THE DEVELOPMENT AND RESPONSE TO INJURY OF NEONATAL RAT HINDLIMB FLEXOR MOTONEURONES AND THEIR AFFERENT CONNECTIONS: A MORPHOLOGICAL STUDY.

A thesis submitted to the University of London for the degree of Doctor of Philosophy in the Faculty of Science.

by

Joanna Dekkers BSc. (Hons)

Department of Anatomy & Developmental Biology

University College London

MARCH 1994

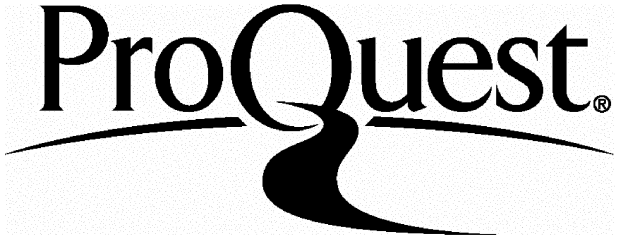

TABLE OF CONTENTS

LIST OF FIGURES

LIST OF TABLES

ACKNOWLEDGEMENTS

I owe a great deal of thanks to all the people that I have had the pleasure of working with during my time at University College. Firstly, to Dr. Roberto Navarrete, for his thorough help and supervision with my Ph.D. project. Next, to Prof. Gerta Vrbova and Dr. Jeremy Cook, for the use of their laboratories and equipment, as well as technical help and advice. Also, to all the miscellaneous individuals, who have made the whole thing such fun; Dr. Linda Greensmith, Dr. Angela Connold, Francois Tyc, Jim Dick, Dr. Angela Hind, Dr. Antal Nogradi, Dr. Gavin Clowry, Claire White, Juneda Sanusi, Dr. Dave Becker, George Mentis and anyone else who was around and offered friendship and assistance when it was needed. Thanks also to other friends and to my family for their support; especially to Kurt, for his love and support, and also for being patient and always ready to help at any time. Very special thanks to Dotty and Flea, just for being.

ABSTRACT

Development of motor function extends into the first three postnatal weeks in rats, and is correlated with maturation of spinal motoneurones and their afferent inputs. This study examined the normal development of somatodendritic morphology of identified ankle flexor motoneurones and the effect of nerve injury on the morphology and survival of cells. The effect of nerve injury upon motoneurone synaptic connectivity was also examined.

Retrogradely labelled motoneurones were injected with fluorescent dyes. One to three days after birth, the soma and dendrites of these motoneurones were covered in filopodial and lamellipodial processes. After four postnatal days there was an elimination of these processes which proceeded from the soma to the distal dendrites. By nine days after birth, these structures were found only distally. There was no significant growth of the soma during the first postnatal week.

After common peroneal (CP) nerve injury on postnatal day two, elimination of processes from the soma and proximal dendrites was halted Some cells showed evidence of dendritic sprouting. Other motoneurones displayed features associated with neuronal degeneration. However, there was no significant difference in soma area of injured motoneurones compared with control motoneurones. Finally, two to three months later only 48-69% of the injured motoneurones survived.

The effect of nerve injury on the distribution of parvalbumin immunoreactive primary afferent fibres and descending serotonergic fibres in the ventral horn was studied. Within five days after nerve injury, there was a decrease in the density of parvalbumin immunoreactivity around the injured CP motoneurone pool. In contrast, the density of serotonergic fibres was apparently unaltered.

The somatodendritic surface of rat flexor motoneurones matures during the first week of postnatal life. Injury during the critical period arrests the maturation of the cell, and results in death of motoneurones.

1. GENERAL INTRODUCTION

The development of the mammalian neuromuscular system may be broadly divided into two stages. In the first stage, muscle and nerves develop independently of each other as isolated systems. In the second stage of development and in the adult mammal, the two systems are mutually and critically dependent upon each other. The development of motoneurones will be described in Chapter 1. Chapter 2 is concerned with the early postnatal development of identified hindlimb flexor motoneurones in the rat. The factors that influence the interdependence of motoneurones and their target are varied. It is thought that some kind of retrograde support is imparted on the motoneurones by the target muscle. Disconnection of the motoneurone from its target and the effects of injury on motoneurones during development, and in the adult, will be addressed in Chapter 1 and in Chapter 3. In addition, afferent inputs onto neurones may effect the development of these cells. Chapter 4 is concerned with the postnatal development and response to peripheral nerve injury, of two types of monosynaptic inputs onto the motoneurones.

1.1. Early development of motoneurones

1.1.1. Neurulation

The central nervous system first appears in the embryo as a piece of thickened ectoderm, the neural plate. This subsequently rises along its lateral edges to form the neural folds, which eventually fuse to form the neural tube. There is a widening of the anterior part of the neural tube to form the brain and the remainder forms the spinal cord. During this period cell division, growth and migration occurs. The forces responsible for these movements of cells are thought to be primarily changes in the shapes and sizes of the cells themselves, and also changes in adhesive properties of surrounding cells (Jacobson, 1982). Neurulation is followed by a period of cellular proliferation and differentiation.

1.1.2. Differentiation

Cells from the neural tube enter a period of mitosis, which results in thickening of the neural tube. Cell division occurs on the inner surface, or ventricular zone, of endothelial cells in the neural tube (see (Purves, Lichtman, 1985)). This lumen eventually becomes the ventricles of the brain and the central canal of the spinal cord (Sauer, 1935; Rakic, 1974). Cells proliferate within the ventricular zone, and from here some migrate to more superficial locations. Others remain and enter the mitotic cycle again (Fujita, 1966).

1.1.3. Migration

As migration progresses, a longitudinal indentation appears in the neural tube and divides it into dorsal and ventral plates. These later become the dorsal and ventral horns of the spinal cord. The neuroblasts, from which motoneurones develop, appear as two longitudinal columns in the ventro-lateral embryonic spinal cord (Fujita, 1963; Jacobson, 1970). There is a rostro-caudal progression of maturation in the development of the spinal cord (Hamburger, 1948), and a ventro-dorsal gradient of proliferation. The motor system in the ventral horn of the spinal cord develops prior to the sensory system in the dorsal horn.

Neuroblasts move by crawling along the surfaces of other cells by means of attachment of extensions of their membrane, and pulling. These lamellipodia extend, attach to the substrate and shorten, pulling the cell forwards (Abercrombie, 1961; Izzard, Lochner, 1976). New adhesion sites are then formed and the process is repeated. This process of movement requires the generation of force within the cells. Muscle-like proteins, such as actin and myosin are present within neurons (Abercrombie, 1982), often associated as microfilaments.

Movement of the cells is partly in response to cues in the local environment of the immature nervous system. Weiss (Weiss, 1939; Weiss, 1941; Weiss, 1961),

showed that cultured epithelial cells tend to move along the scratches in a glass plate. It has been suggested that cells adhere differentially to different surfaces (Letourneau *et al.*1982; Dunn, 1982) and that this is what is responsible for guiding their movements. Relative adhesiveness of certain cells may change during development (Johnson, 1969; Johnson, 1970).

In the cerebral cortex neurones arising early in development end up deep within the cortex, whilst those arising later migrate to more superficial layers (Rakic, 1972). This requires that the younger neurones pass through areas containing older cells. In some regions the neurones may be guided by a specific cell type, radial glia (Rakic, 1972; Rakic, 1971; Henrikson, Vaughn, 1974). These cells appear first, and become oriented to guide other cells to a specific location, extending from the ventricular to the pial surface of the cortex (Levitt, Rakic, 1980).

1.1.4. Axonal outgrowth

Once in position nerve cells may extend growing neurites to make connections within their local environment. The growth cone was first visualised and identified using a Golgi silver stain by S. Ramon y Cajal in 1890 (Ramon y Cajal, 1890), who described the tip of the neurite as the growing region of the cell. Later Harrison (Harrison, 1910), observed that living growth cones in tissue culture were constantly moving and extending. The growth cone has subsequently been described by many authors (Letourneau, 1982; Bray, 1982). It is a club-like structure with extensions, lamellipodia, which are broad, and others, filopodia, which are narrower. These structures contain organelles such as lysosomes, smooth endoplasmic reticulum and cisternae, as well as actin and microfilaments (Bray, Bunge, 1973; Landis, 1983).

Work by Bray has confirmed that neurites grow by membrane addition at the growing tip, the growth cone (Bray, 1970; Bray, 1973b). Whether this mem-

brane is manufactured at the growth cone or in the cell body is unknown, but it is clear that the force for extension is provided by the growth cone itself. Adhesion by the filopodia and contraction by actin and myosin filaments results in a forward pull of the tip of the neurite (Bray, 1973a; Bunge, 1977; Letourneau, 1981). It has also been shown that Ca^{2+} is involved in this event (Anglister *et al.*1982).

Motor axons grow out of the ventral horn of the spinal cord to innervate muscles in the periphery (Tello, 1917). In the chick embryo, axons grow out and form the ventral roots at about the same time as the limb buds develop (Hollyday, Hamburger, 1977). In the rat foetus, axons are seen leaving the ventral root on day 11.5 (Filogamo, Gabella, 1967). The projection pattern of the axons gradually achieves a recognisably adult state, as shown by retrograde labelling with horseradish peroxidase (HRP) (Landmesser, 1978) or other neuronal labels, such as DiI (Snider, Palavali, 1990). Axons have been shown to select a specific direction of outgrowth. In the chick embryo, misrouted axons (either as a result of removal of a part of the spinal cord, or rotation of a portion of the spinal cord), often find their usual targets (Lance-Jones, Landmesser, 1980b; Lance-Jones, Landmesser, 1981a; Lance-Jones, Landmesser, 1981b; Lance-Jones, Landmesser, 1980a). This is only true if the disruptions are quite minor. However, transplantation of duplicate limbs results in the added limb being innervated by nerves that would normally be destined to innervate more distal portions of the original limb (Whitelaw, Hollyday, 1983a; Whitelaw, Hollyday, 1983b).

The mechanisms directing axonal outgrowth are not clearly understood. It is possible that the growing nerves respond to various environmental cues such as mechanical guidance cues (Bray, 1982), differences in adhesiveness ((Nardi, 1983) in the moth), the extracellular matrix ((Schinstine, Cornbrookes, 1990) in the rat), electrical gradients (Jaffe, 1979; Jaffe, 1981) and tropic gradients

((Gundersen, Barrett, 1979; Gundersen, Barrett, 1980) in the chick). Peripheral axons of mammals have the ability to regenerate after injury and to reinnervate the region of their target sites (Gutmann, Young, 1944) although they might not synapse at exactly the same postsynaptic site (Bernstein, Guth, 1961). Axons form synapses as they reach a region of denervated target tissue on a first-come first-served basis. In mammals, regeneration is less likely to occur in the central nervous system (CNS). Nevertheless experiments by Aguayo *et al.* (Aguayo *et al.*1979; Aguayo *et al.*1982) in the rat, using peripheral nerve grafts within the CNS at a site of lesion, show that given the right environment, axons of CNS neurones can regenerate. This suggests that the environment in the CNS, but not in the peripheral nervous system (PNS), prohibits the growth of axons.

The early development of the motoneurone is independent of interaction with the muscle and occurs before the axon has reached its target. If the limb bud of a chick is removed during early development the axons continue to grow into the remaining stump (Chu-Wang, Oppenheim, 1978). Later however, motoneurones become critically dependent on their peripheral connections. The growth of the first axons leads to the formation of immature synapses onto the myotubes.

1.1.5. Developmentally expressed proteins

There are some genes encoding for proteins that are expressed predominantly during growth and development of neurones, and are not normally expressed in adult or mature neurones. These proteins are expressed during axonal and dendritic elongation, and during periods of synaptic rearrangement either during normal development or after injury.

The neurotransmitter enzyme choline acetyltransferase (ChAT) appears in the motoneurones after the final mitotic division (Phelps *et al.*1990). During development the levels of ChAT increase both in the cell body (Phelps *et al.*1984)

and at the nerve terminals (O'Brien, Vrbová, 1978). There is evidence that the interaction with the target muscle (Betz *et al.*1980) and the maintenance of electrical activity are important in maintaining this elevation, as TTX blockade of action potentials in cultured cells results in a delayed development of ChAT activity (Brenneman *et al.*1983) whilst depolarisation of the membrane with K^+ or NMDA receptor activation, causes an increase (Brenneman *et al.*1990; Ishida, Deguchi, 1983).

The gene for GAP-43 is also expressed developmentally. Most neurones reduce the levels of GAP-43 expressed during development as they mature. It is proposed that GAP-43 alters the response of neurones to extracellular signals (see (Skene, 1989)). GAP-43 is found in growth cones (Skene *et al.*1986), and is involved in axonal elongation and synaptic rearrangement. In the visual system of the toad after injury to the optic nerve, the axons grow towards the optic tectum and form synapses. During this period, there is elevated expression of GAP-43 (Skene, Willard, 1981).

Synthesis of tubulin is increased during axonal outgrowth, and one of the genes for tubulin is expressed at higher levels during development and regeneration of axons (Lewis *et al.*1985; Miller *et al.*1987). Tubulin is a major component of the cytoskeleton, but it is transported to the site of growth slowly. It may limit the rate of elongation of axons (Hoffman, Lasek, 1975).

Another example of a group of a developmentally expressed group of proteins are the microtubule associated proteins (MAPs). These proteins regulate the stability of microtubules in the axons and dendrites. They are involved in determining neuronal shape, and regulating the balance between rigidity and plasticity (see (Matus, 1988; Matus, 1990)). MAP1a is not detectable in the rat embryo brain, or at birth. Levels increase up to P20, at a time when neuronal processes are growing, and then remain constant (Riederer, Matus, 1985).

MAP2 is expressed from late embryonic life. One isoform, MAP2c, is present only in neonatal and early postnatal rat brain (Riederer, Matus, 1985). MAP3 levels increase after birth, but drop between P10 and P20. MAP5 is present at higher levels in the brain of neonatal rats than in the adult (Riederer *et al.*1986). The changes in the expression of MAPs coincides with the transition of neurones from a 'growing' to a 'maintenance' state between P10 and P20 in the rat. It also correlates with the efficiency of polymerisation of microtubule proteins. The rate of assembly of microtubules from tubulin is lower in the neonate than in the adult (Fellous *et al.*1979). This can be increased by the addition of adult MAPs (Francon *et al.*1982). Thus, it would appear that MAPs are involved in controlling the rate of polymerisation of tubulin and the stability of developing neuronal processes (see (Tucker, 1990)).

1.1.6. Development of electrical excitability

The firing patterns of motoneurones are influenced by the type and distribution of both ion channels and receptors to neurotransmitters in the membrane of the motoneurones. These change during development (see (Spitzer, 1981)). Inward sodium and calcium currents occur in cultured chick motoneurones at a time when the axon is making connections with the target (E4) for the first time. The size and types of Na^+ currents and their numbers increase with age in chick (McCobb *et al.*1989), and in rat embryos (Ziskind-Conhaim, 1988). Different types of Ca^{2+} conductances contribute to the action potential at various times during development. Motoneurones from E4 chick embryos have mostly low-threshold, T-type Ca^{2+} currents, which are activated near the resting potential. These decrease during development *in vitro*, as the high-threshold, L- and N-type channels increase, and peak at E11 (McCobb *et al.*1990). In the neonatal rat, the low threshold conductances are especially evident during the early postnatal period (Walton, Fulton, 1986), and are associated with spontaneous oscillations in the membrane potential. This may be involved in the generation of spontaneous autorhythmic activity seen in developing neuronal networks

(Llinas, 1988). Another function of the low threshold Ca^{2+} currents may be in the production of "doublet" firing observed in rats only until P7 (Navarrete, Walton, 1989b). This is consistent with the phasic EMG activity pattern seen in neonatal muscle (Navarrete, Vrbová, 1983). It is possible that the changes in the distribution of Ca^{2+} channels may contribute to the matching of the contractile properties of muscle with the firing patterns of the motoneurones (see (Vrbová *et al.*1985)). During postnatal development in the rat, there are changes in the firing patterns of motoneurones and simultaneous changes in the properties of the muscle (Navarrete, Vrbová, 1983). The matching of muscle to motoneurone firing patterns may be as a result of these changes.

In cultured embryonic chick motoneurones, the duration of the action potential is longer than in the adult (McCobb *et al.*1990). This may be due to the relatively small amounts of K^+ currents, which effects the duration of the afterhyperpolarization of the action potential. In the neonatal rat, there is a change in the type of K^+ currents, which may contribute to the changes in the firing patterns of the motoneurones during development (Manabe *et al.*1991). This may also result in an increased entry of Ca^{2+} into the cell through voltage-dependent Ca^{2+} channels. Because of the cell signalling function of Ca^{2+}, this increase in intracellular Ca^{2+} possibly affects the growth and maturation of the motoneurone, as well as altering the firing patterns of the motoneurones.

The activation of the motoneurones is also dependent on the distribution and response to the various neurotransmitters being produced. Synaptic activation is via neurotransmitter mediated ion channels along the membrane. The response of cultured chick motoneurones to the neurotransmitter glutamate shows that the distribution of ion channels is not uniform along the membrane of the motoneurone (O'Brien, Fischbach, 1986b), but is clustered in areas in a similar way to the clustering of AChR on adult skeletal muscle fibres.

1.2. Morphological Development of Motoneurones

1.2.1. Embryonic development

Motoneurones in the rat spinal cord undergo terminal mitosis on E10-11 (Chen, Chui, 1992; Altman, Bayer, 1984) and begin to express ChAT on E12-13 (Phelps *et al.*1990), by which time they have migrated to the ventral horn of the spinal cord (Smith, Hollyday, 1983). They have a smooth, round soma 15-25 μm in diameter (Cummings, Steltzner, 1984), and begin to develop dendritic projections. No new primary dendrites are formed after this period. The dendrites are covered with many irregular hair-like structures, 1-5 μm long, as well as beaded growth cone-like structures. Growth cones and other structures have been observed during development. These are eliminated during maturation, and have been used as an indication of cellular immaturity (Ramon y Cajal, 1929). The varicose structures on secondary dendrites often give rise to much longer filopodial structures, and the long, thin sprouts of tertiary dendrites. By E18 the somata of rat thoracic motoneurones, visualised using the Golgi technique, are covered in thin spines, ranging from 0.5-3 μm in length (Cummings, Steltzner, 1984). These spines are believed to provide sites of synaptic contact for afferent axons that impinge onto the surface of the neurone (Scheibel *et al.*1973; Skoff, Hamburger, 1974). During this period of development dendrites are covered with many spine-like protrusions. It is possible that these take part in the process of synaptogenesis that is occurring during embryonic development, by allowing synapses to become incorporated onto the dendritic shaft as it continues to grow (Skoff, Hamburger, 1974).

1.2.2. Postnatal development of motoneurones

In many mammals locomotion develops and matures during the early postnatal period. This occurs at a time that coincides with the maturation of motor units (see (Vrbová *et al.*1985)), of connectivity between motoneurones and their afferent inputs as well as the maturation of spinal reflexes (Conradi, Skolglund,

1969; Schreyer, Jones, 1988b). During this period there are also changes in the morphology of motoneurones and the orientation of their dendrites (Cullheim, Ulfhake, 1985; Ulfhake *et al.*1988).

There is an increase in the size of the soma of motoneurones, especially between the second and third postnatal weeks, in rat hindlimb motoneurones (Westerga, Gramsbergen, 1992; Kerai *et al.*1993). In cat hind limb motoneurones, there is a 400% increase in the dendritic membrane area, and a 100% increase in the soma area from birth to P46 (Ulfhake, Cullheim, 1988a). The increase in soma area occurs prior to the end of the increase in dendritic membrane area, thus the ratio of dendritic:somatic membrane area increases from 20:1 to 50:1. It is interesting that the growth of the cell body usually precedes that of the dendrites.

The somatodendritic surface of neurones also changes as the cell matures. By P5 in rat thoracic spinal motoneurones, spine-like growth associated processes are eliminated from the surface of the soma (Cummings, Steltzner, 1984). Over the next few days these processes are lost from the surface of proximal dendrites, but they remain on the distal portions. A similar pattern of somatodendritic maturation is observed in hindlimb motoneurones of the cat over the first five postnatal weeks (Ulfhake, Cullheim, 1988b).

In the adult motoneurone the dendritic tree represents the vast majority of the receptive surface of the neurone. The development of this system, and the factors that influence it, are therefore of great importance. Much of the work on the development of the dendritic structures has used the Golgi staining technique (eg. (Cummings, Steltzner, 1984). Dendrites of layer V pyramidal cells in the cortex of the cat increase their complexity by bifurcating at the tip (Petit *et al.*1988) and any growth occurs along the trunk of the dendrite. This is also seen in cells in the the lateral geniculate nucleus of primates (Leuba, Garey, 1984), and in motoneurones (Ulfhake *et al.*1988).

Detailed studies have been done on the postnatal development of kitten hindlimb motoneurones using HRP-filled cells and serial reconstructions by Ulfhake *et al.* (Ulfhake *et al.*1988; Ulfhake, Cullheim, 1988b; Ulfhake, Cullheim, 1988a). Growth of the dendrites in the transverse plane matches the increase in cross-sectional area of the spinal cord over the same period. However, the growth that occurs in the longitudinal, or rostro-caudal axis is much faster, and the dendrites branch more in this plane of orientation. Still, this parallel s the growth of the spinal cord, which is greater in this plane (see also (Scheibel, Scheibel, 1971)). It is possible that dendritic growth at birth is segmental, after which there is a higher degree of intersegmental growth (Ulfhake, Cullheim, 1988b).

The maturation of afferent inputs onto the cell may be one factor determining the direction of dendritic growth (Snider *et al.*1992b). These events occur in parallel with maturation of motor activity. In cat phrenic motoneurones, the development of dendrites along the rostrocaudal axis also orientates the dendrites in a direction so as to receive descending inputs from the respiratory premotor centres (Feldman *et al.*1985) and serotonergic pathways (Pilowsky *et al.*1990).

Additionally, dendrites in various parts and different levels of the spinal cord become'bundled' (Scheibel, Scheibel, 1973; Scheibel, 1991; Bellinger, Anderson, 1987a; Westerga, Gramsbergen, 1992). There is ultrastructural evidence that within these bundles the dendrites of different motoneurones are in direct contact with each other (Kerns, Peters, 1974). But the significance of these bundles is unclear. They may possibly be involved in the reciprocal activity of antagonistic muscles (Scheibel, Scheibel, 1973), and/or be involved in the formation of appropriate inputs onto the motoneurones during development (Bellinger, Anderson, 1987a).

At birth dendritic segments from kitten motoneurones are only 45% of adult length (Ulfhake *et al.*1988). The addition of new membrane initially occurs by the elongation of terminal and preterminal branches. After this, growth is in the terminal branch orders, and lastly there is a period of growth in the preterminal branches. It is clear then that growth of different parts of the neurone does not occur simultaneously. This has also been observed in Purkinje cells of the cerebellum (Berry *et al.*1980), and it is suggested that the interaction of the dendrites with afferents may be partly responsible. Remodelling of the dendrites occurs by the formation of new branches as well as the elimination of existing ones, and results in differential growth in regions of the cell (Berry, 1980; Uylings *et al.*1986; Ulfhake *et al.*1988). The development of the size and orientation of the dendritic tree is greatly influenced by the type and direction of the various types of afferent input onto the cell (Snider *et al.*1992b) and the interaction with other cells (see (Rakic, 1975)). The size and branching structure of the dendritic tree of a motoneurone are important both anatomically, as this will determine where synaptic inputs are made, and also physiologically, as this will determine the relative influence that these inputs have on the functional output of the cell (Rall, 1959).

A feature of embryonic and early postnatal motoneurones is electrotonic coupling of cells (Navarrete, Walton, 1989a; Mazza *et al.*1992). This communication is thought to be mediated via gap junctions (Sotelo, Taxi, 1970). Coupling between motoneurones is possibly involved in establishing the patterns of synchronised firing that is a feature of the activity patterns of early postnatal motoneurones, and is especially evident in motoneurones supplying synergistic muscles (Walton, Navarrete, 1991). This pattern of firing becomes less important over the first two weeks of postnatal development in the rat, as synaptic connections and motor behaviour become refined and mature (Navarrete, Walton, 1989a). The incidence of coupling therefore declines over this period (Mazza *et al.*1992; Navarrete, Walton, 1989a).

1.2.3. Morphology of adult motoneurones

The adult morphology of rat spinal motoneurones is achieved by one month of age (Cummings, Steltzner, 1984). The cell body appears smooth and devoid of any spines; it is up to 50 μm in diameter. The dendrites are mostly smooth (Cummings, Steltzner, 1984). Studies indicate that there are relationships between various morphological and electrophysiological parameters of motoneurones. Thus, in cat a-motoneurones, there is a positive correlation between soma size, axon diameter and axon conduction velocity (Cullheim, 1978; Cullheim *et al.*1987a). The diameter of primary dendrites correlates with the total membrane area of the cell and can be used to give an estimate of total membrane area (Ulfhake, Kellerth, 1981; Burke *et al.*1982; Ulfhake, Cullheim, 1988a). The diameter of the soma is positively correlated with the mean diameter and the combined diameter of the primary dendrites (Ulfhake, Kellerth, 1981), but not with the number of primary dendrites. The firing patterns of slow and fast motoneurones are different. The changes occur during the first three postnatal weeks (Navarrete, Vrbová, 1983), and may partly be dùe to size-related changes in their electrophysiological properties. Small motoneurones have higher input resistances and lower excitation thresholds and so are more active than large ones (Henneman *et al.*1965). Thus, slow motoneurones, which are smaller than fast motoneurones (Cullheim *et al.*1987a), fire more quickly.

The dendritic branching structure of adult motoneurones depends on their location within the spinal cord, and may be influenced by the pattern of afferent innervation (Rose, 1982; Cullheim *et al.*1987a; Cullheim *et al.*1987b). The motoneurones innervating fast motor units are larger than those innervating slow ones (Cullheim *et al.*1987a) and have a more complex branching pattern and more terminal branch points. However, the 'space' that these type-identified motoneurones occupy three-dimensionally does not differ, but reflects the orientation of afferent inputs to the cell (Cullheim *et al.*1987b). In many cases

(though not all), the primary dendrites are oriented radially from the soma, and in this situation any polarity in the orientation of the cell occurs at the distal dendrites. The effectiveness of inputs depends on the site, within the dendritic tree of the cell, at which a synapse is formed (Rall, 1964; Rall, Rinzel, 1973). The greater the order of branching the greater the attenuation of the synaptic potentials of distal synapses with no change in the dendritic electrotonic length (Rall, Rinzel, 1973). This suggests that the complex branching structure of the motoneurone may also be important in determining the integrative properties of the cell which, in turn effect the activity of the muscle fibres that they innervate.

1.3. Early Development of Muscle

Alongside the neural tube in the embryo the somites are formed from the segmentation of the mesodermal tissue. There is a rostro-caudal gradient of formation of the somites, and different areas of the somites develop in different regions of the musculature. The muscles of the trunk develop from the medial region of the somites, the myotome. The cells proliferate and differentiate in the myotome and eventually migrate to their positions within the limbs.

In the rat, somites of the hindlimb muscles (somites 23 to 28), appear on E12 (Christie, 1964). Initially, a few mononucleated cells migrate out of the somite and form the limb bud. Here they proliferate (Chevalier, 1978) and form myoblasts (Tello, 1917). These cells synthesise and contain the elements of muscle: actin, myosin, tropomyosin formed as myofibrils (Holtzner, 1959; Holtzner, Sanger, 1972), and also acetylcholine receptors (AChR's) (Fambrough, Rash, 1971). These myoblasts elongate and fuse with each other to form myotubes (Holtzner *et al.*1957; Schudt *et al.*1976; Holland, MacLennan, 1976). The myotube, even at an early stage, produces active electrogenic responses and conducts along its length (Purves, Vrbová, 1974) although the time course of the response is slow. The AChR responds to acetylcholine (ACh) release with a re-

sulting membrane depolarisation and contraction of the muscle (Dryden *et al.*1974). Later spontaneous contractions occur (Yaffe, 1969) and the T-system develops (Ezerman, Ishikawa, 1967).

The formation of the myotubes from myoblasts is independent of the presence of nerves, or of activity (Harris, 1981). Later during development, however, the muscular and nervous systems do become interdependent.

1.4. Nerve-Muscle Interdependence

1.4.1. Naturally occurring cell death

Death of neurones is a feature of embryonic development in vertebrates. The significance of cell death during development is thought to be in the regulation of neuronal numbers and the control of the interaction between different populations of neurones and their targets (see (Oppenheim, 1991)). In the chick embryo, the greatest number of motoneurones in the spinal cord are found on E6. This then rapidly decreases during a period of target dependent cell death. Up to 50-60% of motoneurones in the chick spinal cord die during this period (Hamburger, 1975). Early experiments showed that the number of neurones innervating a target is proportional to the size of the target, shown by removal of part of the target (Hamburger, 1934). This process occurs not only in response to removal or addition of part of the target field of axons, but as a natural process during development (Hamburger, 1975) in the motor pools of the spinal cord of the chick and is termed apoptosis (Oppenheim, 1991).

Cell death occurs within a precise window of time during the development of the embryo, usually at the time that the axons arrive at their target (Hamburger, 1975; Landmesser, Pilar, 1974). Addition of target tissue has been shown to result in an increase in the number of surviving neurones (Detwiler, 1936) although not necessarily directly in proportion to the amount of target tissue

added (Tanaka, Landmesser, 1986). Using retrograde labelling with HRP, axons are shown to reach their target destination prior to cell death (Chu-Wang, Oppenheim, 1978). Implantation of an additional limb increases the size of the target being innervated. This increases the number of surviving motoneurones that would otherwise die (Hollyday *et al.*1977; Hollyday, Hamburger, 1976). The opposite is also true; by increasing the number of neurones innervating the target, fewer neurones survive (O'Leary, Cohen, 1984). Clearly the target has some effect on the survival of the developing neurones.

1.4.2. Effect of neonatal injury on motoneurone survival

During early postnatal development motoneurones are especially susceptible to injury. The target muscle is thought to provide the motoneurone with retrograde support that sustains them during a critical developmental period when they are particularly vulnerable. It has been established that the interruption of the nerve-muscle interaction during early postnatal development leads to death of motoneurones (LaVelle, 1973).

In the rat the critical period, when the motoneurones are susceptible to loss of contact with their target, continues into the first week of postnatal life. Injury at, or very soon after, birth causes loss of up to 60-70% of the motoneurones innervating hindlimb muscles (Romanes, 1946a). However, the site and severity of the injury inflicted affects the resulting amount of death (LaVelle, 1973). Damage caused to the axon at a site distal to motoneurones, for instance to the sciatic nerve close to the knee, causes less death of motoneurones than a proximally inflicted injury (see (Lieberman, 1974b)). This is possibly due to the amount of reinnervation that is achieved following the injury. The axons growing to a distal lesion have a shorter distance to grow to reinnervate the muscle than those to a proximal lesion. It is also possible to cause death of the motoneurones without inflicting actual damage, eg. by blocking the ACh receptor at the neuromuscular junction with a-bungarotoxin (α-BTX) (Greensmith,

Vrbová, 1989). Additionally, application of α-BTX to block neuromuscular transmission, followed by sciatic crush at 5 days postnatally (which would normally result in little or no motoneurone death (Lowrie *et al.*1982)), causes almost as much death as crush at birth (Burls *et al.*1991). This led to the suggestion that, at least for sciatic motoneurones, it is the loss of interaction with the target that causes death of motoneurones (Kuno, 1990).

1.4.3. Trophic Theory

There are several ways in which the target could retrogradely influence the neurones innervating it. It has been suggested that the target supplies its trophic support via factors produced by the target and taken up by the axons innervating it. During development neurones are thought to be especially dependent on these factors. Hamburger and Levi-Montalcini (Hamburger, Levi-Montalcini, 1949) found that a substance found in the ciliary ganglia of male mice, nerve growth factor (NGF), was able to sustain neurones in the spinal ganglia of chick embryos. Application of anti-NGF antibody resulted in abnormal development of the sympathetic ganglia (Levi-Montalcini, 1972). They suggested that NGF was responsible for imparting trophic support to the neurones. Trophic support would be lent to only those cells that make connections with the NGF-secreting target tissue (Hamburger *et al.*1981; Hamburger, 1992). This would result in competition for the factor, and gives an explanation as to why neurones are vulnerable to disconnection from their target tissue. NGF has been shown to prevent some naturally occurring cell death in the chick embryo spinal cord (Oppenheim *et al.*1982). Nerve growth factor does not, however, affect all types of neurones, but is largely limited to the sympathetic ganglia and the sensory ganglia.

Ciliary neurotrophic factor (CNTF) has been shown to increase the survival of chick spinal motoneurones in culture (Arakawa *et al.*1990). It has been found in adult rat sciatic nerve (Manthorpe *et al.*1986). High levels of CNTF mRNA is

located in the Schwann cells in sciatic nerve (Stockil *et al.*1991) and levels remain high in lesioned nerves (Sendtner *et al.*1992c). CNTF has been shown to prevent the degeneration of facial motor axons in neonatal rats one week after axotomy (Sendtner *et al.*1990) and also to prevent degeneration of motor neurones in mutant *pmn* mice, a proposed model for human spinal motor neurone disease (Sendtner *et al.*1992b).

Whilst CNTF is not expressed during development (Stockli *et al.*1991), another factor, brain derived neurotrophic factor (BDNF) is, and has been shown to prevent some naturally occurring cell death of motoneurones in chick embryos (Oppenheim *et al.*1992). It has also been shown to prevent the death of motoneurones following deafferentation (Oppenheim *et al.*1992) and one week after neonatal nerve injury (Sendtner *et al.*1992a; Yan *et al.*1992).

1.4.4. Role of Activity

When the axons reach the target muscle they form contacts, and there is an increase of transmitter release from the growth cones at the distal tip of the axon. The growth cone has changed from a growing to a transmitting structure (Xie, Poo, 1986). How does the target influence this change? It is possible that the response of the muscle cells to innervation results in changes in the ionic composition of the environment of the neuromuscular junction, and that this triggers the changes that occur. There may also be a feedback mechanism where the increase in transmitter released at the terminal induces the motoneurones to increase their production of transmitter and to become a transmitting cell.

Due to the maturation of spinal reflexes and the formation of afferent synaptic contacts onto the motoneurones in the early postnatal period, there is an increase in the excitatory input onto the motoneurones (Westerga, Gramsbergen, 1990; Navarrete, Vrbová, 1983). The interruption of the contact with the muscle further increases the activity of the immature motoneurones (Navarrete, Vrbová,

1984). It is possible that this increase in activity may be a cause of motoneuronal death following axotomy in the neonate.

The majority of excitatory inputs onto neonatal motoneurones are glutaminergic. The large amount of cell death observed after neonatal injury may be an excitotoxic effect mediated by glutamate (Choi, 1988; Choi, 1992a; Appel, 1993) and specifically the NMDA receptor. NMDA receptors are present on young motoneurones (O'Brien, Fischbach, 1986a), and are activated during locomotion (O'Donovan, Landmesser, 1987). NMDA receptors are transiently expressed in the ventral horn of the rat spinal cord over the first weeks of postnatal life (Kalb *et al.*1992). There is a developmental increase in the resistance to glutamate neurotoxicity in cultured neurones (Brenneman *et al.*1990), that may explain why motoneurones in older animals are less susceptible to injury. This may occur due to the redistribution of the NMDA receptor when contact is made at the neuromuscular junction, so that preventing such a maturation would prolong the susceptibility of the motoneurones to the excitotoxic effects of NMDA (see (Lowrie, Vrbová, 1992)). Support is lent by the finding that axotomy at 5 days postnatally produces motoneurones that are susceptible to the effects of NMDA injected into the spinal cord, whereas those motoneurones that had maintained contact with their muscle were not (Greensmith *et al.*1991). Also that the excitotoxic effects of glutamate can be reduced by the application of an NMDA antagonist such as MK-801 (Mentis *et al.*1993).

The mechanisms of glutamate induced cell death have been proposed. Cortical neurones in culture die when exposed to glutamate (Choi, 1987). They immediately swell, and this may be due to the influx of extracellular Na^+ accompanied by the influx of Cl^-. These osmotic changes result in volume expansion, but are not necessarily lethal. The next phase of glutamate neurotoxicity occurs several hours after exposure and is a result of the excessive influx of Ca^{2+} (Choi, 1985). The Ca^{2+} accumulation is mostly mediated by the NMDA receptor (see (Choi,

1992b; Rothman, Olney, 1987)). This Ca^{2+} overload triggers cytotoxic cascades responsible for neuronal disintegration. There is also a proposed role for glutamate in cell death occurring in some neurodegenerative diseases, via defects in the production of energy from mitochondria (Beal *et al.*1993).

It is clear that at some stage the motoneurones lose their dependence on the target for support. This may be partly due to the changes occurring to the motoneurone synaptic input and receptor distribution, but also due to changes occurring at the neuromuscular junction and the maturation of contacts made by the motoneurones with the target muscle.

1.4.5. Development of neuromuscular connections

The growth cone releases ACh on making contact with the myotube (Young, Poo, 1983), even before the development of synaptic specialisation (Frank, Fischbach, 1979). It appears that the formation of the contact between muscle and nerve induces an increase in the amount of transmitter produced (Xie, Poo, 1986) which is sufficient to trigger muscle contractions (Jaramillo *et al.*1988). Transmission at the immature neuromuscular junction is initially less efficient than that in the adult (Pilar *et al.*1981). The frequency of the spontaneously evoked miniature endplate potentials (MEPPs) and the size of the excitatory postsynaptic potential (EPP) increase during embryonic and early postnatal development (Dennis *et al.*1981; Diamond, Miledi, 1962). There is also an increase of the amount of ACh synthesising enzymes at this time (O'Brien, Vrbová, 1978). As the pre- and postsynaptic membranes develop and become more integrated the efficiency of neuromuscular transmission increases.

During the early postnatal period, there is a reorganisation of the synaptic contacts made at the neuromuscular junction. In the adult state, each muscle fibre is supplied by a single axon from a motoneurone. The most active motor units have the smallest innervation ratio, whilst larger motor units are often less active

(Burke, 1981). During late embryonic and early postnatal development, however, individual muscle fibres are contacted by several motor axons (Redfern, 1970). This is known as polyneuronal innervation. During the early postnatal period, there is a reduction in the number of axons connecting a muscle fibre, until a single muscle fibre is innervated by only one motoneurone. This is achieved by the elimination of polyneuronal innervation. In the rat this occurs during the second and third postnatal weeks (Redfern, 1970) at a time when neuromuscular activity increases (O'Brien *et al.*1978). By blocking the activity of motor units in the neonatal period with TTX it is possible to maintain these large territories characteristic of immature motor units (Callaway *et al.*1987). This suggests a role for activity in the development of neuromuscular contacts.

Application of α-BTX to the soleus muscle of neonatal rats (Greensmith, Vrbová, 1991) results in a loss of synaptic contacts. This can be explained by considering the mechanism for blockade of activity of TTX and α-BTX. TTX reduces the activity at the neuromuscular junction by blocking the action potential, whilst a-BTX blocks the response of the muscle to ACh. The application of TTX blocks activity, but may still allow maturation of the neuromuscular junction as there is still spontaneous release of transmitter in the axon terminals (Gundarsen, 1990). This release may be sufficient to allow the maturation of the developing neuromuscular junction and maintain the contacts formed. In contrast, the application of a-BTX stops differentiation of the postsynaptic membrane as the AChR is blocked (Gordon *et al.*1974). Therefore, it is clear that the maturation of the postsynaptic membrane is crucial for the maintenance of the interaction between the nerve and the muscle, and dictates the innervation ratio of the motor unit.

The dependence of the maturation of the neuromuscular junction upon activity can also be demonstrated by increasing the activity by electrical stimulation. This accelerates the loss of synaptic contacts (O'Brien, Vrbová, 1978). Loss of

contacts can be increased by inhibiting AChE (Duxon, Vrbová, 1985a), the enzyme that hydrolyses ACh. Also during the time that synapse elimination is occurring application of BTX, to block the AChR, prevents further loss of terminals (Srihari, Vrbová, 1978; Duxon, 1982). Prolonged depolarization of the endplate region results in a disruption of many neuromuscular contacts (O'Brien *et al.*1982; O'Brien *et al.*1984; Zhu, Vrbová, 1992) and reduction of Ca^{2+} with BAPT-AM reduces the effects of activity (Zhu, Vrbová, 1992). This suggests that Ca^{2+} ions play an important part, as reduction in the concentration of Ca^{2+} ions slows the disappearance of polyneuronal innervation (Connold *et al.*1986). The Ca^{2+} ions appear to act via a calcium activated neutral protease (CANP) which is involved in the breakdown of cytoskeletal proteins (see (Croall, Demartino, 1991)). A decrease in the number of terminals lost in developing soleus muscle can also be achieved by application of leupeptin, which inhibits CANP (Connold *et al.*1986; O'Brien *et al.*1982; O'Brien *et al.*1984).

Vrbová and colleagues have proposed a mechanism to account for the effects of activity in neuromuscular synapse elimination. During activity there is an accumulation of K^+ in the synaptic cleft (Hohlfield *et al.*1981) which results in the depolarization of the nerve terminal. This opens K^+-dependent Ca^{2+} channels and allows entry of Ca^{2+}. If these Ca^{2+} transient currents are prolonged this will trigger the action of CANP and result in the breakdown of cytoskeletal proteins, such as neurofilament protein, and ultimately the loss of contacts between the nerve and the muscle. Clearly the smaller axon profiles will be more vulnerable, as their surface-to-volume ratio means that the amount of Ca^{2+} will be greater than in bigger terminals (Duxon, Vrbová, 1985b; O'Brien *et al.*1984). Substances that block the action of CANP reduce the loss of contacts (Connold *et al.*1986).

The size of the muscle fibre may also be important in the maintenance of synaptic contact. Primary myotubes are larger and more mature than more recently

formed secondary myotubes and are more able to sustain contacts with the nerve terminals (Sheard *et al.*1991; Duxon *et al.*1986). The oldest primary myotubes are contacted by several nerve terminals from different axons. Secondary myotubes are formed close to primary myotubes and the axons that contact them. In some cases the secondary myotubes share axon terminal profiles with a large primary myotube (Duxon *et al.*1986). Later in development, the contact may be lost and there is a transfer of contact from the primary to the secondary myotube (Duxon *et al.*1986).

The secondary myotube has a high input resistance compared to a primary myotube. The AChRs are less mature and there is less AChE. It responds with a large depolarization and will have a huge response to large amounts of transmitter with a prolonged EPP, as the immature AChRs have long channel opening times (Sheard *et al.*1991). A mature terminal will produce a prolonged response in a secondary myotube. This may lead to retraction of the terminal by the mechanism already described.

The maturation of the neuromuscular junction illustrates the role of activity in the formation of contacts between cells and its importance in the regulation of contacts onto cells and the survival of the neurones themselves.

1.5. Development of Motor Activity

The maturation of the nervous system and motor behaviour is reflected in the movements of the embryo. The changes in patterns of movement of the embryo is correlated to anatomical and electrophysiological changes occurring within the neuromuscular system at this time (Hamburger, Balaban, 1963; Bekoff, 1976). Over a period of development, the movements of the embryo become more complex and coordinated as the neural networks that generate activity mature.

The first movements observed in the chick embryo are in the head and trunk (Hamburger, Balaban, 1963). It is not until E6 that uncoordinated limb movements are seen, although this activity is still only periodic. At this time EMG recordings show that there is coactivation of flexor and extensor muscles (Bekoff, 1976; Landmesser, O'Donovan, 1984; O'Donovan, Landmesser, 1987). Extracellular electrophysiological recordings made *in situ* from the lumbar spinal cord also show this synchronous activity within segments, or even from separate segments (Provine, 1971). There is also firing of both antagonist and agonist muscles together (Landmesser, O'Donovan, 1984). Activity increases from E9, when reciprocal activation of antagonistic muscles emerges (Bekoff, 1976), until just prior to hatching, when activity peaks (Hamburger *et al.*1965). At stage 31 in the chick embryo, firing of the motoneurones is followed by a delayed discharge which is longer in the flexor than in the extensor muscles (O'Donovan, Landmesser, 1987). This accounts for the reciprocal activation of antagonistic muscles.

By removing the afferent inputs onto the motor neurones at various times during the development of motor activity, it has been possible to show that during much of embryonic development motor activity is generated within the spinal cord and is independent of descending or segmental afferent inputs (Hamburger *et al.*1966; Oppenheim, 1975). Until E17 in the chick embryo, interruption of the afferent and descending innervation to motoneurones in the lumbar spinal cord does not influence the patterns of activity. The development of more coordinated movement, however, is dependent on supraspinal influences.

The maturation of motor activity extends into postnatal life in many mammals, including the rat (Navarrete *et al.*1987; Steltzner, 1971; Steltzner, 1982). The elimination of synchronous firing of antagonistic muscles may be due in part to the reduction in inappropriate excitatory connections made by interneurones onto both flexor and extensor motoneurones, during development. There is

also a change in the input resistance of the motoneurones postnatally (Fulton, Walton, 1986; Navarrete *et al.*1987). The morphology of a cell, especially of its dendritic branching, may influence its firing pattern (Rall *et al.*1967).

The rat is an animal which is born relatively immature developmentally, so that it is possible to study the maturation of locomotor behaviour in relation to changes in neuroanatomy (Steltzner, 1982). Crawling is the predominant method of locomotion in the postnatal rat until P10, when it is replaced by walking, and later, adult types of movement (Altman, Sundarshan, 1975; Westerga, Gramsbergen, 1990). After birth the rat has the added factor of coping with the stresses imposed by gravity and the maintenance of posture. Control of locomotion is imposed upon the spinal motor circuits by descending systems. Development of the descending inputs from the cortex, and an increase in connectivity within the spinal cord, occurs between P12 and P20 (Hicks, D'Amato, 1975). On P5 the corticospinal tract fibres reach the lumbar spinal cord (Schreyer, Jones, 1988a), and after this become myelinated. The rubrospinal tract has already reached the lumbar spinal cord by birth in the rat (Shieh *et al.*1983). Development of the cerebellum continues at the same time as the rat begins to walk (Altman, 1982). Disruption of these connections leads to disrupted maturation of locomotion from P14 onwards (Gramsbergen, IJkema-Paasen, 1984). Although there is some evidence of reciprocal activation of antagonistic muscles in the embryo, it is not until some time after birth, when these systems have matured, that true control of posture is achieved. In the neonate these systems do exist, however, as can be seen by administration of L-DOPA (Navarrete, Vrbová, 1985; Iwahara *et al.*1991). This elicits coordinated reciprocal locomotor responses in antagonistic muscles which suggests that the spinal circuitry is able to generate coordinated movement some time before the animal walks.

1.6. Afferent Inputs onto Neurones

1.6.1. Synapse elimination during development

During development there is a period of regulation between the pre- and post-synaptic partners, which may exist to ensure that synapses are appropriately formed. This period of synaptogenesis occurs in most areas of the nervous system after the period of naturally occurring cell death (see (Purves, Lichtman, 1980)). For example, afferent boutons disappear from the surface of the initial segment of the axon of kitten motoneurones in the first two weeks of postnatal life (Conradi, Ronnevi, 1977). At the neuromuscular junction of neonatal rats, there are initially several axons innervating one muscle fibre. In the adult, only one axon remains innervating its target muscle (Redfern, 1970). The pattern of innervation that results after the period of synaptogenesis, differs for different regions of the nervous system.

A good example of synaptic rearrangement in the CNS during development, is seen in the visual cortex. In adult cats, and some primates, neurones of the visual cortex are divided into columns of neurones predominantly from either the right or the left eye (Hubel, Weisel, 1962). These ocular dominance columns are not present at birth, when there is considerable overlap of the cortical innervation from both eyes (Hubel, Weisel, 1963; Hubel *et al.*1977). Thus, cortical inputs must be gradually divided into alternating columns by synaptic rearrangement.

The mechanisms for the elimination of synapses are probably related to the interaction between the axon and its target, and can be explored by interrupting this connection. Competition for trophic factors has been suggested as a mechanism controlling synapse elimination, as has activity (see (Purves, Lichtman, 1980)). A compelling argument for the role of activity is seen in the visual system. Here, unilateral visual deprivation (eg., by occluding one eye), during the

critical period of synapse formation results in errors in the patterns of afferent connections in the tectum, and abnormal pattern of ocular dominance (Weisel, Hubel, 1965).

There have also been many studies on synaptogenesis and the development of appropriate connections at the neuromuscular junction, as it is relatively accessible to study (Redfern, 1970; Brown *et al.*1976; Bennett, Pettigrew, 1974). This has been described previously. Briefly, in adult muscle each muscle fibre is innervated by a single motor axon. In the neonate, there are several axons contacting a single muscle fibre. This has been shown in the rat, where stimulation of the motor nerve in the adult resulted in a single postsynaptic potential, whereas stimulation in the neonate results in several postsynaptic potentials of different strengths (Redfern, 1970; Brown *et al.*1976). It is also seen using histological staining of the motor endplates and counting the number of axons innervating them (Brown *et al.*1976). The elimination of polyneuronal innervation occurs over the first two weeks of postnatal life in the rat.

Synaptogenesis is more difficult to study in the central nervous system. One example of synaptic rearrangement in the CNS is seen in the afferent innervation of Purkinje cells by climbing fibres in the cerebellum of newborn rats. In the adult, there is anatomical and electrophysiological evidence that each Purkinje cell is contacted by only one climbing fibre (Eccles *et al.*1966). However, electrophysiological recordings from neonatal rats suggests that each Purkinje cell is innervated by several climbing fibres, and over the first few postnatal weeks all but one of these inputs are eliminated (Mariani, Changeux, 1981).

Not all vertebrate systems show evidence of synaptic rearrangement during development. In the brachial spinal cord of the bullfrog, the dorsal sensory afferents grow into the ventral horn and arborize before the dendrites of the mo-

toneurones have grown (Jackson, Frank, 1987). These afferents project to the motoneurones innervating specific muscles. Thus, triceps muscle sensory afferents project more to triceps motoneurones (Frank, Westerfield, 1982). However, in most vertebrate nervous systems there is evidence that synapses are rearranged during the developmental period (see (Purves, Lichtman, 1980; Lichtman, Purves, 1980; Purves, 1980)).

By lesioning the spinal cord at different postnatal ages in the rat it is possible to illustrate the maturity of the synaptic connections at these times (see (Steltzner, 1982)). Dorsal root connections appear to be present in the neonatal rat (Gilbert, Steltzner, 1979; Smith, 1983), as are descending connections from the brainstem (Steltzner, 1982), but synaptic remodelling still occurs postnatally. The projection of afferents from the dorsal horn are functionally specific in the adult (Rivero-Melian, Grant, 1990) and these projections appear to develop in a specific way, with different classes of afferents forming terminal arbors in the appropriate laminae (Smith, 1983). There is a proposed chemical affinity between appropriate presynaptic and postsynaptic cells. Trophic factors are also suggested to regulate afferent connectivity during development (see (Barde, 1989)) and in the spinal cord of the adult (Lewin *et al.*1992).

In other systems, such as the visual system, activity may be involved in refining afferent connections. Application of TTX, to block neuromuscular activity, prevents the formation of ocular dominance columns (Reh, Constantine-Paton, 1985), and the adult pattern of connectivity within the retinogeniculate pathway depends on the elimination of functional synapses (Shatz, Kirkwood, 1984). In the neuromuscular system, blockade of neuromuscular transmission arrests the elimination of polyneuronal innervation (Greensmith, Vrbová, 1989; Greensmith, Vrbová, 1991).

The intrinsic connections in the spinal cord of the rat are still immature until

about P15 (Steltzner, 1971; Weber, Steltzner, 1980; Silos-Santiago, Snider, 1992). In preganglionic sympathetic neurons of the spinal cord, the segmental organisation of the inputs to the spinal cord suggests that the rostro-caudal position of the preganglionic cell bodies is a determinant of selective synapse formation (Rubin, Purves, 1980). However, there is considerable evidence of further'fine tuning' of redundant synaptic connections during the early postnatal period (Purves, Lichtman, 1980; Lichtman, Purves, 1980). Synapses may be removed by phagocytosis of synaptic terminal by glia cells (Conradi, Ronnevi, 1975).

The number and position, of direct Ia afferent contacts made onto motoneurones of the adult cat lumbar spinal cord has been studied using intracellular staining of single afferent fibres with HRP (Brown, Fyffe, 1981; Ishizka *et al.*1979). The site of synaptic contact of an afferent bouton has been proposed to influence the excitatory postsynaptic potential (e.p.s.p.) that results (Rall *et al.*1967; Burke *et al.*1979), so the site of contact in the dendritic tree is of importance in dictating their functional effectiveness on the motoneurone. It has been shown that motoneurones receive contact from one collateral of a primary afferent, even though the dendrites of the motoneurones may pass through the areas occupied by other collaterals of the axon (Brown, Fyffe, 1981). Additionally, during the early postnatal period in the rat (P2-3) there is a reduction in the size of the monosynaptic reflex elicited by stimulating dorsal root (Kudo, Yamada, 1987). This may be partly due to a selection and elimination of synapses at some time during development.

1.6.2. Role of afferent inputs in dendritic modelling

The three-dimensional architecture of a motoneurone is partly influenced by the location of synapses on the cell (Rall *et al.*1967) and the direction from which these afferent axons approach the motoneurone within the spinal cord (Cullheim *et al.*1987b; Vaughn *et al.*1988). There is a proposed correlation be-

tween the complexity of the dendritic tree of a neurone and the number of synapses forming on that cell, and dendrites may exist to create distinct spatial domains which act to minimise competition between different afferent axons (see (Purves, Lichtman, 1980)).

The importance of synaptogenesis in influencing dendrites varies in different regions in the nervous system. This question has been studied in the cerebellar cortex, by looking at the growth of dendritic trees following irradiation (Berry, Bradley, 1976b). Irradiation deprives the Purkinje cells of specific afferent connections from granule and stellate cells. The resulting dendritic trees are of a smaller size, the branch length of distal dendrites is increased and covered with abnormally long spines (Chen, Hillman, 1982). Trichotomous branching is observed, as well as an increase in the incidence of collateral branching (Berry, Bradley, 1976b).

Vaughn and colleagues, (Vaughn *et al.*1974; Vaughn, 1989) have proposed that the site and frequency of synapse formation on the dendritic growth cones and filopodia, determines the path of dendritic growth as well as the segment length, order of branching and general architecture of the dendritic tree. The branching structure is influenced by local differences in synaptogenesis, that may result in a predominant direction of growth of the dendrites. This has also been observed in the prenatal development of the dendritic tree of spinal motoneurones in the mouse (Vaughn *et al.*1988). Here, the dendritic lengths and branch densities of motoneurones at E13-14 are greater for marginal zone dendrites, at a time when the majority of synapses are within the marginal zone of the spinal cord. Later, at P0 when the synapses are also within the intermediate zone, there is no difference in the branching. Another example is seen in the retina, where it has been shown that dendrites of retinal ganglion cells grow preferentially towards an area that has been depleted of ganglion cells, and therefore of dendrites (Perry, Linden, 1982). It is suggested that the dendrites compete with

each other for afferents during development.

The postsynaptic site of contact between the afferent axon and its target is proposed to be the dendritic 'spine' (Vaughn *et al.*1974; Skoff, Hamburger, 1974). There is certainly a developmental loss of these processes in many areas of the nervous system, that occurs in parallel with the events of synapse elimination (Cummings, Steltzner, 1984; Lau *et al.*1991; Wong *et al.*1992; Mates, Lund, 1982; Morest, 1968; Berry, Bradley, 1976b; Ramoa *et al.*1988; Henkel, Brunso-Bechtold, 1991).

1.6.3. Interaction of neurones and their afferents

Synapses on the soma and proximal dendrites generate larger amplitude and shorter latency e.p.s.p.s than those on more distal dendrites (Rall *et al.*1967). After injury, the amplitude of the e.p.s.p. reduces and the latency increases (Kuno, Llinas, 1970a; Eccles *et al.*1958). It is possible that this is partly due to a loss of the proximal synapses onto the cell (Mendell *et al.*1976). As the number of afferent synapses decreases following axotomy, the e.p.s.p. rise time slows (Mendell *et al.*1976).

Injury to the peripheral nerve results in death of up to 30-60% of cells in the dorsal root ganglion (Risling *et al.*1983b; Arvidsson *et al.*1986a; Ygge, 1989; Bondok, Sansone, 1984). Injury to the neonate results in a greater amount of cell death (Himes, Tessler, 1989; Aldskoguis, Risling, 1981), but immature neurones seem to have a greater capacity to reorganise themselves anatomically and recover their function than adult neurones (Himes, Tessler, 1989; Bregman, Goldberger, 1982). There is transganglionic death of cells in the dorsal horn after injury to the peripheral nerve in the rat (Grant, Ygge, 1981; Arvidsson *et al.*1986a; Aldskoguis *et al.*1985). However, not all of the cells die. Some damaged cells respond to the injury by sprouting axons into areas that are not normally occupied, as well as occupying sites that are vacated due to death of

other cells. After partial denervation of cat spinal nerves the intact roots sprout into adjacent vacated area (Goldberger, Murray, 1982). There is some reorganisation of the synapses in the dorsal horn following injury in the adult (Shortland, Woolf, 1993; Linda *et al.*1990b) and it is possible that the amount of plasticity and sprouting is greatest in those neurones that survive after injury that results in the greatest amount of cell death.

The synaptic input onto a motoneurone changes as a result of axotomy and damage to its afferents (Linda *et al.*1990a; Clowry *et al.*1991; Mendell *et al.*1976). This can result in changes in the dendritic morphology of the efferent motoneurones (Yawo, 1987). In the rat spinal cord, following deafferentation there is an increase in the diameter of the dendrites and some dendritic branching (Bernstein, Standler, 1983). The response of different regions of the cell may vary; in some areas there may be dendritic expansion and in others, retraction and so a change in the overall orientation of the dendrites of the cell may result.

These events occur over a relatively short period of time, though effects may be long-lasting if reinnervation is prevented. The motoneurone itself also responds to the axotomy by undergoing a series of morphological and electrophysiological changes elicited by the interruption of connections with its target.

1.7. Cellular responses to axonal injury

1.7.1. Response of the soma to injury

Separation of an axon from its cell body, in vertebrate PNS neurones, leads to Wallerian degeneration of the distal portion of the nerve (West, Collins, 1991), and a series of morphological changes to the proximal portion and cell body of the neurone (Lieberman, 1971; Watson, 1974). The most striking changes are seen in the endoplasmic reticulum (Nissl substance), which occur 24 hours after injury, and continue for 2-3 days. This was first described by Nissl (Nissl, 1892),

as a disintegration and redistribution of the Nissl substance, and later termed chromatolysis. Nissl bodies are observed to break up into many small aggregates of polyribosomes and within these aggregates, RER is not arranged as stacks, but exists as small fragments (Johnson, Sears, 1989b). The chromatolytic reaction appears to start in the centre of the soma, and to spread to the periphery and the dendrites later (Barron *et al.*1971). It has been suggested that it is only in those cells that are degenerating that the Nissl substance disappears altogether, and that in regenerating cells, which later reinnervate their target, it becomes granular and is limited to the periphery of the soma (Lieberman, 1971). Since the disorganisation of the Nissl substance involves a decrease in the ratio of RER to polyribosomes, this could reflect the reorganisation of the protein synthetic 'machinery' of the motoneurones, from transmission to growth (Grafstein, McQuarrie, 1979) for the production of neurofilament and other proteins that are up-regulated after axotomy (Price, Porter, 1972).

Soon after injury the cell body is seen to swell considerably (Watson, 1974). Cellular enlargement is most striking after injury that results in cell death (Murphey *et al.*1990). This response is partly caused by water uptake by the cell due to its increased osmolarity (LaVelle, Sechrist, 1970). This is probably partly as a result of increased protein synthesis in the soma and dendrites in response to injury. Later on after injury, swelling occurs due to a proliferation in the number of cell organelles, RNA and other proteins (Watson, 1972; Watson, 1974; Price, Porter, 1972). Some studies report that after a period following permanent axotomy the soma returns to its normal size (Brannstrom *et al.*1992a) and in others there is no change observed (Delgado-Garcia *et al.*1988). It is worth mentioning that not all neurones respond in the same way. Following axotomy of the trochlear nerve in adult cats, the soma initially undergoes hypotrophy, then gradually increases in size when contact with the target is regained (Murphey *et al.*1990).

There is some evidence of an increase in the number of lysosomes following axotomy (Hudson *et al.*1961), as well as an increase in the size of the lysosomes (Barron, Tuncbay, 1964). Lysosomal activity remains especially elevated in those cells that do not recover from axotomy and fail to reinnervate their targets (Barron, Tuncbay, 1964). The response of lysosomes is anabolic, and may be related to the production of phosphates for increased protein synthesis (Barron *et al.*1966).

Another response to injury is seen in the changes in the nucleus. This is often seen to become eccentric and swelling may also be observed (LaVelle, Sechrist, 1970). The reason for this eccentricity is unclear, though it may be due to changes in axoplasmic flow within the cell (Lieberman, 1971). Additionally, the volume of the nucleus appears to increase slightly immediately after axotomy (Barr, Hamilton, 1948), and later to decrease if reinnervation does not occur (Cavanaugh, 1951). There may also be an increase in the size of the nucleolus (Watson, 1965). These changes in nucleolar volume may be up to two times the normal size (Murray, Grafstein, 1969) and may be due to an increase in the RNA and protein content of the nucleolus and to an increase in synthesis (Watson, 1965). This increase in synthesis may also be accompanied by the appearance of vacuoles within the nucleolus (Lindsay, Barr, 1955).

Cytoskeletal proteins also change in response to injury. There is an increase in the production of neurofilaments and neurotubules in the soma of frog ventral horn motoneurones after injury (Price, Porter, 1972). These may be synthesized in the free polyribosomes which are prominent during chromatolysis. This increase in the production of protein may be in response to the loss of part of the cell by axotomy, and also may be an effort to regrow an axon to re-establish connection with the target.

After axotomy of cholinergic neurones, there are changes in the activity of sev-

eral enzymes. There is a decrease in the amount of AChE (Barron *et al.*1971; Engel, Kreutzberg, 1986) and ChAT (Watson, 1974). The developmental up-regulation of the ChAT is delayed if functional connections between nerve and muscle are interrupted during the early postnatal period (Greensmith, Vrbová, 1990). The enzyme is expressed when the connections are reestablished (Engel *et al.*1988).

Respiratory and metabolic enzymes, as well as mitochondria, undergo change after axotomy. Mitochondria are reported to swell and hypertrophy. The increase in size is due to an increase in the number, and density, of the crista (Barron *et al.*1971). However, there is an observed decrease in the expression of the enzyme cytochrome oxidase (CO) following injury (Wong-Riley, 1989). This is the terminal enzyme in the electron transport chain, and is found on the inner mitochondrial membrane of all eukaryotes. Levels of CO activity within neurones positively correlates with the activity of the cell (Wong-Riley, 1979). Reduced afferent activity results in a reduction in the levels of CO ((Wong-Riley *et al.*1978), in the auditory system; (Hevner, Wong-Riley, 1990), in the visual cortex). It appears that inhibiting the transmission of the neurone reduces its metabolic activity and results in a reduction in CO. There is also evidence that cells that express CO in the retina may be more resistant to injury than others that do not (von Bussmann *et al.*1993), perhaps indicating that the ability of a cell to survive, and regenerate its axon after injury is related to its metabolic state.

A reflection of the increase in protein synthesis and metabolic state of motoneurones after injury, is seen in the use of glucose. There is an increase in the use of glucose in the hypoglossal nucleus of the rat following injury (Singer, Mehler, 1980). This could be due to the regenerative synthetic activity of the motoneurone in the production of proteins, RNA and lipids after axotomy. It is also possible that it reflects increase in electrical activity at the site of transection

(Singer, Mehler, 1983).

1.7.2. Response of microglia

Microglial cells are present near motoneurones reacting to axotomy, and it is suggested that they respond when a motoneurone is disconnected from its target (Watson, 1974). Perry and colleagues (Perry *et al.*1985), showed that microglia divide from macrophages which invade the developing brain to differentiate into mature, resting microglia. They suggested that the microglia are phagocytic and respond to the production of cellular debris during development. There have been numerous reports of the incidence of microglia in areas of the developing brain (Perry *et al.*1985; Innoceti *et al.*1983; Ling, TAn, 1974; Murabe, Samo, 1982; Valentino, Jones, 1982; Ashwell, 1991). Microglia have also been reported to appear in response to injury (Sumner, Sunderland, 1973). The process of the inflammatory reaction after injury could be triggered through the induction of the expression of major histocompatibility complex (MHC) antigens. This has been seen in the visual system after eye enucleation (Rao, Lund, 1989) and in the lumbar spinal cord of adult (Maehlen *et al.*1989) and neonatal rats (Greensmith, Navarrete, 1991) where an up-regulation in MHC expression is observed after injury.

Microglia are also present in diseased nervous tissue (Giulian, Robertson, 1990), after ischemic injury; (McGreer *et al.*1987), in Alzheimer's disease). It is possible that microglia release cytotoxic agents, including free radicals (Giulian, Baker, 1986). Giulian and colleagues (Giulian *et al.*1993) have proposed that the neurotoxins released by microglia act in a way similar to glutamate-induced neurotoxicity and that the action of microglia might partly account for the inability of CNS neurons to recover after injury.

Astrocytes become reactive following injury and may wrap around the regenerating neurones (Tetzlaff *et al.*1988). This is a long-lasting response, and may be

partly responsible for the redistribution of the synapses on the cell (Lux, Schubert, 1975).

1.7.3. Effect of injury in the adult

Injury to peripheral nerves in the adult does not inevitably lead to death of the parent cell body, whilst injury to nerves in the CNS often does. The response of cells which will eventually reinnervate their target is different to those that do not; these cells are destined to die ((Kashihara *et al.*1987) see (Lieberman, 1971)). The site and severity of the injury inflicted, as well as the type of neurone and species of animal, will also influence the amount of cell death or reinnervation that follows (Watson, 1974; Murphey *et al.*1990; Brown, Butler, 1976; Bowe *et al.*1989). The most pronounced reactions occur after proximal the injury to the axon, especially if reinnervation is prevented (see (Lieberman, 1974a; Lowrie, Vrbová, 1992)). A crush injury results in more complete recovery than nerve section (Brown, Butler, 1976), although there is often failure to restore normal function fully (Gordon, 1988).

The ability of a neuron to reinnervate its target depends on its ability to regrow an axon. Following axotomy, the diameter of the axon proximal to the cut, has been shown to decrease due to a reduction in the transport of neurofilaments to the axon and neurofilament gene expression within the soma (Murphey *et al.*1990; Hoffman *et al.*1987; Cragg, Thomas, 1961). Since the diameter of the axon affects its conduction velocity (Kernell, Zwaagstra, 1981; Cullheim, 1978), after axotomy there is a reduction in conduction velocity of up to 40% in cat spinal alpha-motoneurones (Kuno *et al.*1974; Cragg, Thomas, 1961). This is an especially fast response in large diameter axons with a large neurofilament content (see (Titmus, Faber, 1990)), which respond by shrinking the diameter of the axon. The conduction velocity in regenerating dorsal root axons a few days after injury is reduced (Feasby *et al.*1981). Reports indicate that conduction velocity returns to normal when the axon reinnervates the muscle (Foehring *et*

*al.*1986), and conversely, that if reinnervation is prevented the changes in conduction velocity are more permanent (Sanders, Whitteridge, 1946). There is evidence that the diameter of the axon increases during the first few months following injury, after which it becomes smaller than is normal (Murphey *et al.*1990). It is clear that the type of lesion and the ability of the axons to regenerate is important, as well as the time after injury that the observation is made. The diameter of the axon and its conduction velocity return to normal upon reinnervation of the target. Myelination of the regrowing axons does occur. This is fastest after crush injury, where intact Schwann cell tubes and basal lamina provide guidance for regenerating sprouts (Risling *et al.*1984).

Neurons may respond to injury by 'sprouting' of supernumerary axons (Ramon y Cajal, 1929; Havton, Kellerth, 1987). Axons sprout to regenerate and reinnervate the target in response to injury and the number of sprouts that remain after reinnervating the muscle is determined by the availability of synaptic sites (Murphey *et al.*1990). Growth occurs through the proximal stump, and results in the re-matching of the axon with its target, and the restoration of function. There may also be growth of 'supernumerary' axons from the soma or even dendrites, which have different trajectories from the original primary axon. Many anomalous projections may result (Havton, Kellerth, 1987). The axons may themselves have collateral branches or even arise from dendrites as myelinated 'dendraxons' of uniform diameter (Havton, Kellerth, 1987; Linda *et al.*1985; Hall *et al.*1989; Hall, Cohen, 1988), and which have cytoskeletal structures dominated by neurofilament. In some cases they may be still apposed by synaptic boutons (Hall *et al.*1989).

Collateral sprouts grow in response to partial or complete denervation of the target and originate from an intact axon. These sprouts may innervate the site vacated by the damaged primary axons before these axons can themselves grow (Seil, 1988). In cases where reinnervation of the primary axon is pre-

vented, these axons may maintain contact between the neurone and its target. However, when the primary axons do eventually reach the target they will displace the collateral sprouts (Jackson, Diamond, 1981).

Recurrent axon collaterals found in some motoneurones, such as medial gastrocnemius of the cat, respond to axotomy by retracting soon after injury if reinnervation is prevented (Havton, Kellerth, 1990b) whilst other axon-like processes grow out of the cell body (Havton, Kellerth, 1987). There is evidence that the collaterals with proximal origins are preferentially eliminated, and it is suggested that these axons are lost as they are making monosynaptic contact with neurones that are also axotomised. However, no histological evidence was found of degeneration of these collaterals, despite the fact that they are gradually lost (Havton, Kellerth, 1990b). It therefore appears that axotomy causes both degenerative and regenerative axonal responses. Despite the reduction in the number of recurrent axon collaterals (Havton, Kellerth, 1989), no changes in the amount of recurrent inhibition was found 12 weeks postoperatively (Havton, Kellerth, 1984), despite a transient reduction at 3 weeks (Havton, Kellerth, 1990a). This suggests that there are changes in the recurrent inhibitory pathways of the injured motoneurones and of the intact synergists (Havton, Kellerth, 1990a). A few supernumerary axons do grow from the soma of injured cells to the region of lamina VII after proximal injury, where they may innervate Renshaw cells (Havton, Kellerth, 1987). There is also a change in the activity pattern of the Renshaw cells themselves. This will lead to alteration in the balance of inhibition on to the motoneurones (Renshaw, 1946; Ryall, Piercy, 1971). Some axon collaterals are normally seen to make direct contact with other motoneurones (Cullheim *et al.*1977; Cullheim *et al.*1984) and since these are eliminated there may be a reduction in the excitatory input to the cells and a shift in the reflex balance towards inhibition. There may also be changes in the afferent inputs from other sources onto the motoneurones.

The dendritic tree also responds to the injury inflicted on the neurone. The dendrites have been reported to retract, shrink or degenerate following axotomy ((Cerf, Chako, 1958) in the frog, (Grant, 1965; Grant, Westman, 1968) in the kitten, (Sumner, Watson, 1971; Sumner, Sunderland, 1973) in the rat). This effect is reversible following reinnervation, which suggests that loss of neuromuscular contact is deleterious to the cell (Sumner, Watson, 1971). The response of the primary dendrites appears to be a little different. There is evidence that after long periods following injury and reinnervation, primary dendrites remain larger than normal (Bowe *et al.*1992) and that sprouting may occur. There is evidence in the lamprey, that the site of the lesion influences the amount and site of sprouting that occurs. Thus, a proximal lesion will produce profuse sprouting from the dendritic tips in the short-term, whereas more distal lesion result in less sprouting from the dendrites and more profuse sprouting from the axonal stump, although total amounts of sprouting remain constant (Hall, Cohen, 1988). After a longer period, when reinnervation has occurred, the cell responds by retracting these sprouts (Hall, Cohen, 1988). Other studies report that there is a decrease in the diameter of primary dendrites following axotomy (Brannstrom *et al.*1992a), and that the loss of dendritic territory occurs in the preterminal and terminal segments. There is a reported 30% loss in the total membrane area of the cells, although the relationship between the primary dendrite diameter and the total dendritic size remained unchanged. When reinnervation is allowed, the membrane area returns to normal, but combined dendritic length and number of dendritic terminals remains 25% below normal (Brannstrom *et al.*1992b). The appearance of the dendrites is also seen to change, often reported as looking 'beaded' (Lagerback, Ulfhake, 1987). These varicosities are found mostly on the distal segments of the dendrites (Ulfhake, Kellerth, 1981; Grant, 1975; Becker, Cook, 1990). Beads are also a feature of developing motoneurones but in this case they are more probably large growth-cone-like structures ((Ulfhake, Cullheim, 1988b) and present study).

The appearance of abnormally long spine-like appendages is sometimes observed following axotomy in the adult. It has been described in the vagal motor nucleus of the guinea pig (Engel, Kreutzberg, 1988), as have flaps and protrusions of stacks composed of thin, elongated lamellipodia, some of which appear to have the ultrastructure of growth cones. These grow form the soma and dendrites. These authors suggest that spine-like protrusions may represent a plastic area on the surface of the cell which is able to respond dynamically to insult with an increase in the synthesis of cytoskeletal proteins.

With such dramatic morphological changes occurring, it is no surprise that there are also changes in excitability following axotomy, although the response of different types of neurones varies. Sodium channels, which are normally concentrated at the nodes of Ranvier (Waxman, Foster, 1980), become more evenly distributed along the nerve, a situation that is reminiscent of the developing axon prior to myelination (Black *et al.*1982). Sodium channels that are normally in the initial segment of the axon, spread to the soma following injury (Eccles *et al.*1958; Titmus *et al.*1986). Smaller neurones have a lower threshold for excitation and a more sustained discharge than larger neurones (Henneman, 1979) although the function of a motoneurone is also related to resistivity and geometry (Gustafsson, Pinter, 1984). In the majority of neurones there is an increase in the input resistance after injury (eg. (Gustafsson, 1979)), but this is by no means a universal response to injury (see (Titmus, Faber, 1990)). This may be the result of an increase in the specific membrane resistivity, due to a decrease in the motoneurone surface area and a change in the dendritic geometry, most notably a simplification of the dendritic architecture (Gustafsson, Pinter, 1984). There is also an overall decrease in the amount of recorded motor activity following injury (Gordon *et al.*1980). There is an increase in the duration of the afterhyperpolarization of the action potential (Gustafsson, Pinter, 1984) and some afferent inputs onto the cells may be lost (Mendell *et al.*1974; Sumner, 1975). Presynaptic boutons are lost from the surface of the neurone over the

period following axotomy, but not uniformly from the soma and dendrites (Sumner, Sunderland, 1973). These will return to normal unless reinnervation is prevented (Sumner, Sunderland, 1973). In cat motoneurones there is also a change in the membrane excitability of both soma and dendrites and the appearance of dendritic membrane potentials (Kuno, Llinas, 1970b) immediately after injury. This is also seen in the goldfish Mauthner cells (Faber, Zottoli, 1981) and is believed to be due to the insertion of sodium channels into the proximal dendritic region.

If reinnervation is prevented there is a very different response of the cell that in severe cases may lead to death of the neurone (Sumner, 1976; Brannstrom *et al.*1992a). Even after the axons have been able to reinnervate their targets there may still be long-term effects of injury to the nerve (Bowe *et al.*1989; Bowe *et al.*1992; Brannstrom *et al.*1992a; Brannstrom *et al.*1992b). This is not due to cell loss, but to a change in the axon and/or target following injury (Bowe *et al.*1989). In fact, changes in size of reinnervated motoneurones are not evident until sometime after injury (5-10 months in rat spinal motoneurones (Bowe *et al.*1992)), and show that the motoneurones have a delayed and progressive response after successful reinnervating their targets. In reinnervated sciatic motoneurones in the rat, the soma size and diameter of the primary dendrites was found to be larger on the ipsilateral side than in control age-matched animals.

Adult motoneurones depend on their contact with the target muscle for survival, but as long as it is possible to reestablish contact following axotomy most cells will survive and the chromatolytic reaction will be reversed (Lieberman, 1971). However, disruption of the interaction of the nerve and the muscle during the critical period of neonatal development will invariably result in the death of the motoneurone, and ultimately atrophy of the target muscle (Romanes, 1946a; Lowrie *et al.*1987).

1.7.4. Effect of injury during development

Generally, early postnatal motoneurones degenerate in response to injury, often not displaying the classical chromatolytic reactions described by Nissl ((Nissl, 1892) and see (LaVelle, LaVelle, 1958)). Romanes (Romanes, 1946b), observed that many motoneurones die following sciatic nerve crush in young mice, and it is generally accepted that injury to neurones in newborn animals produces greater retrograde death than in adults (Aldskoguis, Risling, 1981).

The recovery of postnatal neurones following injury varies with the severity of the injury inflicted. Thus, after crush injury to the sciatic nerve of the rat, 60-70% of motoneurones die (Lowrie *et al.*1987). Additionally, there is a critical period in development when the motoneurones are especially sensitive to disruption of connections with the target; in the rat this is between birth and P6 (Lowrie *et al.*1987; Navarrete, Vrbová, 1984; Kashihara *et al.*1987). There may be some, or even complete functional recovery, though there is also a difference in the response of slow and fast muscles (Zelena, Hnìk, 1960; Lowrie *et al.*1982; Navarrete, Vrbová, 1984; Kashihara *et al.*1987). The long term effects of injury at birth are especially evident in the fast muscle, which develops a more tonic firing pattern characteristic of slow muscle. There is also an increase in fatigue resistance and activity of oxidative enzymes in the muscle, even in the absence of motoneuronal cell death (Lowrie *et al.*1982; Navarrete, Vrbová, 1984). This is due to an increase in the muscle activity (Navarrete, Vrbová, 1984). Such an effect is not seen if injury is at an older age (Lowrie *et al.*1987). In this situation the axons do reinnervate the appropriate muscle, and the degree of motoneuronal death does not differ between the slow and fast muscles studies (Lowrie *et al.*1987). However, the response to injury does. There is a reduction in the size of the fast motoneurones (Lowrie *et al.*1987) which may account for their higher excitability (Navarrete, Vrbová, 1984) and the change in activity pattern.

Following neonatal nerve injury, sensory afferent fibres expand their territory (Fitzgerald, 1985b) and as synaptogenesis is still occurring during this period (Steltzner, 1982) the motoneurones that are regenerating may preferentially receive these afferent synaptic contacts. As many of the inputs onto the motoneurones are from interneurones this may explain the effects on the polysynaptic reflexes (Navarrete *et al.*1986; Navarrete *et al.*1990). Injury to the sciatic nerve in early postnatal rats results in an enhancement of the reflex response evoked from the contralateral afferents, which results in inappropriate activation during locomotion (Navarrete, Vrbová, 1984; Vejsada *et al.*1991) and to a permanent increase in the reflex response from reinnervated fast muscles (Navarrete *et al.*1990).

The morphological changes that occur in a neonatal neurone are not totally dissimilar to what has already been described in the adult. The major difference is that the majority of neonatal neurones do not survive injury during this critical period, and therefore there is atrophy and eventual death of the cell. In the kitten, section of the sciatic nerve leads to degeneration of the soma, dendrites and axon of the cell (Grant, 1975; Grant, 1968). The dendrites often appear beaded, or fragmented and contained large mitochondria (Grant, 1965). If the motoneurone survives to adulthood, long-term morphological changes are observed. In the rat, the dendritic tree of hindlimb motoneurones was seen to be larger at P14, following nerve crush at birth, but after this grew more slowly (O'Hanlon, Lowrie, 1993a). Since there is a reduction in the branching density of dendrites in the adult motoneurones after injury, this suggests that the reduction is due to a failure to grow, rather than retraction of dendrites that already exist. Other effects of neonatal injury will be addressed in Chapter 3.

Therefore, it appears that the changes that occur in neonatal motoneurones in response to injury are a result of the immature state of the nerve cell, its morphology and of its synaptic connections.

In conclusion, the interaction of the motoneurone and its target is of vital importance in allowing normal postnatal maturation of the motoneurone and of the motor function. Disruption of this contact results in death of many neurones both in the neonate and in the adult. In the process of 'dying' the motoneurone undergoes changes in size and of morphology and orientation of its dendrites as well as metabolic and biochemical changes. The afferent inputs onto the motoneurone are involved in the formation of the 3-dimensional structure of the cell, and its excitability. Their removal, therefore, results in changes in the morphology and architecture of the cells.

2. MORPHOLOGICAL DEVELOPMENT OF EARLY POSTNATAL FLEXOR MOTONEURONES IN THE RAT

2.1. INTRODUCTION

The adult motoneurone comprises of a cell body, containing the majority of the organelles of the cell, the axon, which is specialised for the conduction of electrical activity by action potentials over long distances, nerve terminals which are specialised for neurotransmitter release and the dendrites, where most of the synaptic inputs onto the motoneurones impinge. Motoneurones receive and integrate a variety of synaptic inputs, and the morphology of the cell influences the functional effectiveness of these inputs. The geometry of the dendrites can modify the spread of current from different regions of the dendritic tree to the soma (Rall *et al.*1967) and the current flow at the initial segment determines the generation of the impulse that eventually elicits muscle contraction. The dendrites occupy over 95% of the total membrane area of the motoneurones (Cullheim *et al.*1987b) and 75% of the volume, extending hundreds of microns away from the soma (Ulfhake, Kellerth, 1981). They receive several thousands of synaptic contacts from different types of afferent inputs, both excitatory and inhibitory. The position of the dendrites within three-dimensional space and their conducting properties, as well as the position of the synapses on the dendrites themselves, influence the resulting e.p.s.p. recorded at the soma (Rall *et al.*1967). Thus, a knowledge of the morphology of the motoneurone is important for the understanding of its function.

2.1.1. Morphology of adult motoneurones

Numerous studies on the morphology of motoneurones have revealed that there are relationships between various parameters of the soma, the dendrites of the cell and the conduction velocity of the axon (Burke *et al.*1982; Zwaagstra, Kernell, 1981; Cullheim, Ulfhake, 1979b; Ulfhake, Cullheim, 1981; Cullheim,

1978; Cameron *et al.*1988). The α-motoneurone of the cat has been studied using retrograde labelling with HRP and shows that there is a positive correlation between the conduction velocity of the axon, the mean diameter of the soma and the diameter of the axon (Cullheim, 1978). The mean diameter of the soma is correlated to both the mean and combined diameter of the primary dendrites (Ulfhake, Kellerth, 1981), and the diameter of primary dendrites is positively correlated with the combined length of the entire dendrite, the number of dendritic branch points and the number of dendritic terminations. Similar correlations have been observed in phrenic motoneurones of the cat (Cameron *et al.*1988). A strong correlation was found for the diameter of the primary dendrites and the combined dendritic length, number of terminal branches, dendritic surface area and volume.

There is evidence that the dendritic organisation of motoneurones may differ according to the function of the muscles that they innervate. The recruitment of motor units during the performance of different motor tasks reflects the metabolic demands of the muscle fibres (Burke, 1981), slow motor units usually being recruited before fast. The factors that determine which motor units are recruited first may depend on their synaptic input and on the geometry of the motoneurone, its size and the electrical properties of its membrane (Henneman, 1957). The excitability of flexor motoneurones has been shown to vary inversely with size (Henneman, 1957; Henneman *et al.*1965). Reconstructions of motoneurones innervating slow and fast motor units have been compared (Cullheim *et al.*1987a; Cullheim *et al.*1987b; Zwaagstra, Kernell, 1981; Burke *et al.*1982). These comparisons show that both the cell body and the dendritic tree of motoneurones to fast muscles are larger and more complex than those innervating slow motor units. In cat triceps surae motoneurones the average total membrane area of motoneurones of slow motor units was 22% smaller than that of fast (Cullheim *et al.*1987a). Additionally, the branching structure of 'slow' motoneurones was less complex and more radial than that of 'fast' mo-

toneurones. The smaller size of slow motoneurones and their smaller input resistance (Kernell, Zwaagstra, 1981; Ulfhake, Kellerth, 1984) may partially account for the differences in recruitment order of these two types of motoneurone (Henneman, 1957).

A study of the spatial distribution of the dendrites of cat motoneurones showed that there was little difference in the way in which the dendrites of fast and slow motoneurones occupy three-dimensional space (Cullheim *et al.*1987b). The mediolateral and rostrocaudal axes to the soma are more extensively invaded than dorsal and ventral areas. The span of the dendritic territory gives an indication of the region within which the dendrites can receive synaptic inputs. The probability of synaptic contacts occurring within a given area depends partly on the local density of postsynaptic membrane. Highly branched, relatively thin dendrites offer a large surface area for the reception of synaptic inputs. Other factors, such as metabolic and cytoskeletal constraints also dictate the formation of dendritic structure, but dendrites probably project preferentially into areas containing an abundance of synaptic inputs. Motoneurones in the ventral horn of the spinal cord form synaptic contacts with sensory afferents (Brown, Fyffe, 1981) which approach from a dorsomedial direction. In addition, motoneurones form contacts with systems of afferents descending from the brain. These include the serotonergic (Holstege, Kuypers, 1987a; Ulfhake *et al.*1978) and noradrenergic (Stevens *et al.*1985) systems in the ventrolateral part of the spinal cord. The shape of the dendritic tree in other neuronal systems (eg cerebellar Purkinje cells (Berry, Bradley, 1976b; Berry, Bradley, 1976a)) are asymmetrical and have a polarised structure due to the spatial position of afferent projections. It has been suggested that the spatial pattern of dendritic trees of motoneurones may be influenced by their afferent inputs (Vaughn *et al.*1988).

There is evidence for direct interaction between spinal motoneurones which possibly account for the formation of dendritic 'bundles (Scheibel, Scheibel,

1970). This is particularly prominent in the phrenic nucleus (Cameron *et al.*1983). The presence of gap junctions has been reported in other spinal nuclei that form bundles (Matsumoto *et al.*1989) and these bundle formations could be related to cell-cell interactions in the control of patterned activity (Scheibel, Scheibel, 1971).

The anatomical constraints of the structures within which neurones lie also dictates the pattern of dendritic form. Subcortical structures impose anatomical limits on the shape of the dendritic tree of cortical neurones (Yelnik *et al.*1984). The morphology of a motoneurone is influenced by its position within the grey matter of the spinal cord. The dendrites of motoneurones situated medially within the cat lumbosac ral spinal cord project radially around the soma (Cullheim *et al.*1987b; Ulfhake, Kellerth, 1981; Brown, Fyffe, 1981), whereas those situated more laterally lack dendrites projecting ventrally and extend around the perimeter of the grey matter.

2.1.2. Postnatal development of motoneurones

Use of retrograde dyes such as HRP, has allowed the structure of identified populations of developing motoneurones to be studied. In phrenic motoneurones the mean surface area of the soma increased 2.5 times during the postnatal period, and this change was correlated to changes in the mean conduction velocity of the axon (Cameron *et al.*1990). A similar correlation was found for lumbosaccral motoneurones of the cat during development (Cullheim, Ulfhake, 1979a). Growth was also shown in developing postnatal motoneurones innervating gastrocnemius muscles of the cat (Cameron, Fang, 1989) and shows that the volume of the soma increases from birth until adult.

The postnatal development of cat hindlimb motoneurones has been studied in great detail (Ulfhake *et al.*1988; Ulfhake, Cullheim, 1988b; Ulfhake, Cullheim, 1988a). These authors report that there is growth of the soma and dendrites during postnatal development. The territory of the dendrites increased in paral-

lel with the overall growth of the spinal cord, resulting in preferential growth of rostrocaudally projecting dendrites. A similar pattern of growth was observed in phrenic motoneurones (Cameron *et al.*1991). The size of the dendritic fields in the rostrocaudal plane was also greater. The increases in the lengths of dendritic branches was not uniform, but mostly occurred in the terminal branches. There was about a 400% increase in the total membrane area and 100% increase in soma area of motoneurones innervating triceps surae motoneurones during postnatal development (Ulfhake, Cullheim, 1988a).

Studies using the Golgi technique indicate that there are changes in the size, complexity and orientation of motoneurone dendritic trees during prenatal and postnatal development (Scheibel, Scheibel, 1970; Scheibel *et al.*1973; Cummings, Steltzner, 1984; Bellinger, Anderson, 1987a; Bellinger, Anderson, 1987b). The maturation of the somatodendritic surface of Lamina IX neurones in the rat thoracic spinal cord (Cummings, Steltzner, 1984) has been described. Spine-like structures and growth cones are present in all parts of the motoneurones until P5. There is then a reduction in the growth associated processes on proximal dendrites, but they still remain in more distal parts of the cell. The adult morphology, which is devoid of these processes, is attained after the third postnatal week. In the brain stem of the cat, spine-like structures are eliminated from the surface of motoneurones during the first months of postnatal life (Scheibel *et al.*1973).

The formation of dendritic bundles during postnatal development has been described in spinal motoneurones of the cat (Scheibel, Scheibel, 1970), where they were proposed to play a role in the development of reciprocal activation of antagonist muscles (Scheibel, Scheibel, 1971). In the lumbosacral spinal cord of the rat, the postnatal development of dendritic bundles has been described in the ventrolateral (Bellinger, Anderson, 1987a) and the ventromedial cell columns (Bellinger, Anderson, 1987b), where they may integrate autonomic inputs. In these motoneurones the most extensive dendritic growth was during

the postnatal period; dendritic bundles appear later. This suggests that bundles form by a redirection of existing dendrites, rather than the outgrowth of new branches. Growth associated, spine-like processes were eliminated from the surface of the motoneurones in the first two postnatal weeks, during which time the dendrites increased in length and reorganised into bundles. Using retrograde labelling with cholera toxin the development of motoneurones from two specific motor pools innervating hindlimb muscles has recently been studied in the rat (Westerga, Gramsbergen, 1992). This study showed that bundling only occurred in motoneurones innervating the tonically active soleus muscle, and not from the phasically active tibialis anterior muscles. These authors also found that the formation of dendritic bundles coincided with the maturation of locomotion (Altman, Sundarshan, 1975; Westerga, Gramsbergen, 1990).

In developing cat hindlimb motoneurones (Ulfhake, Cullheim, 1988a), growth associated processes are gradually eliminated from the surface of the cells. The presence of these processes can be used to provide an indication of the maturity of the motoneurones. Motoneurones innervating the short plantar muscles of the foot showed less mature characteristics at birth than those innervating the triceps surae muscles (Ulfhake, Cullheim, 1988b). The postnatal development of the sizes of motoneurones innervating fast and slow twitch muscles was examined in the cat (Sato *et al.*1977). This study suggests that motoneurones innervating fast muscles may attain adult morphology before slow motoneurones. Motoneurones at different levels of the spinal cord have been shown to reach their adult soma areas in a rostrocaudal sequence (Cameron *et al.*1989). It does appear that dendritic maturation is completed at different times in different motor pools.

In the rat, locomotor function develops during the first three postnatal weeks (Altman, Sundarshan, 1975). There are changes in the intrinsic electrophysiological properties of flexor and extensor motoneurones during this period (Navarrete *et al.*1988a; Navarrete *et al.*1988b; Walton, Navarrete, 1991). This is

the time when distinct differences in the activity patterns of slow extensor and fast flexor muscles appear (Navarrete, Vrbová, 1983) and the adult phasic firing pattern of fast muscles develops.

This chapter is a study of the early postnatal changes in the somatodendritic structure of identified hindlimb ankle flexor motoneurones in the rat using intracellular injection of Lucifer Yellow in an *in vitro* hemisected spinal cord preparation. Qualitative and quantitative analyses were carried out on images obtained using a confocal microscope. These results have been presented as a paper (Dekkers *et al.*1994).

2.2. METHODS

2.2.1. Surgery

All experiments were performed on neonatal, albino, Wistar rats of both sexes, bred in the Joint Animal House at University College London. Operations were performed under ether or halothane anaesthesia and in sterile conditions.

On the day of birth (P0), a small incision was made in the skin of the lateral aspect of the leg, which exposed the underlying muscles. The physiological ankle flexor muscles tibialis anterior (TA) and extensor digitorum longus (EDL) were identified and injected bilaterally with 0.5 µl of a suspension of 3% Fast Blue and 2 %Diamidino Yellow (FB/DY; Illing), made by sonication of the solids in distilled water, to label the motoneurone pools. Fast Blue is a cytoplasmic label and Diamidino Yellow labels the nucleus of the cell.

On P2, after at least 24 hours, allowing time for retrograde transport of the dyes to the motoneurone somata, and up to 9 days later, the animals were deeply re-anaesthetised, decapitated and eviscerated. The spinal cord was exposed by a ventral laminectomy (Fig. 2.1). The dura was carefully cut in the sagittal plane up the midline and the left and right hemicords were allowed to part under their

own weight by raising them with a pair of fine scissors (Otsuka, Konishi, 1975). Dissection and intracellular injection were performed in oxygenated Krebs (Walton, Fulton, 1983) at room temperature.

2.2.2. Intracellular injection

The pia mater was stripped from the lateral surface of each hemicord, which was then pinned out on the fixed stage of a purpose-built injection microscope (Microtec M2; MicroInstruments, Oxford). Individual retrogradely labelled motoneurones were visualized under epifluorescence from the ventro-lateral aspect of the hemicord, with long working distance objectives. Filters optimal for Fast Blue (Zeiss 48 77 18) and Lucifer Yellow (Zeiss 48 77 05) were interchanged as appropriate, though each dye could be seen with either filter. The FB filter was used during the injecting process as both of the dyes were visible using this filter.

Glass micropipettes were pulled on a Kopf 720 vertical electrode puller. Electrodes with a very fine tip and a long shank were considered optimal for injection of the cells, and so the filament heat and solenoid strength were adjusted accordingly. Their typical resistance when filled with 3 M potassium acetate was 30 -70 mohns. As the tips were very fine, the electrodes were prone to blockage; this could sometimes be cleared by reversal of the injecting current. Electrodes were filled, by capillary action, with Lucifer Yellow CH (LY; 3% in distilled water; Sigma L-0259). The electrode itself formed the cathode and a spatula made of a conducting metal was connected and placed within the perfusing bath to form the anode.

The prelabelled pool was located visually, under low magnification objectives (x2.5; Nikon). The electrode tip was also visibly fluorescing, and so it could be manoeuvred using gross manipulation, over the vicinity of the motor pool. The x20 magnification lens was then substituted, and the tip of the electrode was manipulated over the pool using fine pneumatic control, and visually selected

prelabelled motoneurones were impaled. When a small pulse of negative current was applied, the cell body and some primary dendrites filled rapidly (Fig. 2.2). LY was injected iontophoretically, using negative currents of 0.8-3.6 nA for 15-20 minutes into lumbar motoneurones which were selected for clear retrograde labelling with FB/DY. If the electrode was still located within the extracellular space however, the dye leaked diffusely around the cell. The filling was stopped under these circumstances, the electrode was removed and another motoneurone was selected for intracellular injection. In some favourable cases it was possible to inject several motoneurones along the length of the same motor pool (see Fig. 2.3a,b,c). Since living tissue was used, it was necessary to keep changing the oxygenated Krebs bathing solution and it was impossible to inject each cell for more than 20 mins (see also (Buhl, Lubke, 1988)).

In cells close to the surface of the hemicord, LY fluorescence in the soma and dendrites could be observed directly and was used as a criterion to assessthe success of the intracellular fill. However, in more deeply located neurones, most typically in those of older animals, penetration was less reliable and the extent of filling could only be assessed in the most superficial dendrites.

After injection, hemicords were fixed for up to one week in fresh paraformaldehyde (4%in phosphate buffer, pH 7.6), then dehydrated through graded ethanol and cleared in methyl salicylate (Sigma). Clearing has been found to enhance the visualization of Lucifer Yellow filled cells, especially under the laser scanning confocal microscope (LSCM), and to reduce photobleaching (Becker *et al.*1991). Lucifer Yellow filled cells were examined in the whole mount.

2.2.3. Confocal microscopy

Laser scanning confocal microscopy was required both to achieve high resolution of fine structural detail and to solve the problem of depth-of-field presented by large, multipolar neurones in wholemounts (Wilke, 1984). The confocal microscope produces images of narrow focal planes. This results in difficulty in

obtaining an image of the whole neurone. The system used here overcomes this problem by superimposing the component images obtained at different depths through the tissue in the z-axis, to form a projected, or sum image of the entire selected piece of tissue. The depth of tissue scanned and the increment of the steps taken through the tissue could be changed to suit the requirements of the operator and the type of image being created (Boyde, 1992).

All filled motoneurones included in this study were therefore analysed on a BioRad 600 laser scanning confocal microscope (LSCM). A series of images of confocal optical sections in successive, adjacent, parasagittal planes (Fig. 2.4) was created through the tissue (the z-axis, hence the term 'z-series'), digitized and stored on optical disc for later computer-assisted analyses. All the images in each z-series were then projected onto a single plane to create a 2-dimensional view of the 3-dimensional cell. In this way, all fluorescent structures in a block of tissue up to 250 μm deep could be brought into focus in a single projected image without loss of resolution, eliminating the need for manual registration and reconstruction. Images for manual analyses were printed on a Sony Multiscan video printer (UP-930).

For each cell, image series were collected at several different magnifications. At low power (x10 or x20) an image of the whole cell was acquired first, and used to asses the orientation and distance of projection of the dendrites of the cell. Representative regions of the cell were then imaged at the highest possible resolution (Nikon x 60/1.4 oil immersion) to give information about its finer structures. The following image series were acquired for each cell; (i) the soma and all visible dendrites at low power (30-50 sections, 3-6 μm apart); (ii) the soma and proximal dendrites at high power (up to 15 sections, 1-2 μm apart); (iii) representative first and second order dendrites at high power (up to 15 sections, 1-2 μm apart); and (iv) representative distal dendrites at high power (up to 6 sections , 0.5-2 μm apart). The confocal aperture was manipulated to adjust the thickness of the optical sections according to their spacing. In addition, a single

high-resolution optical section was acquired through the centre of the soma, if possible showing the nucleus and nucleolus.

2.2.4. Analyses

In total, 96 cells from 3 age groups were scored for specific developmental features and entered on a database to simplify the analyses of age-related changes. At 1-3 days postnatal 60 cells from 26 animals were scored; at 4-6 days postnatal 20 cells from 17 animals were used; at 7-9 days there were 16 cells from 12 animals. Not all images were of good enough quality to provide information about every feature. In some cases, the limiting factor was the quality of intracellular injection: in others, detail may have been lost during image acquisition, since the resolution of optical sections was noticeably reduced at depths greater than 250 μm from the surface of the wholemount. However, in most cases the number of primary dendrites and the incidence of spines on the soma, on primary dendrites, on secondary dendrites, and on more distal dendrites was recorded. Primary dendrites are defined as those arising from the soma of the motoneurones; secondary, as those arising from primary dendrites, etc.; distal dendrites here as those of higher branch order than the third, usually more than 100 μm from the soma of the cell.

Projected soma area, diameter and length of all dendrites were measured directly from the digitized image, using the image capture and analyses software of the BioRad LSCM (SOM). From this, it was possible to reconstruct the cell as closely as possible, to create dendrograms and to calculate the total membrane surface area and the volume of the cell (Fig. 2.5).

Fifteen cells (at the extremes of the period of study, P2 and P9) that showed at least 4th order branching, Sholl analyses of dendritic branching were used (Sholl, 1953) to study the direction of orientation of the dendrites with respect to the dorsoventral and rostrocaudal axes of the spinal cord.

2.2.5. Surgery for animals processed for HRP histochemistry

The retrograde horseradish peroxidase (HRP) technique was used to estimate the sizes of the motoneurones during this early postnatal developmental period and beyond, to adulthood. This was necessary to confirm the measurements obtained using intracellular filling with LY and the LSCM.

One day before the desired age point, animals were anaesthetised using halothane in sterile conditions. The TA and EDL were identified as described previously, and dissected free of the surrounding muscles to avoid spread of the dye to these muscles. Using a fine Hamilton syringe, the TA and EDL muscles were each injected bilaterally with a 15% solution of HRP (Sigma Type IV) made in sterile saline (0.9%). The injection was performed in 3-4 parts of the muscle, to ensure that the HRP was distributed evenly through the muscle. The amount of HRP that was injected was estimated according to the weight of the animal (1 μm HRP per 25 mg of muscle). This was estimated from the body weight of the animal based on previous work in this laboratory (Krishnan *et al.*1985). Any excess or leakage from the muscle was immediately mopped up. The wound was sutured with silk thread (Ethicon).

HRP is taken up by the motor endings of the nerve and retrogradely transported up the axons to the cell bodies of the motoneurones within the spinal cord. Extreme caution must be used to ensure that the HRP is not allowed to come into contact with any other muscles, as this will result in the labelling of other motor pools. Due to the tiny size of the muscles, especially EDL, in the neonate, the accuracy of the injection was often in doubt. Therefore, when counting or measuring the labelled cells it was necessary to eliminate many of the motoneurones that were not thought to be situated within the flexor pool. This was judged in reference to previous studies using retrograde transport of HRP in flexor muscles in the neonate (Krishnan *et al.*1985). To avoid counting motoneurones more than once, only those cells in which the nucleolus was visible were counted.

The animals were left for 24 hours before perfusion and processing for HRP visualisation. Animals were used at P1 (n=3), P7 (n=3), P14 (n=4), and adult (n=2).

2.2.6. Intracardial perfusion

24 hours after HRP injection, the animals were anaesthetised with a lethal dose of chloral hydrate(4.5%) by intraperitoneal injection. When the animal was deeply anaesthetised, the thorax was exposed from the ventral aspect. The heart was quickly exposed and a blunt needle was inserted into an incision in the apex. This was secured in place with artery forceps. Another incision was made in the right atrium to allow the perfusate to escape. Saline solution (0.9%) was first passed through the animal using a Watson-Marlow perfusion pump, for a brief period until the liver was blanched. Next, a solution of 2.5% gluteraldehyde (1 ml per gram of body weight) in Millonigs phosphate buffer, pH 7.3 was perfused through for about 20 minutes, until the animal was rigid.

The lumbar region of the spinal cord was carefully removed. It was identified as the area of lumbar enlargement. The cord was postfixed in 2.5% gluteraldehyde for 2 hours at 4 C. This was then transferred to 30% sucrose in Millonig's phosphate buffer, pH 7.3, and kept overnight at 4 ^{o}C.

The lumbar region of the spinal cord was identified and the ventral roots from L3 - L6 were carefully pinned out in a dissection dish. The cord was cut above L3 and below L6. The right dorsal horn of the cord was penetrated with a fine micropin, to enable the right and left sides to be distinguished after sectioning. The block of tissue was then mounted in TissuTec on a freezing microtome (Pelcool). If the tissue was small enough it was not necessary to use dry ice to ensure that it remained frozen, but this was needed with older spinal cords. Serial transverse sections of 50 μm were cut and collected in wells containing Millonigs phosphate buffer and then processed for HRP histochemistry.

2.2.7. HRP histochemistry

The process for HRP histochemistry is described in detail in Appendix 1. Staining was done semi-serially, in purpose-built staining trays. Each well contained 3 sections and the wells could be drained and refilled without need to remove the sections and potentially cause damage. Sections were washed in Millonig's phosphate buffer (pH 7.3) and after a brief wash in distilled water, were immersed in cobalt 1% chloride/ 1% nickel solution for 15 minutes. After washing twice for 10 minutes each in Millonig's phosphate buffer, sections were incubated in Hanker Yates solution until the HRP was visibly developed (about 20 minutes). The Hanker Yates reaction allowed the HRP to be visualised within the soma, some dendrites and often the axon of the motoneurones. It appeared as dark grains within the cells. Sections were rinsed in Millonig's phosphate buffer before being mounted onto gelatinised slides.

Slides were dried and counterstained with gallocyanin to stain the RNA and Nissl substance. The sections were stained until they were a purple/brown colour and the nucleolus was visible. They were then dehydrated through alcohols, cleared in xylene and coverslipped.

2.2.8. Microscopy

Sections were examined using a conventional light microscope (Zeiss). The HRP-labelled motoneurones were visible on both sides of the spinal cord. Since the pin-hole was in the right dorsal horn, the sides could be distinguished. The microscope was fitted with a camera lucida drawing tube, which allowed the profiles of the cells to be drawn.

The sections were viewed under low power objective (x 2.5) to see if there was any spread of the HRP into the motor pools of adjacent muscles. Then the high power objective (x 40) was used to draw around only those cells within the flexor motor pool. Only cells with a visible nucleolus were measured, as this ensured that the cell was measured at its largest point, and that cells would not be

measured twice. This was still a subjective measurement, as a decision had to be made as to were the outline of the soma was drawn.

The outlines of the cells were then redrawn using a graphics tablet interfaced with an IBM compatible microcomputer. A stereometry program written by Dr. J. E. Cook was used to measured the area of the soma of the cells. Frequency histograms were created for the individual cells and pooled data at P1, P7, P14 and adult, to show the changes in distribution of the soma areas.

2.2.9. Statistics

Throughout the entire study Statistical tests were calculated using a MacIntosh microcomputer. The statistical package StatView for MacIntosh was used. For each parameter, the statistical differences between two age groups, or between operated and control sides of the spinal cord, were tested either using the non-parametric MannWhitney U test. Changes in relation of one parameter on another were accomplished using the non-parametric Spearman's rank correlation test, to obtain Spearman's rank correlation coefficient R_S. Levels of significance are indicated by the number of symbols, where * = 0.05, ** = 0.01 and *** = 0.001.

2.3. RESULTS

2.3.1. Location and imaging of flexor motoneurones

The motoneurones innervating the physiological ankle hindlimb flexor muscles tibialis anterior and extensor digitorum longus (TA and EDL) appeared in the living hemicord as a discrete, compact column of fluorescent FB/DY filled cells in the dorsolateral part of the lumbar spinal cord spanning the 4th and 5th lumbar segments (Fig. 2.6). This location corresponds with that previously reported in the adult animal in studies in which horseradish peroxidase was used as the retrograde tracer (Nicolopoulos-Stournaras, Iles, 1983; Peyronnard *et al.*1988; Lowrie *et al.*1987). In addition, the position of motoneurones within the flexor

motor pool was shown with retrograde labelling with HRP (Fig. 2.7). This shows the position of the motoneurones within the ventral horn of the spinal cord (Fig. 2.7a). A higher magnification (Fig. 2.7b), the axons can be seen coursing towards the ventral horn. A high power image of a motoneurone from this pool (Fig. 2.7c) shows the granular nature of the HRP when visualised with the Hanker Yates method.

The somata of individual, prelabelled motoneurones were visible on the lateral aspect of the hemisected spinal cord, and could be selected for intracellular injection. Since Fast Blue was localised in the cytoplasm and Diamidino Yellow was localised in the nucleus, cells in which both of the retrograde labels were co-localised were selected for injection (Fig. 2.6). P1 was the first day on which motoneurones could be injected, since at least 24 hours was required for retrograde transport of the dyes from the target muscle. At this age the prelabelled pool was located close to surface of the spinal cord. Later, due to myelination of the axons in the white matter and the overall increase in the size of the cord, the pool was more deeply located. After this time motoneurone cell bodies were more difficult to locate under epifluorescence and so could not be reliably injected in the hemisected preparation.

Filling was stopped if the dye was seen to be leaking from the cell. In cells close to the surface it was possible to see the soma and dendrites filling, and to keep a close visual check on the quality of the fills. However, in cells more deeply situated within the tissue the soma was obscured and it was necessary to keep changing the plane of focus to see any dendrites close to the surface and this was used as a criterion for a successful fill. Consequently, at later stages the filling was more difficult. In a wholemounted hemicord the soma and dendrites were intact as there was no sectioning of the tissue, and dye leakage occurred due to rupture of the cell membrane, or to a poor penetration of the electrode.

After dehydration and clearing of the wholemounted preparation, individual Lucifer Yellow filled cells were clearly seen by conventional epifluorescence

microscopy (Fig. 2.6c). The use of the LSCM conferred several advantages for the visualization of the three dimensional structure of intact, unsectioned motoneurones (Dekkers *et al.*1994). At low magnifications (Fig. 2.8a and Fig. 2.9a), the digital superimposition of successive optical sections allowed dendrites in widely differing planes to be brought into focus. In some exceptionally good cases, the axon in the ventral root could be traced out of the ventral root (Fig. 2.8b). At high magnifications (Fig. 2.8c-f and Fig. 2.9b-d) the use of thin optical sections greatly reduced the background fluorescence and produced images of high resolution even deep within the tissue. This made it possible to record finer details of the neuronal structure than would otherwise have been possible.

To describe and quantify the features of the motoneurones I have arbitrarily divided the cells into 3 'compartments': (i) the soma, (ii) the primary dendrites, (iii) the distal dendrites (also see methods).

2.3.2. Somatodendritic surface features of neonatal flexor motoneurones

At the earliest times studied, P1 and P2, the most characteristic feature of the somatodendritic morphology was the large number of spine-like, or hair-like growth associated processes covering the soma as well as the dendrites of these immature motoneurones. Somatic appendages were generally hair-like: typically 2-8 μm long and 0.5 μm or less in diameter (Fig. 2.8c). Appendages found on proximal dendrites (primary and secondary) were equally long and thin (Fig. 2.8d). However, in contrast, growth associated processes found on distal dendrites were more irregular and showed a variety of morphologies. Some were hair-like as found on the soma and proximal dendrites, but others, the majority, were much shorter and more club-like than those found more proximally: less than 5 μm long and more than 1 μm in maximum diameter. Generally these distal dendrites had a denser covering of spines which gave the dendrite a 'barbed-wire' appearance (Fig. 2.8e, f) as has been described in other neuronal types at certain periods of development (Lund, 1978). The termination of these

distal dendrites was often thin, sharp lanceolate processes, or less often, classical growth cones (Fig. 2.8e).

2.3.3. Postnatal changes in somatodendritc surface features

The morphological features which characterise the somatodendritic surface of flexor motoneurones during the immediate neonatal period (P1-P3) were quantitatively and qualitatively different to those found at later stages during development. From P4 onwards the somatic appendages seen earlier were no longer evident (Fig. 2.9b). The growth associated processes on proximal dendrites were also reduced in length and number by P4, and had disappeared by P7-9 (Fig. 2.9c). Appendages were still found on distal dendrites, but were shorter, thicker and sparser than those found at earlier stages: 1 μm or more in diameter and 1-2 μm in length. (Fig. 2.9d). They were also more difficult to visualise in the thicker hemicords of older animals. The proportion of distal dendrites bearing growth associated processes did not change over the period studied.

To gain a more quantitative estimate of the incidence, location and developmental changes of the dendritic and somatic appendages during the period studied, a systematic scoring of the 96 most adequately filled motoneurones for spines on somata, on proximal dendrites, on secondary dendrites and on distal dendrites was undertaken. The results are shown in Figure 2.10. As can be seen, at P1-P3, more than 20% of the motoneurones possessed growth associated processes on the soma, whereas the incidence of these processes in primary dendrites was 50% and in distal dendrites near 100%. By P4-P6, none of the motoneurones scored contained somatic appendages. In contrast, 20% of the primary dendrites still had dendritic spines, and the incidence of spines on the distal dendrites remained high. By P9, there was a complete elimination of appendages on the primary dendrites and a great loss on the secondary dendrites. However, the incidence of dendritic appendages remained high on the most distal dendrites.

These results suggest that there is a progressive change in the character and distribution of growth associated processes during the first 10 days of postnatal life in the rat. This eventually leads to an elimination of dendritic appendages from most 'compartments' of the motoneurones over the period studied. There was, additionally, a tendency for this process to proceed in a somatofugal direction.

2.3.4. Growth in the early postnatal period

In the majority of motoneurones studied (n=96), the soma and the primary dendrites were filled well enough to permit basic morphometric analyses. The results are shown in Table 2.1.

The mean projected area of motoneurone somata at all ages studied using intracellular injection of Lucifer Yellow into prelabelled flexor motoneurones was very much smaller than that previously shown in adults (Lowrie *et al.*1987). The mean projected area of the soma at P2 was 342.2 ± 131.4 μm^2 and at P9 was 410.4 ± 193.6 μm^2 (mean ± SD). The difference between P2 and P9 was not significant. However, the relatively small number of cells studied and the possible bias to successful microinjection of relatively large cells precluded detailed analyses of somatic growth. To overcome this problem, soma sizes of motoneurones were obtained using a standard technique of retrograde filling with HRP. The results are shown in Table 2.2, Figure 2.11 and 2.12. The mean soma area at P1 was 371.7 ± 110.3 μm^2 (mean ± SD) and at P7 it is 283.0 ± 110.1 μm^2. There was no significant increase. At P14 the mean soma area was 781.6 ± 280.9 μm^2; this is significantly different from the mean area at P1 ($p>0.0001$) and at P7 ($p>0.001$). Additionally the mean area in the adult was significantly different to that at P14 ($p>0.001$). The growth of the soma area, over the period from P1 to the adult, was found to be significant ($R_S=0.799$; $p>0.001$; Spearman rank correlation test for pooled data) and is shown in Figure 2.12. This shows histograms from the soma areas of animals pooled at P1 (n=132 motoneurones), P7 (n=344), P14 (n=215) and adult (n=288). The histograms in Figure 2.11

show the distribution of soma sizes for one animal at each of the ages P1 (n=22), P7 (n=94), P14 (n=29) and adult (n=126). Both figures show that there is a pronounced period of growth between P7 and P14, which continues to adult. Before P7 the range in sizes of the soma are relatively small, from about 100-500 μm^2. At P14 the range of soma sizes is from 100-2000 μm^2, and is similar in the adult. This confirms the findings of Westerga and Gramsbergen (Westerga, Gramsbergen, 1992) who showed that there is a significant increase in the soma areas of motoneurones between P8 and P20. These authors report that at P30 the bimodal distribution (due to the presence of gamma motoneurones) observed in motoneurones from the soleus motor pool is not observed in the TA motor pool. In this study, a bimodal distribution was not observed in the motoneurones from TA/EDL.

The overall mean number of primary dendrites (Table 2.1) for the intracellularly filled motoneurones over the period P1-P9 was 7.97 ± 0.21 (range 4-12). Neither the number nor their mean diameter changed significantly between P1 and P9.

2.3.5. Morphometric data on individual motoneurones

Seventeen motoneurones were selected for their apparently complete dendritic fill. These were reconstructed from serial optical sections and additional morphometric variables associated with the soma, primary dendrites and distal dendrites were measured. The results are presented in Table 2.3. Due to the limited age range, no attempt was made to study developmental trends. However, there was some variability in the size of the parameters measured. The total membrane area of the motoneurones varied from 2202-28943 μm^2. This indicates that there are large differences in the sizes of individual motoneurones over the first 10 days of postnatal life. Figure 2.13 shows a positive correlation ($R_S = 0.644$; $P < 0.01$; Spearman rank correlation test) between mean soma diameter and the combined diameter of the primary dendrites of the 17 cells in Table 2.3. A positive correlation ($R_S = 0.583$; $P < 0.001$; Spearman rank

correlation test) was also found between the diameter of a primary dendrite and the combined length of the dendritic tree arising from it for each of the 17 cells (Figure 2.14). This confirms the strong relationship between these parameters in immature motoneurones that has been observed in various studies in adult cat motoneurones (Cameron *et al.*1988; Luscher, Clamann, 1992). This suggests that the growth of dendrites is proportional, and that larger stem dendrites give rise to larger dendritic trees. It also suggests that the dendritic tree of the motoneurones have been extensively filled with the intracellular dye, Lucifer Yellow.

The primary dendrites extended in all directions around the soma, but the extent of dendritic outgrowth was not radially symmetrical (see also Fig. 2.16a,b), showing a consistent dorsal bias. Dendrites extended for distances from the soma ranging from 137 to 293 μm, the diameter of the primary dendrite of the smaller being 1.6 μm and that of the larger being 2.9 μm. The maximum branch orders ranged from 4 to 7 orders of branching (Table 2.3), suggesting that most, if not all, of each dendritic tree was visible in the 2-D projections from which the measurements were made.

2.3.6. Spatial analysis of dendritic trees

Sholl analyses were performed on the dendritic trees of a sample of 15 motoneurones, suitable for analyses, at the two extremes of the period studied, P2 and P9 to reveal any changes in the relationship between dendritic branch number and distance from the soma. These cells were selected for apparently complete dendritic imaging in the projection plane. Figure 2.15 shows Sholl analyses for motoneurones at P2 (Fig. 2.15a; n=10) and P9 (Fig. 2.15b; n=5). At both ages, the greatest number of dendritic intersections (points at which the dendrites crossed uniformly spaced at 20 μm rings concentric with the soma) occurred at about 80 μm from the soma, and the maximum dendritic length was in the range 220-240 μm.

To analyse dendritic orientation in the parasagittal plane, dendritic intersections were counted separately for 12 sectors of 30 ^{o} and pooled into quadrants, each quadrant being the group of three sectors centred on either the dorsoventral or rostrocaudal axis. No significant changes could be demonstrated between P2 and P9. However, a general dorsal bias was present at both ages, more intersections being found in the central of the dorsal sectors than any other ($p < 0.005$, $p < 0.024$ and $p < 0.016$: two-tailed MannWhitney U-tests for dorsal against rostral, ventral and caudal respectively). Polar plots of the data for the individual sectors (Fig. 2.16) suggest a particular bias towards the most dorsal 30^{o} sector at both P2 and P9. In contrast to this particularly dorsal 'spray' of dendrites, also seen of Figure 2.16a, dendrites that were directed rostrally, ventrally and caudally tended to be more uniform in angular distribution and length.

2.4. DISCUSSION

This chapter examined early postnatal changes in the somatodendritic morphology of retrogradely labelled flexor motoneurones in the rat. A combination of *in vitro* intracellular labelling and confocal microscopy was used. The length of the period of study was limited to between the second and the ninth postnatal days. This was due to the thickness of the hemisected spinal cord at periods later than P9. Motoneurones were injected in a wholemount preparation to avoid the need for sectioning and manual reconstruction of the cells. Use of the confocal microscope allowed high resolution images of the motoneurones to be created through the thickness of the tissue. However, the limit of the depth of resolution of the confocal microscope was about 250 μm. The flexor motor pool was located on the lateral surface of the ventral horn of the spinal cord. During the period of early postnatal growth, there was an increase in the thickness of the white matter of the spinal cord as the axons were myelinated, and this resulted in the flexor motor pool being located deeper within the tissue of

the spinal cord. Due to the increase in the thickness of the spinal cord it became increasing difficulty to identify individual prelabelled motoneurones for injection with Lucifer Yellow. By P9, the motor pool was located too deeply within the ventral horn to be injected or to allow the visualization of motoneurones in the wholemount. Embryonic tissue was not used due to the difficulty in accurately prelabelling and identifying a specific motor pool.

The study was limited to the first 10 days postnatally. However, during this period these motoneurones and their target muscles are undergoing important functional changes (Navarrete, Vrbová, 1983; Vrbová *et al.*1985; Navarrete *et al.*1988a; Navarrete, Vrbová, 1993). The characteristically different firing patterns of slow and fast muscles develop during this period of postnatal development (Navarrete, Vrbová, 1983). Smaller motoneurones generally fire tonically, for longer periods of time, than larger motoneurones which fire phasically. In the newborn rat, motor units in both soleus and EDL fire phasically, but in EDL the interspike intervals are larger than in adults. Over the period of postnatal development there is a shift towards the adult pattern. Motor units of slow soleus muscle begin to fire tonically, whilst the interspike intervals of fast EDL become shorter. These changes occur over P1-P9. Since the activity of a motoneurone depends of both its size (Henneman, 1957) and patterns of afferent connections (Rall *et al.*1967), there are likely to be changes in either one or both of these during during the postnatal period.

2.4.1. Postnatal changes in the somatodendritic surface features

During the immediate postnatal period (P2-P3) the somatodendritc surface of the motoneurone is covered by numerous growth associated processes. These spine-like or hair-like processes decrease in number and change in character and distribution over the first postnatal week. The elimination of these structures during the first nine days of postnatal development proceeds in a somatofugal direction, so that they are still present on the distal dendrites at the end of the time period studied here (P9). This confirms previous work using the Golgi

technique, where growth associated processes were seen between embryonic days E13 and E18 and gradually disappeared between P5 and P11. The smooth somatodendritic morphology characteristic of the adult was attained by P18 (Cummings, Steltzner, 1984).

During this early postnatal period, when the entire somatodendritic surface of the motoneurone is covered by growth associated processes, the peripheral field of the axon (the motor unit) is also at its largest. The motor unit size of a neonatal rat is up to five times that of the adult (Brown *et al.*1976; Balice-Gordon, Thompson, 1988; Connold *et al.*1992). This large motor unit size is due to the fact that individual muscle fibres have several inputs. This polyneuronal innervation decreases with age. In EDL the elimination of polyneuronal innervation of muscle fibres begins at around P3. By P18 the majority of the muscle fibres have the adult pattern of innervation, with one axon innervating a single motor end plate (Balice-Gordon, Thompson, 1988). This occurs at the same time that the immature surface features disappear from the soma and dendrites of the motoneurone membrane. This also coincides with elimination of electrotonic and dye coupling between functionally related motoneurones (Becker, Navarrete, 1990). Thus, during this period of early postnatal development there are important changes occurring in the motoneurones (see (Lowrie, Vrbová, 1992; Navarrete, Vrbová, 1993)), as they change from a growing to a transmitting cell. There is an increase in the release of the neurotransmitter ACh during development (O'Brien, Vrbová, 1978). During this period, motor activity becomes more mature due to the development of both the motoneurones and the spinal circuitry. Interruption of the nerve-muscle interaction during this critical period of development results in long-lasting alterations in the function and structure of the motoneurones (Navarrete, Vrbová, 1984; Lowrie *et al.*1987; Navarrete *et al.*1990; Greensmith, Vrbová, 1991; Vejsada *et al.*1991).

2.4.2. Mechanisms involved in somatodendritic surface changes

The presence of somatodendritic growth associated surface features and their

elimination during development, has been described in many parts of the nervous system (in the cerebellum (Morest, 1968; Berry, Bradley, 1976b); brain stem (Scheibel *et al.*1973); retina (Ramoa *et al.*1988); see (Lund, 1978)). During the first month of postnatal life, growth associated processes are lost from the neurones in the brainstem auditory nucleus of the ferret (Henkel, Brunso-Bechtold, 1991). As in the present study, these processes are lost somatofugally. In cat retinal ganglion cells, spine-like processes were eliminated in the first postnatal month (Ramoa *et al.*1988).

These changes in the morphology of the cell are possibly a result of changes in the neuronal cytoskeleton. Microtubule-associated proteins (MAPs) are responsible for regulating the stability of microtubules within neurones, and are necessary in order for dendritic growth to occur (Matus, 1988). Different MAPs are developmentally expressed and the changes in MAP2 expression coincides with the end of axonal and dendritic growth ((Viereck *et al.*1988), see (Tucker, 1990)). When neuroblastoma cells are exposed to microtubule-depolymerising substances in culture, processes similar to those observed during development arise along the neurite (Bray *et al.*1978; Anglister *et al.*1982; Matus *et al.*1986). In cultured neurones of the hippocampus, the dendrites lose their cylindrical shape and the outline becomes irregular ((Matus, 1987), see (Matus, 1988)).

In addition to binding tubulin, MAPs have been shown to bind actin (Nishida *et al.*1981) and neurofilaments (Letterier, Shelanski, 1982). The transition from plastic, highly motile growth cones to rigid neurites may depend on a change in the amount of polymerised actin in relation to polymerised tubulin, which is linked to the changes in MAP2 which occur developmentally (Matus, 1988). It is proposed that the interaction of MAP2 with microtubules and other cytoskeletal elements is mediated by the phosphorylation of the microtubule-associated protein. Phosphorylation reduces the affinity of MAP2 for binding tubulin (Murphy, Flavin, 1983) and increases the interaction with both actin (Nishida *et al.*1981) and neurofilament (Letterier, Shelanski, 1982) whilst de-

phosphorylation of MAP2 reverses this (Halpain, Greengard, 1990). At present, the levels of expression and the phosphorylation state of microtubule-associated proteins in neonatal motoneurones is not known.

2.4.3. Synaptogenesis

Several studies of the developing nervous system, using electron microscopy, have shown that synapses are formed on growth cones and filopodia (Hinds, Hinds, 1972; Vaughn *et al.*1974; Vaughn, Simms, 1978; Skoff, Hamburger, 1974; Ulfhake, Cullheim, 1988b). It is suggested that the growth associated processes form the major receptive area of membrane for the synaptic contacts onto developing neurones (Vaughn, 1989). Vaughn *et al.* (Vaughn *et al.*1974) found that there was a relationship between the proportions of growth cones and dendritic synapses. They suggested that presynaptic boutons first make contact with dendritic filopodia and growth cones, and that, after the synapses are formed, the dendrites continue to grow, leaving behind the synapse (Vaughn *et al.*1974). The point of growth of the dendrites is the growth cone, and after the contact is made with the synapse the growth cone differentiates into an area of dendrite. A filopodial process grows from the growth cone and when contacted it continues to grow, leaving behind newly formed synapses on the segment of the dendrite. This would suggest that dendritic branching patterns of motor neurone dendrites are influenced by the way in which the dendritic growth cone filopodia come into contact, and form synapses with afferent axons (see also (Berry, Bradley, 1976a)).

Other studies have failed to find conventional synaptic contacts on filopodial structures. During development of the retinal ganglion cells of the cat, transient growth associated processes have been observed (Ramoa *et al.*1988), reaching a peak during the first postnatal week and the declining to adult. However, an ultrastructural study by Wong *et al.*. did not reveal synaptic contacts on the dendritic spines of developing retinal ganglion cells , though they were seen on the dendrites themselves (Wong *et al.*1992). They propose that these processes

do play a role in synaptogenesis, and facilitate early interactions between potential presynaptic processes or their growth cones that may eventually result in the formation of synaptic contacts. This was also proposed by Wassle (see (Wassle, 1988)) who described them as 'tentacles' with which the ganglion cell 'catches' its afferent connections. By retracting the 'tentacle' the synapse is formed on the dendritic shaft. A further possibility is suggested by experiments that show that growth cones in cultures of immature neurones can release neurotransmitters and produce postsynaptic responses without the presence of synaptic specialisation (Hume *et al.*1983; Young, Poo, 1983).

During the period of early postnatal development the descending and interneuronal inputs onto the motoneurones are maturing (Gilbert, Steltzner, 1979). This results in changes in afferent synaptic activity which may actively result in the retraction of growth associated processes from the somatodendritic surface of the motoneurone. Growth cone motility is affected by neurotransmitters (Haydon *et al.*1987) and activity (Patel, Poo, 1982), via calcium mediated mechanisms (Kater *et al.*1988). This could result in changes in the cytoskeleton of the dendrites, as described in other areas of the nervous system (Llinas, Sugimori, 1979; Kater *et al.*1988).

It is interesting to note that there is evidence for plasticity in dendrites of motoneurones of aged cats, where growth cone-like processes appear to sprout, though in fewer numbers than observed during development (Ramirez, Ulfhake, 1992). It appears that the loss of the growth associated processes is reversed during aging. In this situation the renewed growth of collateral dendritic branches could be due to the degenerative loss of afferent connections and/or neighbouring motoneurones.

During the first three weeks of postnatal life, a period of dendritic remodelling in the kitten (Ulfhake, Cullheim, 1988b; Ulfhake *et al.*1988), up to half of the synapses onto the motoneurones are lost (Conradi, Ronnevi, 1975; Purves, Lichtman, 1980). With growth associated processes being eliminated, any

synaptic inputs on these structures would be either lost or relocated elsewhere on the motoneurone dendritic tree. At present there is little information on the pattern of synapse elimination and its possible relation to changes in the surface of the soma and dendrites of rat motoneurones. Chapter 4 will examine the number and distribution of primary afferent and descending inputs onto the somatodendritic surface of rat flexor motoneurones (Clowry *et al.*1991; Greensmith *et al.*1992).

2.4.4. Dendritic branching and orientation

In ankle flexor motoneurones Sholl analyses showed that there was little evidence of dendritic growth during the first 10 days of postnatal life. The dendrites within the most dorsal 30° sector were consistently longer, and branching occurred at greater distances from the soma than dendrites in other sectors. In a study using lipid-soluble fluorescent tracers to show the projection patterns of developing rat neurones and their afferent connections, the dendrites of motoneurones innervating the limb were seen to have a prominent dorsomedial or medial projection (Snider *et al.*1992b; Snider, Tsering, 1990). This projection was directly in the path of the dorsal root afferents and was already evident at E15, the first day on which sensory afferent axons can be seen entering the spinal cord (compare with the growth of dendrites in the amphibian into a preformed neuropil (Jackson, Frank, 1987)). The dendrites of motoneurones of the foot sole muscles of the kitten also form these dorsomedially projecting bundles (Ramirez, Ulfhake, 1991). The projection of clusters of dendrites into the dorsal sector in this study, may be exactly the equivalent, but the growth along the medial axes was not assessed, as hemicord preparations were viewed most clearly from the lateral aspect. Nevertheless, these patterns of growth may represent dendrites preferentially forming connections with axons from dorsal afferents.

Other studies have reported a pronounced degree of dendritic growth along the rostrocaudal axis that was not observed in this study. This may be due to the

lengthening of the spinal cord along that axis (Ulfhake *et al.*1988; Cameron *et al.*1991). However, since this phase of growth happens relatively late in the kitten cervical spinal cord, which is relatively more mature, it is probable that this lengthening of the spinal cord would occur after P10 in the rat (Westerga, Gramsbergen, 1992), and so would not be observed within the period of this study.

The pattern of dendritic growth in the ventral quadrant appeared to be most compact. The ankle flexor motoneurones are located in the dorsolateral part of the ventral horn of the spinal cord. Their lateral positioning imposes restrictions on growth in the ventral direction, which can be clearly seen in transverse sections of spinal cord containing motoneurones. In these preparations, the dendrites of flexor motoneurones follow the ventral curvature of the limits of the grey matter. There is also limited growth along the medial axes. This is in direct contrast to more medially located soleus motoneurones, which exhibit radial dendritic growth.

2.4.5. Relevance to functional development of flexor motoneurones

As suggested in the introduction to this chapter, the size and branching structure of a motoneurone dendritic tree determines both the position of the synaptic inputs and the relative influence of these inputs on the functional output of the neurone (Rall *et al.*1967). In the adult, various parameters related to the size and complexity of the dendritic tree are seen to be correlated with the contractile properties of the motor units that they innervate (see (Luscher, Clamann, 1992)).

The dendritic structure of motoneurones innervating slow muscle fibres in triceps suroe muscles in the adult cat are smaller and less complex than those of fast muscles supplying fast muscle fibres (Cullheim *et al.*1987a). Correlations have also been found between the size of the soma of a motoneurone and the complexity of its dendritic tree (Zwaagstra, Kernell, 1981; Cameron *et al.*1991;

Ulfhake, Kellerth, 1983; Ulfhake, Cullheim, 1988a). Due to the limited optical penetration of the confocal microscope, the possibility of bleaching of dendrites (especially distally) during the acquisition of an image, and the small sample size, complete dendritic reconstructions were not attempted, and these relationships were not studied in great detail. A significant correlation was found in the small sample of motoneurones, between both the soma size and combined diameter of the primary dendrites, and the diameter of a stem dendrite and the total membrane area that it supports. If other correlations found in cat motoneurones also apply to these flexor motoneurones of the rat, there may be a large degree of variability in the total membrane area of individual neonatal motoneurones. This is also seen in the variability of the total membrane area of the motoneurones that were reconstructed.

During the first three postnatal weeks there is a maturation of locomotor function. The firing patterns of slow and fast motoneurones in the hindlimb of the rat change during this period in association with the development of locomotion ((Navarrete *et al.*1988a), see (Navarrete, Vrbová, 1993)). These changes may reflect changes in the size of the motoneurones resulting in changes in the intrinsic electrophysiological properties of the cells. Small motoneurones are known to have higher input resistance and lower excitation thresholds, and are therefore more active, than larger motoneurones (Henneman *et al.*1965). The developmental changes in the morphology of the motoneurones might be expected to occur at the same time as the functional changes.

In this study, there was little observed change in the area of motoneurones filled with Lucifer Yellow (Table 2.1 and 2.3) during the first postnatal week. However, in motoneurones retrogradely labelled with HRP, a significant increase was observed (Table 2.2, Figures 2.11 and 2.12). This was probably due to the small size of the group of intracellularly filled motoneurones. Other studies have shown that the most rapid period of somatic growth of motoneurones supplying soleus (Kerai *et al.*1993) and TA (Westerga, Gramsbergen, 1992) is

during the second and third postnatal weeks. These results confirm that the major period of growth of hindlimb flexor motoneurones is between P14 and adult.

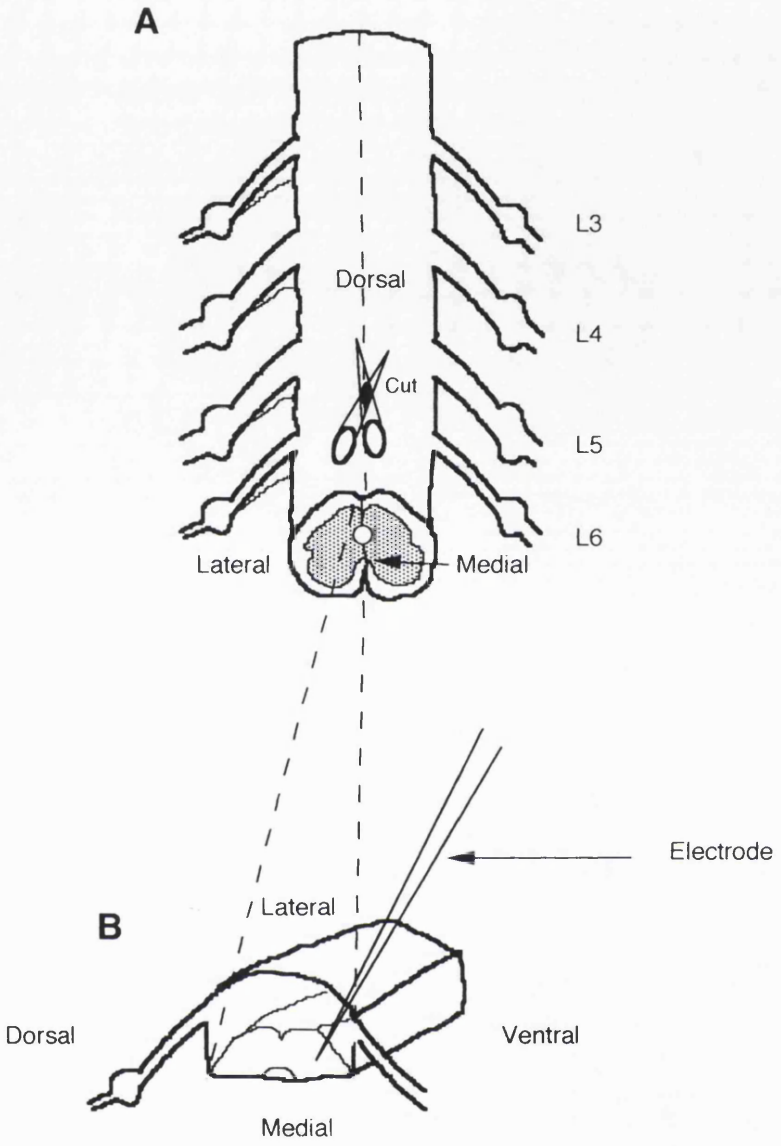

Figure 2.1 shows the orientation of the spinal cord when exposed for intracellular injection of Lucifer Yellow. **(A)** shows a pictorial representation of the spinal cord when removed from the animal. The two sides of the spinal cord are hemisected up the midline, as shown. Each hemicord is then injected separately. The hemicord is injected in the lateral side, resting on the medial side as shown in **(B)**.

Figure 2.2 The process of filling individual retrogradely labelled flexor motoneurones with the fluorescent dye, Lucifer Yellow. The motoneurones are retrogradely labelled with Fast Blue and Diamidino yellow, which allows the cells to be located in the ventral horn of the spinal cord (shown in Figure 2.6). An individual motoneurone is then selected and impaled with a microelectrode filled with Lucifer Yellow. The electrode is clearly visible on the right of each frame. Motoneurones were filled iontophoretically using negative currents of 0.8-3.6 nA for 15-20 minutes.

(1) Shows a rather faintly labelled motoneurone impaled by the electrode. The process of filling with Lucifer Yellow has just begun. In **(2)**, **(3)** and **(4)** the motoneurone is gradually filled with Lucifer Yellow. The dendrites become visible as the dye spreads through the motoneurone. About three minutes have elapsed between each frame. In **(5)** and **(6)** the motoneurone has been filled for about 15 minutes. The whole of the dendritic tree is not visible in one plane of focus, and **(5)** and **(6)** show two different planes of focus of the motoneurone. Scale bar = 50 μm.

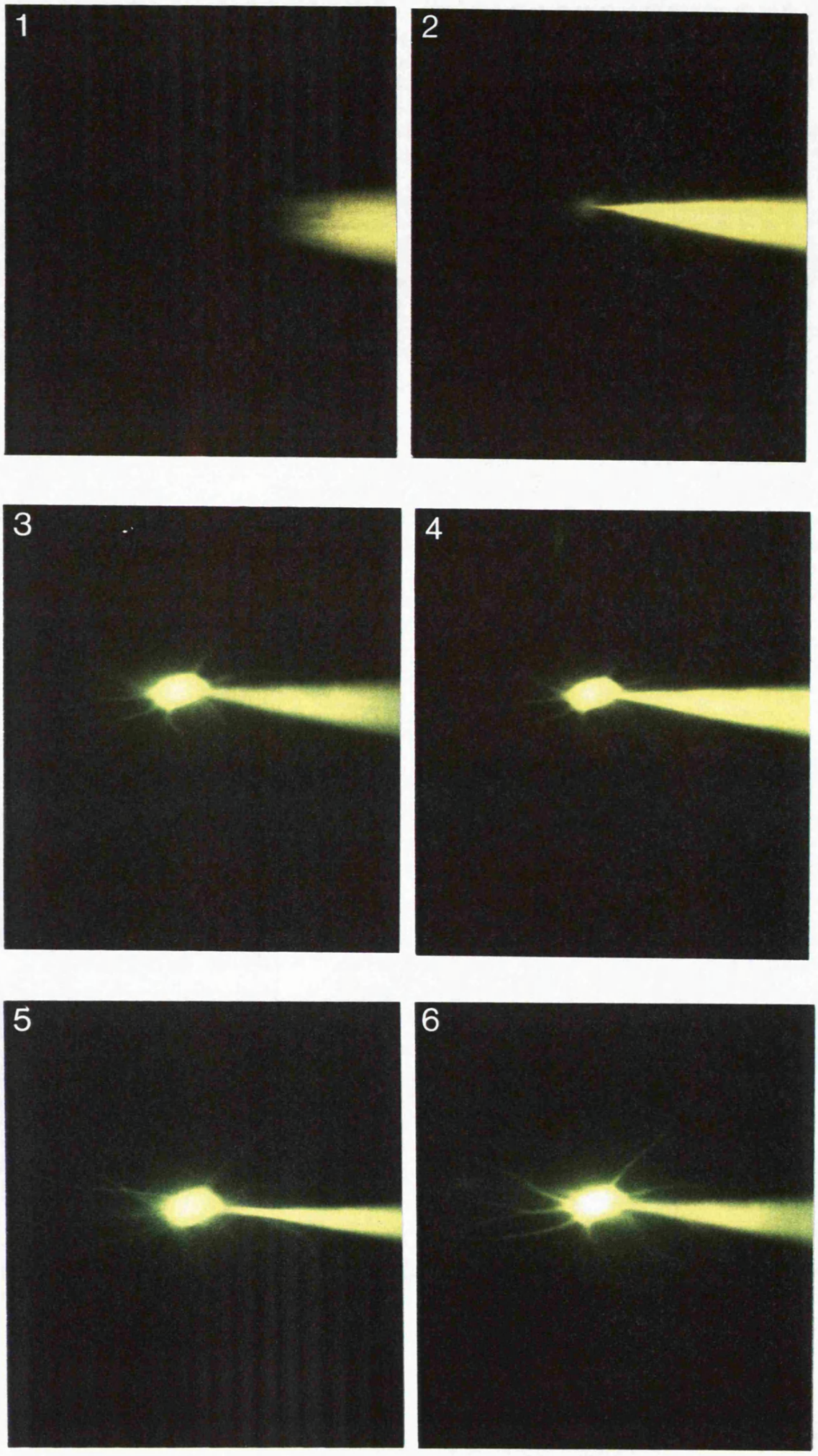

92

Figure 2.3 Motoneurones from the tibialis anterior/extensor digitorum longus motor pool, that have been intracellularly filled with Lucifer Yellow (LY).
(A) The wholemounted hemisected spinal cord is viewed from the lateral aspect using epifluorescence microscopy. LY filled motoneurones are clearly visible in the motor pool, as are the Fast Blue/Diamidino Yellow prelabelled cells. Compass points mark the dorsal and ventral axes. Scale bar = 250 μm.
(B) The boxed area from **(A)**. This shows a LY filled flexor motoneurone at higher power (x25) using conventional epifluorescence microscopy. Scale bar = 50 μm.
(C) Transverse section of spinal cord containing motoneurones that have been filled with LY. The motoneurones were filled in the wholemounted hemicord, which was then sectioned at 50 μm. Note the orientation of the dendrites of the motoneurones. They appear to be polarised along the lateral border of the ventral horn. Scale bar = 50 μm.

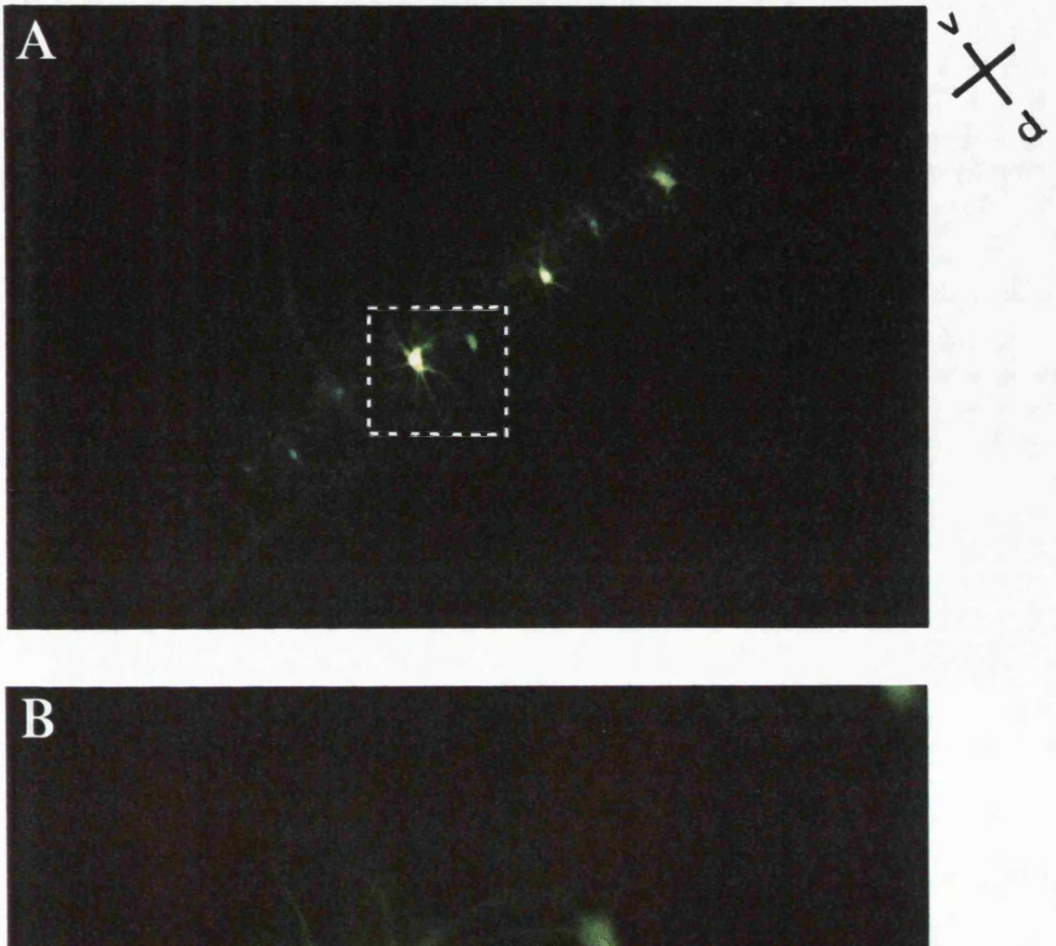
A
v
d

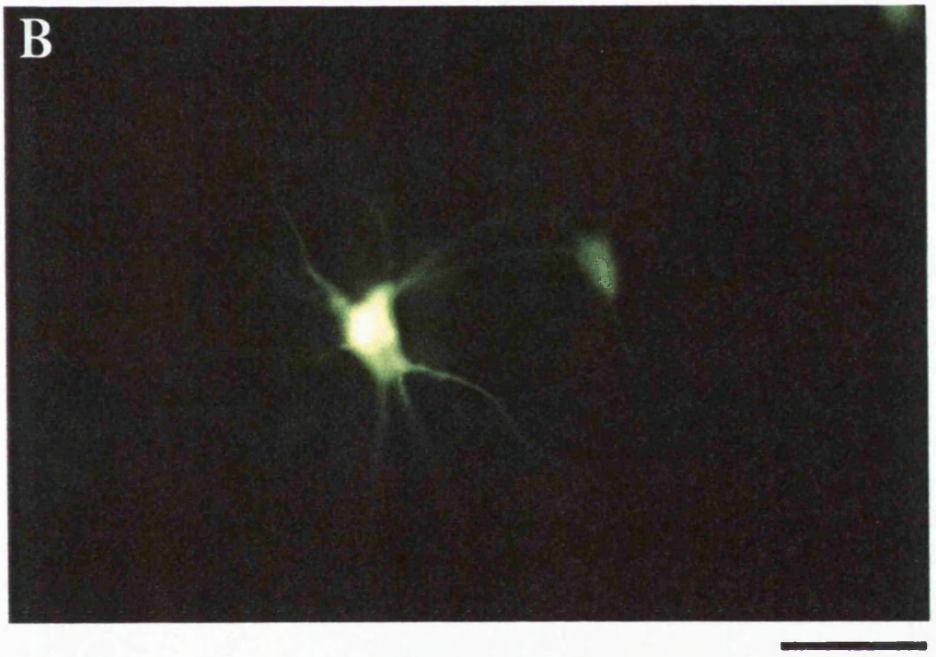
B

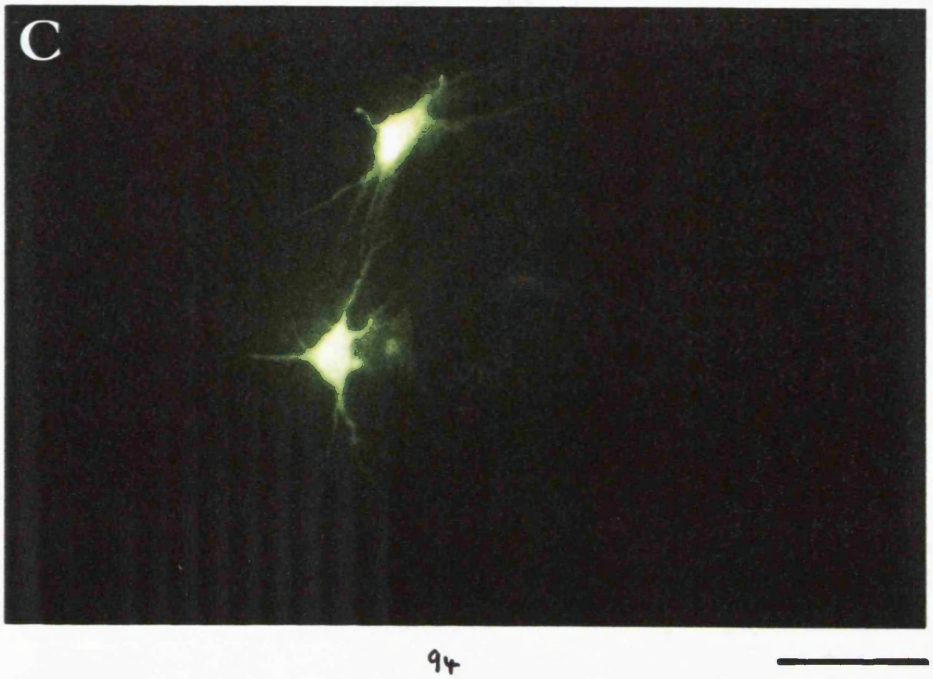
C

Figure 2.4 The acquisition of a 'z-series' of images through the soma and primary dendrites of a motoneurone along the z-axes using the laser scanning confocal microscope (LSCM). The LSCM was used to obtain high resolution images showing fine structural detail. It solves the problem of depth-of-field by creating a series of images through the depth of the motoneurone. Each image is obtained at a different focal plane. There are 3 μm between each image in this z-series. The z-series of images are then projected onto a single plane to create a 2-dimensional view of the 3-dimensional cell.
Images **(1)** to **(8)** show the series of images created through at P7 motoneurone at high power (x60/1.4 oil immersion, zoom 1). These images will be projected, to form a single image of the motoneurone. Scale bar = 10μm.

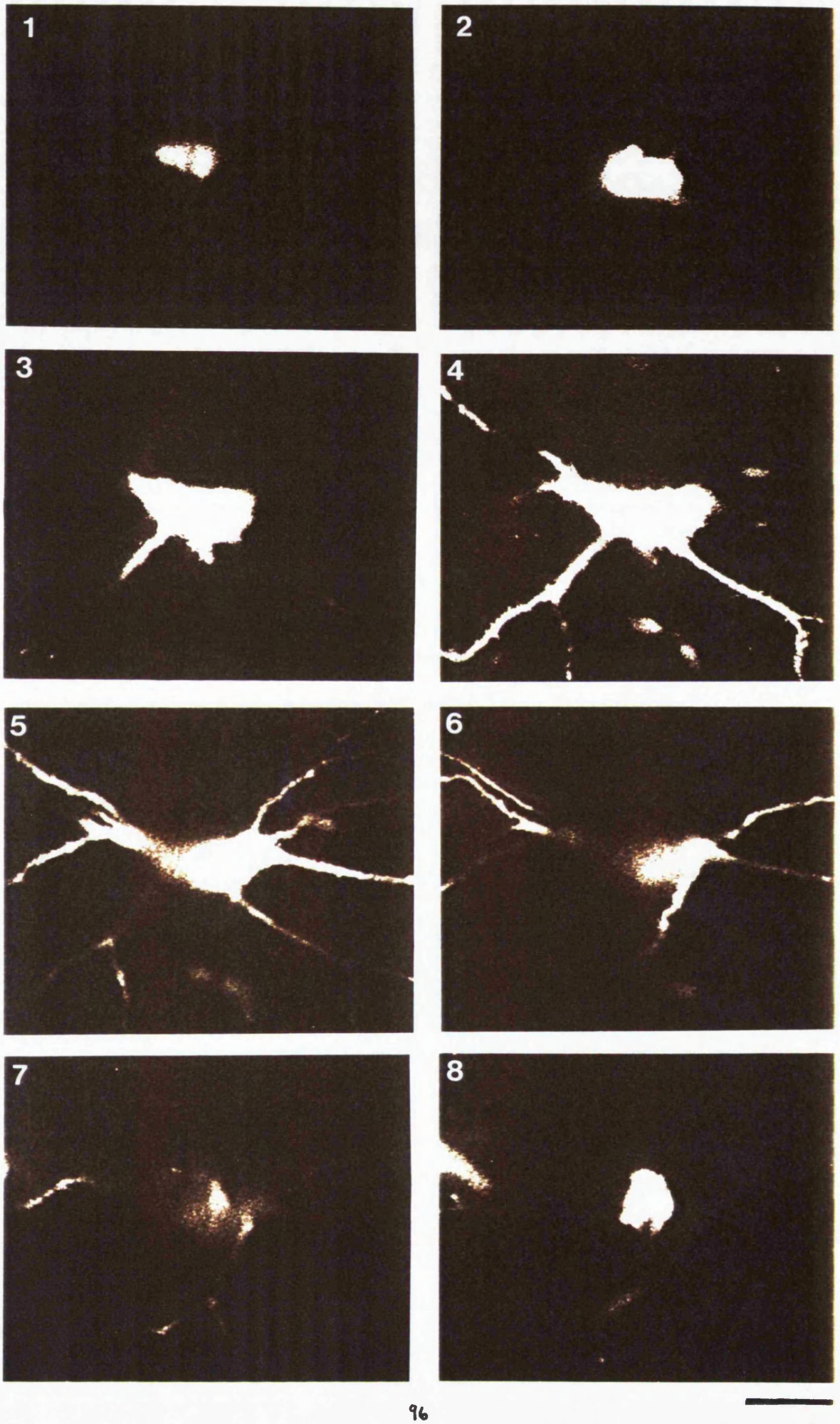
1
2
3
4
5
6
7
8

Figure 2.5 Camera lucida-like drawings of flexor motoneurones. This shows examples of cells that were used to examine the morphology of the developing motoneurones. The drawings (A) and (C), were obtained from low power (x20, zoom 1) projection images through the motoneurones at P2. Sholl analyses (Sholl 1953) was performed on these images. Concentric rings were placed over the image of the motoneurone and the number of dendritic intersections made at distances of 20 μm increments from the soma were counted (see Figures 2.15, 2.16).

Using these projection images, the length and diameter of each dendrite was measured from the computer screen using the resident BioRad software, SOM. Particular regions of the motoneurone were enlarged to provide more accurate measurements. **(B)** shows a example of a dendrogram obtained by measuring the dendrite indicated by the arrowhead in **(A)**. The scale is in microns. Dendrograms were obtained for all the dendrites of the 17 motoneurones (see Table 2.3). From these measurements the total surface area and volume of the motoneurones could be calculated. Scale bar for (A) and (C) = 250 μm.

A

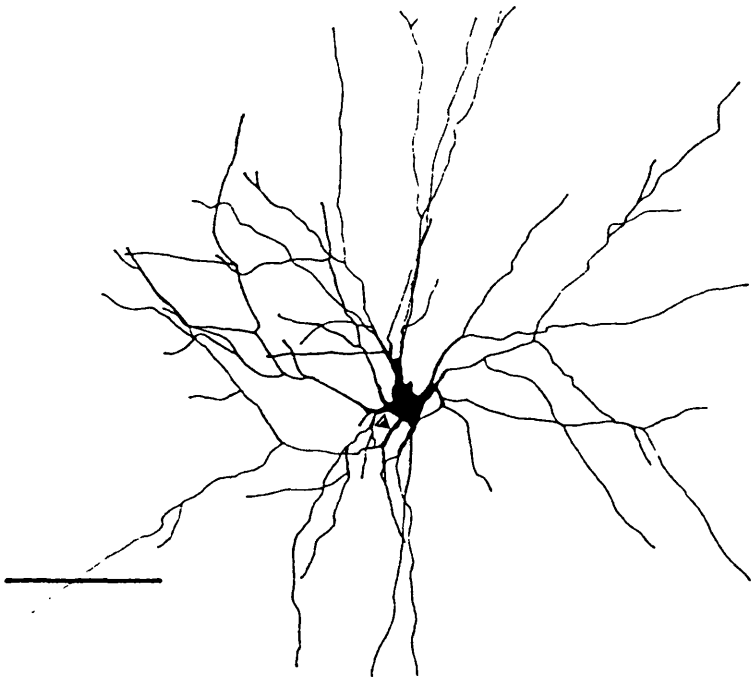

B

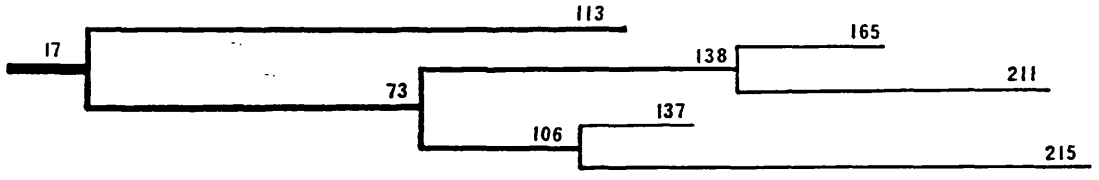

C

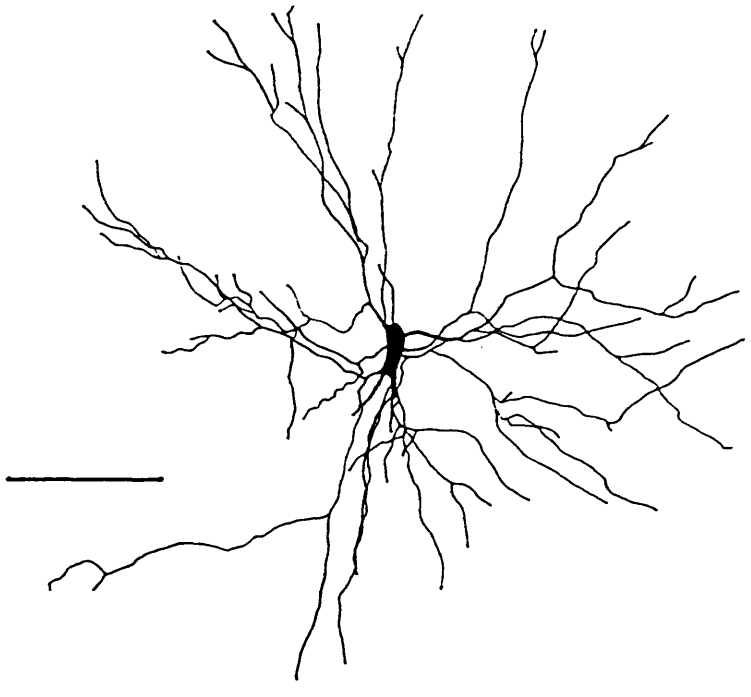

Figure 2.6 The identification, location and imaging of retrogradely labelled ankle flexor motoneurones in a spinal hemicord preparation.

(A) Part of an intact P3 hemicord viewed by conventional epifluorescence microscopy, showing a compact pool of ankle flexor motoneurones (arrows) labelled with Fast Blue and Diamidino Yellow from tibialis anterior and extensor digitorum longus. Scale bar = 1mm.

(B) A Vibroslice section of a similar cord at P3, cut transversely at the level of the tibialis anterior/extensor digitorum longus pool. Dorsal is up and the midline to the left. The Fast Blue labelled motoneurones (arrows) can be seen to lie dorsolaterally within the ventral horn. Scale bar = 250 μm.

(C) A single flexor motoneurone of the tibialis anterior/extensor digitorum longus pool, injected with Lucifer Yellow on P2 and viewed by conventional epifluorescence. Much of the dendritic tree inevitably lies well outside the focal plane. Increasing the depth of field by reducing the aperture of the objectives is not practical with epifluorescence, since image brightness varies as the fourth power of aperture. With the confocal microscope, the problem can be solved by the digital recombination of many individual optical sections. Scale bar = 50 μm.

In some cases there was spread of the prelabel dyes into adjacent muscles and other motor pools may have been labelled. However, in the majority of preparations the prelabelling was restricted to a defined area of the CP motor pool.

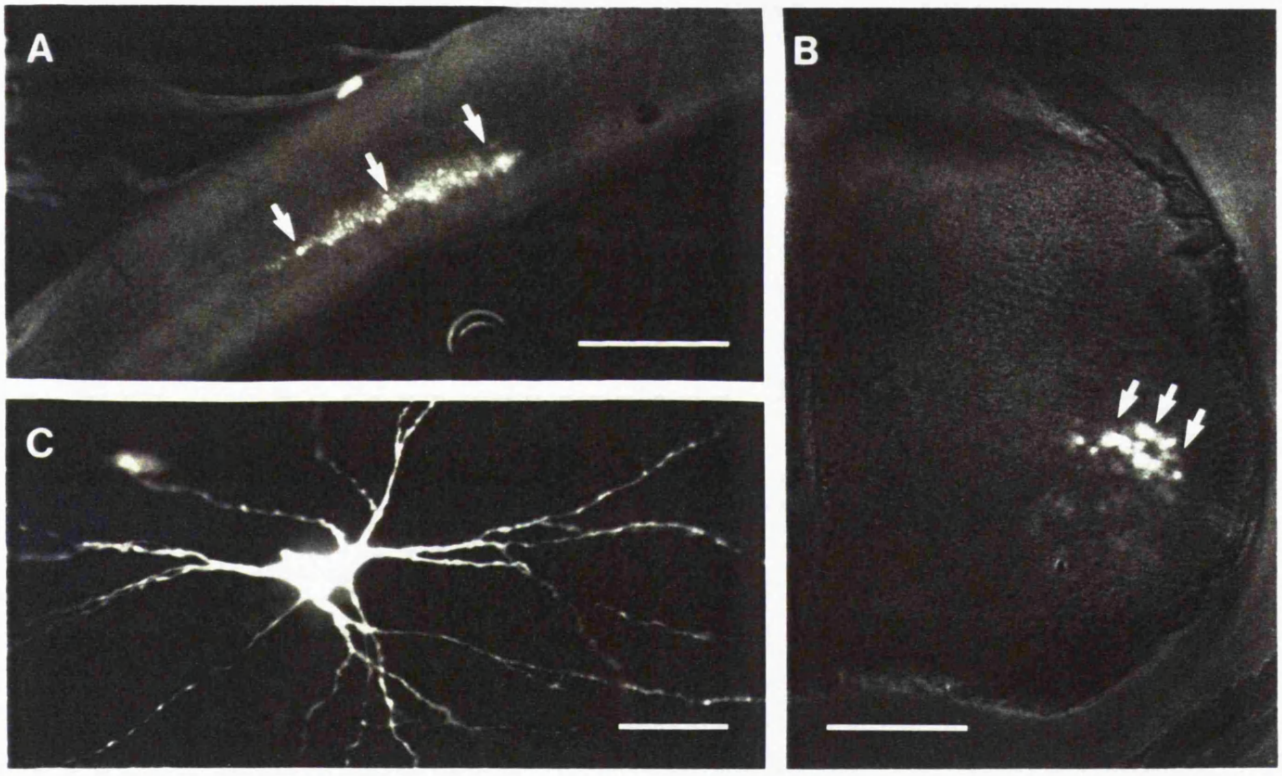
A
B
C

Figure 2.7 Motoneurones retrogradely filled with horseradish peroxidase (HRP) by microinjection of HRP into the flexor muscles tibialis anterior and extensor digitorum longus (TA/EDL). The animals were transcardially perfused with 2.5% gluteraldehyde 24 hours after injection of the HRP. The tissue was cut at 50 μm and processed using the Hanker Yates method for visualisation of HRP.

(A) View of a transverse section of an adult spinal cord through the tibialis anterior/extensor digitorum longus motor pool. The HRP filled motoneurones are clearly visible in the dorsolateral part of the ventral horn. The large hole in the ventral horn on the right side of the spinal cord was produced by a pin, and serves to distinguish one side of the spinal cord from the other. Scale bar = 800 μm.

(C) The right side of the same adult spinal cord as in **(A)**. At this magnification (x10) the axons of HRP filled motoneurones from the TA/EDL motor pool are visible traversing towards the ventral root (arrows). Scale bar = 200 μm.

(B) An HRP filled motoneurone (x40) from the TA/EDL pool shown in **(A)** and **(C)**. Only cells with a visible nucleolus, as this one has, were counted. Note the granular appearance of the HRP in the cytoplasm of the motoneurone, characteristic of processing of HRP by the Hanker Yates method. This allows clearer visualisation of the nucleolus. Scale bar = 50 μm.

Spread of HRP into adjacent muscles was a problem at younger ages. Only motoneurones well within the boundaries of the CP pool were included in the analysis. This resulted in sampling of the motoneurones.

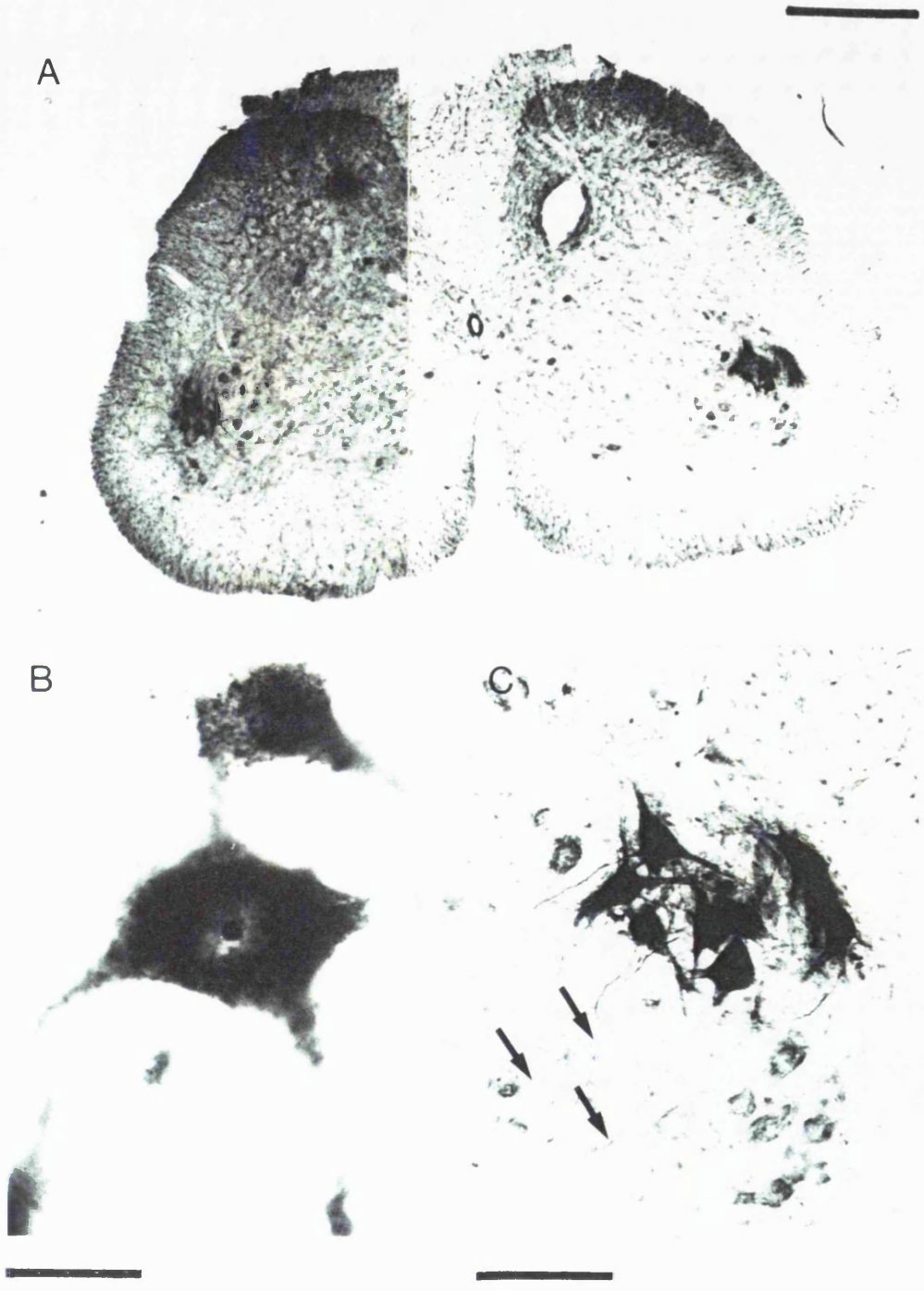
A
B
C

Figure 2.8 Laser scanning confocal microscope images showing morphological features of neonatal ankle flexor motoneurones, injected with Lucifer Yellow on P2 or P3, in whole-mounted hemicords.

(A) Low power projection of such a motoneurone, viewed from the lateral surface of the hemicord, showing the extensive dendritic tree. Compass points mark the dorsal, rostral, ventral and caudal axes, which for this cell closely correspond to the major directions of dendritic outgrowth. Note that the dendrites seem to form loose 'sprays' or bundles. Dendrites from a second, more caudal motoneurone are seen on the left. Scale bar = 80 μm.

(B) Similar projection of another motoneurone, reoriented to show the ventral root and the Lucifer Yellow filled axon (arrows) leaving the cord. In the cell, the soma and proximal dendrites show a strong dorso-ventral polarity. Scale bar = 80 μm.

(C) High power (x60/1.4 oil-immersion) view of a motoneurone soma and primary dendrites at P2. The entire somatodendritic surface is covered in appendages. Most are fine and hair-like (arrows) but some are stubbier. Many filled somata, though by no means all, bore such appendages at this stage. Scale bar = 10 μm.

(D) High power view of proximal (second order) dendrites at P2, clearly showing long, hair-like appendages (arrows), many of which are almost perpendicular to the main axis of the dendrite. Scale bar = 10 μm.

(E) Distal (fourth order) dendrites viewed at the same scale showed more complex surface features. Here they include long hairs (arrows), short club-like extensions resembling classical dendritic spines (arrowheads), an incipient dendritic branch point (open arrow) and a classical growth cone with filopodia (star). Scale bar = 10 μm.

(F) In some cases, distal dendrites also adopted patterns of branching and fasciculation, with immature side-branches. Scale bar = 10 μm.

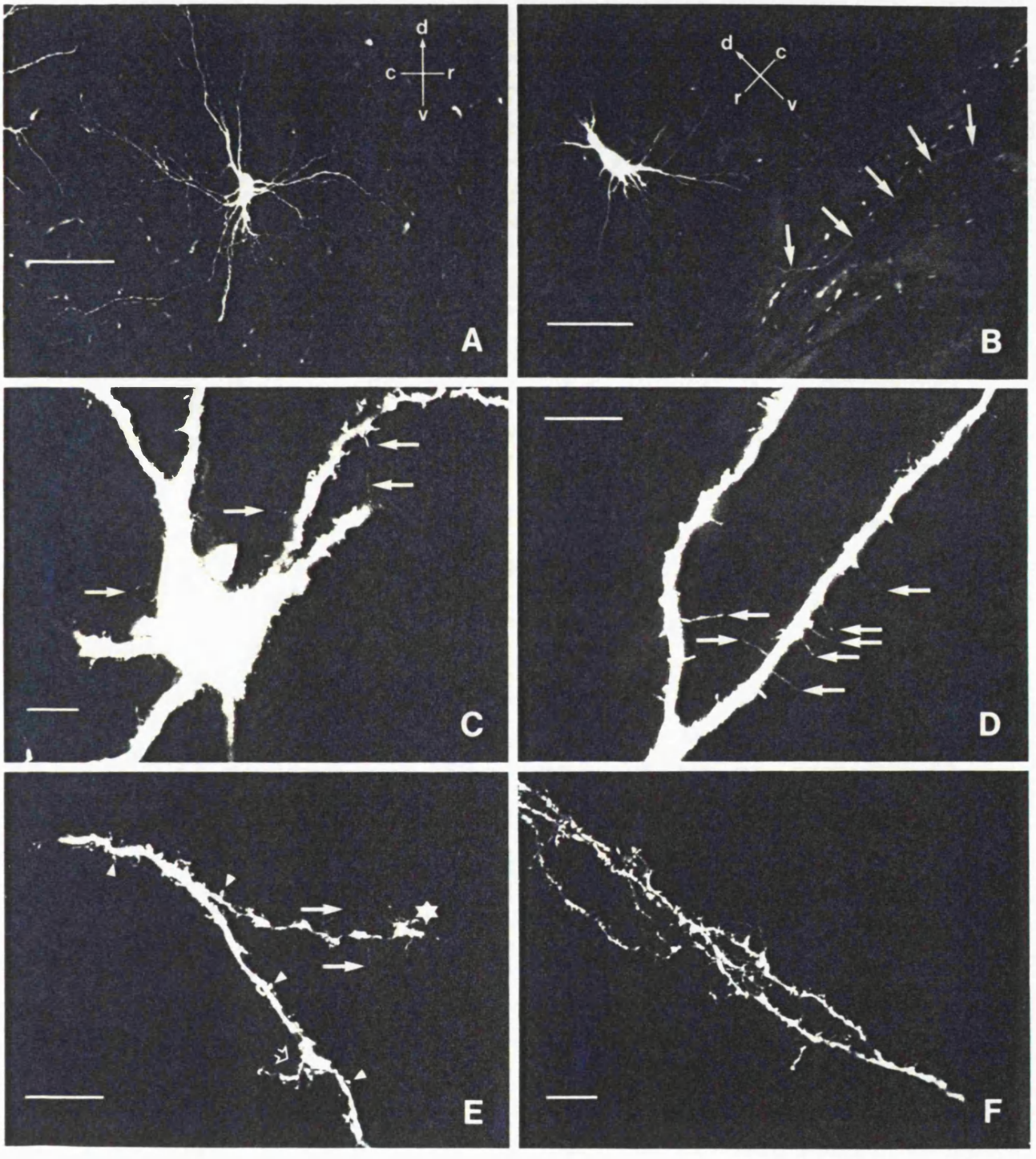
d
c
r
v
A
d
c
r
v
B
C
D
E
F

Figure 2.9 Laser scanning confocal microscope images of postnatal ankle flexor motoneurones, filled with Lucifer Yellow on P8 or P9.

(A) Low power projection of a P9 motoneurone, together with dendrites from others lying rostral and caudal to it in the pool. Compass points mark the dorsal, rostral, ventral and caudal axes. A prominent 'spray' of slender, almost parallel dendrites extends dorsally (to the right). By comparison, the dendrites passing rostroventrally and caudoventrally are thicker. Scale bar = 80 μm.

(B) High power(x60/1.4 oil-immersion) view of a motoneurone soma and primary dendrites at P9, comparable to Figure 2.8c at P2. The surface is smooth with no sign of the hairs and spiny appendages seen earlier. From P4 onwards, none of the somata showed such appendages. Scale bar = 10 μm.

(C) High power view of proximal dendrites at P8, comparable to Figure 2.8d on P2. The surface is free of prominent hairs and relatively smooth, though some processes remain (arrows). Scale bar = 10 μm.

(D) High power view of distal dendrites at P8, comparable to Figure 2.8f on P2. These dendrites show varicosities and a few short lateral spines, but lack the exuberant processes seen soon after birth. Scale bar = 10 μm.

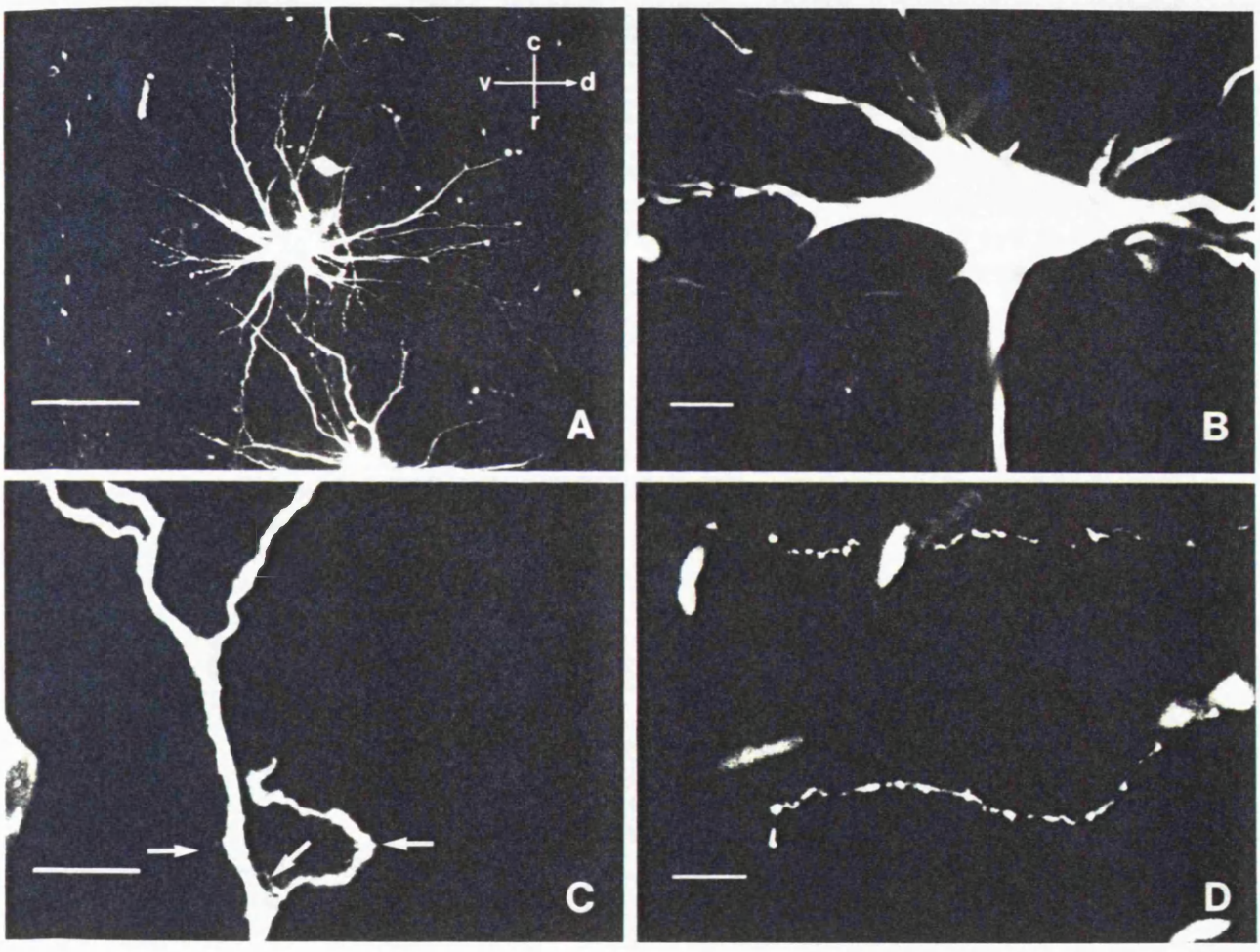
c
v
d
r
A
B
C
D

Figure 2.10 Postnatal changes in the incidence of exuberant surface features on different regions of ankle flexor motoneurones. The elimination of hairs and spiny appendages can be seen to proceed from the soma outwards and presumably continues well beyond the latest age studied. For each region, incidence is expressed as a percentage of the number of cells filled and judged to be well enough filled *in the region* to be scored. This number ranged from 96 for the soma to 81 for the distal dendrites.

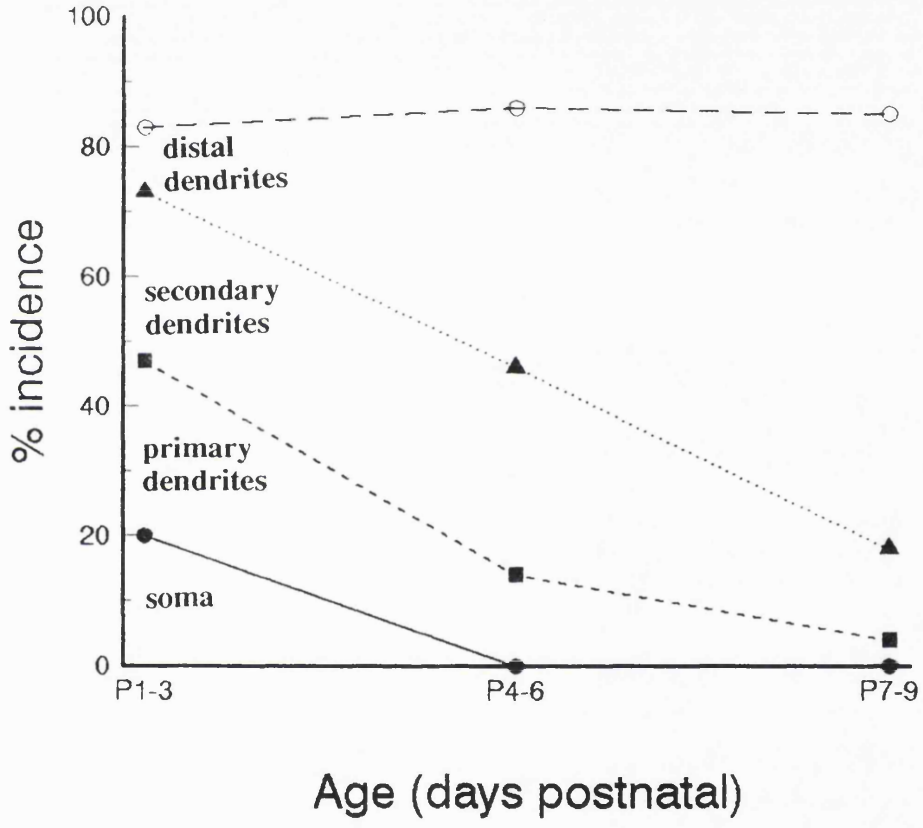
100
80
60
40
20
0
% incidence
distal
dendrites
secondary
dendrites
primary
dendrites
soma
P1-3
P4-6
P7-9
Age (days postnatal)

Figure 2.11 Histograms of soma areas of motoneurones of the tibilalis anterior/extensor digitorum longus (TA/EDL) motor pool retrogradely labelled with HRP from the hindlimb. One animal at each of the ages P1, P7, P14 and adult. The soma areas of retrogradely filled motoneurones were measured using camera lucida and a graphics tablet interfaced with a microcomputer. Only those cells that had a nucleolus (see Fig. 2.7c) were measured. The number of motoneurones measured in each animal at each age is shown. Considerably fewer motoneurones were measured in the animal at P1 (n=22, compared with n=126 in adult). This is due to the difficulty in reliably injecting young muscles with HRP and avoiding spread to other muscles. Only cells considered to be well within the limits of the TA/EDL motor pool were included.
The mean soma area of motoneurones at P1 is 404.6 ± 98.6 μm^2 (mean ± SD) and at P7 is 320.5 ± 88.2 μm^2. The mean soma area at P14 is 628.9 ± 137.0 μm^2 and in the adult is 1027.9 ± 324.8 μm^2.

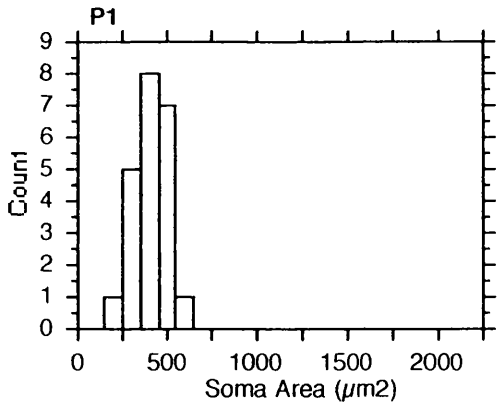

n=22

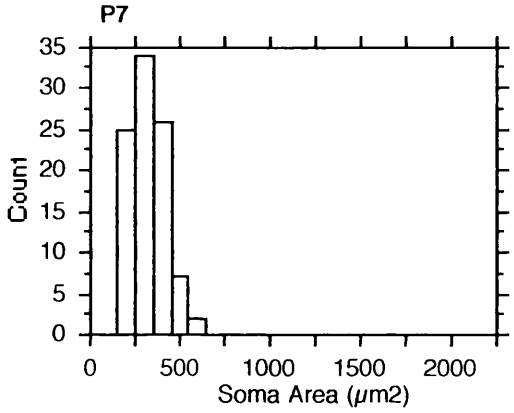

n=94

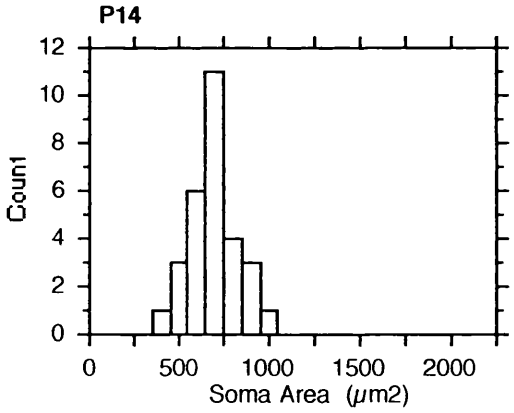

n=29

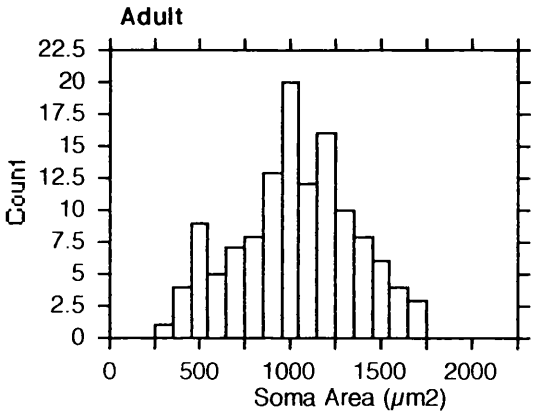

n=126

Figure 2.12 Histograms of soma areas of all HRP filled motoneurones of the tibialis anterior/extensor digitorum longus motor pool from the hindlimbs of animals at P1 (n=132), P7 (n=344), P14 (n=215) and adult (n=288). These results are also shown in Table 2.2.

There is no significant growth of soma areas of motoneurones during the first postnatal week (P1-P7). The mean soma area of motoneurones at P1 is 371.7 ± 110.3 μm^2 (mean ± SD) and at P7 is 283.0 ± 110.1 μm^2. After this, at P14, there is a significant increase in the soma area of the motoneurones. The mean soma area at P14 is 781.6 ± 280.9 μm^2 and in the adult is 1226.8 ± 368.4 μm^2.

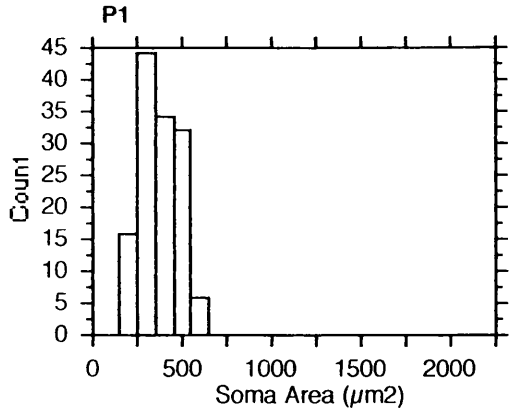

n=132

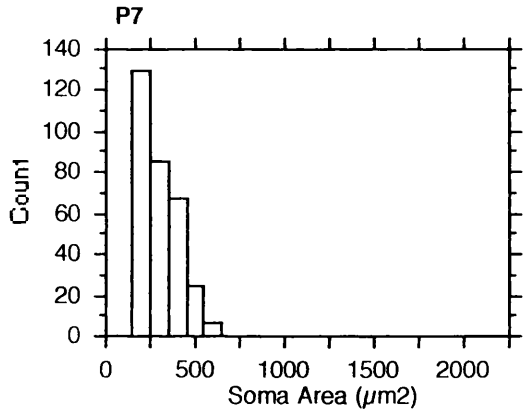

n=344

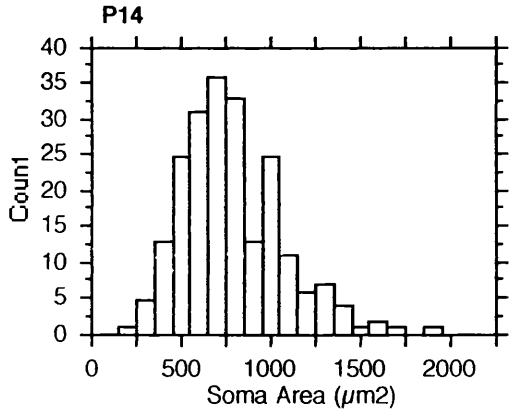

n=215

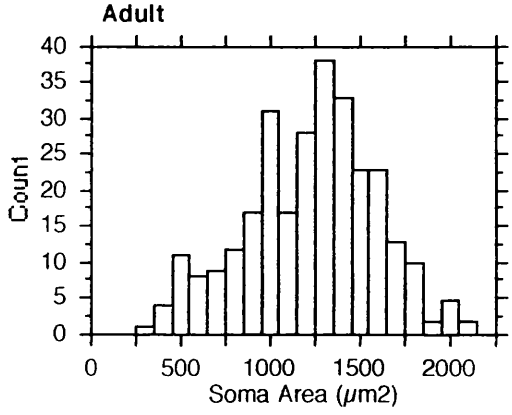

n=288

Figure 2.13 Scatter plot of the sum of the individual diameters of all primary dendrites arising from each motoneurone against the mean soma diameter, for the 17 neurones of Table 2.3. The diagonal line represents the linear regression of the combined dendritic diameter on soma diameter: the slope is 0.903 and the intercept -1.4 μm. The results of Spearman's rank correlation test are given in the text.

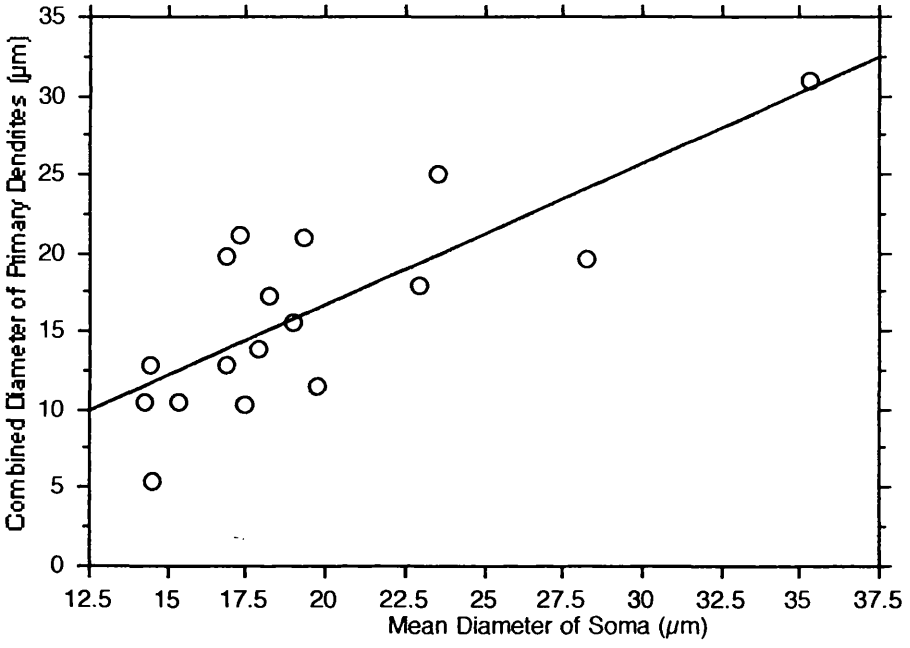
Combined Diameter of Primary Dendrites (µm)
35
30
25
20
15
10
5
0
12.5
15
17.5
20
22.5
25
27.5
30
32.5
35
37.5
Mean Diameter of Soma (µm)

Figure 2.14 Scatter plot of individual diameters of primary dendrites arising from a motoneurone against the combined length *of that dendrite*, for the 17 neurones in Table 2.3. The diagonal line represents the linear regression of the dendritic diameter on dendritic length: the slope is 80.2 and the intercept 192.9 μm. The results of Spearman's rank correlation test are given in the text.

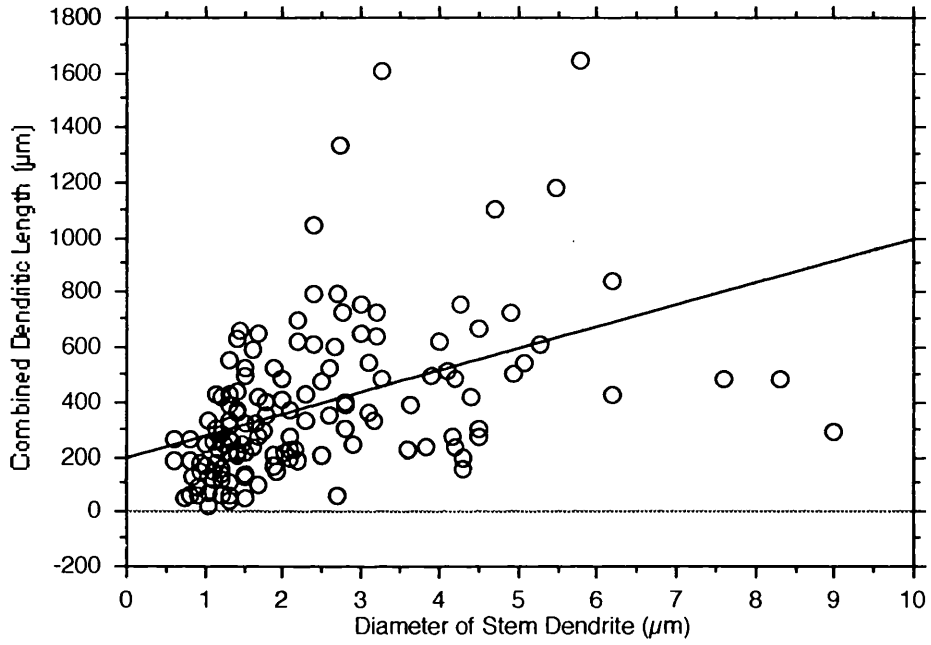
Combined Dendritic Length (µm)
1800
1600
1400
1200
1000
800
600
400
200
0
-200
0
1
2
3
4
5
6
7
8
9
10
Diameter of Stem Dendrite (µm)

Figure 2.15 Sholl diagram (Sholl, 1953) showing the extent of dendritic outgrowth as a function of distance from the soma for ankle flexor motoneurones at P2 an P9. The vertical scale denotes dendritic intersections per 20 μm increment of radius, expressed as a percentage of all such intersections.
(A) At P2 intersections with dendrites in the ten cells analysed were commonest 60 μm and 80 μm from the soma. However, some dendrites (usually dorsal) extended beyond 200 μm.
(B) At P9 the same method of analyses applied to five cells detected only a very modest shift to longer radial distances.

A Sholl Analysis P2

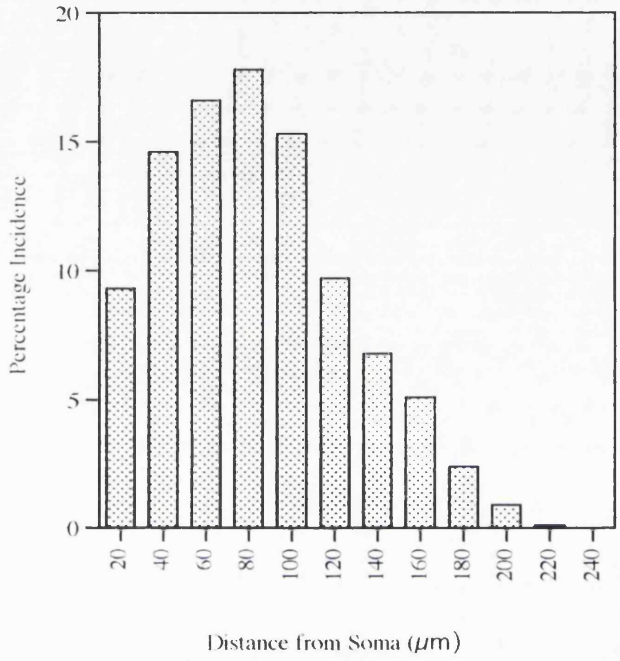

B Sholl Analysis P9

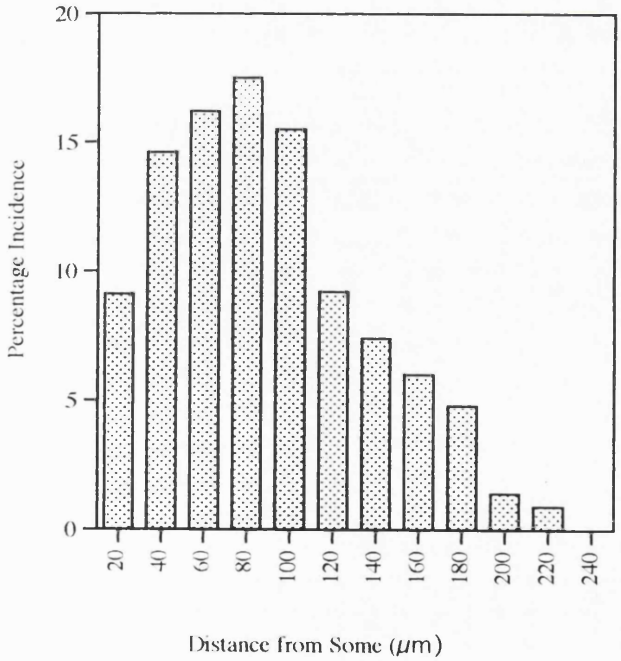

Figure 2.16 Circular graphs showing the summed dendritic distribution of identified flexor motoneurones (**A**) at P2 (10 cells) and (**B**) at P9 (5 cells). D, V, C and R denote the dorsal, ventral, caudal and rostral axes. Each point represents a length that is proportional to the dendritic density (in the plane of the image projection) within one 30 ^{o} sector around the soma. To measure this density, all the intersections between dendrites and concentric circles spaced at 20 μm intervals (as for Sholl analyses but sector by sector) were counted and summed within each sector. The scale denotes intersections per sector as a percentage of total intersections. No significant changes with age were found, but dendrites at both ages showed a consistent dorso-ventral polarity, as in Figure 2.8b, and a significant dorsal bias (see text). The long dorsal point at P9 (**B**) represents a general trend for dorsal dendrites to be not only longer but also more numerous and grouped into a 'spray', as in Figure 2.9a. This 'spray' was also quite well aimed: the sectors flanking the most dorsal one were in more densely populated by dendrites than some on the ventral side.

A Orientation P2

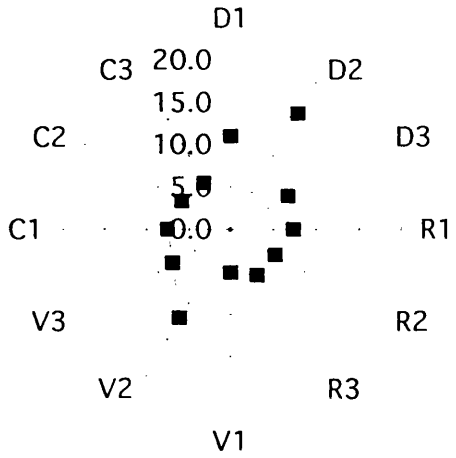

B Orientation P9

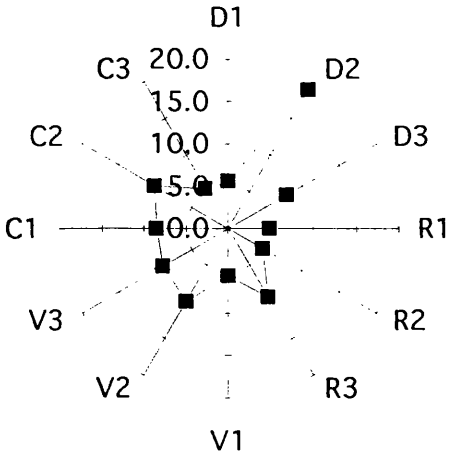

Table 2.1

Morphometric characteristics of the soma and primary dendrites of Lucifer Yellow filled ankle flexor motoneurones during early postnatal development[*].

Age (days)	Number in group	Projected soma area (μm^2)	Mean diam. of soma (μm)	Number of primary dendrites	Mean diam. of primary dendrites (μm)
P1-3	n=60	342.2 ± 131.4	17.9 ± 0.6	8.1 ± 0.3	1.9 ± 0.1
P4-6	n=20	359.7 ± 102.5	16.6 ± 0.3	7.4 ± 0.4	2.1 ± 0.1
P7-9	n=16	410.4 ± 193.3	19.2 ± 3.5	8.3 ± 0.5	2.0 ± 0.5

[*]Values for each parameter correspond to the mean and standard deviation in each age group.

Table 2.2

Soma areas of ankle flexor motoneurones retrogradely labelled with horseradish peroxidase from postnatal day 1 to adult[*].

Age (days postnatal)	**1**	**7**	**14**	**Adult**
Soma Area (μm^2)	371.7 ± 110.3	283.0 ± 110.1	781.6 ± 280.9	1226.8 ± 368.4
Number of cells	n=132	n=344	n=215	n=288

[*]Values correspond to the mean and standard deviation in each age group.

Table 2.3

Morphometric characteristics of individual reconstructed Lucifer Yellow filled ankle flexor motoneurones during early postnatal development.

Age	Max/min diam.	Mean diam. (μm)	Projected area (μm2)	Number	Combined diam. primary dend. (μm)	Mean diam. (μm)	Max. branch order	Max. distance from soma (μm)	Diam. distal dendrites (μm)	Combined dend. length (μm)	Surface area of dend. (μm2)	Total memb. area (μm2)
2	1.2	16.9	185.7	8.0	19.7	2.5	6	237.2	0.4	2702.2	8366.9	8552.6
2	1.3	19.0	341.0	7.0	15.5	2.2	7	184.5	0.5	1981.4	5185.0	5526.0
2	1.5	14.4	245.7	8.0	12.9	1.6	5	200.6	0.6	1950.8	5354.8	5600.5
2	2.4	18.2	263.7	6.0	17.3	2.9	6	293.3	0.7	3833.5	10759.8	11023.5
2	1.4	19.7	342.5	9.0	11.5	1.3	4	237.2	0.7	1938.0	5238.1	5580 6
2	1.7	14.5	174.1	5.0	5.4	1.1	4	242.3	0.6	807.5	2027.3	2201.5
2	3.3	14.3	168.3	9.0	10.5	1.2	4	232.1	0.6	3093.2	7499.9	7668.3
2	2.5	17.9	218.9	9.0	13.8	1.5	7	209.1	0.6	7415.4	3338.3	3557.2
Mean	**1.9 ± 0.7**	**16.9 ± 2.2**	**242.5 ± 69.8**	**7.1 ± 1.5**	**13.4 ± 4.3**	**1.8 ± 0.6**	**5.5 ± 1.2**	**229.5 ± 33.1**	**0.6 ± 0.1**	**2965 ± 2013**	**9721 ± 9889**	**6214 ± 2806**
4	1.4	17.3	264.4	9.0	21.2	2.4	5	172.6	0.7	8553.6	28678.9	28943.4
4	2.0	23.5	488.4	7.0	25.0	3.6	5	223.6	0.7	2929.1	10305.4	10793.8
4	2.3	35.3	535.4	9.0	30.9	3.4	7	193.0	0.7	2978.4	12892.7	13428.0
7	1.3	22.9	511.5	6.0	18.0	3.0	5	244.0	0.7	2548.3	7535.3	8046.8
7	1.4	16.9	465.9	8.0	12.9	1.6	4	136.9	0.7	2947 8	7054.1	7520 1
Mean	**1.7 ± 0.4**	**23.2 ± 7.4**	**453.1 ± 108.6**	**7.8 ± 1.3**	**19.8 ± 8.0**	**2.8 ± 0.8**	**5.2 ± 1.1**	**195.9 ± 44.1**	**0.7 ± 0**	**3991 ± 2556**	**13293 ± 8915**	**13746 ± 8818**
9	1 8	19.3	356.9	9.0	21.0	2.3	7	227.0	0.8	3297.2	9296.4	9653.3
9	2.0	28.2	693.6	9.0	19.6	2.2	5	197.2	0.5	2446.3	5613.1	6306.7
9	2.2	17.5	161.1	8.0	10.3	1.3	6	234.6	0.8	3485.9	8239.8	8400.8
9	2.6	15.4	164.7	9.0	10.4	1.2	6	149.6	0.8	2132 7	5004.0	5168.8
Mean	**2.2 ± 0.3**	**20.1 ± 5.6**	**344.1 + 250.3**	**8.0 ± 0.5**	**15.3 ± 2.8**	**1.7 ± 0.6**	**6.0 ± 0.8**	**202.3 ± 38.5**	**0.7 ± 0.1**	**2841 ± 654**	**7038 ± 2059**	**7382 ± 2029**

3. MORPHOLOGY OF RAT FLEXOR MOTONEURONES FOLLOWING NEONATAL INJURY

3.1. INTRODUCTION

3.1.1. Target dependence of neonatal neurones

The interaction of the motoneurone with its target muscle is vital for normal development and the maintenance of function in the immature neuromuscular system. Axotomy in the early postnatal period results in varying degrees of death of neurones (Lowrie *et al.*1982; Schmalbruch, 1984; Lowrie *et al.*1987; Burls *et al.*1991; Crews, Wigston, 1990; Romanes, 1946a) in spinal motoneurones; (Sendtner *et al.*1990) in cranial motoneurones (also (Aldskoguis, Risling, 1981; Yip *et al.*1984; Himes, Tessler, 1989) in DRG cells; (Bregman, Goldberger, 1982) in corticospinal neurones; (Cho, So, 1992) in retina). The disruption of the nerve-muscle interaction results in impaired recovery of the target muscle, fast muscles being more effected than slow muscle (Lowrie *et al.*1982; Lowrie *et al.*1987).

There are differences in the magnitude of the response to injury in these different systems. The developmental stage of the cells at the time of injury (Pollin *et al.*1991) and the location of the lesion site affects the amount of death that results (see (Snider *et al.*1992a). The age at which the axotomy is performed greatly influences the response of mammalian neurones to injury. In the hypoglossal nerve of the rat, axotomy at 1 week of age results in 60% death of the motoneurones, whereas an identical procedure at 3 weeks (or in the adult if reinnervation is prevented) only results in 30% death of cells (Snider, Thanedar, 1989). In the facial nerve of the rat, axotomy on postnatal day 1 (P1) results in 80% loss of cells, whereas axotomy in the adult results in only 25% loss of cells (Sendtner *et al.*1990; Yu, 1988). Similarly, injury to developing lumbar motoneurones in the rat before P5, results in up to 70% of the cells dying; after this

critical age less death occurs ((Burls *et al.*1991; Lowrie *et al.*1987; Schmalbruch, 1984) and (Crews, Wigston, 1990), in the mouse). In immature motoneurones, the response of the cells to injury is also faster than in the adult ((Romanes, 1946a; Pollin *et al.*1991) in mouse, (LaVelle, LaVelle, 1958) in hamster). In neonates, the death of the cells happens within a week of the injury (Sendtner *et al.*1990; Yan *et al.*1992; Sendtner *et al.*1992a; Pollin *et al.*1991) whereas the response in adults occurs over several weeks (Snider, Thanedar, 1989). The site and type of injury will also affect the amount of cells that are lost. Axotomy at a site distal to the cell body of the neurone results in less cell death than a proximal lesion (Burls *et al.*1991) and a crush injury results in less death than a cut injury (Kashihara *et al.*1987; Crews, Wigston, 1990). The reason for the improved survival of crushed neurones is possibly that they are able to reinnervate their target and are guided by the remaining endoneurial tubes (Ramon y Cajal, 1929).

Thus, it is clear that the muscle exerts a retrograde trophic influence on the developing motoneurones during a critical period of their development when they are extremely susceptible to injury, as well as in the mature adult muscle (Kuno, 1990). In rat hindlimb flexor motoneurones, the critical period of development when the nerve is especially vulnerable to disconnection from the target, occurs during the first few days of postnatal life. During this time injury to the nerve, in the form of either complete axotomy or crush, results in a loss of up to 60% of the motoneurones form the sciatic pool (Lowrie *et al.*1982; Schmalbruch, 1984). Whether this influence is mediated by a' trophic factor' supplied by the muscle (Sendtner *et al.*1992a; Oppenheim, 1992; Kuno, 1990), or by some factor associated with functional neuromuscular activity (Greensmith, Vrbová, 1989; Connold *et al.*1986; Lowrie, Vrbová, 1992) is still disputed.

3.1.2. Morphological responses to injury

The response of many types of neurones to axotomy has been studied extensively both in adult and immature animals (see (Lieberman, 1971)). These in-

clude enlargement of the soma, nuclear eccentricity, enlargement of the nucleolus, chromolytic response, consisting of dispersal of the endoplasmic reticulum ((Price, Porter, 1972; Johnson, Sears, 1989a), see (Barron *et al.*1971; Lieberman, 1971)). There is an increase in the synthesis of RNA (Watson, 1968a). The number of microglia in the area of the injured neurones increase immediately after injury (Sumner, Sunderland, 1973; Sumner, 1976) and astrocytes proliferate and surround the injured neurones (Watson, 1974; Watson, 1972). After injury to the sciatic nerve, a transient increase in the area of the soma has been observed (Swett *et al.*1991). This returns to normal at later times after injury. However, whilst there is some evidence that the results of injury in the adult can be reversed if reinnervation is permitted (Sumner, Sunderland, 1973; Sumner, Watson, 1971; Sumner, 1976), there may be also be more long-term effects (Bowe *et al.*1989). In rats, 12-15 months after sciatic crush there is a change in the distribution of retrogradely labelled motoneurones in the sciatic pool, becoming more clustered (Bowe *et al.*1988). There is also an increase in the mean soma area of injured motoneurones after long-term survival following adult injury. These changes are progressive and take place even after the axons have reinnervated their target muscle. Indeed, dendritic thickening was only observed at longer intervals after injury, long after reinnervation had occurred (Bowe *et al.*1992).

The response of neonatal neurones to injury is different to that of adults (Lieberman, 1971; Bowe *et al.*1989). LaVelle and LaVelle (LaVelle, LaVelle, 1958), observed the response of hypoglossal neurones in the hamster to injury. They suggested that the response of neurones to injury depended on their maturity, and that after a critical period of development they reacted as adult neurones. The initial reaction to injury in early development was nucleolar loss without chromatolysis and early death of neurones. After P7, injury results in chromatolysis without swelling of the cell or changes in the structure of the nucleolus and about 40% of the cells survive (LaVelle, LaVelle, 1958). After 15 days postnatal injury resulted in somatic swelling, and as in the adult, the major-

ity of the cells survived. In hypoglossal motoneurones, the reaction of the nucleus and cytoplasm after injury to the hypoglossal nerve in young and adult rats was compared (Borke, 1983). Nuclear eccentricity and cytoplasmic infoldings were observed sooner after neonatal injury than injury in the adult. This suggests that there may be a difference in the response of immature and mature neurones to injury. Work in kittens in unidentified lumbar motor pools after ventral root transection (Grant, 1968; Grant, 1975; Grant, Westman, 1968; Grant, 1965), suggests that the motoneurones retract their dendrites distally and display characteristic degenerative features such as swelling and beading. In adult hypoglossal motoneurones, dendritic retraction as a result of peripheral injury has been shown to be reversible (Sumner, Watson, 1971). The effect of injury on dendritic spread in immature motoneurones is different (O'Hanlon, Lowrie, 1993c). The dendritic tree of adult animals that had undergone sciatic nerve crush at birth showed a 30% reduction in dendritic length. This suggests that motoneurones do react to neonatal injury, and that this has long-lasting effects on their dendritic morphology. Neonatal motoneurones are still growing, and the ultrastructure of the cells differs from the adult (LaVelle, Sechrist, 1970). The morphological changes that occur in neonatal neurones after injury are possibly an exaggeration of the normal features of the immature neurone, which result from the increased protein synthesis in the immature neurone at the time of injury.

The role of afferent inputs in the modelling of dendritic form has been clearly shown in the Purkinje cells (Berry, Bradley, 1976b). Following irradiation and elimination of afferent inputs to the developing cells, there is aberrant growth and branching of the dendrites. The pattern of growth of dendrites in mouse spinal motoneurones may be directed by the way in which the growth cones contact the axons making afferent connections with the dendrites (Vaughn *et al.*1974; Vaughn *et al.*1988). The spine-like or hair-like growth associated processes, covering the somatodendritic surface of immature motoneurones, are proposed to be sites of synaptic contact onto the motoneurones (Cummings,

Steltzner, 1984; Vaughn, 1989). During development, these processes are eliminated from the surface of the soma by P5 in the rat, and over the next few days spines are lost from the surface of proximal dendrites, until they remain only distally ((Cummings, Steltzner, 1984; Dekkers *et al.*1994) see also (Ulfhake, Cullheim, 1988b) in cat). It is possible that this synaptic remodelling is involved in the development of dendritic form as well as the maturation of the spinal reflexes and motor function.

Damage to the peripheral nerve at this critical period in development results in damage to the Ia dorsal sensory afferents (Himes, Tessler, 1989; Wang *et al.*1991a; Tessler *et al.*1985), and will affect the maturation of some of the afferent inputs onto the motoneurones. This in turn may affect the morphology of the motoneurone dendritic tree. Following axotomy in the cat there are changes in the electrophysiological properties of the motoneurones which is partly attributed to the 'stripping' of Ia fibres from the surface of the neurone (Mendell *et al.*1976). Additionally, the maturation of a motoneurone is critically dependent on the maintenance of contact with its target (Burls *et al.*1991). Even in the adult, functional neuromuscular connection is crucial for the normal electrophysiological activity of the motoneurones (see (Titmus, Faber, 1990)). After axotomy, the electrophysiological properties of the adult motoneurones become similar to that seen in the immature state (Kuno *et al.*1974). However, after reinnervation in the adult the electrical properties return to normal in most motoneurones (Foehring *et al.*1986) whilst it appears that in immature motoneurones the effects of axotomy are more long-lasting (Navarrete, Vrbová, 1984).

Chapter 2 examined the normal morphological development and dendritic characteristics hindlimb flexor motoneurones (see also (Dekkers *et al.*1990; Dekkers *et al.*1994)) in the neonatal rat. In this Chapter, the effect of disconnection from the target on the survival and maturation of somatodendritic morphology of rat hindlimb flexor motoneurones is examined. Since peripheral nerve injury results in damage to the sensory afferent fibres, the effect of afferent inputs on den-

dritic maturation must also be considered.

3.2. METHODS

The methods used here for intracellular filling of the prelabelled injured motoneurones were identical to those described in Chapter 2, for normal development. The description here will be brief.

3.2.1. Surgery

On the day of birth (P0), the ankle flexor muscles TA and EDL, were bilaterally injected with 1µl of 5% FB/DY, to retrogradely label the motoneurone pool. On P2, allowing time for retrograde transport of the dyes to the motoneurone cell body, the animals were reanaesthetised, and the common peroneal (CP) nerve was crushed unilaterally about 3mm from the entry of the nerve into the TA/EDL muscles (Fig. 3.1). In some cases a few crystals of FB/DY were also crushed onto the nerve in order to enhance the retrograde labelling.

At intervals up to P9 the animals were deeply anaesthetised, decapitated and eviscerated. As previously described (Chapter 2), the spinal cord was exposed from the ventral aspect and cut in the sagittal plane up the midline to separate the hemicords. Dissection and intracellular injection were performed in oxygenated Krebs at room temperature.

3.2.2. Intracellular injection

The prelabelled pool was located visually, and LY was injected iontophoretically into lumbar motoneurones which were selected for clear retrograde labelling with FB/DY, as described in Chapter 2. The motor pool of the operated side of the spinal cord was less distinctly prelabelled than that on the contralateral side.

The criteria to assess the success of the intracellular injection were the same as

described previously. However, it was considerably more difficult to fill motoneurones that had been damaged by axotomy, than normal cells. In addition, there were fewer motoneurones on the operated side of the spinal cord, making it more difficult to select cells for intracellular injection.

After injection, hemicords were fixed for up to one week in fresh paraformaldehyde (4%in phosphate buffer, pH 7.6), then dehydrated through graded ethanol and cleared in methyl salicylate (Sigma). Lucifer Yellow filled cells were examined in the whole mount.

3.2.3. Confocal microscopy and analyses

All filled motoneurones were visualised using a BioRad 600 laser scanning confocal microscope (LSCM). The methods of analyses have been described in detail in Chapter 2. In total, 78 axotomised cells (from 40 animals) were studied. These were compared with data from normal (n=43) from 32 animals and contralateral control cells (n=54) from 32 animals.

The best filled cells, (that is, those that showed at least 4th order branching), were used for Sholl analyses of dendritic branching (Sholl, 1953). The total dendritic length and diameter of all the dendrites were measured. Sholl analyses and orientation after axotomy was compared with that during normal development as described in the previous chapter.

3.2.4. HRP histochemistry

In order to determine the number of motoneurones that died in the common peroneal pool as a result of crushing the CP nerve on P2, retrograde filling with HRP was used. The CP crush was performed exactly as described above, but the animals were allowed to survive until adult (10 -12 weeks postnatal). HRP (Sigma Type IV) was injected into the TA and EDL muscles bilaterally (1 µl HRP per 25 mg of muscle). Excess was immediately mopped up and the wound was sutured.

The animals were left for 24 hours, to allow time for retrograde transport, before being perfused intracardially with 2.5% gluteraldehyde in Millonig's phosphate buffer. The processing for HRP is described in Chapter 2 and Appendix 1.

The number of cells was counted on both the control and operated sides of the spinal cord (distinguished by the pinhole, created by the insertion of a micropin into the dorsal horn on one of the spinal cord) and expressed as a percentage. Only those cells that were considered to be within the CP motor pool and had a visible nucleolus were counted. The soma areas of motoneurones on the operated and control sides of the spinal cord were measured using a graphics tablet interfaced with a microcomputer, and software for morphometric analyses (written by Dr. J.E. Cook, 1993). The soma area of the motoneurones following axotomy was compared with that of normal motoneurones of the same age. Histograms were drawn to show the changes in the soma area following injury and the differences were tested for significance.

The soma areas of motoneurones on the operated and contralateral control sides of the spinal cord in sections counterstained with gallocyanin were counted at P3, P7 and P14. The sections contained motoneurones prelabelled with FB/DY. These were then counterstained with gallocyanin, and only the cells considered to be well within the CP motor pool, and that had a visible nucleolus, were included. The sizes of the motoneurones were presented as histograms and a comparison was made between operated and control cells.

3.2.5. Statistics

The statistical methods used are as described in the Methods of Chapter 2. A Mann-Whitney U test was used to test the difference between two groups of means. A Kolmogorov-Smirnov test was used to test the difference between the number of motoneurones surviving neonatal injury compared to the number of motoneurones in the normal animal.

3.3. RESULTS

3.3.1. General features

Motoneurones supplying the physiological flexor muscles TA and EDL were retrogradely labelled on both sides of the spinal cord by intramuscular injection of FB/DY at birth. Two days later (P2), the common peroneal (CP) nerve was crushed unilaterally, and the morphology of the injured and contralateral control motoneurones was examined at various intervals after the operation.

As described in Chapter 2, the individual fluorescent prelabelled motoneurones were brightly labelled on the lateral aspect of the hemisected spinal cord between L4 and L5 and could be selected for intracellular injection. The nerve crush was performed on P2. There were fewer prelabelled motoneurones visible in the flexor motor pool following injury, making it more difficult to select cells for intracellular injection. The labelling was improved by crushing crystals of the fluorescent dyes onto the CP nerve when the injury was being inflicted. In addition, injured cells were less robust, than normal motoneurones, and were prone to membrane rupture, resulting in dye leakage. The criteria for quality of the filling of the prelabelled motoneurones was the same as described in Chapter 2 for normal motoneurones.

After dehydration and clearing of the wholemounted preparation, individual LY filled cells were clearly seen by conventional epifluorescence microscopy and the laser scanning confocal microscope (LSCM) as previously described. To quantify the features of the motoneurones, the cells were divided into 'compartments' as in chapter 2: (i) the soma, (ii) the primary dendrites, (iii) the distal dendrites.

3.3.2. Cell death in the flexor motoneurone pool after nerve injury

At P3, 24 hours after nerve injury, flexor motoneurones were brightly labelled on both the operated and control sides of the spinal cord. At this time, a few fluorescent microglia-like cells were observed in the region of the motoneurone

pool. At longer intervals (P5-P9) there was an apparent reduction in the number of retrogradely labelled motoneurones on the injured side of the spinal cord. In some experiments crystals of FB/DY were crushed directly onto the nerve at the time of injury to ensure that the retrograde transport of the dyes from the muscle was not reduced due to damage to the nerve. Additionally, the use of gallocyanin-stained sections confirmed that fewer motoneurones were present in the injured flexor motoneurone pool at P7 than at P3, and that the amount of cell death in the second week after injury was not as great as during the first week (data not shown). Figure 3.2 shows a comparison of the retrograde labelling in the control (Fig. 3.2a) and operated (Fig. 3.2b) sides of the spinal cord, 5 days after nerve injury (P7). It can be seen that there are fewer prelabelled motoneurones on the operated side of the spinal cord. A high power image obtained on the LSCM (Fig. 3.2c) shows a motoneurones from the injured side of the spinal cord at P7 surrounded by numerous small microglia. By P7 the area of the motor pool and regions close to it, was densely populated with small fluorescently labelled microglia-like cells. The number of these cells increased during the first week after injury, presumably acquiring the label by phagocytosis of the degenerating injured motoneurones. This has been observed in other studies (Crews, Wigston, 1990). A few microglial cells were occasionally seen on the contralateral control side of the spinal cord. This probably resulted from damage caused to the motor endings during the injection of the fluorescent dyes two days earlier.

Examination of the Nissl stained tissue allowed an estimate of the number of injured motoneurones with eccentric nuclei to be made. At P3, about 29% (n=114) of the injured motoneurones had eccentric nuclei compared to about 13% (n=116) of the contralateral control neurones. The percentage of injured motoneurones with displaced nuclei increased to 47% (n=71) at P7, and at this time eccentric nuclei were observed in 21% (n=99) of the control neurones. By P14 36% (n=43) injured and 13% (n=60) of contralateral control motoneurones had eccentric nuclei. This suggests that nuclear eccentricity is a feature of mo-

toneurones injured at birth. This has previously been shown in the hypoglossal nerve following neonatal injury (Borke, 1983).

The number of motoneurones that died as a result of neonatal injury was assessed 2-3 months later using retrograde transport of HRP. An example of a section from an adult spinal cord, after unilateral nerve crush on P2, is shown in Figure 3.3. It is clear that there are fewer HRP filled motoneurones on the operated side of the spinal cord. Table 3.1 shows that the average number of motoneurones on the injured side of the spinal cord was only 44.1% (range 31-52%) of that on the contralateral unoperated side. The number of motoneurones remaining 2-3 months after neonatal crush injury was compared with the number of motoneurones in the contralateral control side of the spinal cord ($p=0.0366$), the number of motoneurones in a normal adult spinal cord ($p=0.0366$) and the number of cells in normal and contralateral sides together ($p=0.0097$; Kolmogorov-Smirnov test). Thus, common peroneal nerve injury in neonates leads to rapid loss of motoneurones during the first week after injury, resulting in a permanent depletion of more than 50% of the TA/EDL flexor motoneurone pool.

3.3.3. Changes in somatodendritic surface induced by neonatal injury

To study the somatodendritic morphology of the surviving flexor motoneurones during the time when some of then were degenerating, individual motoneurones were injected intracellularly with Lucifer Yellow and examined on a confocal microscope. Figure 3.4 illustrates the appearance of the soma, proximal and distal dendrites of an injured motoneurone at P7, and two control motoneurones at P3 and P7. As described previously, during normal development (see Chapter 2), at P1-3, the soma (Fig. 3.4a) and dendrites (Fig. 3.4d,g) are covered by numerous growth associated processes. The processes located proximally were filopodial-like; up to 8 mm long and 0.5 mm in diameter (Fig. 3.4d) whereas those on more distal dendrites were shorter (up to 4 mm long) and more irregular (Fig. 3.4g). The dendrites terminated in either growth cone-like lamellipodial

structures (Fig. 3.4g open arrows) or, more often, tapered to a point .

During normal development, growth associated processes were mostly eliminated from the soma by P4, and were totally absent by P7 (compare Fig. 3.4a and 3.4b). These processes also disappeared from the primary dendrites (compare Fig. 3.4d and 3.4e) However, after neonatal injury, the elimination of the growth associated processes was halted, so that at P7 there was a clear difference between the appearance of injured and normal motoneurones (compare Fig. 3.4b,e,h with Fig. 3.4c,f,i). The somatic membrane of injured motoneurones at P7 was covered by a large number of spine-like processes, 3 μm or more in length and 0.5 μm in diameter, as found in normal cells of an earlier developmental stage (compare Fig. 3.4a with Fig. 3.4c). The growth associated processes found on proximal dendrites (Fig. 3.4f) appeared to be even longer and more numerous than those found during normal development at P1-3 (Fig. 3.4d). There were also many growth cone-like structures, some of which bore lamellipodial outgrowths (Fig. 3.4f). The processes on the distal dendrites of injured motoneurones (Fig. 3.4i) were similar to those at the same age during normal development (Fig. 3.4h).

To provide a more quantitative comparison of somatodendritic maturation in control and injured cells, the incidence of growth associated processes on the soma, primary dendrites, secondary dendrites and distal dendrites was systematically studied in a group of adequately stained motoneurones. These results are shown in Figure 3.5, where the incidence of growth associated processes is plotted as a function of age for injured (Fig. 3.5a) and contralateral unoperated motoneurones (Fig. 3.5b). Throughout the period studied, growth associated processes on injured motoneurones were present on all orders of branching, from primary to distal dendrites. However, the most striking difference was seen in the soma, where the incidence of growth associated processes remained highest, at about 50% to 60% between P3-P6, and declined slightly to about 40% at P7-P9 compared to a near complete elimination in contralateral control

motoneurones (Fig. 3.5b) and normal cells (Chapter 2). This is also clearly seen in Figure 3.4 which shows motoneurones from the injured (Fig. 3.4c) and contralateral unoperated side (Fig. 3.4b) of the spinal cord in a P7 rat. The soma of the contralateral control motoneurone has a smooth surface, whilst that of the injured cell from the operated side of the spinal cord in the same animal, was covered in many growth associated processes. These results suggest that neonatal nerve injury halts the elimination of the growth associated processes which normally occurs during the first postnatal week (Chapter 2). Whether elimination of the growth associated processes is completed in the motoneurones that survive nerve injury and reinnervate their target muscles is not yet known.

3.3.4. Dendritic sprouting after neonatal nerve injury

In a few cases long, fine, unbranched dendritic processes were observed, which often originated from proximal dendrites (Fig. 3.6a, arrows). These thin branches 'sprouted' from the soma and proximal dendrites dendrites, and continued for distances, up to 200 μm or more without forming branches. They often crossed other dendrites at unusual trajectories and could not be traced to their site of termination. The proximal origin and appearance of these processes is similar to the dendritic sprouts described by Havton and Kellerth (Havton, Kellerth, 1987) after axotomy in adult cats. They have not been previously described after distal nerve injury either in adult or immature animals.

There is also an increase in the incidence of growth cone-like (Fig. 3.6b) and lamellipodial processes (3.6c, d, arrows). Some of these processes are long, and have the appearance of dendrites.

3.3.5. Features associated with neuronal degeneration

Since a large fraction of motoneurone death after neonatal nerve injury probably occurs during the first week after injury (Yan *et al.*1992; Sendtner *et al.*1992a), I sought to determine whether a proportion of the sampled cells dis-

played features associated with neuronal degeneration. Figure 3.7 shows examples of pathological changes of motoneurone somatodendritic morphology following injury. The cell shown (Fig. 3.7a,c) illustrates the presence of dendritic varicosities in both primary (see detail in Fig. 3.7c) and more distal dendrites (Fig. 3.7a, arrows) seen in some of the injured motoneurones. Varicosities were observed on both proximal (primary and secondary) dendrites in 39% of the cells and on distal dendrites in 84% of the cells. Dendritic varicosities were not observed in proximal dendrites of flexor motoneurones during normal development or in the contralateral side to the injury, though in a few cases varicosities were seen in distal dendrites of normal motoneurones. The presence of these features, though not observed in the whole population studied, does suggest that some cells undergo changes in response to injury.

Abnormal, trichotomous branching was seen in a few cells (Fig. 3.7b, arrow). This is a departure from the normal dichotomous pattern of branching that is observed in healthy cells of the same age.

3.3.6. Changes in size of the motoneurones following neonatal injury

To determine whether neonatal injury influenced the dimensional growth of the soma and dendrites, a comparison was made between injured motoneurones and those from the contralateral side and normal unoperated animals. Table 3.2 shows the morphometric characteristics of the intracellularly filled motoneurones following injury in 78 cells. Over the period studied there was no significant difference in the soma area of the intracellularly filled injured motoneurones compared to either contralateral or normal neurones. The mean area of the soma changed from 380.4 ± 135.0 μm^2 at P3, to 434.5 ± 208.5 μm^2 at P7-9, but these values were not significantly different for contralateral controls or normal controls at the same ages. Additionally, there was no significant difference between the sizes of injured motoneurones at P3 and P7. Figure 3.8 shows histograms of the soma area of intracellularly filled motoneurones over the period P3-P9. The soma areas of motoneurones from pooled injured mo-

toneurones over the period P3-P9 had a mean value of 403.8 ± 175.2 μm^2 (Fig. 3.8a), those for normal had a mean soma area of 385.6 ± 141.9 μm^2 (Fig. 3.8b), and contralateral controls had a mean soma area of 347.8 ± 119.3 μm^2 (Fig. 3.8c). These values were not significantly different. As the size of the sample of intracellularly labelled cells was relatively small, similar measurements of soma area were made using gallocyanin-stained sections of spinal cord (Fig. 3.9). It was not possible to use retrograde filling of HRP in young injured motoneurones as there was excessive spread of the dye to neighbouring muscles, so counterstained sections were used.

At P3 the mean soma area of injured motoneurones was 431.6 ± 106.8 μm^2; this increased to 562.1 ± 270.4 μm^2 at P7 and by P14 the mean soma area was 843.0 ± 344.0 μm^2. The results are shown in Table 3.3. There is a significant difference between the mean soma area at P3 and P7 in the contralateral control ($p<0.0001$) and injured motoneurones ($p<0.006$; Mann-Whitney U test). There is also a significant difference in the mean soma area of both control and injured motoneurones from P7 to P14 ($p<0.0001$ and $p<0.0001$ respectively). The period of greatest growth of the motoneurones occurred after P7. There was no significant difference in the sizes of control compared to injured motoneurones at either P3, P7 or P14. The soma area of motoneurones at P3, P7 and P14 in both injured and contralateral control sides of the spinal cord are shown in Figure 3.9. This shows histograms of the sizes of motoneurones on the injured (Fig. 3.9a,b,c) and contralateral control (Fig. 3.9d,e,f) sides of the spinal cord at P3, P7 and P14. After injury, the mean soma area did not change significantly from contralateral control cells.

The sizes of the motoneurones 10-12 weeks after injury were measured using retrograde filling with HRP after crushing the common peroneal nerve at P2. The results are shown in Table 3.4 and Figure 3.10. There is a significant difference in the sizes of injured motoneurones and both normal and contralateral control cells ($p<0.0001$ and $p<0.0005$ respectively). The motoneurones that

survive neonatal injury are smaller than normal motoneurones and the injury has resulted either in shrinkage of the cells or selective death of larger motoneurones.

In some motoneurones, 1-3 of the primary dendrites appeared to be larger (up to 4 μm in diameter) than others (Fig. 3.7b). The mean diameter of primary dendrites at P3 was 2.2 ± 0.8 μm and at P7 was 2.1 ± 0.8 μm (see Table 3.2). This was not significantly different from either the contralateral or normal controls. The mean number of the primary dendrites of injured motoneurones at P3 was 8.4 ± 1.4 μm and at P7 was 8.2 ± 1.8 μm. This did not differ significantly from contralateral or normal controls.

Eight motoneurones, 4 at P3 and 4 at P7 were selected for apparently complete dendritic filling and were reconstructed from serial optical sections. The results are presented in Table 3.5. This shows measurements of the soma, primary and distal dendrites. Despite the small size and age-range of this group, a comparison was made with the some of the parameters from normal motoneurones (Table 2.3, Chapter 2). The mean combined dendritic length at P3 in injured motoneurones was 2444 ± 875 μm, and that at P2 in normal motoneurones was 2965 ± 2013. This was not statistically significant. The total membrane area of injured motoneurones at P3 was 2083 ± 1120 μm^2 and at P7 was 8360 ± 6771 μm^2; that of normal motoneurones at P2 was 6214 ± 2806 μm^2 and at P7 was 7783 ± 372 μm^2. There is no significant difference between injured and normal motoneurones.

The correlation between the mean soma diameter and the combined diameter of the primary dendrites for the 8 selected motoneurones, is not significant (see Fig. 3.11). However, the correlation between the diameter of the stem dendrite and the combined length of that dendrite (R_S=0.743; $p<0.0001$; Spearman's rank correlation test) is significant (Fig. 3.12). Thus, it appears that there is a change in the relationship between the soma and primary dendrites immediately following neonatal injury, whilst that between the diameter of the primary den-

drite and its combined dendritic length remains.

The primary dendrites projected around the soma of the motoneurones. Dendrites extended for 139.3 to 327 μm from the soma. The maximum branch order of the dendrites was from 4 to 6 orders of branching.

3.3.7. Spatial analyses of dendritic trees

Sholl analyses were performed on the dendritic trees of 8 motoneurones (4 at P3 and 4 at P7), to show if there were any changes in the relationship between the dendritic branch number and the distance from the soma following neonatal injury. Figure 3.13 shows Sholl histograms for motoneurones at P3 (Fig. 3.13a) and P7 (Fig. 3.13b). At both ages the greatest number of intersections occurred at 60 μm from the soma. At P3 the maximum dendritic length was 180 μm and at P7 the maximum length was 200 μm. At P7 there was also a greater number of intersections between 60-120 μm from the soma than at P3. Figure 3.14 shows Sholl analyses of pooled data of the 8 injured motoneurones at P3-P7 (Fig. 3.14a) and the 14 normal motoneurones at P2-9. After injury the greatest number of intersection was 60 μm from the soma; in the normal motoneurones maximum branching was 80 μm from the soma. Sprouting was observed, from the soma and primary dendrites, following neonatal injury. The increased incidence of proximal branching that was observed may have reflected this. The sample of motoneurones was very small, however.

Analyses of the orientation in the parasagittal plane was done by counting the number of dendritic intersections for 12 sectors of 30^{o}, and pooling the data into quadrants so that each quadrant was composed of 3 sectors each, at P3 and P7 (Fig. 3.15). There was no significant difference between injured motoneurones at P3 and P7. Additionally, the dorsal bias observed during normal development was still present ($p=0.128$, $p=0.036$, $p=0.066$; Mann-Whitney U tests for dorsal against rostral, ventral and caudal respectively for pooled data at P3 and P7). Figure 3.16 shows the pooled data for the orientation of injured mo-

toneurones (P3-7) and control motoneurones (P2-9). During normal development the dorsal bias is strong, being predominantly in the most dorsal sector, D2. After injury this bias is not as clear, though it does still exist. A comparison was made between the orientation during normal development and that after neonatal injury for pooled data. There was no significant difference in the dorsal, rostral, ventral or caudal orientations following injury. Neither was there any significant difference between the orientation of the dendrites after injury at P3 compared to P7. Thus, from this data it would appear that the factors influencing the growth of motoneurone dendrites into the dorsal sector are still present, and injury does not result in any significant changes in the orientation of the dendrites.

3.4. DISCUSSION

Injury to the sciatic nerve during the early postnatal period has been shown to result in death of 60-70% of the motoneurones innervating the hindlimb muscles (Lowrie *et al.*1987). The present study shows that after injury to the common peroneal nerve on P2 there is also death of over 50% of the motoneurones. The early changes in the somatodendritic morphology of flexor motoneurones during the first week after postnatal injury were studied and compared to motoneurones during the same period of normal development (see Chapter 2).

3.4.1. Microglial response to injury

Microglia were present in the injured motor pool, in small numbers, 24 hours after the crush was performed. Figure 3.2 shows that by P7, there were many more microglia-like cells present in the region of the injured motor pool. These cells were intensely labelled with the fluorescent dyes FB/DY, which were previously restricted to the prelabelled motoneurones This suggests that the microglia had ingested the dyes during phagocytosis of the injured motoneurones. The fact that microglia were occasionally observed on the contralateral side of

the spinal cord may be due to damage inflicted to some of the motor endings within the muscle during the injection of the prelabel into the muscle. The presence of microglia has been described previously using fluorogold labelling after limb amputation (Crews, Wigston, 1990). Microglia are proposed to have a phagocytic role in the developing central nervous system (Perry *et al.*1985). They respond to the production of cellular debris during development. It has been shown that the number of microglia increases in some regions of the developing brain that are undergoing cell death (Ashwell, 1991). The expression of class II MHC antigens in small cells which express the microglial marker OX-42, in the region of degenerating motoneurones indicates that these cells may be activated and are involved in phagocytosis (Greensmith, Navarrete, 1991). Microglia are thought to arise from macrophages that invade the region of dying neurones (Perry, Gordon, 1988). Such cells were observed closely apposing the motoneurones. Additionally, microglia have been shown to have a neurotoxic effect *in vitro* (Giulian *et al.*1993). It appears that microglia are associated with neuronal cell death in response to many types of injury and disease ((Rio-Hortega, 1939) after stroke, trauma, infection; (Giulian, Robertson, 1990), after ischemic injury to the spinal cord; (McGreer *et al.*1987) in Alzheimer's disease). Therefore, after injury to the common peroneal nerve, the presence of microglia may be associated with the death of the neurones themselves as well as with the process of phagocytosis.

3.4.2. Morphological responses of flexor motoneurones to neonatal injury

Previous studies have shown that neurones respond to injury by displaying distinct morphological characteristics (see (Lieberman, 1971)). However, most work has been done following axotomy in PNS neurons in the adult. It has been suggested that the response of immature cells (LaVelle, LaVelle, 1958; LaVelle, 1973; Schmalbruch, 1984) destined to die after injury may not be the same as the classical reaction, involving chromatolysis, somatic and nuclear swelling, Nissl ((Nissl, 1892) see (Lieberman, 1971)). Swelling possibly occurs

*

NB. There was a significant increase in the soma area of motoneurones between P3 and P7 using counterstained material (see Table 3.3). However, there was no significant difference in the soma size of the Lucifer Yellow filled motoneurones over the same period (see Table 3.2). The size of the group of intracellularly filled motoneurones was much smaller than that of the gallocyanin group. In addition, the process of selection of cells for intracellular injection resulted in sampling. The difference in tissue thickness and clearing methods may partly explain these differences, though no wholly adequate explanation is available.

due to changes in the osmolarity of the cytoplasm of the cell. This may be due to a disruption in the cell membrane, resulting in a change in the ion balance of the cell. It may also result from the altered production of proteins following injury. At the time of injury to the neonate, the activity of the cell and its cytoplasm are directed towards growth and the production of proteins necessary for the creation of new membrane and expansion of dendritic territory. There was not a significant increase in the size of flexor motoneurones in the first 10 postnatal days of development (Chapter 2), when measured in Lucifer Yellow filled identified flexor motoneurones or HRP filled cells. However, somatic growth does occur between P9 and P14 (also (Westerga, Gramsbergen, 1992)). The measurement of gallocyanin counterstained sections showed a significant increase in the soma area of both injured and control motoneurones between P3 and P7 as well as between P7 and P14. These cells were from counterstained sections containing retrogradely labelled motoneurones. Only those cells judged to be well within the limits of the TA/EDL motor pool were included. This was a larger sample of motoneurones than was obtained using either of the other methods, and this could account for the difference. It is also possible that some of the motoneurones included were not CP motoneurones, but were from an adjacent, uninjured pool. The soma area of the rat hindlimb motoneurone increases from about 400 μm^2 to about 2500 μm^2 from birth until adult (this study and (Lowrie *et al.*1987)) and there is a 400% increase in the dendritic membrane area of cat hindlimb motoneurones (Ulfhake, Cullheim, 1988a) from birth until adult. There is evidence of a redistribution of the dendritic branch distribution during development (Bellinger, Anderson, 1987a; Ulfhake *et al.*1988; Nunez-Abades *et al.*1993), specifically in distal dendrites. Clearly there is a substantial amount of protein synthesis occurring during postnatal development. The intrasomatic reactions observed in young hypoglossal neurones following injury, such as nuclear eccentricity and infoldings of the nuclear membrane (Borke, 1983) occur more quickly than after injury in the adult, but are less distinct. They can be described as an exaggeration of the normal features

of immature motoneurones. In this study, motoneurones were observed that displayed abnormal features. Nuclear eccentricity was observed in a greater proportion of the injured cells on P7 when compared with normal cells. Some motoneurones had varicose swellings along the length of dendrites, both proximally and distally. This could be indicative of fragility of the cell membrane as a result of the injury, making it prone to rupture. The increased protein production in young motoneurones may result in a degree of somatic swelling, so that the response of the neurones after injury is not pronounced. This may account for the fact that significant increases in the soma area of the motoneurones or their dendrites, in response to injury was not observed (see Table 3.2). This shows that the mean soma size at P1-3 was 380.4 ± 135.0 μm and at P7-9 was 434.5 ± 208.5 μm. The study extended over only the first 10 days of postnatal life, a short time period, and it is possible that there may be evidence of cellular swelling, or other changes, at a later time. The time period of the study was limited by the thickness of the hemisected spinal cord which made it impossible to inject the motoneurones in the wholemount after P9. There is evidence of effects of injury to the adult nerve being observed in surviving motoneurones at very long periods after injury (Bowe *et al.*1992), even following reinnervation of the target. The effects of neonatal injury to rat flexor motoneurones appear to be long-lasting (O'Hanlon, Lowrie, 1993c). In this study motoneurones that survived a period of disconnection, and successfully reinnervated their target muscle had a significantly smaller soma area than control neurones (see Table 3.4). It has been shown that motoneurones of the rat sciatic nerve have impaired dendritic growth at long periods after neonatal injury (O'Hanlon, Lowrie, 1993c). The activity patterns of these neurones and their muscle has been investigated six months after neonatal injury (Navarrete, Vrbová, 1984). The development of phasic firing patterns of fast motor units is impaired, and there is a resulting shift towards tonic activity. This suggests that the effects of neonatal injury are long-lasting.

Crushing the CP nerve presumably causes damage to the axons of all of the mo-

toneurones within the nerve. Not all of the motoneurones die, but many successfully reinnervate their target muscle. Over 50% of the motoneurones died following neonatal nerve injury (this study and (Lowrie *et al.*1987)). There is virtually no information on the changes in dendritic structures of cells undergoing degeneration. Previous studies, using silver impregnation techniques, have described features of degenerating neonatal motoneurones and their dendrites (Grant, 1975; Grant, 1968; Grant, 1965; Grant, Westman, 1968) in the kitten. Dendritic degeneration has been observed. There is even evidence of a transient increase in dendritic length two weeks after neonatal injury, followed by a retarded growth rate (O'Hanlon, Lowrie, 1993a). However, degenerating cells were not frequently observed. This could be due to the method of selection of motoneurones for intracellular injection with Lucifer Yellow. The prelabelled cells were often indistinct within the motor pool, especially after injury, and in choosing a cell to inject the largest and most clearly visible neurones were selected. This was especially true at P7-P9. Whether this gave an accurate representation of neurones within the motor pool is not possible to assess. Figure 3.9 shows histograms of the soma areas of motoneurones from gallocyanin-stained sections. At P7 the injured motoneurones display 2 peaks in the soma areas, one of neurones with an area of about 300 μm^2 and the other of about 800 μm^2 (Fig. 3.9b). The peak for control motoneurones at P7 is about 750 μm^2 (Fig. 3.9e). This may represent two populations of cell, one destined to die and the other in the process of reinnervation, although these two peaks may be artifactual.

Death of the motoneurones probably occurs in the first week after neonatal injury (this study and (Pollin *et al.*1991)), and so the study covered the period when cells were dying and features associated with degeneration would be observed. Figure 3.7 shows some of the abnormal features, associated with neuronal degeneration, that were observed following neonatal injury to the CP nerve. Varicosities were never observed on the proximal dendrites of flexor motoneurones during normal development (Dekkers *et al.*1994). Varicosities have been described in Golgi-stained tissue after neonatal injury and may be part of

the process of dendritic retraction and neuronal degeneration (Grant, 1968; Grant, 1975; Sumner, Watson, 1971; Grant, 1965). Nuclear eccentricity increased from 13-30% in apparently normal, contralateral control motoneurones between P3 and P7. Eccentric nuclei are a feature of immature hypoglossal, and probably other, motoneurones (Borke, 1983). The incidence of nuclear eccentricity remained at around 33% in injured motoneurones at P3 and P7.

3.4.3. Changes in the somatodendritic surface of motoneurones after injury

The most dramatic response of the motoneurone to injury was observed in the somatic and dendritic growth associated processes, or filopodial hair-like structures. As previously described during normal development (Chapter 2), growth associated processes are eliminated somatofugally. By P9, they remain predominantly on the distal dendrites and have been eliminated from the soma and most of the proximal dendrites. As can be clearly seen in Figure 3.4 and Figure 3.5, this is not the case following axotomy. Growth associated processes were retained on proximal as well as distal dendrites until after P9. There was, in fact, an increase in the incidence of these processes on the soma from 50% at P3 to 60% from P3 to P4-6, declining slightly to 40% at P7-9 (Fig. 3.5). It is not possible to distinguish the two groups of motoneurones that are present in the first week after injury. Some of the motoneurones are destined to die (there are only 44.1% of the motoneurones remaining 2-3 months after injury). The other group of motoneurones consists of those cells that do survive the injury. There is probably a bias towards the selection of large motoneurones that are clearly labelled with the retrograde dyes, for intracellular injection. These may be the motoneurones that subsequently reinnervate their target and survive. The response of motoneurones that are destined to die may be different, and it may only be those cells that are regenerating that display such features. This must represent an immediate period of growth and sprouting of processes from the somatodendritic surface of the motoneurone following injury to the nerve. It is not known if these processes disappear and the normal maturation of the soma-

todendritic surface of the motoneurone is resumed when functional reconnections are re-established with the target muscle. It has been shown that the effects of injury during the neonatal period have both immediate (O'Hanlon, Lowrie, 1993a) and long-lasting consequences on the morphology of the motoneurones (O'Hanlon, Lowrie, 1993c). It is possible that the growth of some of these processes is responsible for the changes in morphology observed in these studies.

Sprouting has been described in the period following axotomy in the adult in many systems ((Cho, So, 1992), in hamster retina; (Linda *et al.*1985), in spinal motoneurones of cat; (Hall *et al.*1989; Hall, Cohen, 1988), in Lamprey central neurones). In these circumstances regeneration of axon-like structures occurs, often from dendritic origins. Axon collaterals and supernumerary axons have been described following injury to the adult (Havton, Kellerth, 1987). Some of the processes observed after neonatal injury to the flexor motoneurones may have been supernumerary 'dendraxons' involved in the attempt to grow an axon and form a connection with the target. The long, unbranched process seen in Figure 3.6c is an example of this. Collateral sprouting of damaged axons was not observed, but this could have been due to the plane of acquisition of the images on the LSCM. Other studies suggest that it is only after very proximal lesion that axon collaterals are seen (Rose, 1991). Some of the motoneurones must regenerate their axons, as a proportion of the motoneurones survive. Another possibility is that not all of the axons are damaged as a result of injury, and it is only the undamaged axons that survive.

In this study, the pattern of dendritic branching of motoneurones following injury did not change (see Figs. 3.13 and 3.15). There was no evidence of the production of the significant number of long processes, or either sprouting or retraction of dendrites as has been described after injury in the adult (Standler, Bernstein, 1982; Bernstein, Standler, 1983), or the changes in morphology observed in the neonate (O'Hanlon, Lowrie, 1993a). However, the number of mo-

toneurones that were measured and analysed was relatively small, and the method did have certain limitations. During the acquisition of images from fluorescent material there was bleaching, especially of distal parts of the dendritic tree. In addition, information was lost in deeper tissue, even using the LSCM. Lastly, the images produced were 2-dimensional representations of 3-dimensional structures, and parts of the dendritic tree were distorted. These factors probably contributed to the incomplete imaging of the motoneurones and may explain why changes in dendritic morphology were not observed.

The majority of the 'sprouting' observed after neonatal injury could be described as a proliferation of growth associated processes on the soma and dendrites of the motoneurones. The retention of these processes and the halting of the maturation of the somatodendritic surface of the neurone are indicative of hasty increase in the production and insertion of membrane and, though it would be difficult to measure accurately, a significant increase in membrane area must result. Many of the growth associated processes were filopodial-like and it would be useful to examine their cytoskeletal elements and ultrastructure. Since immature motoneurones at the time of injury are still actively growing, there may have been a large amount of proteins destined for transport to the areas of the neurone that were expanding. This protein would have been sequestered within cytoplasmic vesicles as described in developing neurones (Landis, 1983; Chang, Reese, 1986) and could be transported and incorporated into the membrane.

The functional significance of the retention of growth-associated processes can only be speculated. There is evidence that motoneurones respond to axotomy by reverting to a growth state (Watson, 1974). After disconnection of the motoneurones with its target, there is an increase in the production of DNA (Watson, 1968b) and of proteins (Watson, 1970). Motoneurones during the neonatal period are still growing, and production of proteins is high. The loss of connection of the motoneurones with its target may prolong or halt the matura-

tion of the protein synthetic machinery of the cell, and result in the maintenance and even proliferation of the growth associated processes.

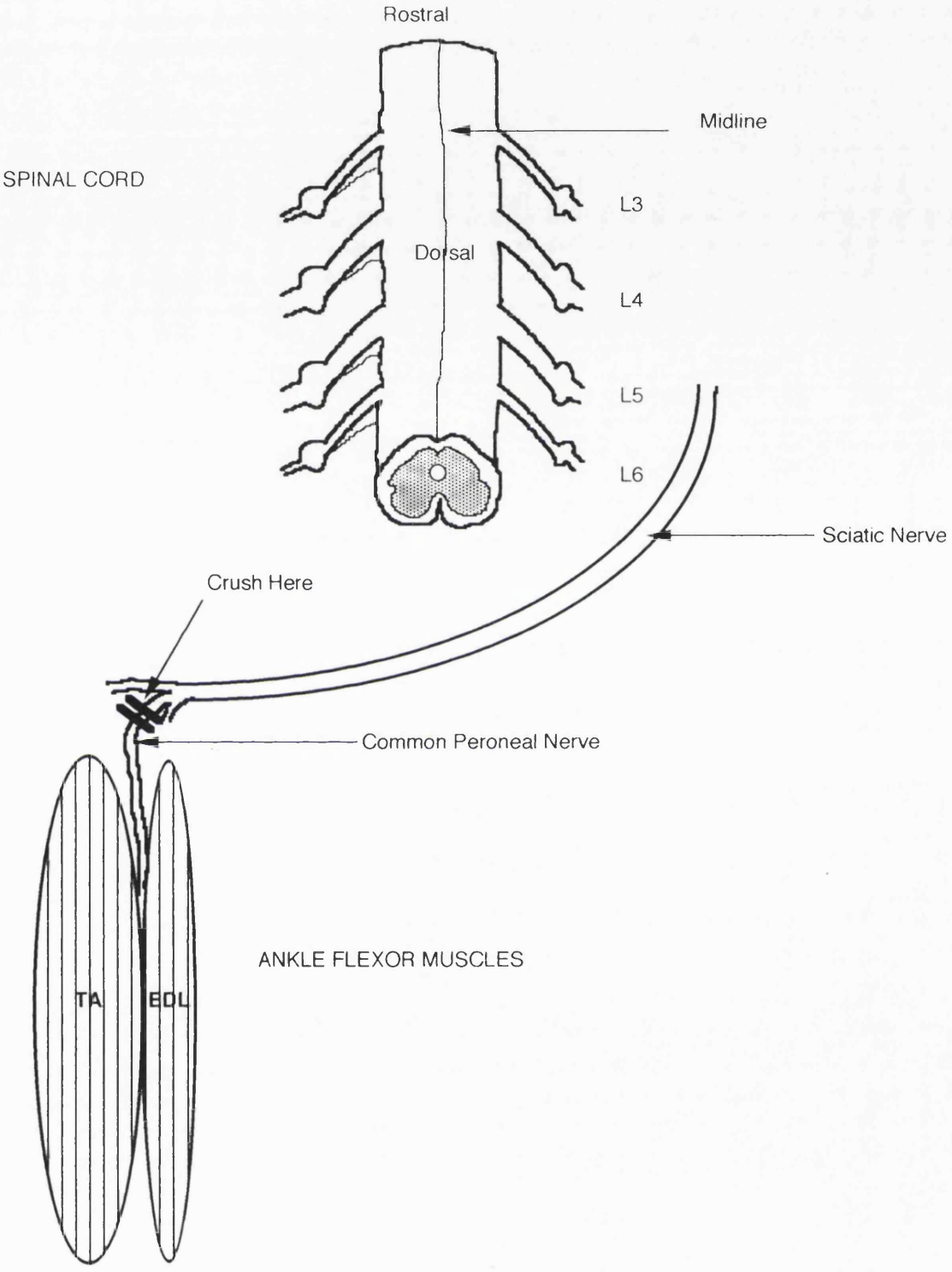

Figure 3.1 shows a diagram of the spinal cord and sciatic nerve innervating the ankle flexor muscles, tibialis antrior (TA) and extensor digitorum longus (EDL). The common peroneal nerve, which is a branch of the sciatic nerve, was crushed just before entry into the muscels, as shown, on P2.

Figure 3.2 Retrogradely labelled flexor motoneurones after injury. This shows fluorescently labelled motoneurones innervating the ankle flexor muscles tibialis anterior and extensor digitorum longus (TA/EDL) from the control **(A)** and operated **(B)** sides of the spinal cord 5 days following unilateral crush of the common peroneal nerve on P2. The flexor motoneurone pool is situated dorsolaterally within the ventral horn between segments L4 and L5.
(A) and **(B)** show several Fast Blue and Diamidino Yellow (FB/DY) prelabelled motoneurones from an 7 day old animal. There are many small, brightly fluorescent microglial cells (arrows) within the injured motor pool on the operated side **(B)**. Note also that there are fewer motoneurones on the operated side **(B)** compared to the control side **(A)**. This may be due to neuronal degeneration. Scale bar = 100 μm.
(C) A prelabelled motoneurone form the injured side of the spinal cord of a P7 animal. The image was obtained using the confocal laser scanning microscope and consists of a projected z-series of 5 images. The motoneurone is surrounded by numerous small microglial cells (arrows). The nucleolus is visible (arrowhead). Scale bar = 10 μm.

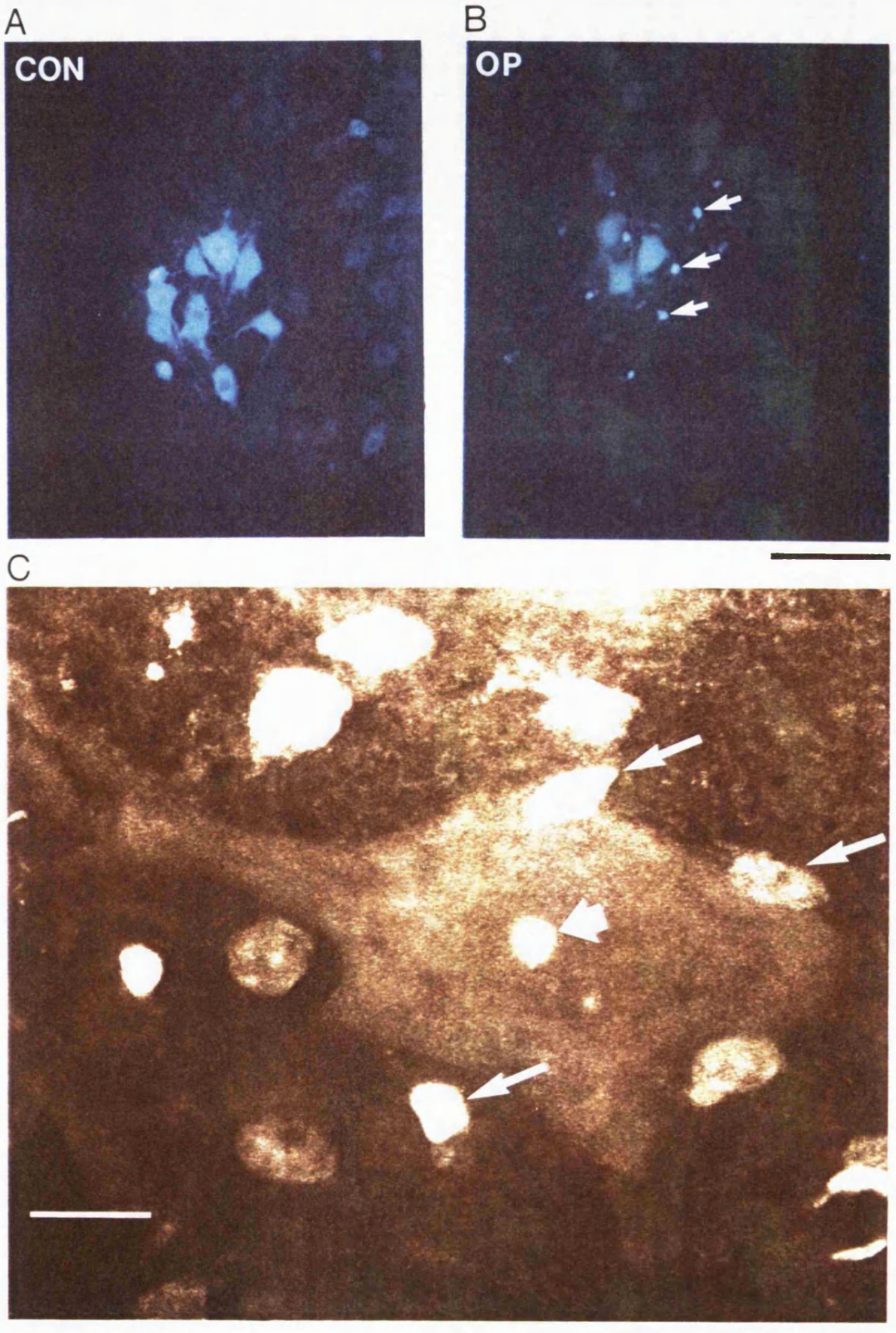
A
CON
B
OP
C

Figure 3.3 Motoneurones of the tibialis anterior/extensor (TA/EDL) digitorum longus motor pool retrogradely filled with HRP. The TA/EDL muscles were injected with HRP in adult animals after unilateral common peroneal nerve crush on postnatal day 2. The operated side of the spinal cord is marked with a pinhole. There are fewer retrogradely labelled motoneurones on the operated side. Scale bar = 500 μm.

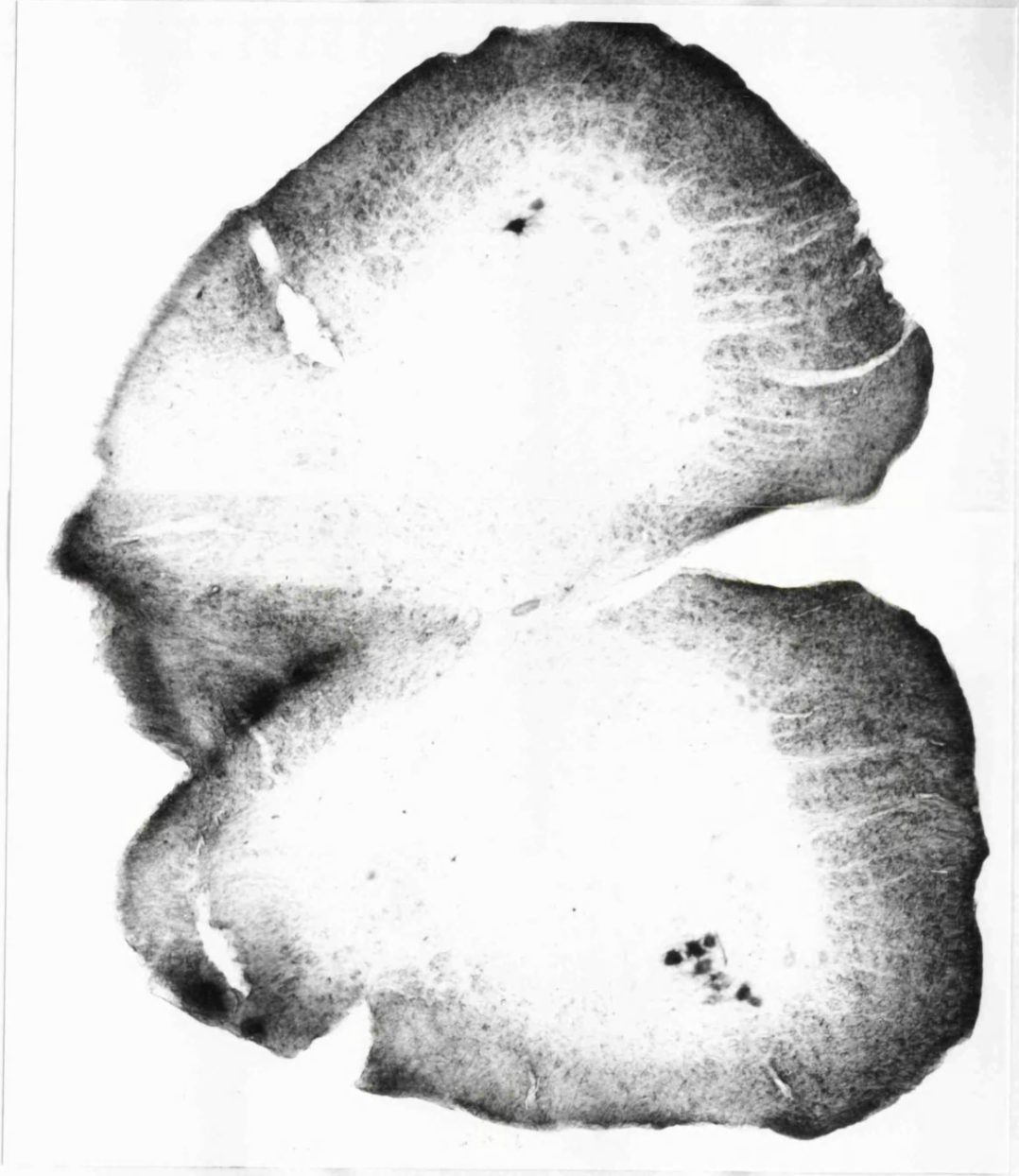

Figure 3.4 Shows Lucifer Yellow filled motoneurones form the ankle flexor pool at 3, and 7 days postnatal age. There is a developmental elimination of surface growth associated features from the proximal region of the cells. A comparison is made between P7 injured motoneurones and P7 normal motoneurones.

(A) Motoneurone from a 2 day old animal (P2). The surface of the soma, proximal and distal dendrites are densely covered in numerous long, thin, growth associated processes. Scale bar = 10 μm.

(B) Motoneurone from a P7 animal. By this time soma and proximal dendrites are largely devoid of these growth associated processes. Scale bar = 25 μm.

(C) Motoneurone 5 days after CP nerve injury (P7). Taken from the contralateral side of the spinal cord of the same animal as in **(B)**. Note: unlike the cell shown in **(B)** the surface of the soma and proximal dendrites of the injured motoneurone are still covered in numerous hair-like processes. This is similar to those seen in normal younger animals **(A)** and suggests that maturation of the motoneurone may have been delayed by the injury. Scale bar = 25 μm.

(D) High power image (x60/1.4 oil immersion) of the proximal (second order) dendrites of a normal P2 motoneurone. Arrows show very long, hair-like appendages. Scale bar = 10 μm.

(E) An image of the proximal portion of a P8 motoneurone. The surface is free of prominent hairs and is relatively smooth. Scale bar = 10 μm.

(F) A P7 motoneurone. The long, hair-like structures still remain on the dendrite (compare **(D)**). The density of these processes is even greater than in normal development. Scale bar = 10 μm.

(G) Distal (fourth order) portion of a 2 day old motoneurone (P2) at high power. The large arrows indicate long, fine hairs. There are also shorter processes (smaller arrows) that resemble classical dendritic spines. One branch of the dendrite terminates in a growth cone with filopodia (open arrow). There is also a long process (arrow heads) that may continue to grow into a dendrite. Scale bar = 10 μm.

(H) High power view of the distal dendrite from an 8 day old motoneurone. Some of the dendritic structures are filopodial in nature (large arrow) and others are lamellipodial (small arrows). At this stage the growth associated structures are still found, but only on the distal dendrites. The Scale bar = 10 μm.

(I) Distal portion of a motoneurone 5 days after injury (P7). There are still numerous processes along the dendrite as is the case during normal development **(H)**. The large arrow shows a growth cone-like structure, the smaller arrows show filopodial processes. Scale bar = 10 μm.

a
b
c
d
e
f
g
h
i

Figure 3.5 Changes in the incidence of exuberant surface features on different regions of ankle flexor motoneurones after injury to the common peroneal (CP) nerve on postnatal day two (P2). The elimination of growth associated processes from the soma and proximal regions of the dendrites can be seen to be halted (compare with Fig. 2.10 during normal development). There is even evidence of an increase in the incidence of processes on the soma between P3 and P4-6, which then declines at P7-9.
There is evidence of possible contralateral effects of injury, especially in the incidence of growth associated processes on the soma and primary dendrites (compare Fig. 3.5b with Fig. 2.10).

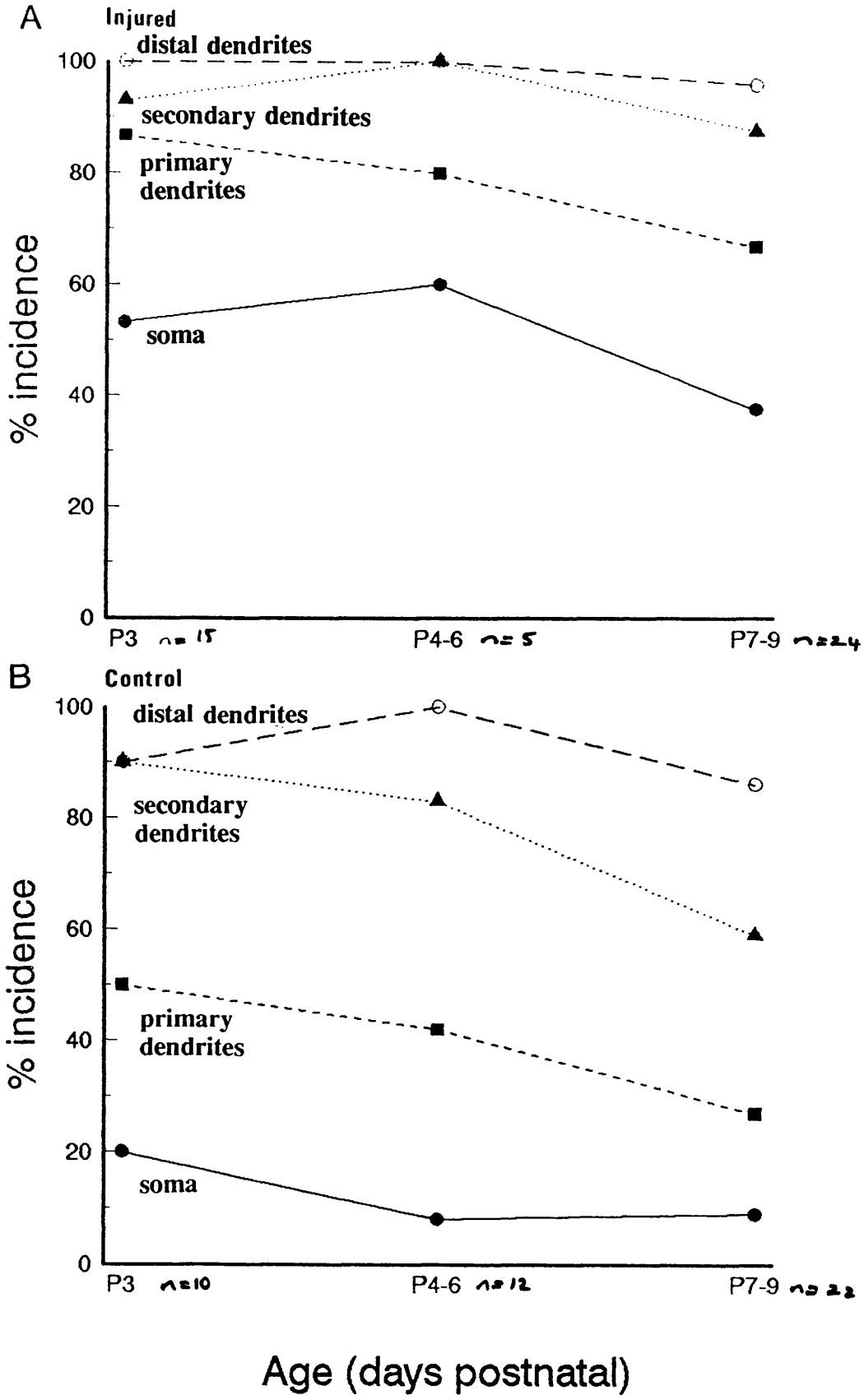
A
Injured
distal dendrites
secondary dendrites
primary dendrites
soma
% incidence
100
80
60
40
20
0
P3 n= 15
P4-6 n= 5
P7-9 n=24
B
Control
distal dendrites
secondary dendrites
primary dendrites
soma
% incidence
100
80
60
40
20
0
P3 n=10
P4-6 n=12
P7-9 n=22
Age (days postnatal)

Figure 3.6 This figure shows several examples of unusual growth seen in a few of the motoneurones following injury to the common peroneal (CP) nerve on P2.

(A) A (P7) motoneurone, 5 days after damage to the axon. Arrows indicate the growth of long, thin unbranched processes arising from a primary dendrite. This unequal branching pattern is a deviation from that observed during normal dendrites where the daughter branches are of equal diameter. The process is covered in many fine hair-like lamellipodia, which suggests that it is dendritic in origin. Scale bar = 25 μm.

(B) High power image (x60/1.4 oil immersion) of a proximal dendrite of a P3 motoneurone after CP crush on P2. There are many growth cone-like or lamellipodial structures. Scale bar = 25 μm.

(C) High power view from a proximal dendrite of a P3 motoneurone. The dendrite is covered with numerous small 'hairs'. In addition there is one large process (arrows) growing from the dendrite. It is, itself, covered in hair-like structure suggesting dendritic origins. Scale bar = 10 μm.

(D) High power image of a distal dendrite of a 3 day old cell (1 day after CP crush). Arrows point to long, thin spine-like outgrowths of more than 10 μm in length. Scale bar = 10 μm.

a

b

c

d

Figure 3.7 'Degenerative' features of axotomised motoneurones. The features illustrated below were seen in relatively few cells. The expression of these abnormal features is suggestive of degeneration.
(A) Shows an example of a 7 day motoneurone (5 days after injury). The cell body of this motoneurone is greatly swollen. There are many varicose structures along proximal and distal dendrites (arrows). These structures may arise as a result of osmotic damage to the cell. The boxed area relates to that area shown in **(C)**. Scale bar = 25 μm.
(B) The arrow indicates an example of a swollen primary dendrite. This is an example of trichotomous branching in a P8 motoneurone (6 days after injury). Note also the enlarged appearance of some of the primary dendrites of this cell. Scale bar = 10 μm.
(C) is a high power image of a region of a primary dendrite of a P7 motoneurone from the boxed area in **(A)**. Large arrows show varicose enlargements of the proximal dendrites which are never seen in a normal motoneurone of this age. Smaller arrows show the fine spine-like processes. Scale bar = 10 μm.
(D) An example of a eccentrically displaced nucleus. Scale bar = 25 μm.

b
d
a
c

Figure 3.8 Histograms showing the soma areas of motoneurones intracellularly filled with Lucifer Yellow, at P3-9 after common peroneal (CP) crush on P2. Injured (CP crush) cells are compared with controls from normal animals and motoneurones from the contralateral side of the spinal cord to the injury. The number of motoneurones in each group is shown. There is no significant difference in the mean area of the soma of injured (403.8 ± 175.2; mean ± SD), normal (385.6 ± 141.9) or contralateral control (347.8 ± 119.3) motoneurones over this early postnatal period. This data is shown in Table 3.2.

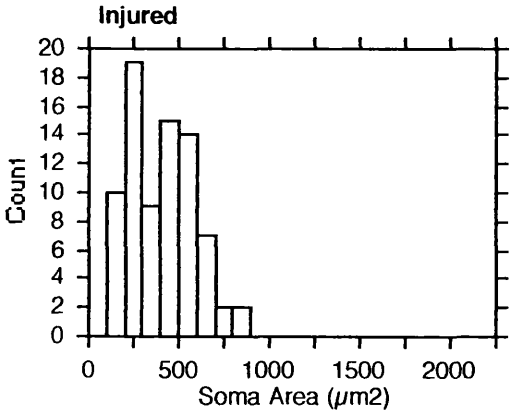
Injured
Count
20
18
16
14
12
10
8
6
4
2
0
0
500
1000
1500
2000
Soma Area (μm2)

n=78

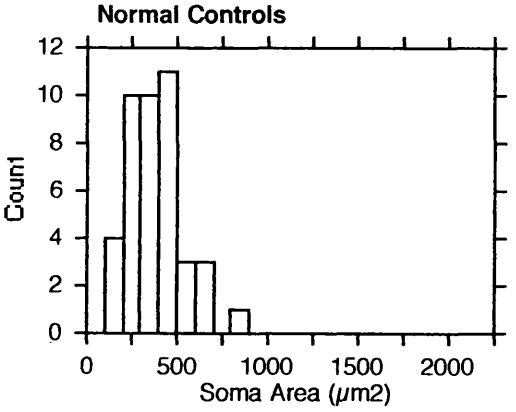
Normal Controls
Count
12
10
8
6
4
2
0
0
500
1000
1500
2000
Soma Area (μm2)

n=42

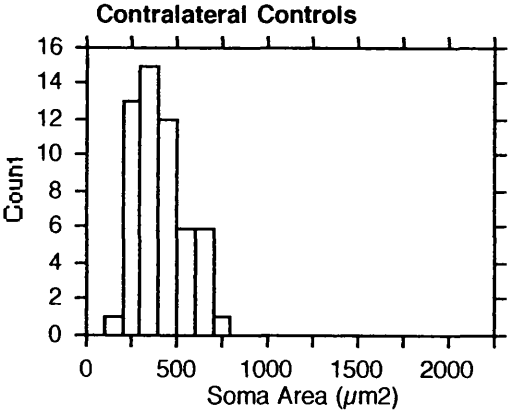
Contralateral Controls
Count
16
14
12
10
8
6
4
2
0
0
500
1000
1500
2000
Soma Area (μm2)

n=54

Figure 3.9 Histograms showing the soma areas of counterstained motoneurones from the tibialis anterior/extensor digitorum longus (TA/EDL) motor pool after common peroneal (CP) crush on P2, and in contralateral control motoneurones. Sections of spinal cord 20 μm thick, containing motoneurones retrogradely labelled with Fast Blue and Diamidino Yellow (FB/DY) were counterstained with gallocyanin. The soma areas of these motoneurones in the CP pool were measured using camera lucida and a graphics tablet interfaced with a microcomputer at P3, P7 and P14. Injured (CP crush) cells are compared with controls motoneurones from the contralateral side of the spinal cord to the injury. The number of motoneurones in each group is shown. This data is shown in Table 3.3.

At all ages there was not a significant difference in the mean soma area of injured and control motoneurones. However, there was a significant difference in the mean soma area between P3 and P7, as well as P7 and P14 (see Table 3.3).

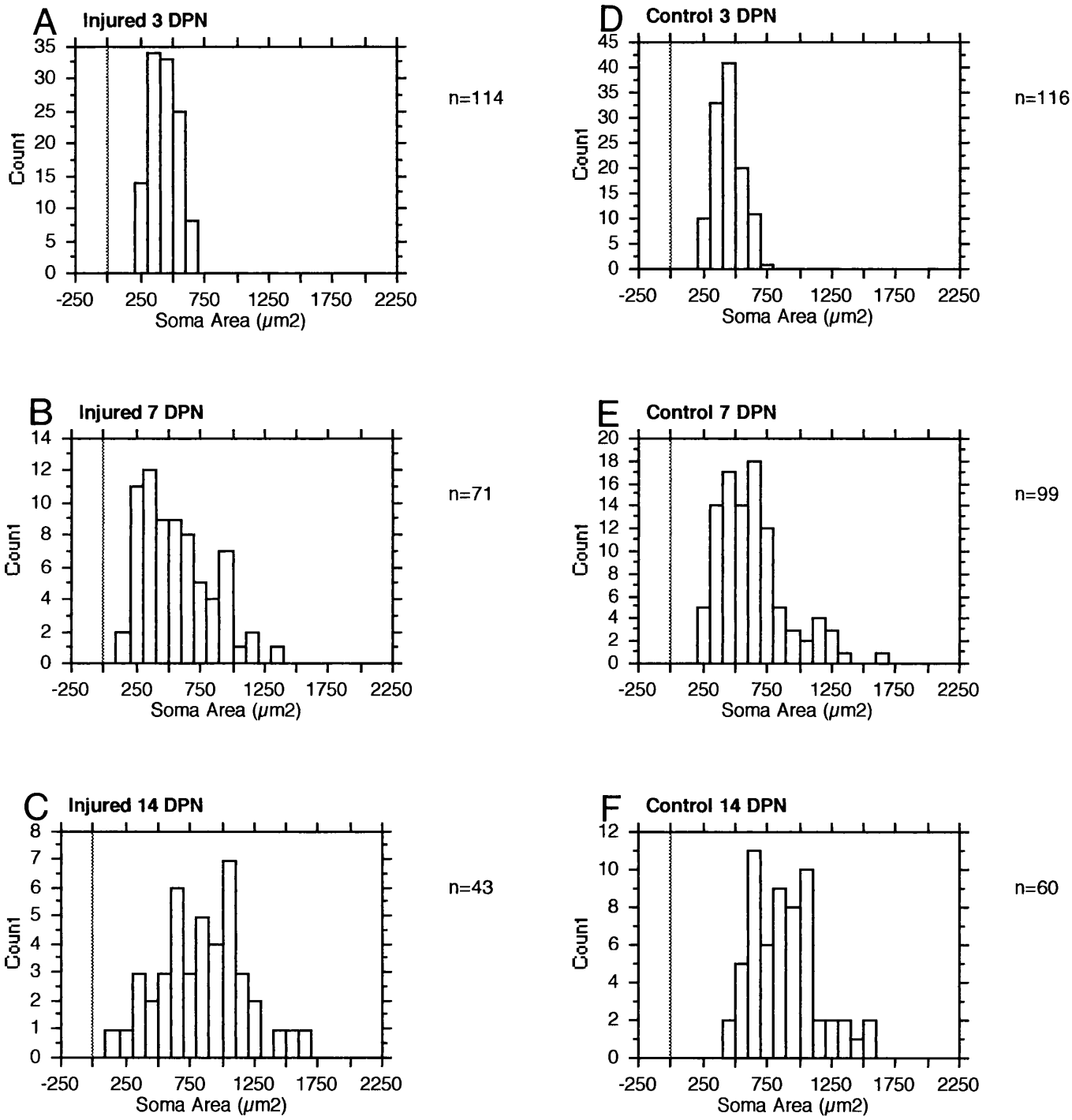
A
Injured 3 DPN
Count
Soma Area (μm2)
n=114
D
Control 3 DPN
n=116
B
Injured 7 DPN
n=71
E
Control 7 DPN
n=99
C
Injured 14 DPN
n=43
F
Control 14 DPN
n=60

Figure 3.10 Histograms showing the soma areas of motoneurones retrogradely filled with HRP 2-3 months after common peroneal (CP) crush on P2. Injured (CP crush) cells are compared with controls from normal animals, motoneurones from the contralateral side of the spinal cord to the injury, as well as the pooled control motoneurones. The number of motoneurones in each group is shown. The mean soma area of the injured motoneurones is 1147.8 ± 137.4 (mean +SD), and that of the contralateral control motoneurones is 1237.5 ± 192.6. This shows that 2-3 months after injury there is a significant reduction in the mean soma area of the surviving motoneurones (see Table 3.4).

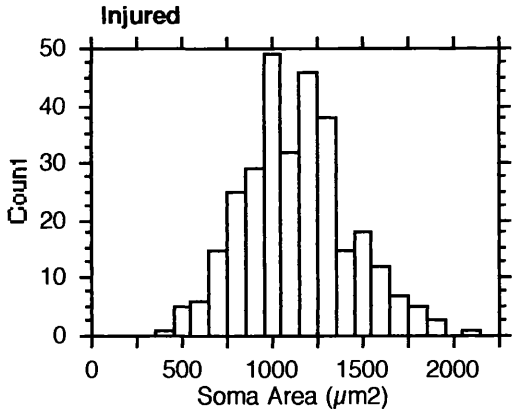

n=307

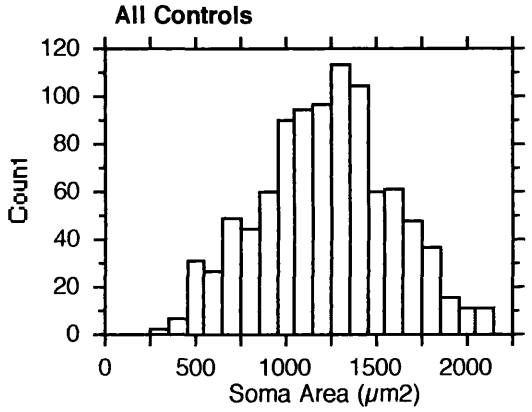

n=967

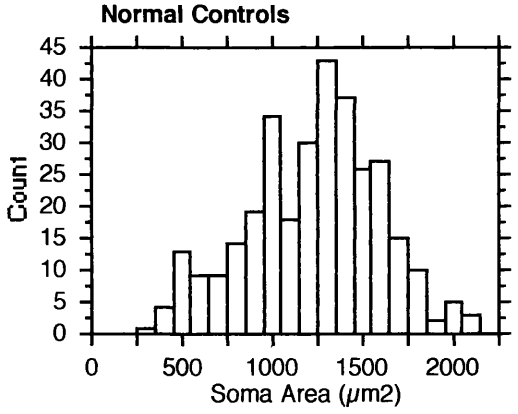

n=321

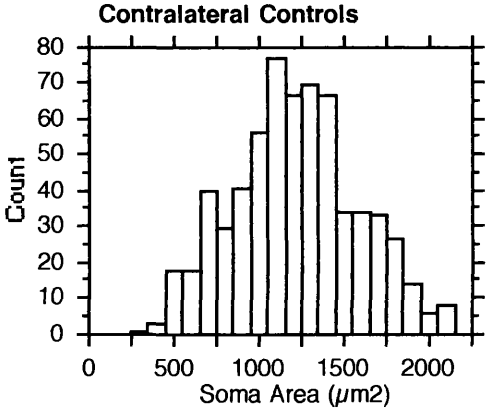

n=646

Figure 3.11 Scatter plot of the sum of the individual diameters of all primary dendrites arising from each injured motoneurone against the mean soma diameter, for the eight neurones of Table 3.5. The diagonal line represents the linear regression of the combined dendritic diameter on soma diameter: the slope is 0.226 and the intercept 17.17 μm.

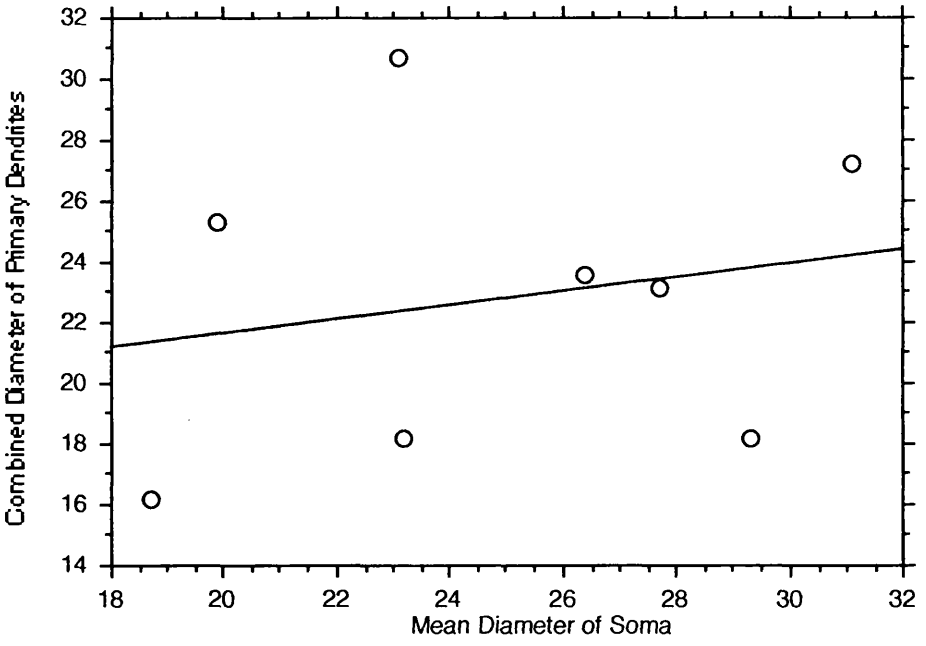
Combined Diameter of Primary Dendrites
32
30
28
26
24
22
20
18
16
14
18
20
22
24
26
28
30
32
Mean Diameter of Soma

Figure 3.12 Scatter plot of individual diameters of primary dendrites arising from a motoneurone after common peroneal crush on P2, against the combined length, for the 8 neurones in Table 3.5. The diagonal line represents the linear regression of the dendritic diameter on dendritic length: the slope is 122.13 and the intercept 11.02 μm. The results of Spearman's rank correlation test are given in the text.

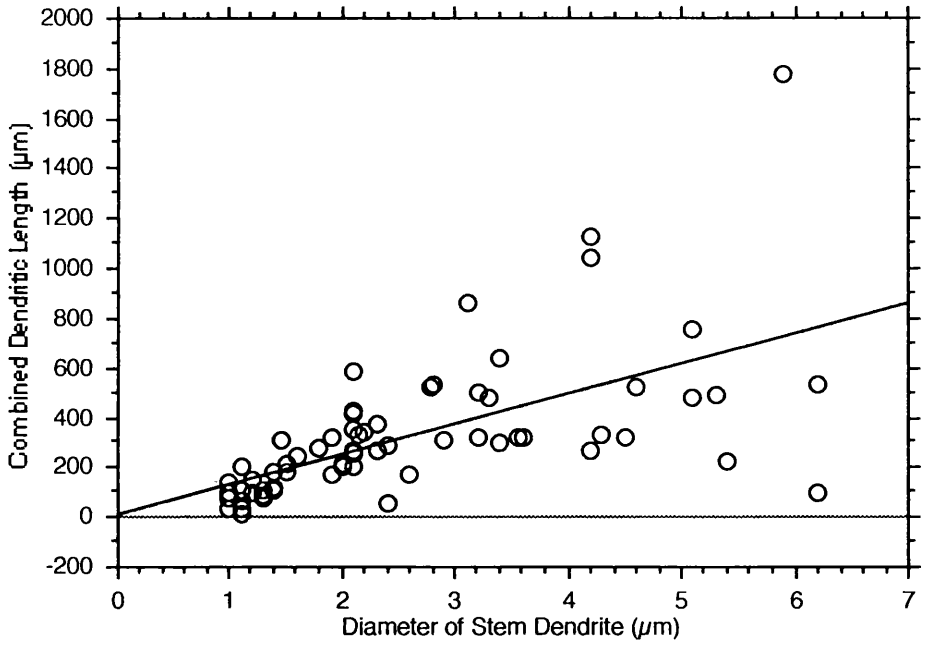
Combined Dendritic Length (µm)
2000
1800
1600
1400
1200
1000
800
600
400
200
0
-200
0
1
2
3
4
5
6
7
Diameter of Stem Dendrite (µm)

Figure 3.13 Sholl diagram (Sholl, 1953) showing the extent of dendritic outgrowth as a function of distance from the soma for ankle flexor motoneurones at P3 and P7 after common peroneal crush on P2. The vertical scale denotes dendritic intersections per 20 μm increment of radius, expressed as a percentage of all such intersections.
(A) At P3 intersections with dendrites in the four cells analysed were commonest 40 μm and 60 μm from the soma. Some dendrites extended beyond 180 μm.
(B) At P7 the same method of analyses applied to four cells detected a large shift to longer radial distances. Distances of 60-120 μm occurred most often.

A

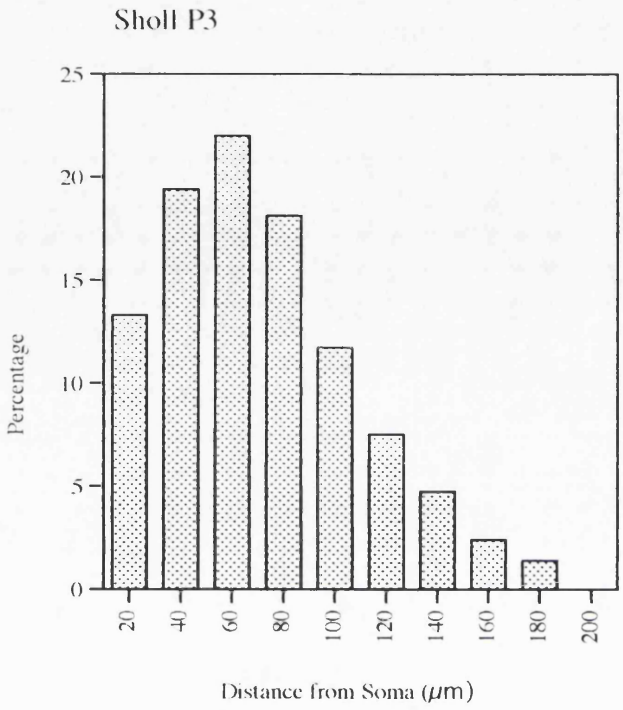
Sholl P3
25
20
15
10
5
0
Percentage
20
40
60
80
100
120
140
160
180
200
Distance from Soma (μm)

B

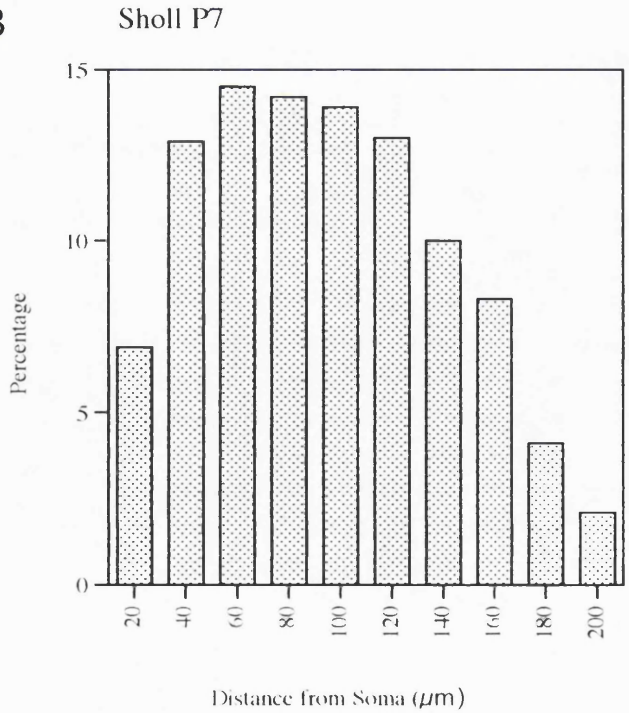
Sholl P7
15
10
5
0
Percentage
20
40
60
80
100
120
140
160
180
200
Distance from Soma (μm)

Figure 3.14 Sholl diagram showing the extent of dendritic outgrowth of flexor motoneurones.
(A) Pooled data of motoneurones eight at P3-7, after common peroneal crush on P2. Intersections in the eight cells analysed were commonest 60 μm from the soma. Some dendrites extended 220 μm from the soma.
(B) Pooled data for 15 normal motoneurones at P2-9. Intersections most frequently occur at 60-80 μm from the soma. Distances of over 220 μm occurred most often.

A Sholl Injured 3-7DPN

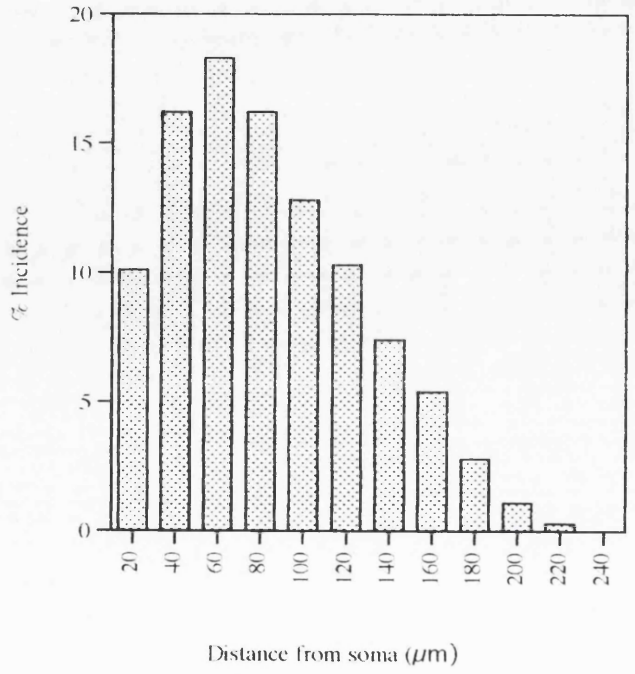

B Sholl Control 2-9DPN

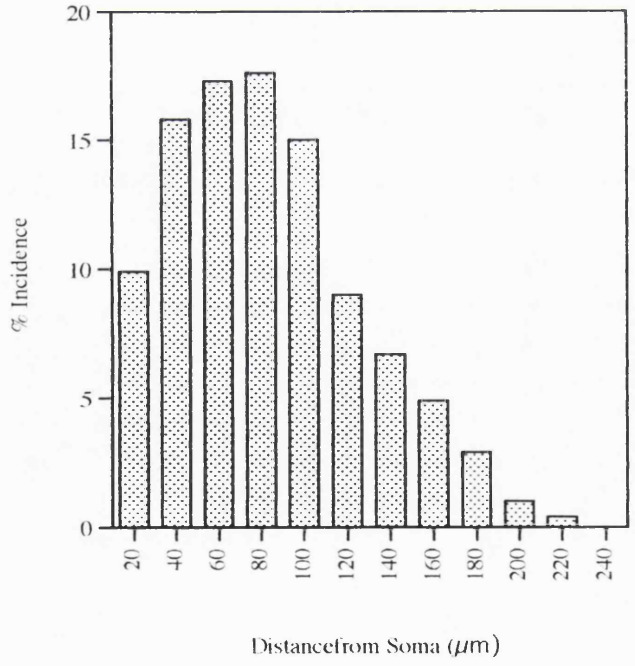

Figure 3.15 Circular graphs showing the summed dendritic distribution of identified flexor motoneurones (**A**) at P3 (4 cells) and (**B**) at P7 (4 cells). D, V, C and R denote the dorsal, ventral, caudal and rostral axes. Each point represents a length that is proportional to the dendritic density within one 30 ^{o} sector around the soma. To measure this density, all the intersections between dendrites and concentric circles spaced at 20 μm intervals were counted and summed within each sector. The scale denotes intersections per sector as a percentage of total intersections. Dendrites at P7 showed a dorso-ventral polarity, and a dorsal bias.

A Orientation P3

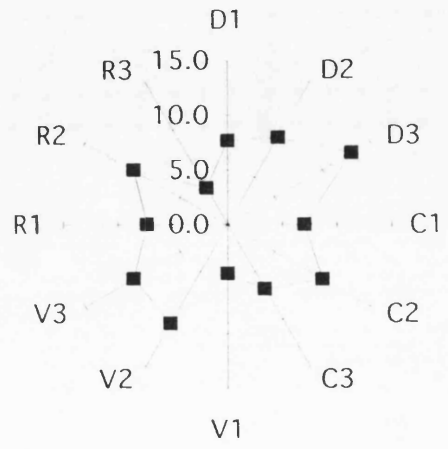

B Orientation P7

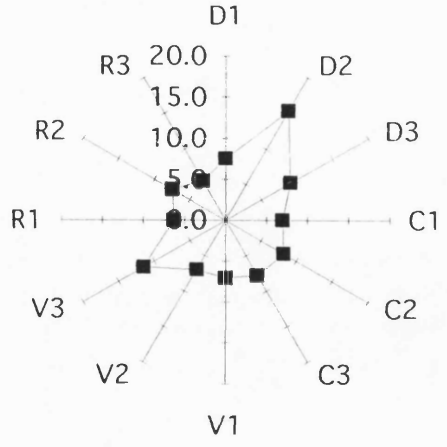

Figure 3.16 Circular graphs. **(A)** at P3-7, in eight motoneurones after common peroneal nerve crush on P2. **(B)** In 15 normal motoneurones. D, V, C and R denote the dorsal, ventral, caudal and rostral axes. Dendrites from control motoneurones showed a stronger dorsal bias than those from injured motoneurones.

A Orientation Injured P3-7

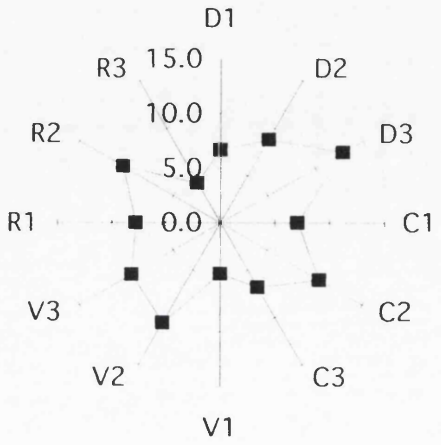

B Orientation Control P2-9

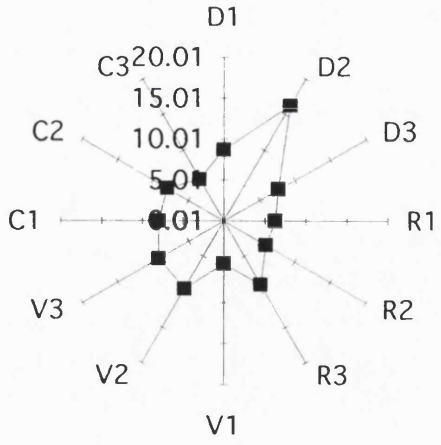

Table 3.1

Number of motoneurones, retrogradely filled with horseradish peroxidase, from the control and operated side of the spinal cord, surviving 2-3 months after left common peroneal nerve crush on postnatal day 2. Animals 5 and 6 are normal controls.

	Animal	LS	RS	% op/con	Kolmorogov-Smirnov test
Number of Cells	1: operated	84	183	46	
	2: operated	98	190	52	
	3: operated	82	172	48	
	4: operated	46	147	31	
Mean (±SD)		**77.5 ± 22.2**	**173 ± 18.9**	**44.1 ± 9.2**	**p=0.0366**
	5: control	193	133	69	
	6: control	189	176	93	
Mean (±SD)		**191 ± 2.8**	**155 ± 30.4**	**81.0 ± 17.0**	**p=0.2707**

Table 3.2

Morphometric characteristics of the soma and primary dendrites of Lucifer Yellow filled ankle flexor motoneurones during the early postnatal period[•]. Motoneurones after common peroneal nerve crush injury on postnatal day 2 are compared with motoneurones form the contralateral control side of the spinal cord, and others from normal animals.

	Projected Soma Area (μm2)			Mean Diameter of Soma (μm)			Number of Primary Dendrites			Mean Diamter of Primary Dendrites		
Age	Injured	Contralateral Control	Control	Injured	Contralateral Control	Control	Injured	Contralateral Control	Control	Injured	Contralateral Control	Control
P3	380.4 ± 135.0 n=17	445.3 ± 107.6 n=8	401.2 ± 82.6 n=7	21.8 ± 4.4 n=17	16.6 ± 4.8 n=5	18.4 ± 3.4 n=5	8.4 ± 1.4 n=13	8.7 ± 1.5 n=7	8.3 ± 1.2 n=6	2.2 ± 0.5 n=15	2.1 ± 0.8 n=7	1.6 ± 0.5 n=4
P4-6	367.4 ± 128.1 n=22	389.2 ± 95.3 n=13	359.7 ± 102.4 n=20	21.6 ± 3.2 n=15 **	17.9 ± 3.1 n=9	16.6 ± 0.6 n=4	8.3 ± 2.5 n=14	7.4 ± 1.4 n=13	7.4 ± 1.6 n=19	2.3 ± 0.7 n=14	2.2 ± 0.6 n=13	2.1 ± 0.6 n=19
P7-9	434.5 ± 208.5 n=39	408.3 ± 161.8 n=33	410.4 ± 193.3 n=16	26.7 ± 4.5 n=15 |||	19.0 ± 3.8 n=22	21.7 ± 4.7 n=4	8.2 ± 1.8 n=37	7.2 ± 2.0 n=33	8.3 ± 0.5 n=16	2.1 ± 0.8 n=30	2.1 ± 0.8 n=31	2.0 ± 0.6 n=14

[•]Values for each parameter correspond to the mean and standard deviation in each group. The levels of statistical significance are shown by the symbols:

* denotes injured vs normal; | denotes injured vs contralateral controls. The number of symbols represents the levels of significance.

Table 3.3

Mean soma areas of gallocyanin counterstained motoneurones flexor motoneurones at postnatal days 3, 7 and 14[apple].

Age	Mean Soma Area Control (μm^2)	Mean Soma Area Operated (μm^2)
P3	443.8 ± 107.1 n=116 ***$$$	431.6 ± 106.8 n=114 $$$
P7	631.8 ± 268.3 n=99 !!!	562.1± 270.4 n=71 !!!
P14	887.5 ± 261.7 n=60	843.0 ± 344.0 n=43

[apple]Values for each parameter correspond to the mean and standard deviation in each group. The statistical significance levels are shown by the symbols: * denotes P3 vs P7; $ denotes P3 vs P14; ! denotes P7 vs P14. The number of symbols represents the levels of significance.

Table 3.4

Mean soma area of HRP filled motoneurones form the injured and control sides of the spinal cord 2-3 months after common peroneal crush on postnatal day 2.

	Animal	LS Injured	RS Control
Mean Soma Area (μm^2)	1	1119 n=98	1069 n=190
	2	967 n=84	1234 n=183
	3	1277 n=82	1508 n=172
	4	1228 n=46	1139 n=147
Mean ± SD (μm^2)		**1147.8 ± 137.4**	**1237.5 ± 192.6**
		Control	**Control**
	5	1407 n=193	1260 n=133
	6	1086 n=189	964 n=176
Mean ± SD (μm^2)		**1246.5 ± 226.9**	**1111.8 ± 209.2**

Table 3.5

Morphometric characteristics if individual Lucifer Yellow filled motoneurones during the early postnatal period after common peroneal nerve crush on postnatal day 2[*].

Age	Max/min diam.	Mean diam. (μm)	Projected area (μm2)	Number	Combined diam. primary dend. (μm)	Mean diam. (μm)	Max. branch order	Max. distance from soma (μm)	Diam. distal dendrites (μm)	Combined dend. length (μm)	Surface area of dend. (μm2)	Total memb. area (μm2)
3	1.4	19.9	314.8	10.0	25.3	2.5	5	223.4	0.8	2360.4	1468.7	1783.5
3	1.8	29.3	259.6	10.0	18.2	1.8	4	139.3	0.7	1915.9	852.0	1111.6
3	1.6	18.7	325.5	8.0	16.2	2.0	5	186.9	0.8	1611.7	1412.1	1737.6
3	1.0	23.1	452.4	10.0	30.7	3.1	6	220.6	0.7	3887.1	3246.8	3699.2
Mean	**1.5 ± 0.3**	**22.8 ± 4.7**	**338.1 ± 81.5**	**9.5 ± 1.0**	**22.6 ± 6.7**	**2.4 ± 0.6**	**5.0 ± 0.8**	**192.6 ± 39.2**	**0.75 ± 0.1**	**2444 ± 875**	**1745 ± 1039**	**2083 ± 1120**
7	2.5	31.1	856.0	11.0	27.2	2.5	5	327.0	0.8	3275.1	14748.7	15604.7
7	1.8	23.2	515.5	5.0	18.2	3.6	5	205.7	0.7	1993.9	1636.6	2152.1
7	2.0	26.4	506.3	9.0	23.6	2.6	5	282.3	0.8	3726.8	2539.8	3046.1
7	2.4	27.7	640.1	9.0	23.1	2.6	4	243.6	0.8	3036.2	11996.2	12636.3
Mean	**2.2 ± .3**	**27.1 ± 3.3**	**629.5 ± 162.9**	**8.5 ± 2.5**	**23.0 ± 3.7**	**2.8 ± 0.5**	**4.8 ± 0.5**	**264.7 ± 52.0**	**0.8 ± 0.1**	**3008 ± 734**	**7730 ± 6621**	**8360 ± 6771**

[*]Values for each parameter in 8 cells are shown, together with means and standard deviations for motoneurones from animals at P3 and P7.

4. PARVALBUMIN- AND SEROTONIN-POSITIVE APPOSITIONS CONTACTING RAT FLEXOR MOTONEURONES DURING EARLY POSTNATAL DEVELOPMENT AND AFTER NEONATAL INJURY

4.1. INTRODUCTION

The afferent inputs onto motoneurones provide the synaptic drive that results in the patterns of motor activity generated by the spinal cord. These inputs include sensory afferents from the periphery, descending afferents from the brain, and interneurones. The majority of the synaptic inputs onto motoneurones are from interneurones located in laminae VI and VII of the spinal cord. They form part of the polysynaptic reflex pathways from skin, joint and muscle afferents as well as from descending inputs. The majority of monosynaptic contacts onto motoneurones are from the 1a primary afferents forming part of the stretch reflex.

4.1.1. Primary afferents

The group 1a afferents, in the mammal, are the largest diameter and fastest conducting primary afferents originating from the muscle spindles. They enter the spinal cord in the same segment that contains their target motoneurones, which usually innervate the same muscles from which the afferents originate (Eccles *et al.*1957; Luscher *et al.*1980). These afferents form the basis of the monosynaptic stretch reflex (see (Luscher, Clamann, 1992)). After entering the spinal cord, each 1a afferent divides into a large ascending and a smaller descending branch, which project rostrally or caudally in the ipsilateral dorsal column ((Ishizka *et al.*1979) in the cat, (Rivero-Melian, Grant, 1990) in the rat). These branch again, and give off collaterals (Brown, Fyffe, 1981; Rivero-Melian, Grant, 1990), some of which terminate in the region of large neurones in Clarke's column nucleus in laminae V and VI (Rivero-Melian, Grant, 1987; Rivero-Melian, Grant, 1990). The neurones in Clarke's column send ascending axons to the cerebellum, in

the spinocerebellar tract. Other collaterals terminate in the region of inhibitory interneurones in lamina VII and VIII (Jankowska, Lindstrom, 1972), which may themselves project to the motor pools. There are also monosynaptic contacts onto the soma and dendrites of alpha-motoneurones in lamina IX (Burke *et al.*1979; Brown, Fyffe, 1981). Some 1a afferents make polysynaptic contacts onto motoneurones via interneurones, and others convey sensory information to the contralateral sensory-cortex through the spinothalamic tracts.

The motoneurones from a muscle receive functional contacts from most of the group 1a afferents originating from that muscle. This forms the homonymous connection (Mendell, Henneman, 1971; Fleshman *et al.*1981). There are fewer heteronymous projections from synergistically acting muscles. Connections may also occur between muscles acting at different joints, possibly to facilitate the coordinated action of different muscles during movement (Eccles *et al.*1957).

The spatial distribution and number of contacts made by 1a afferent axon collaterals onto motoneurones have been studied using electrophysiological and anatomical methods. There is electrophysiological evidence suggesting that 1a afferents make connections on both the dendrites and soma of the motoneurones (Burke, 1967; Iansek, Redman, 1973; Mendell, Henneman, 1971; Rall *et al.*1967; Luscher *et al.*1980). Intracellular labelling of single 1a afferents with HRP has allowed the anatomical connections between identified motoneurones and their afferents to be studied. This has shown that boutons (swellings) on the axons, contact the soma and dendrites (Burke *et al.*1979; Brown, Fyffe, 1981) and confirms the findings of electrophysiological studies. Primary afferent axons contact the motoneurone dendrites at distances of 800 μm or more from the soma in the cat (Brown, Fyffe, 1981). However, the majority of the synapses were in the proximal region of the dendritic tree. A single 1a afferent collateral may make between 3 and 35 contacts onto a homonymous motoneu-

rone, averaging about 10 (Brown, Fyffe, 1981). An estimate of the total number of 1a afferent boutons on a motoneurone in the lumbosaccral region of the cat spinal cord suggests that 1a afferent inputs form less than 1% of the total synaptic contacts onto motoneurones. Single fibre 1a e.p.s.p.s usually have a simple time course, which suggests that a motoneurone receives contacts from only one axon collateral (Mendell, Henneman, 1971). Anatomical evidence seems to confirm this finding (Brown, Fyffe, 1981). Despite the fact that the dendrites of a motoneurone may pass through the field of projection of several collateral fibres, contacts are only made with one of the collaterals. This suggests that appropriate connections are selected during development.

4.1.2. Development of 1a afferent fibres

The developmental sequence of projections of primary afferents into the spinal cord of the rat has been studied using transport of HRP onto cut lumbar dorsal roots (Kudo, Yamada, 1987; Chymkhova *et al.*1991). Between embryonic day 15.5 and 16.5, collaterals were present and projected from the dorsal funiculus into the dorsal horn of the lumbar region of the spinal cord (Kudo, Yamada, 1987). Some collaterals also project towards the ventral horn. In the lumbar spinal cord the afferent fibres first enter the region of the motor nuclei in the ventral horn on E17.5. Many of the growing collaterals terminate in growth cones or other growth associated processes, and have numerous varicose boutons. These boutons form the *en passant* sites of synaptic contact between the afferents and the motoneurones. By stimulating the dorsal root it has been shown that monosynaptic transmission from the primary afferent fibres first appears on E18.5. The size of the response increases, becoming maximal at P2-P3, and decreasing between P4-P8 (Kudo, Yamada, 1987). The development of the monosynaptic reflex occurs slightly earlier in the thoracic spinal cord (Saito, 1979), on E17.5. The number of boutons on each collateral increases with age (Kudo, Yamada, 1987; Chymkhova *et al.*1991), but the increase in the size of the monosynaptic reflex with age is less marked (Kudo, Yamada, 1987). The in-

crease in the size of the monosynaptic reflex may be partly due to developmental changes in the input resistance of the motoneurones (Fulton, Walton, 1986), but may also be influenced by the shape and branching pattern of the dendritic tree, and the location of the afferent contacts (Rall *et al.*1967).

In the frog (Frank, Westerfield, 1983) and chick (Lee, O'Donovan, 1991) the connections between motoneurones and their afferents has been shown to be formed at an early developmental stage, and might not undergo rearrangement. In the frog there is evidence that the afferents arrive in the region of the ventral horn first, and that the dendrites grow into an area already occupied by afferent axons (Jackson, Frank, 1987). In mammals, the dendrites of motoneurones and their afferent connections project to an area of interaction at the same time, and connections can be demonstrated almost immediately (Kudo, Yamada, 1987). The interactions of the developing motoneurones and their afferents in the rat has recently been studied using fluorescent, lipid-soluble dyes which were placed on the dorsal and ventral roots (Snider *et al.*1992b). This study shows that the afferent axons and motoneurone dendrites develop independently of each other. In fact, the 1a afferent fibres grow through regions containing distal dendrites of many developing motoneurones, forming synapses in the region of the soma and proximal dendrites of motoneurones innervating honomynous muscles.

4.1.3. Response to injury of segmental afferents

Injury to the peripherally projecting process (but not the centrally projecting process) causes death of neurones in the dorsal root ganglion (DRG), both in neonates and in adult rats (Himes, Tessler, 1989). However, the extent of cell death depends on the type and site of the injury, as well as the age at which injury is inflicted. Generally, the more proximal and disruptive the lesion, the greater the resultant cell death. Up to 52% of DRG neurones die after sciatic nerve section in the adult cat (Risling *et al.*1983a; Carlson *et al.*1979). There is

some evidence of shrinkage of surviving cells following injury (Risling *et al.*1983a), but another study failed to find any change in cell size (Ygge, Aldskoguis, 1984b).

As described in other neuronal systems after neonatal injury (LaVelle, LaVelle, 1958), more cell death results after neonatal injury than in the adult (Aldskoguis, Risling, 1981; Himes, Tessler, 1989). A comparison of the amount, and time-course, of cell death in the L5 DRG of adult and neonatal rats, after section and ligation of the sciatic nerve, shows that 30% of axotomised neurones in adults die and 75% of the axotomised neurones in neonates die (Himes, Tessler, 1989). Sciatic nerve section on the day of birth also results in retardation of the growth of the dorsal horn (Fitzgerald, Shortland, 1988). This may result in a reduction of the dorsal horn area of up to 40% compared to the contralateral control side, and dorsal horn cells with abnormal morphologies (Fitzgerald, Vrbová, 1985; Fitzgerald, Shortland, 1988). Neonatal sciatic nerve crush results in cell death in the dorsal root ganglion (Yip *et al.*1984), but if the target is reinnervated (as, for instance, after crush injury) there is less retardation in the growth of the dorsal grey matter (Fitzgerald, Vrbová, 1985).

Collateral sprouting of axons following injury has been observed in the central nervous system of mammals, both in neonates (Fitzgerald, 1985b) and adults (Molander *et al.*1988). After injury to the peripheral nerve in young rats, there is death of injured dorsal root neurones and expansion of the axons of neighbouring intact neurones, into the denervated dorsal horn (Fitzgerald, 1985b; Fitzgerald *et al.*1990). The conditions that allow sprouting to occur are different in the neonate compared to the adult. After peripheral nerve section in the neonatal rat on P1, there is sprouting of adjacent nerve terminals into the territory of the injured nerve (Fitzgerald, 1985b; Fitzgerald, Vrbová, 1985; Fitzgerald *et al.*1990). There is little or no sprouting of uninjured nerve terminals if the injury is inflicted after P5 (Fitzgerald, 1985b). In addition, crushing the sciatic

nerve results in less sprouting of adjacent nerve terminals than cutting the same nerve (Fitzgerald, 1985b). In the adult rat, sprouting of adjacent nerve terminals has been shown to occur only after this nerve has been damaged itself. Molander *et al.* showed that, after cutting the sciatic nerve in the adult rat there is no discernible sprouting of the adjacent saphenous nerve terminals unless this nerve itself has also been crushed (Molander *et al.*1988). The difference in the amount of sprouting after neonatal injury compared to injury in the adult, is possibly because there is a greater amount of cell death of sensory neurones following neonatal injury (Yip *et al.*1984) than in the adult (Rich *et al.*1987). This may provide a greater stimulus for axons to sprout in the neonate. After dorsal rhizotomy in the adult, resulting in injury to the central projection of the nerve, where one root has been spared, there is also sprouting of the uninjured nerve terminals (Piehl *et al.*1991).

Parvalbumin immunoreactivity has been shown to preferentially label the large diameter primary afferents, and not the smaller diameter afferents terminating in the dorsal horn (Zhang *et al.*1993; Celio, 1990). Parvalbumin-positive neurones have been observed in the spinal cord of the rat in the adult (Celio, 1990) and during development (Zhang *et al.*1990; Solbach, Celio, 1991). PV-immunoreactive fibres are first seen in the spinal cord between E15 and E17. They reach a peak of expression of P14, and then PV staining declines. The immunoreactive fibres can be traced to the dorsal root, and some neurones in the dorsal ganglion are also PV-positive (Zhang *et al.*1990). The expression of PV in the lumbar spinal cord of the rat coincides with the first appearance of the monosynaptic reflex (Kudo, Yamada, 1987) and PV is also expressed in the annulospiral endings of muscle fibres in neonatal rats (Celio, 1990). This suggests that PV can be used as an early marker for large diameter 1a afferent fibres.

Injury to the peripheral nerve during the early postnatal period results in substantial death of DRG cells (Aldskoguis, Risling, 1981; Himes, Tessler, 1989;

Bondok, Sansone, 1984) and this is usually accompanied by evidence of collateral sprouting of adjacent nerves into the territory vacated as a result of injury (Fitzgerald, 1985b; Risling *et al.*1984). This is especially pronounced if the injury is inflicted at birth.

Parvalbumin belongs to a family of low molecular weight calcium-binding proteins, with a common evolutionary origin and similar structure (see (Heizmann *et al.*1990)). Ca^{2+} is frequently implicated in the transduction of external signals into intracellular information. It is involved in numerous biological functions in the adult, such as muscle contraction, transmission between nerves, and release of neurotransmitters (see (Baimbridge *et al.*1992)). Uncontrolled elevation in the amount of intracellular Ca^{2+} leads to cell death (see (Heizmann, Braun, 1992)). Calcium is also involved in many events during development, such as neurite elongation and growth cone motility (Anglister *et al.*1982; Kater *et al.*1988; Mattson, Kater, 1987). By virtue of the fact that PV binds Ca^{2+} it affects Ca^{2+}-mediated events. Cells transfected with PV cDNA have a decreased mitotic rate (Rasmussen, Means, 1989) and increased motility (Andressen C., Gotzos V., Celio M.R. *unpublished*). It is possible that the developmental changes in PV reflect changes in the maturation of the neurones. Levels of PV increase in the primary afferent fibres at a time when they were growing through the spinal cord and forming connections with the motoneurones. When these connections have been established, after the second postnatal week, the levels of PV decrease.

4.1.4. Descending serotonergic afferents

The white matter of the spinal cord contains axons which carry information to and from the brain, as well as locally within the spinal cord. There are descending pathways, from the brain to spinal neurones (see (Tracey, 1985; Holstege, Kuypers, 1987b)) one of which originates in the raphe nuclei of the brain stem (see (Tork, 1985)). A characteristic feature of the raphe nuclei is that a large

proportion of the neurones within them are serotonergic (Dahlstrom, Fuxe, 1964). Neurones from the raphe pallidus and raphe obscurus nuclei project to the ventral horn of the spinal cord through the ventral funiculus (Bowker *et al.*1981; Bowker, Abbott, 1990), whilst neurones from the nucleus raphe magnus project via the dorsolateral funiculus (where they are assumed to be involved in the control of sensation (Eide *et al.*1990; Gharagozloo *et al.*1990)) and terminate in the dorsal horn.

Studies of the projections of these brain stem nuclei have been conducted using both anterograde (Holstege, Kuypers, 1987c; Basbaum *et al.*1978; Holstege, Kuypers, 1987b; Jones, Light, 1990) and retrograde (Bowker *et al.*1981; Bowker, Abbott, 1990; Skagerberg, Bjorkland, 1985; Tan, Miletic, 1990; Jones, Light, 1992; Pilowsky *et al.*1990) techniques. A combination of these tracers and immunocytochemical techniques has allowed the chemical identity of the pathways to be studied. In addition to serotonin, neurones containing other peptides such as substance P, thyrotropin-releasing hormone (TRH), CGRP, enkephalin, GAP-43 and somatostatin have been found (Bowker, Abbott, 1990; Bowker, 1986; Bowker *et al.*1983; Tashiro *et al.*1988; Ulfhake *et al.*1978; Azvidsson *et al.*1990; Arvidsson *et al.*1992; Nicholas *et al.*1992). The pharmacological effects produced by the application of agonists and antagonists of serotonin and the other peptides, suggest that the descending systems have a neuromodulatory effect on the spinal cord ((Anderson, 1972), see (Holstege, Kuypers, 1987b)). Serotonin has been shown to cause a reduction in the after-hyperpolarization of lamprey interneurones (van Donger *et al.*1986). This results in an increased frequency of firing of lamprey neurones, and will affect the motor activity of the spinal cord. In identified motoneurones of the rat, serotonin has been shown to exert an excitatory effect (Berger, Takahashi, 1990). Serotonergic pathways have a facilitatory effect on motoneurones, as does substance P, possibly by modulating the effect of serotonin on the motoneurone membrane (Tremblay *et al.*1986). The action of the serotonin-containing fibres

projecting to the ventral motoneurones from the raphe pallidus and raphe obscurus, enhance the responsiveness of the motoneurones. Neurones from the raphe magnus, which project to the dorsal horn, have an inhibitory effect on the transmission of pain. If these two systems were to act together there would be a resulting enhanced responsiveness of the motor system accompanied by decreased awareness of pain.

4.1.5. Development of serotonergic afferents

The development of the serotonergic system has been studied in the nervous system of the chick and the rat ((Okado *et al.*1991) in the chick; (Tanaka *et al.*1992) in the rat). Development of serotonin positive fibres occurs in a rostral to caudal direction, and the ventral horn is innervated before the dorsal horn. Serotonin positive fibres were first seen in the cervical cord of the chick on E6 and in the lumbar spinal cord on E8. They were first located in the lateral and ventral parts of the white matter in the ventral horn. Between E8 and E16 there is an increase in the levels of serotonin and the density of serotonin positive axons in the spinal cord of the chick. Lamina IX contains serotonin positive fibres on E16, however the pattern of innervation suggests that the fibres were just invading the ventral horn. The pattern of innervation changes after hatching, as the serotonergic axons arborize and form contacts with the motoneurones. The serotonergic fibres are within the lateral and medial parts of the lateral motor column. The axons are varicose and are located around the somal profiles of the motoneurones. The pattern of innervation is less dense in the dorsal horn at this time. In the first week after hatching the density of serotonin positive fibres continues to increase. Between one and two weeks after hatching the density of serotonin positive axons decreases in the neuropil. However, the serotonin positive varicosities become more densely located around the profiles of the motoneurones. In the adult spinal cord, the serotonin positive fibres are unevenly distributed through the spinal cord, with dense innervation around motoneurones in the ventral horn.

In the rat, the first projections from the brain stem to the spinal cord are on E15.5 (Kudo *et al.*1993). The density of serotonin positive appositions increases around hindlimb extensor motoneurones during the first two postnatal weeks (Tanaka *et al.*1992), at a time when there are changes in the activity of motoneurones (Navarrete *et al.*1988a). The adult pattern and density of innervation is not achieved until P14 in the cervical spinal cord and P21 in the thoracic and lumbar spinal cord (Bregman, 1987; Tanaka *et al.*1992). This may be partly responsible for the gradual development of motor function, and for this reason serotonin was selected for this study. Serotonergic descending inputs to the ventral horn of the spinal cord have been shown to be involved in the modulation of motor function (see (Holstege, Kuypers, 1987b)). In addition, serotonin may be involved in the development of dendritic form ((Goldberg *et al.*1991; Haydon *et al.*1987), see (Lipton, Kater, 1989). Serotonin has been shown to have an inhibitory effect on the outgrowth of extending neurites of embryonic snail neurones in culture (Haydon *et al.*1987; Goldberg *et al.*1991), by direct inhibition of growth cone motility. In those neurites that were stable, serotonin caused a reinitiation of growth. There was no observed effect on adult cultured neurites. Thus, it appears that serotonin regulates neurite outgrowth in embryonic neurones.

In this study, the early postnatal changes in two types of afferent inputs onto the flexor motoneurones were studied: the parvalbumin-positive sensory afferents, and the serotonin-positive descending afferents. The changes in the afferent innervation was also studied after injury to the peripheral nerve. This causes damage to the 1a afferents, but might not effect the descending afferent fibres.

4.2. METHODS

4.2.1. Surgery

Wistar rat pups were used throughout. On the day of birth (P0), the tibialis anterior and extensor digitorum (TA/EDL) muscles were injected with 1 µl of Fast Blue and Diamidino Yellow (FB/DY; Illing) with 5% FITC-dextran amine (10K MW; Sigma) in distilled water, in both hindlimbs under halothane anaesthesia. On P2, allowing time for retrograde transport of the dyes from the muscle to the motoneurones within the spinal cord, the common peroneal (CP) nerve was crushed unilaterally about 3 mm from the entry of the nerve into the flexor muscles.

4.2.2. Intracellular injection

In some preparations the spinal cord was dissected out hemisected and mounted on the fixed stage of a purpose-built injection microscope. Motoneurones retrogradely labelled with FB/DY and the fluorescinated Dextran, were visualised under epifluorescence using Fast Blue and Lucifer Yellow filters. Individual cells were iontophoretically filled with Lucifer Yellow using negative currents for 15-20 minutes (see Chapter 2).

After injection, hemicords were fixed in 4% paraformaldehyde for up to a week, transferred to 30% sucrose, cut at 100 µm on a freezing microtome (Pelcool) and processed for serotonin immunocytochemistry as free-floating sections in the same way as sections on slides. The sections were incubated in wells, and transferred carefully, to avoid damage to the tissue, through the processing using a paintbrush. There were spinal cords from P4 (n=2 motoneurones), P6 (n=3 motoneurones), P7 (n=5 motoneurones) or P8 (n=4 motoneurones) day old animals.

4.2.3. DiI labelling of fixed tissue

In a preliminary study, small amounts of the carbocyanin dye, DiI (1,1'-dioctadecyl-3,3,3',3'-tetramethylindo-carbocyanine perchlorate) were placed on the L4 dorsal and/or ventral roots to label the afferent axons and the motoneurones. The spinal cord was removed and placed in 4% paraformaldehyde. The dorsal and ventral roots were carefully dissected free, whilst the tissue was in the fixative. The spinal cord and its spinal roots were pinned out on a petri dish that had been coated in silgard(DOW). A small amount of DiI was carefully crushed onto the L4 dorsal and/or ventral roots, ensuring that there was no contamination of other regions of the spinal cord. The preparation was then kept in fixative (4% paraformaldehyde), at 38 ^{o} C for about 2 months. After this the tissue was removed, washed in PBS, embedded in agar (Sigma), sectioned at 100 μm and visualised using epifluorescence.

4.2.4. Immunocytochemistry

At P3, P7 and P14 the animals were deeply reanaesthetised and perfused intracardially with 4% paraformaldehyde. Their spinal cords were removed, postfixed for 3 hours in 4% paraformaldehyde and the placed in 30% sucrose as a cryoprotectant. Sections were cut at 50 μm and put onto gelatinised slides (0.05%). Only those slides that contained sections with the FB/DY prelabel were processed for immunocytochemistry.

4.2.5. Parvalbumin

Sections, on slides, were immersed in phosphate buffered saline (PBS; 0.01%) with 0.3% Triton-X-100 (T). They were then incubated for 1 hour in 3% Normal Horse Serum (NHS; Vector). After washes in PBS-T, the sections were incubated in 1:1000 primary antibody, monoclonal mouse anti-Parvalbumin (Sigma) for 48 hours at 4^{o}C in PBS-T. Negative control sections in which the primary antibody was omitted were also prepared. The sections were thoroughly washed before incubation in the secondary, biotinilated layer, 1:100 biotinilated

horse anti-mouse (adsorbed in rat; Vector) at room temperature in PBS.

The sections were then processed either with HRP as the chromagen, or for fluorescence with Texas Red as the chromagen.

4.2.6. HRP-visualisation of PV-immunoreactivity

After washing, the sections were immersed in the avidin-biotin complex (Vector ABC kit). This was mixed 1/2 an hour prior to use and incubated for one hour. Following a wash in PBS the sections were then reacted with diaminobenzamine (DAB; 20 µg/1 ml) with 5 µl hydrogen peroxide for 20-25 minutes, until darkly stained.

The sections were examined under conventional light microscopy. Using camera lucida, drawings of the operated and control sides of the spinal cords were made (see Fig. 4.4). The number of PV-positive appositions contacting the soma of the motoneurones were counted. The appositions were often in a different plane of focus to the outline of the soma, and it was necessary to constantly change the focus to accurately plot the position of the PV-positive boutons (see Fig. 4.3).

The soma areas were measured using a graphics tablet interfaced with a microcomputer and morphometric software written by Dr. J. Cook. The number of appositions per 100 µm of soma perimeter was calculated. The operated side was compared for significant difference with the normal, contralateral control side, using the Mann-Whitney U test.

4.2.7. Texas red visualisation of PV-immunoreactivity

The sections were washed in bicarbonate buffered saline prior to incubation in 1:100 solution of Texas Red Avidin D (Vector) in bicarbonate buffered saline for 2 hours.

Sections were examined using the LSCM. A 'z-series' of five separate 1 μm steps was created through a high power image containing 1 or 2 prelabelled motoneurones, using firstly the BHS filter optimal for FITC (exciter, 488 BP; reflector, 510 LP; barrier, 515 LP; manufacturer's data). The LSCM uses an argon laser with light emitted at wavelengths in the range of 458-514 nm, too long to excite FB and DY. However, it was possible to see the FITC-dextran amine dye, which had a granular appearance in the cytoplasm of the neurone.

Without changing the focus, the identical series of optical sections were collected using the GHS filter, optimal for Texas Red (exciter, 514 DF; reflector, 540 LP; barrier, 550 LP). The software provided with the LSCM (SOM) enabled me to 'merge' each single image from one filter with its counterpart image obtained on the other filter. This created a 'merged image' with pseudocolours to indicate which features were obtained with each filter. From this merged image the number of appositions within 0.2 μm of the soma in each of these five 1μm thick sections through the motoneurone were counted. The soma area of the motoneurone was measured, and the number of appositions per unit area was calculated. The operated side was compared with the control side.

4.2.8. Serotonin immunocytochemistry

Sections were immersed in phosphate buffered saline (PBS; 0.01%) with 0.3% Triton-X-100 (T). They were then incubated for 1 hour in 3% Normal Goat Serum (NGS; Vector). After washes in PBS-T, the sections were incubated in 1:1000 primary antibody, polyclonal rabbit anti-serotonin (Chemicon) for 48 hours at 4 ^{o} C in PBS-T. Negative controls, without the primary antibody, were also prepared. The sections were thoroughly washed before incubation in the secondary, biotinilated layer, 1:200 biotinilated goat anti-rabbit (Vector) at room temperature in PBS.

The sections were then processed either with HRP as the chromagen, or for fluorescence with Texas Red as the chromagen. Free-floating sections containing LY filled motoneurones were processed only for fluorescence.

4.2.9. HRP-visualisation of serotonin-immunoreactivity

After washing the sections were immersed in the avidin-biotin complex (Vector ABC kit). This was mixed 1/2 an hour prior to use and incubated for one hour. Following a wash in PBS the sections were then reacted with diaminobenzamine (DAB; 20 µg/1 ml) with 5 µl hydrogen peroxide until darkly stained.

The sections were examined using light microscopy. The density of serotonin-positive boutons within the ventral horn of the spinal cord was calculated by using a camera lucida drawing tube, with a x40 objective, to obtain a drawing of the area of the flexor motor pool. A grid of 50 x 50 µm squares was placed over the area to be measured and the number of boutons falling within this grid were counted for four samples. The density of appositions at P7, P14 and the adult was compared in the operated and contralateral control sides of the spinal cord.

Camera lucida drawings of individual motoneurones (x 40) were made from the injured and contralateral control sides of the spinal cords. The contacts made by serotonin-positive axons onto individual motoneurones considered to be within the flexor motor pool were drawn. The number of serotonin-positive appositions contacting the perimeter of the soma of these motoneurones were counted.

The soma perimeter was measured using a graphics tablet and a morphometric software (J. E. Cook, 1993), and the number of appositions per 100 µm of perimeter of the soma was calculated. The operated side was compared with the normal, contralateral control side.

4.2.10. Texas red visualisation of serotonin-immunoreactivity

Prelabelled sections were washed in bicarbonate buffered saline prior to incubation in 1:100 solution of Texas Red Avidin D (Vector) in bicarbonate buffered saline for 2 hours.

Sections were visualised on the LSCM as described previously. The LY filled motoneurones were imaged firstly using the BHS filter optimal for FITC. Then, without changing the focus, the identical series of optical sections were created using the GHS filter, optimal for Texas Red to show serotonin-immunoreactivity. As for parvalbumin, a series of images was obtained along the z-axis, in different regions of the dendrites and soma of the cell, at 1 μm intervals. These images were 'merged', with pseudocolours to indicate which features were obtained with each separate filter (see Fig. 4.12). From this merged image the number of serotonin-immunoreactive appositions within 0.2 μm (the limit of resolution of the LSCM; manufacturer's data) of the soma in this region through the motoneurone was recorded. The whole of the motoneurone was systematically imaged in this way, and the position of serotonin appositions in all regions of the neurone were mapped using both filters.

The soma diameter and dendritic lengths and diameters were measured in individual intracellularly filled motoneurones. The number of serotonin-positive appositions per unit membrane area was calculated. The percentage of the appositions on the soma within 75 μm of the centre of the soma and greater than 75 μm from the centre of the soma were calculated. The percentage of appositions within the dorsal, ventral, rostral and caudal quadrants were calculated. This allowed a comparison to be made between the distribution of appositions on the soma and dendrites of normal and injured motoneurones.

4.3. RESULTS

As described previously (Chapter 2), the fluorescent retrogradely labelled motoneurones innervating the hindlimb flexor muscles TA and EDL are located between L3 and L5 in the lumbar spinal cord of the rat. Sections of the spinal cord, cut at 20 μm, containing sections in which fluorescently prelabelled motoneurones were visible, were selected for parvalbumin or serotonin immunocytochemistry. In some cases 100 μm sections containing motoneurones intracellularly filled with Lucifer Yellow (LY) were processed for immunocytochemistry.

4.3.1. Primary afferents

In a few preliminary experiments, the pattern of primary afferent innervation in the spinal cord was studied using anterograde labelling with the fluorescent carbocyanin dye, DiI in fixed tissue (Fig. 4.1). In these preparations both the dorsal and ventral L4 roots were labelled with a few crystals of DiI. This fluorescent dye labels the plasma membrane of the cell (see (Honig, Hume, 1989)), and can also be used to retrogradely label motoneurones in the spinal cord. Figure 4.1 shows the primary afferent fibres from one L4 dorsal root in a longitudinal section of the spinal cord. The primary afferent fibres pass through the dorsal horn (Fig. 4.1a; top) into the ventral horn (Fig. 4.1b; bottom). Here they enter the territory of dendrites from the motoneurones (Fig. 4.1b; the dendrites are also labelled with DiI, and are located to the right of the frame) in the ventral horn.

DiI labels all the afferent fibres entering the spinal cord through the labelled dorsal roots. Sensory afferent axons terminate throughout the dorsal horn in laminae I-V. There is somatotopic organisation of the terminating afferents arranged according to their origin (Rivero-Melian, Grant, 1990; Fitzgerald, 1985a). Some sensory afferents terminate on the large neurones of Clarke's column in

laminae V and VI (Rivero-Melian, Grant, 1987). Other axons terminate in the region of the interneurones in laminae VII and VIII. There are some monosynaptic terminations in lamina VIII in the region of the motor pools.

4.3.2. Developmental expression of parvalbumin in the rat spinal cord

Parvalbumin immunoreactivity preferentially labels the large diameter primary afferent axons during the early postnatal period (Zhang *et al.*1990; Solbach, Celio, 1991; Celio, 1990), and does not label the smaller diameter afferents that terminate in the dorsal horn. (Some axon collaterals terminate in laminae V and VI as well as in the ventral horn on the motoneurones (see also (Ishizka *et al.*1979))). The pattern of PV staining was compared at P3, P7 and P14. Since PV immunoreactivity disappeared in the ventral horn of the lumbar spinal cord by P21 in the rat (Zhang *et al.*1990), a comparison was not made with the adult.

The general pattern of PV staining was similar at the three ages studied. There was PV-positive staining in the dorsal funiculus of the spinal cord and the dorsal root entry zone (see Fig. 4.2). The afferent axon collaterals passed through the medial part of the dorsal horn, to the deeper parts of the grey matter. Some axon collaterals appeared to terminate in lamina VI, in the region of Clarke's nucleus which corresponds to the origin of the posterior spinocerebellar tract (Fig. 4.2). Most afferent axons terminated in lamina IX, around the motoneurone cell bodies.

The pattern of PV-immunoreactive staining in the spinal cord at P3 is shown in Figure 4.2a. In the grey matter of the ventral horn there was strong labelling of axons in laminae VI, VIII and IX. The overall amount of PV-staining appeared to increase in the spinal cord from P3 to P7 (Fig. 4.2b). There was also considerable growth of the spinal cord (compare the sizes of spinal cord cross sections in Fig. 4.2) over this period. The amount of PV-immunoreactive labelling of primary afferents remained high up to P14 (Fig. 4.2c).

The density of PV-immunoreactive afferent axons terminating around identified flexor motoneurones was quantified by counting the number of boutons (enlargements along the primary afferent axon collateral; also referred to as 'appositions') apposing the perimeter of the soma. Using conventional light microscopy, only those boutons that appeared to touch the outline of the motoneurone cell body were counted at high magnification. Figure 4.3 shows a gallocyanin counterstained motoneurone from a section of spinal cord at P3 containing FB/DY prelabelled motoneurones that has been processed for PV immunocytochemistry. This shows that only a few of the appositions were in focus at any single focal plane. The focal plane was changed as the appositions were counted. The number of appositions around the outline of the soma of the motoneurone were drawn (see Fig. 4.4), allowing the total number of appositions per unit motoneurone membrane area to be calculated. However, using this method it was not possible to discriminate between a bouton that was touching the outline of the motoneurone and one that was close to it. The confocal microscope was used, as it allowed better resolution of the proximity of the appositions to the motoneurones. The limit of resolution of the confocal microscope was 0.2 μm, so boutons were within 0.2 μm of the outline of the soma (see Fig. 4.5). In all preparations there was some variability of immuno-staining, but those sections with poor staining were discarded.

Table 4.1 shows the data of the number of boutons contacting the perimeter of flexor motoneurones at P3 (n=116 motoneurones), P7 (n=99 motoneurones) and P14 (n=60 motoneurones). There are no significant changes (Mann-Whitney U test) in the mean number of boutons contacting the soma of motoneurones between P3 (9.9 ± 4.7; mean ± SD) and P7 (11.8 ± 5.7) or P7 and P14 (11.8 ± 7.4). However, the soma perimeter increased significantly between P3 (89.0 ± 11.5 μm) and P7 (111.8 ± 23.5 μm), and also between P7 and P14 (127.3 ± 17.2 μm). The mean number of appositions per 100 μm of the soma

perimeter decreased slightly between P3 (11.1 ± 4.9 per 100 μm) and P7 (10.8 ± 4.5 per 100μm). There was a significant decrease in the number of appositions per 100 μm of perimeter between P7 and P14 (9.0 ± 5.3 per 100 μm). Thus, it would appear that the number of PV-positive fibres contacting the motoneurone does not change at a time when there is an increase in the soma area of the motoneurones. This results in a reduction in the density of appositions around individual hindlimb flexor motoneurones.

Figure 4.5 illustrates the pattern of PV immunoreactivity around an individual motoneurone at P7, imaged using the LSCM. The motoneurone was retrogradely labelled with fluorescinated dextran dye, which appears as an indistinct granular label in the cytoplasm of the cell (Fig. 4.5a). The motoneurone was imaged using the BHS filter. Texas red was used as a chromagen to label the PV-positive afferent axons. Texas red was visualised using the GHS filter. The images were 'merged' to create a pseudocolour image of the information collected from both filters (see Fig. 4.5). The number of boutons (Fig. 4.5a, arrows) apposing the outline of these motoneurones was counted in each of five separate sections at 1μm intervals through the soma at the level of the nucleolus. The number of boutons was calculated per 100 μm^2 unit area of the motoneurone. The use of the LSCM to visualise and quantify the PV-positive afferent inputs onto the motoneurones was intended to verify the results of counting appositions using light microscopy, with an alternative, and more accurate technique. Only a small number of animals were used.

Table 4.2 shows the results of counting the appositions contacting motoneurones at P3 (n=104 motoneurones), at P7 (n=85 motoneurones) and at P14 (n=29 motoneurones). As observed with conventional light microscopy (see Table 4.1), there is no change in the number of boutons apposing a motoneurone at P3, P7 and P14 at a time when there is a significant increase in the size of the soma. This results in a developmental decrease in the density of appositions

onto flexor motoneurones. The mean number of appositions contacting the soma at P3 was 7.6 ± 5.0, at P7 was 7.6 ± 4.2 and at P14 was 8.1 ± 4.0. The mean area of the soma was 462.8 ± 139 μm^2 at P3, 601.5 ± 237.5 μm^2 at P7 and 937.2 ± 251.1 μm^2 at P14. This resulted in a significant reduction in the mean number of apposition per 100 μm of soma area from 1.7 ± 1.1 μm^2, at P3, to 1.3 ± 0.8 to P7 μm^2 and 0.9 ± 0.4 μm^2 at P14.

In one experiment a single motoneurone was intracellularly filled with Lucifer Yellow and visualised under fluorescence using confocal microscopy (Fig. 4.5c). No attempt was made to count the number of PV-positive contacts onto the soma and dendrites of the cell, due to the large number of PV-positive axons in the region of the soma and dendrites of the motoneurone. This proved difficult, and no attempt was made to investigate developmental trends in the topographical location of PV-immunoreactive appositions contacting the motoneurones using this method.

Figure 4.6 shows the distribution of PV-positive neurones throughout the spinal cord. On P3 (Fig. 4.6a), there were few PV-positive neurones, and these were located in the ventral horn in laminae VII, VIII and IX. By P7 (Fig. 4.6b), there was an increase in the number of PV-positive neurones in the ventral horn especially in lamina VIII. Judged by their location and morphology, these PV-positive cells were probably mostly interneurones (Jankowska, Lindstrom, 1972). At P14 (Fig. 4.6c), there was a further increase in the number of PV-positive neurones, some of which were located in the dorsal horn. No PV-immunoreactive neurones were considered to be motoneurones.

4.3.3. Changes in parvalbumin expression after injury

Following CP crush at P2, the pattern of PV staining in the injured ventral horn was compared with that on the control side at P3, P7 and P14 (see Figs. 4.2 and 4.7, 4.8, 4.9). Using conventional light microscopy, at P3 (Fig. 4.2a and Fig.

4.7) very little difference was observed in the pattern of PV-positive staining in the ventral horn on the injured compared to the control side of the spinal cord. By P7 (Fig. 4.2b and Fig. 4.8) there was less PV-positive staining on the operated side of the spinal cord, and this continued to decrease, so that by P14 (Fig. 4.2c and Fig. 4.9) there was a clear reduction in the PV-immunoreactivity on the operated side of the ventral horn. In addition, there was a decrease in the density of PV-immunoreactivity in the region of the dorsal root entry zone. This was especially marked at P14 (Fig. 4.2c). This result is consistent with the death of some dorsal root ganglion neurones following neonatal nerve injury reported in previous studies (Himes, Tessler, 1989).

The number of boutons contacting injured flexor motoneurones was quantified and compared with the values on the contralateral unoperated side of the spinal cord reported in the previous section. Table 4.1 shows the data at P3 (n=115 motoneurones), P7 (n=71 motoneurones) and P14 (n=43 motoneurones). There was no significant difference in the number of appositions at P3 (9.5 ± 4.6) and P7 (11.2 ± 6.9), or P14 (11.7 ± 7.2). As on the control side of the spinal cord, there was a significant increase in the perimeter of the soma between P3 (87.3 ± 13.4 μm) and P7 (103.4 ± 22.7 μm), and between P7 and P14 (123.6 ± 28.0 μm). In this sample there was no significant difference in the perimeter of the soma of injured compared to control motoneurones at any of the ages studied. In addition, there was no significant change in the number of appositions per 100 μm of soma perimeter at P3, P7, or P14 after injury on P2.

These results were somewhat surprising as previous studies have shown that neonatal injury results in death of a large number of dorsal root ganglion neurones (Himes, Tessler, 1989; Bowker *et al.*1983). It might, then, be expected that there would be a reduction in the innervation to the spinal cord from the dorsal root, but these results did not indicate that this was the case. Since it was possible that conventional light microscopy did not provide adequate resolu-

tion of the separation of the PV-positive afferent appositions and the outline of the motoneurones, the LSCM was used. The number of appositions contacting a relatively small number of identified CP motoneurones after injury on P2 was counted. Texas Red was used as a fluorescent chromagen to label PV-immunoreactive afferent contacts. The limit of resolution of the confocal microscope is about 0.2 μm, so that it was possible to discern with greater accuracy the proximity of the boutons to the soma outline. By using optical sectioning throughout the motoneurone, it was also possible to have the entire depth of tissue being visualised in focus. This revealed that there were discrepancies in the results of the counts using these two different methods.

The greatest problem in using this method was that the prelabel, injected into the muscles TA and EDL at birth, was not clearly visible using the wavelengths emitted by the argon laser. Fast Blue/Diamidino Yellow were not visible at all, and so a fluorescinated dextran amine was also injected. In many cases this was indistinctly visible as granules in the cytoplasm of the motoneurone (see Fig. 4.5a), but it still did not provide a clear outline of the soma. This led to selectivity in the quality of the motoneurones imaged, resulting in a bias in sampling, and consequently only a small number were counted.

Figure 4.5 shows examples of PV-positive afferents contacting an injured (Fig. 4.5b) and a contralateral control (Fig. 4.5a) motoneurone at P7. It can be seen that there are fewer appositions (arrows) touching the outline of the injured motoneurone than the control cell. Table 4.2 summarises the results of counts of the numbers of these appositions. Here it can be seen that there was a reduction in the number of PV-positive appositions contacting the flexor motoneurones after injury. Even at P3, 24 hours after the injury, there was a significant reduction (23%) in the number of PV-positive appositions contacting the somata of flexor motoneurones. There was no difference in the mean soma area of injured compared to control motoneurones at any of the ages studied. Over the

period there was a significant increase in the mean soma area of injured and control motoneurones from 449.2 ± 124.0 at P3, to 590.8 ± 193.7 at P7, and 983.9 ± 240.6 at P14. There was a significant difference in the number of appositions per 100 μm^2 of soma area in operated motoneurones compared to controls at P3 (81%), P7 (32%) and P14 (33%). Clearly there are some discrepancies in the numbers of afferent inputs onto motoneurones found using these two different counting techniques.

4.3.4. Density of descending serotonergic afferents in the CP motor pool

Serotonin-positive axons appeared in the spinal cord as varicose fibres. They were observed throughout the ventral horn (see Fig. 4.10a and 4.11a). A gross estimate of the density of serotonin-positive axons in the ventral horn was obtained by counting the number of axon profiles within 50 μm^2 squares in a grid placed over the area of the CP pool in four animals at each of the ages P7, P14, P22 and adult. HRP was used as a chromogen, and the sections were visualized using light microscopy. The changes in density of serotonin immunoreactive fibres from P7 to adult is shown in Table 4.3. There is a significant increase in the density of serotonin-positive fibres in the ventral horn between P7, P14, P22 compared to in the adult.

A similar increase was seen over the period studied after neonatal crush (Table 4.3 and Figs. 4.10a and 4.11a). There was no significant difference between the control and operated sides of the spinal cord. The overall density of the serotonin afferent fibres did not change within the ventral horn after neonatal injury.

4.3.5. Serotonin immunoreactive appositions onto individual motoneurones

The number of serotonin-immunoreactive boutons contacting individual prelabelled motoneurones was quantified by counting the number of boutons closely apposing the perimeter of the soma of motoneurones in the CP motor

pool at P3 and P7 using conventional light microscopy (Fig. 4.10b and 4.11b). The number of appositions per 100 μm soma perimeter was calculated. Table 4.4 shows the mean number of appositions on motoneurones at P3 (n=58 motoneurones) and P7 (n=53 motoneurones). The mean number of appositions on each motoneurone was 4.8 ± 3.5 at P3, and at P7 it was 8.7 ± 5.2. At P3 there were 6.4 ± 4.3 appositions per 100 μm soma perimeter; this increased to 11.0 ± 6.0 at P7. The perimeter of the motoneurones increased significantly over this period. There was an increase in the number of serotonin-positive contacts onto individual motoneurones from P3 to P7.

Table 4.4 shows a comparison of the number of serotonin-positive appositions contacting control and injured CP motoneurones at P3 (n=54 motoneurones) and P7 (n=55 motoneurones). At P3, the mean number of appositions contacting injured motoneurones was 6.6 ± 3.3, compared to 4.8 ± 3.5 on the control side. This was significantly different, as was the mean number of appositions on injured motoneurones at P7 (11.2 ± 5.5), compared to the control side (8.7 ± 5.2). There was no significant difference in the perimeter of injured and control motoneurones at either P3 or P7. The number of appositions per 100 μm soma perimeter was calculated for injured and control sides of the spinal cord at both P3 and P7. At P3, there were 6.4 ± 4.3 appositions per 100 μm perimeter on the control side and 9.1 ± 4.8 on the injured side. At P7 there were 11.0 ± 6.0 apposition per 100 μm perimeter on the control side and 15.2 ± 7.5 on the injured side. There were significant differences between the control and injured sides of the spinal cord at P3 and P7 (see Fig. 4.10c,d and 4.11c,d). This suggests that, whilst there may not be an overall increase in the serotonin innervation to the ventral horn after neonatal injury (see Table 4.3), there are more serotonin afferents contacting CP motoneurones (see Table 4.4).

4.3.6. Mapping of serotonin innervation onto LY-filled motoneurones

The topographic distribution of serotonergic contacts onto the soma and den-

drites of flexor motoneurones was investigated by mapping the position of serotonin-positive boutons onto individual, intracellularly filled flexor motoneurones. The whole motoneurone was systematically mapped, using a series of images at 1 μm steps through the depth of the Lucifer Yellow filled motoneurone (Fig. 4.12a, b). In each optical section, those contacts that appeared to be in direct apposition (i.e. within less than 0.2 μm) of the dendrites or soma of the motoneurone were included. Figure 4.13 shows a pseudocolour 2-dimensional projection image of P7 motoneurones filled with Lucifer Yellow. Serotonin immunoreactive boutons can be seen contacting the soma (Fig. 4.13c), proximal dendrites (Fig. 4.13b) and distal dendrites (Fig. 4.13d) of the motoneurone. The position of these boutons was carefully mapped for seven injured and seven control motoneurones. Figure 4.14 shows a camera lucida-type drawing of the position of serotonin immunoreactive contacts on a control (Fig. 4.14a) and an injured (Fig. 4.14b) motoneurone. It can be seen that the majority of the contacts are made in the distal (further than 75 μm from the soma) parts of the dendritic tree of the motoneurone.

Table 4.5 shows the location of serotonin-positive afferent boutons on control and injured motoneurones. The variability of immunostaining in different experiments was reflected in the differences in the total number of appositions contacting each motoneurone. There may also have been problems in photobleaching during image acquisition, especially of very distal dendrites. The problems associated with this method will be addressed in the discussion. The number of afferent contacts was expressed as a percentage of the total number of contacts for different regions of the motoneurone.

The most striking difference in topographic position of serotonergic appositions on injured and control motoneurones was seen in the number of boutons contacting the soma (see Table 4.5). In control motoneurones, only 1.5% of the total number of contacts were made on the soma of the motoneurone. This in-

creased to 12.3% after neonatal injury. In both control and injured cells, about 60% of the contacts were found at distances greater than 75 μm from the soma. In control cells, 36% of the appositions contacted the motoneurones closer than 75 μm from the soma, compared to 30% after injury. Thus, it appears that there is a redistribution of some of the most proximal contacts onto the motoneurones following injury during the postnatal period. This confirms the observations found by counting the number of appositions onto the cell bodies of individual retrogradely prelabelled motoneurones (see Table 4.4).

Table 4.6 shows the percentage of contacts made in dorsal, ventral, rostral and caudal 90^{o} quadrants oriented around the soma of the intracellularly filled motoneurones. From this it can be seen that the majority of the afferents make contact with the motoneurones from the dorsal quadrant in both control (37.7 ± 12.7) and injured (42.4 ± 17.4) cells. Fewest serotonergic appositions are in the ventral quadrant (11.0 ± 5.7) in control motoneurones and from the rostral quadrant (13.7 ± 8.9) in injured motoneurones. However the sample was too small to determine if this represented a real change in the projection fields of serotonin afferents onto motoneurones after injury during the early postnatal period.

4.4. DISCUSSION

This chapter has examined the early postnatal development of afferent inputs onto flexor motoneurones and the response of these afferents to crushing of the common peroneal nerve during the early postnatal period. Two types of afferent connections, selected by the use of monoclonal antibodies for PV and serotonin, were studied. Only those structures that appeared as distinct, punctate boutons, or as a swellings along an axonal profile, and apposing the soma of the motoneurones were counted. These boutons were presumed to be sites of synaptic contact. Some of the contacts formed are of the *en passant* type and

have previously been demonstrated to be synaptic contacts using electron microscopy. This has been shown for serotonin-immunoreactive afferents (Ulfhake *et al.*1978) and for 1a afferents (Conradi *et al.*1983). Serotonin-positive boutons have been shown to form synaptic contacts with phrenic motoneurones in the cat (Pilowsky *et al.*1990), and 1a primary afferent connections have been observed in the cat (Brown, Fyffe, 1981; Burke *et al.*1979) and the rat (Chimykhova *et al.*1991). In the present study, the injection of a fluorescent retrograde prelabel ensured that the study was confined to the flexor motoneurones. Only sections containing the prelabel were processed for immunocytochemistry, and the number of boutons in close apposition to the soma outline were counted. This was not intended to give an exact quantification of the number of appositions contacting motoneurones, but rather, to indicate if there are any differences in the relative expression of both parvalbumin and serotonin both developmentally and after injury.

Some difficulties were encountered in quantifying the number of immunoreactive contacts onto motoneurones. The major difficulty was in assessing if the axons were in fact apposing the outline of the soma. An example of a motoneurone with PV-stained afferents, using HRP as the chromagen and visualised using conventional light microscopy is shown in Figure 4.3. It can be seen that some of the boutons are out of the plane of focus. When counting the appositions using conventional light microscopy, for both PV and serotonin, it was necessary to change the focus to include all visible boutons apposing the soma outline through the visible depth of the motoneurone. This may have introduced errors, resulting in a possible over-estimation of the number of appositions. A similar method has been previously used, to quantify the number of serotonin-positive appositions around quadriceps motoneurones identified by retrograde labelling with HRP or fluorescinated dextran amine (Tanaka *et al.*1992).

Parvalbumin has been shown to be a label of large diameter primary afferent axons. However, it is possible that some of the immunoreactive boutons are from other sources such as interneurones in laminae VII and VIII, although there is no evidence for this. A comparison of the pattern of staining revealed by using parvalbumin with staining for instance of the L4 dorsal root with HRP, would confirm whether PV labels exclusively primary afferents from the periphery.

4.4.1. Primary afferents

Parvalbumin immunoreactivity has been shown to preferentially label large diameter primary afferent fibres during early postnatal development (Zhang *et al.*1990; Solbach, Celio, 1991). Here, it has been used to label the large diameter primary afferents which form monosynaptic connections with motoneurones and to investigate changes in the afferent synaptic inputs onto flexor motoneurones after neonatal injury. The pattern of PV staining was similar to that described previously during development (Zhang *et al.*1990; Solbach, Celio, 1991). The greatest number of terminations were in the ventral horn, in laminae VII, VIII and IX. These PV-positive fibres were observed projecting transversely through to the ventral horn and traversing the region of the motoneurones in the flexor motor pool. ✻

Other studies have observed developmental changes in the intensity and distribution of PV in the spinal cord of the rat (Zhang *et al.*1990; Solbach, Celio, 1991). In general, these changes were confirmed in the present experiments, although a detailed study of the types and numbers of PV-immunoreactive neurones was not undertaken. Over the period studied there was an increase in the total amount of PV staining in the spinal cord. However, during the second postnatal week there was a decrease in the number of appositions around individual motoneurones. This confirms the findings of another study (Zhang *et al.*1990), where an increase in the density of PV innervation was observed in the ventral horn during the prenatal and early postnatal period, followed by a decrease during the second postnatal week. Possible reasons for this decrease postnatally may be a reduction in the number of collateral fibres or a developmental decrease in parvalbumin expression. The number of fibres in the dorsal root has been shown to decrease during the first two postnatal weeks, despite the fact that there is no change in the number of DRG neurones (Hulsebosch *et al.*1986). This phenomenon may be important in the development of synaptic connections within the nervous system, and has been observed in other central

systems such as the tract of Lissauer (Chung, Coggeshall, 1984).

Another reason may be a reduction in the transport of PV from the cell bodies of the neurones, possibly after myelination of the maturing axon. A similar pattern has been observed in Purkinje cells (Braun *et al.*1986). This would suggest that parvalbumin may play a role in some events related to the maturation of primary afferents during development and that once these events have occurred, the expression of parvalbumin diminishes.

4.4.2. Effect of CP nerve injury on PV-immunoreactive primary afferents

Damage to a peripheral nerve results in a variety of morphological, biochemical and physiological changes to the dorsal root ganglion cells and in the dorsal horn of the spinal cord (see (Aldskoguis *et al.*1985)). Death of dorsal root ganglion cells following peripheral nerve injury has been shown in the neonate (Yip *et al.*1984; Himes, Tessler, 1989; Bondok, Sansone, 1984) and the adult (Ygge, Aldskoguis, 1984a; Ygge, 1989; Tessler *et al.*1985; Himes, Tessler, 1989), the effect of injury in the neonate being greater than in the adult. This can be expected to result in a reduction in the number of central projections from the dorsal root to the motoneurones.

In this study, the changes in the density of PV-positive appositions around motoneurones after CP nerve injury on P2, were assessed using two techniques. In the first, using conventional light microscopy, no significant reduction in PV-immunoreactive afferent contacts onto flexor motoneurones was found after injury (see Table 4. 1). As already discussed, this technique had inherent inaccuracies arising from the difficulties in assessing if a bouton was directly apposing the soma (see Fig. 4.3). The use of confocal microscopy in a smaller sample of motoneurones, indicated that there was a significant reduction in the PV-immunoreactive afferent contacts after injury (see Table 4.2). This showed that about 70% of the appositions were lost at P7. The appositions were counted in

a series of five steps at 1μm intervals, and summed. It was possible to discern with greater accuracy if a bouton was directly apposing the motoneurone soma, rather than merely in the vicinity. It is conceivable that the discrepancies arose because, using conventional light microscopy, it is not possible to distinguish between a bouton that is close to the motoneurone, from one that is forming a functional contact, especially when there is a lot of immunoreactivity. If, after injury to the nerve, boutons are 'stripped' away from the motoneurone by the insertion of astrocytic processes (see (Sumner, 1975; Mendell *et al.*1976)), but do not immediately disappear, this type of error would result. The use of the LSCM should be more accurate, and further work should be done to increase the sample of motoneurones counted using this method.

As was shown in Chapter 3, over 50% of the motoneurones are lost after neonatal CP crush. This injury would have also caused damage to the sensory afferents, and a reduction in the PV-immunoreactive afferent contacts may be predicted based on other studies that show DRG cell death after neonatal injury (Yip *et al.*1984; Himes, Tessler, 1989). There is some evidence of 'sprouting' of undamaged afferents in the dorsal horn after injury to the peripheral nerve in both the adult (Molander *et al.*1988) and the neonate (Fitzgerald, 1985b; Fitzgerald *et al.*1990).

In this study, the two methods used to quantify the number of PV-immunoreactive afferents contacting the flexor motoneurones did not yield the same results. Using conventional light microscopy, no significant decrease in the PV-immunoreactive innervation to the motoneurones was observed. This may be due to the inaccuracies of the method used in being unable to discern between appositions and boutons that are close to the outline of the soma. Alternatively, there may not have been any death of 1a afferent projections at any of the times studied. This seems unlikely as there is substantial loss of central projections to the dorsal horn, and a reduction in the overall size of the dorsal horn following

*

The use of the two methods gave conflicting results for the number of PV-positive appositions contacting the soma of the injured motoneurones. The limitations of both sets of results have been discussed in detail, but it is necessary to note that probably neither are wholly correct. It is likely that the true reduction in the number of contacts onto injured motoneurones is in the region of 40%, somewhere between the two results.

neonatal injury to the sciatic nerve in the rat (Fitzgerald, 1985b; Fitzgerald, Vrbová, 1985). It is also possible that there was sprouting of uninjured adjacent nerve terminals into the field of projection of the common peroneal nerve. Other studies have shown considerable sprouting after neonatal injury, but not complete invasion of the depleted terminal field of a nerve (Fitzgerald, 1985b). Therefore, it is most probable that this method does not yield accurate results.

The second method, confocal microscopy, showed that there was about 70% loss of PV-immunoreactive afferents at P7. This method was more accurate, but the numbers of animals used, especially at P14, were possibly too small to be conclusive. However, considering previous studies and the apparent reduction in the pattern of PV-immunoreactivity in the ventral horn after injury (see Fig. 4.2), it would appear that this method gives a better indication of the response of 1a afferent terminal axons to neonatal injury. *

After neonatal injury there is death of many of the dorsal root ganglion cells, and their central projections (Bondok, Sansone, 1984; Himes, Tessler, 1989). Yip *et al.*, showed that there was a 40 to 50% reduction in the number of DRGs following crush of the sciatic nerve on P1, and that all of the cells were lost one day after the injury (Yip *et al.*1984). Therefore, in this study, a similar reduction in the primary afferent projections to the motoneurones might be expected. However, as shown in Chapter 3, there was also considerable death (over 50%) of the motoneurones after common peroneal crush on P2 (see Table 3.1). There is evidence, using retrograde labelling with fluorescent dyes, that this death takes place within 5 days of the injury being inflicted (G.Z.Mentis and R.Navarrete; pers. comm.). It is possible that some, or all, of the surviving afferents are redistributed, and form contacts with the surviving motoneurones.

There are several possible scenarios for the events taking place after neonatal injury. If there is death of about 50% of the DRGs immediately after injury (Yip

*et al.*1984), a similar reduction in the number of afferent axons contacting the motoneurones might be expected. However, there is probably sprouting of some of the surviving primary afferents (Fitzgerald, 1985b). There was a 70% decrease in the number of contacts onto the motoneurones five days after the injury. In this case 20% sprouting would be predicted. In addition, 50% of the motoneurones died after injury, and some of the surviving afferents may be re-located to the surviving motoneurones. There may be a combination of sprouting of some of the surviving collaterals and relocation of others onto a depleted population of motoneurones following injury.

This suggests that there would be radical changes in the amount of monosynaptic innervation from primary afferents following injury. There was a mean reduction in the number of PV-immunoreactive contacts onto the motoneurones by 70%. These contacts are made predominately onto the soma and proximal dendrites (Brown, Fyffe, 1981; Burke *et al.*1979), and their loss, or relocation to more distal locations, would result in a reduction in the excitability of the cells (Rall *et al.*1967). Since there is actually an increase in excitability of flexor motoneurones after neonatal injury (Navarrete *et al.*1988a; Navarrete *et al.*1986), this suggests that there may also be a reduction in the inhibitory innervation to the motoneurones. Death of the DRGs may also result in a decrease in the central projection to the interneurones, and so a decrease in the polysynaptic, inhibitory innervation to the motoneurones. There may also be a compensatory increase in the excitatory inputs of some other afferent system, for example the descending serotonergic system (Polistina *et al.*1990; Wang *et al.*1991b).

4.4.3. Descending serotonergic afferents

Serotonin-positive afferent axons project from the raphe nuclei in the brain stem (Holstege, Kuypers, 1987b; Tork, 1985) to the dorsal and ventral horn of the spinal cord. Serotonin-positive axons have been shown to make monosynaptic contacts with phrenic motoneurones in the spinal cord of the cat (Pilowsky *et*

*al.*1990). In the chick spinal cord serotonin-positive fibres have been shown to be unevenly distributed around motoneurones of different motor pools (Homma *et al.*1988). The motor pools most densely innervated by serotonin are those projecting to postural muscles (Okado *et al.*1991; Homma *et al.*1988).

Serotonin-positive axons appeared in the spinal cord as thin fibres, with numerous boutons. This is similar to the pattern observed in the adult rat (Jones, Light, 1990; Jones, Light, 1992) and in the cat (Pilowsky *et al.*1990). There is electronmicroscopic evidence from cat phrenic motoneurones, that the serotonin-immunoreactive boutons make synaptic contact onto the motoneurones (Pilowsky *et al.*1990). Since these contacts were most common on the dendrites of the phrenic motoneurones, where they formed synapses with well-defined postsynaptic densities, it is possible that they directly affect the excitability of these motoneurones. A similar thing has been observed in the motor pools of the adult rat (Holstege, Kuypers, 1987a) and the cat (Ulfhake *et al.*1978). Here, serotonin-immunoreactive boutons have been observed to form synapses with the dendrites of motoneurones in the ventral horn.

In this study, an increase in the density of serotonin immunoreactive fibres was observed in the ventral horn of the spinal cord, from P7 to adult (Table 4.3) based on counts of the number of axons within 50 μm^2 grids. The density of serotonin-immunoreactive boutons around identified flexor motoneurones also increased from P3 to P7 (Table 4.4). An increase in the amount of serotonin-positive innervation during postnatal development has also been observed in the chick (Sako *et al.*1986; Okado *et al.*1991) in the rat (Ozaki *et al.*1991; Rajaofetra *et al.*1989b; Bregman, 1987; Rajaofetra *et al.*1989a) and in the opossum (Martin *et al.*1991). In the rat spinal cord, the development of serotonergic projections to the ventral horn of the spinal cord precedes that to the dorsal horn (Rajaofetra *et al.*1989a), the adult pattern of innervation being reached on about P21.

The distribution of serotonin-positive appositions onto the somatodendritic surface of intracellularly filled motoneurones revealed that the majority of the contacts were not made on the soma, but on the distal dendrites, of the motoneurones (see Table 4.6). This has also been described in other studies (Pilowsky *et al.*1990; Ulfhake *et al.*1987). The majority of the appositions appeared to be made on dendrites projecting into the dorsal quadrant (see Table 4.7). In the chick spinal cord, many of the serotonin-positive fibres were observed in the lateral part of the spinal cord, in the white matter (Sako *et al.*1986), and serotonin immunoreactivity was not evenly distributed through the motor pools of the spinal cord (Homma *et al.*1988), being more dense in the medial extensor motor pools. To project to motor pools located medially in the spinal cord, the serotonergic axons would pass through the dendritic fields of more laterally placed pools, such as the flexor motor pool. This would allow many opportunities for contacting the flexor motoneurones in all quadrants. It is not clear why there should be an apparent preference for contacts to be made in the dorsal segment.

4.4.4. Effect of CP nerve injury on descending afferents

Injury to the common peroneal nerve does not cause direct damage to the serotonin-positive descending afferents axons. However, there is evidence of heterotypical sprouting of serotonergic projections following dorsal rhizotomy in the adult rat (Polistina *et al.*1990; Wang *et al.*1991b). In the small number of motoneurones examined in this study there was a significant increase in the absolute number of appositions touching the soma, as well as the number of appositions contacting 100 μm of the perimeter of identified flexor motoneurones both at P3 (one day after injury) and at P7 (see Table 4.4). At this time there was no significant increase in the overall density of serotonin-positive axons in the ventral horn of the spinal cord (see Table 4.3). Thus, it would appear that the increase in serotonin-positive innervation onto injured motoneurones may

be due to a redistribution of synaptic boutons, rather than sprouting of new collaterals. This is also suggested by the results from motoneurones intracellularly filled with Lucifer Yellow (see Table 4.5). This showed that, after injury to the CP nerve on P2, the proportion of serotonin-immunoreactive boutons apposing the soma of a small sample of motoneurones increased from 1.5% to 12.3%. This relocation in the number of contacts made onto the soma of the motoneurones may be partly responsible for the increase in excitability reported in flexor motoneurones following injury (Navarrete *et al.*1988a; Navarrete *et al.*1986).

There is clearly some variability in the quality of serotonin immuno-staining. It is possible that some of this difference could be due to this. In the two control cells with serotonin-immunoreactive boutons observed on the soma (cells no. 8 and 14 in Table 4.6), the overall amount of staining is also exceptionally high. This suggests that the quality of staining influences the apparent distribution of inputs. However, in other injured motoneurones (eg. cell no.1 in Table 4.6), that do not have many serotonergic contacts, a large proportion of these contacts (26.7%) are found on the soma.

A stimulus for the redistribution of the inputs could be the appearance of vacant synaptic sites arising from the removal of the central connections of damaged DRGs. There is evidence of competition between the descending serotonergic axons and central projections of DRG's to Clarke's column neurones (Polistina *et al.*1990). Additionally, damage to the postsynaptic motoneurone itself may result in a reduction in the total number of presynaptic boutons contacting the motoneurone (Sumner, 1975). It is also possible that the position of contacts of the PV-immunoreactive 1a afferents and serotonin-immunoreactive afferents on the motoneurones are different. For instance, serotonin-positive inputs do not normally make synaptic contacts with spines on the dendrites of dorsal horn neurones, but form synapses predominantly on the dendritic shafts (Miletic *et*

*al.*1984; Hylden *et al.*1986). After injury to the common peroneal nerve there is an increase in the number of spine-like, growth associated processes on the somatodendritic surface of the damaged motoneurones (see Chapter 3). If these processes are sites of synaptic contact (Vaughn *et al.*1974; Skoff, Hamburger, 1974), it is possible that they represent 'new' sites of synaptic contact that were not present before the injury. This may form the site of contact for either sprouting PV-positive primary afferents, or descending serotonin-positive afferents. It is not known if these processes remain after injury, or if the maturation of the motoneurone surface continues in those cells that survive neonatal injury.

Figure 4.1 DiI on L4 dorsal and ventral roots in fixed tissue. The DiI was applied onto the roots of a fixed spinal cord preparation, and kept at 38°C for up to two months. The tissue was embedded in agar, sectioned using a Vibratome, and visualised under epifluorescence.

(A) View of the dorsal horn of the lumbar area of the spinal cord in longitudinal section. The afferent axons are clearly visible, labelled by the DiI. These axons are projecting towards the ventral horn. Compass points mark the dorsal and ventral axes.

(B) Shows the point at which the dendrites from the motoneurones (towards the right) and the afferents axons (towards the left), meet. Compass points mark the dorsal and ventral axes.

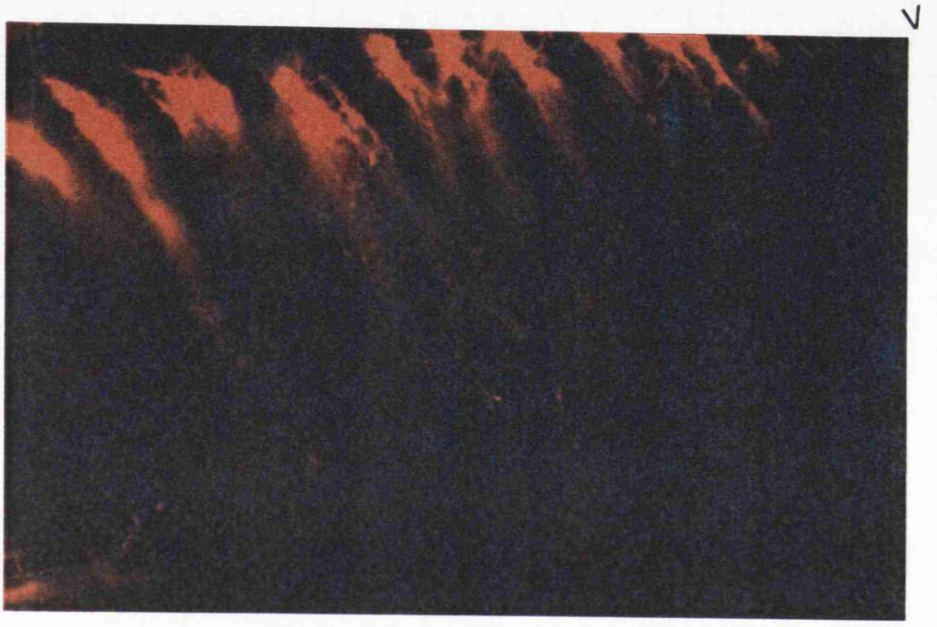
d
v

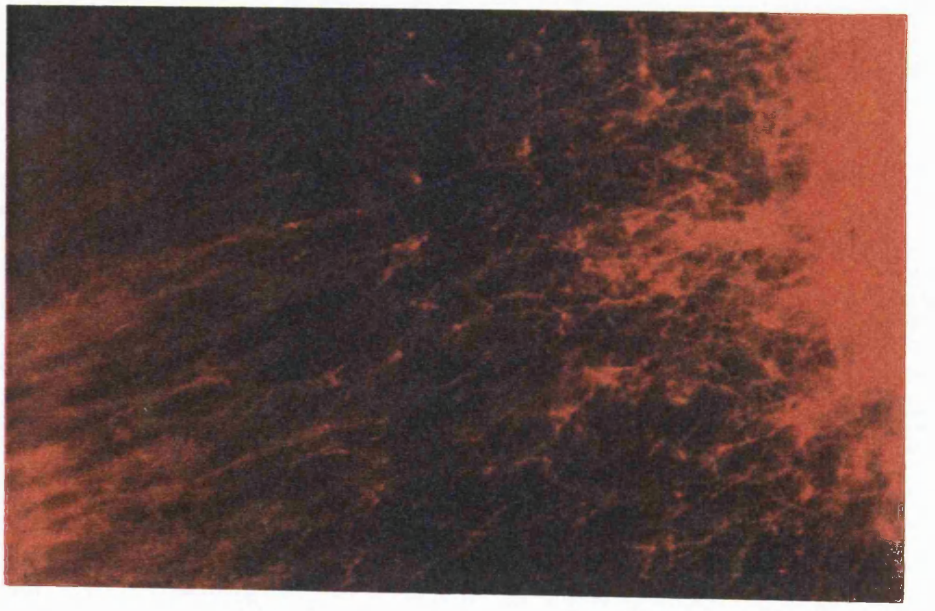
d
v

Figure 4.2 Pattern of immuno-staining in 20 μm transverse sections (x 2.5) of the spinal cord using the monoclonal antibody to parvalbumin (PV). On the left is the pattern of PV-immunoreactivity after common peroneal (CP) nerve crush on postnatal day 2 (P2). The right is the contralateral control. PV-immunoreactivity showed a restricted pattern of staining within the spinal cord. PV-immunoreactive fibres entered the dorsal columns medially, corresponding to the path followed by large diameter myelinated primary afferent fibres. These fibres coursed towards the motor columns of the ventral horn.
(A) The pattern of PV-immunoreactivity in the spinal cord at P3. Even one day after injury there appears to be some difference between the amount of PV-immunoreactivity on the injured compared to the control side.
(B) The pattern of PV-immunoreactivity in the spinal cord at P7. The overall pattern of staining is similar to that at P3. However, the intensity of the PV-immunoreactivity is stronger than at P3. There is less PV-immunoreactivity on the injured compared to the control side of the spinal cord.
(C) The pattern of PV-immunoreactivity in the spinal cord at P14. Again, there is an increase in the intensity of staining. There is also reduced staining on the injured side. In addition, many PV-immunoreactive neurones are visible, especially in laminae VII and VIII. These are possibly interneurones. Scale bar = 500 μm.

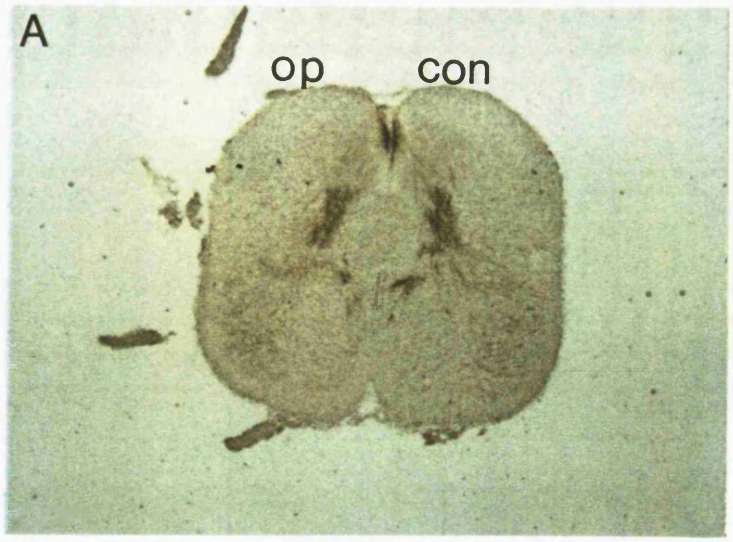
A
op
con

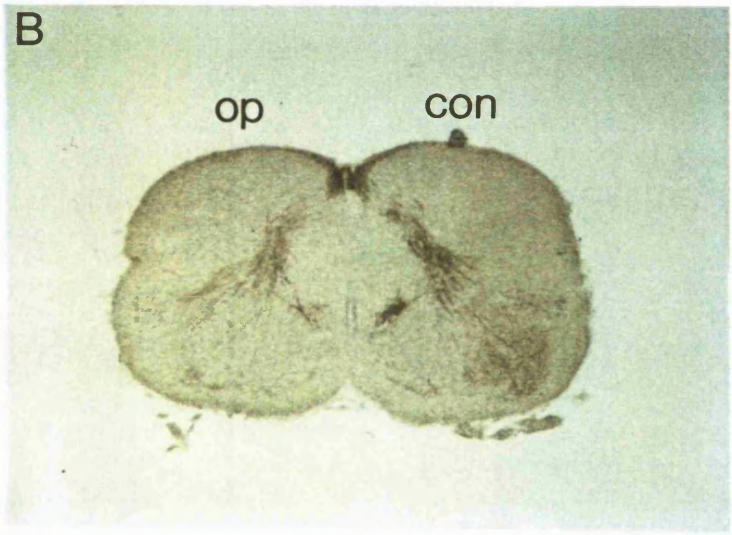
B
op
con

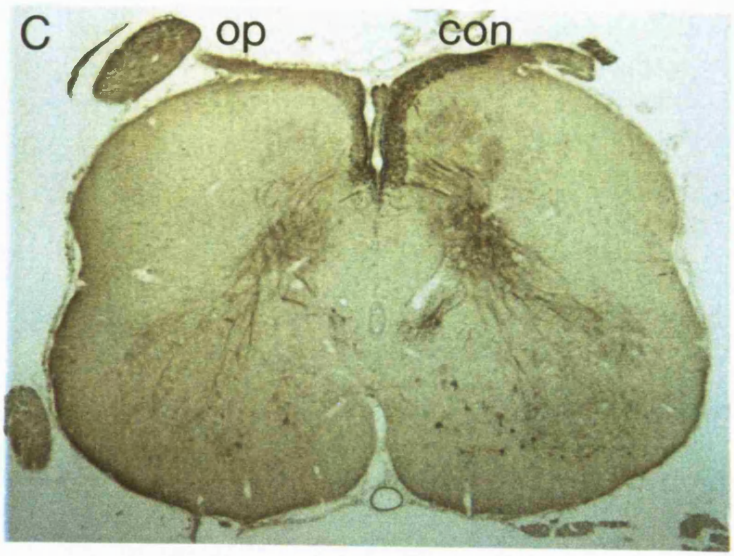
C
op
con

Figure 4.3 Parvalbumin (PV) immunoreactivity around a gallocyanin counterstained motoneurone form the tibialis anterior/extensor digitorum (TA/EDL) motor pool. Transverse 20 μm sections, containing motoneurones prelabelled with the fluorescent dyes Fast Blue and Diamidino Yellow, were processed for PV immunocytochemistry, using HRP as a chromogen.
A high power (x100 oil immersion) view of a motoneurone from a P3 spinal cord. The PV-immunoreactive 1a afferent axons are seen around the outline of the cell. Only the contacts that appear as punctate boutons apposing the outline of the soma of the motoneurone (arrows), were counted. Many of the appositions appear out-of-focus. This created problems in counting accurately the number of contacts that were touching the outline of the cell. Scale bar = 25 μm.

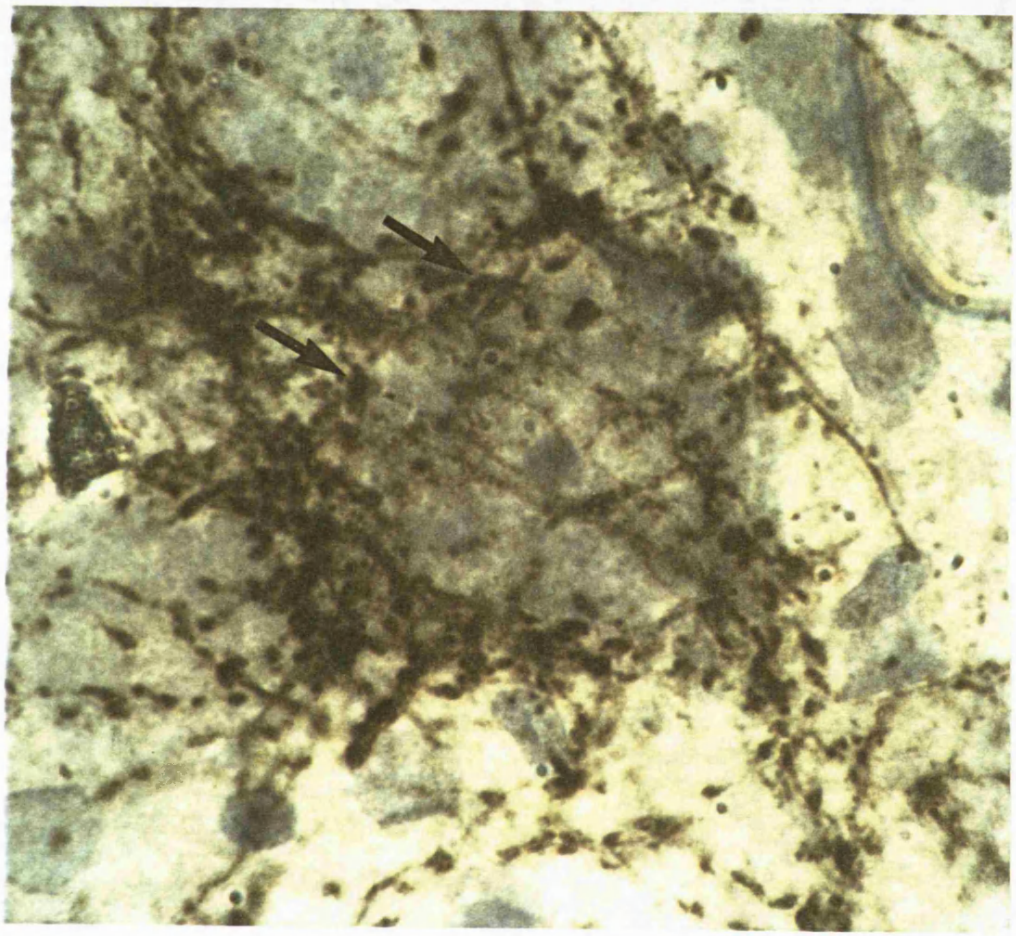

Figure 4.4 Examples of camera lucida drawings of normal and injured motoneurones from the tibialis anterior/extensor digitorum longus motor pool. The motoneurones are surrounded by parvalbumin-immunoreactive boutons. Only those boutons that contacted the outline of the soma (ringed) were counted. The number of boutons that were counted in these examples is shown. The nucleolus is marked with an asterisk.

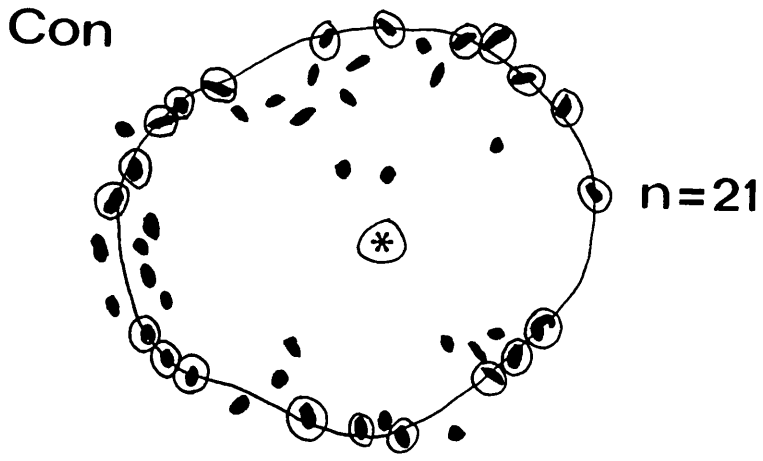
Con
n=21

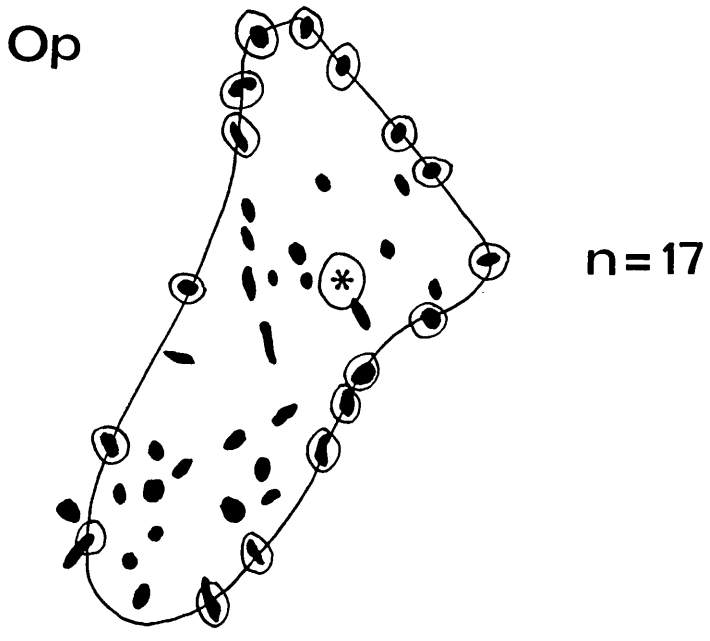
Op
n=17

Figure 4.5 PV-immunoreactivity around tibialis anterior/extensor digitorum longus (TA/EDL) motoneurones visualised using confocal laser scanning microscopy. A series of images was obtained through the tissue at 1 μm steps. The Texas Red-labelled PV immunoreactivity was visualised using the GHS filter, and the Fluorescinated dextran amine (FDA) or Lucifer Yellow (LY) was visualised using the BHS filter. The two separated images were the 'merged' to create pseudocolour images containing the information from both filters.
(A) Five 1 μm sections projected to form an image of a motoneurone from a normal animal on postnatal day 7 (P7). FDA dye was used as a prelabel to identify the TA/EDL motor pool, and can be seen as indistinct spots in the cytoplasm of the motoneurone. The arrows indicate two examples of PV-immunoreactive boutons apposing the outline of the soma. The number of such boutons contacting the soma was counted. Scale bar = 10 μm.
(B) Motoneurone from the TA/EDL motor pool after common peroneal nerve crush on P2. Arrow indicates a PV-immunoreactive bouton. Scale bar = 10 μm.
(C) A P7 LY filled motoneurone with PV-immunoreactive axons. The PV-immunoreactive boutons (arrow) apposing the soma and dendrites of the flexor motoneurone were too numerous to count. Scale bar = 15 μm.

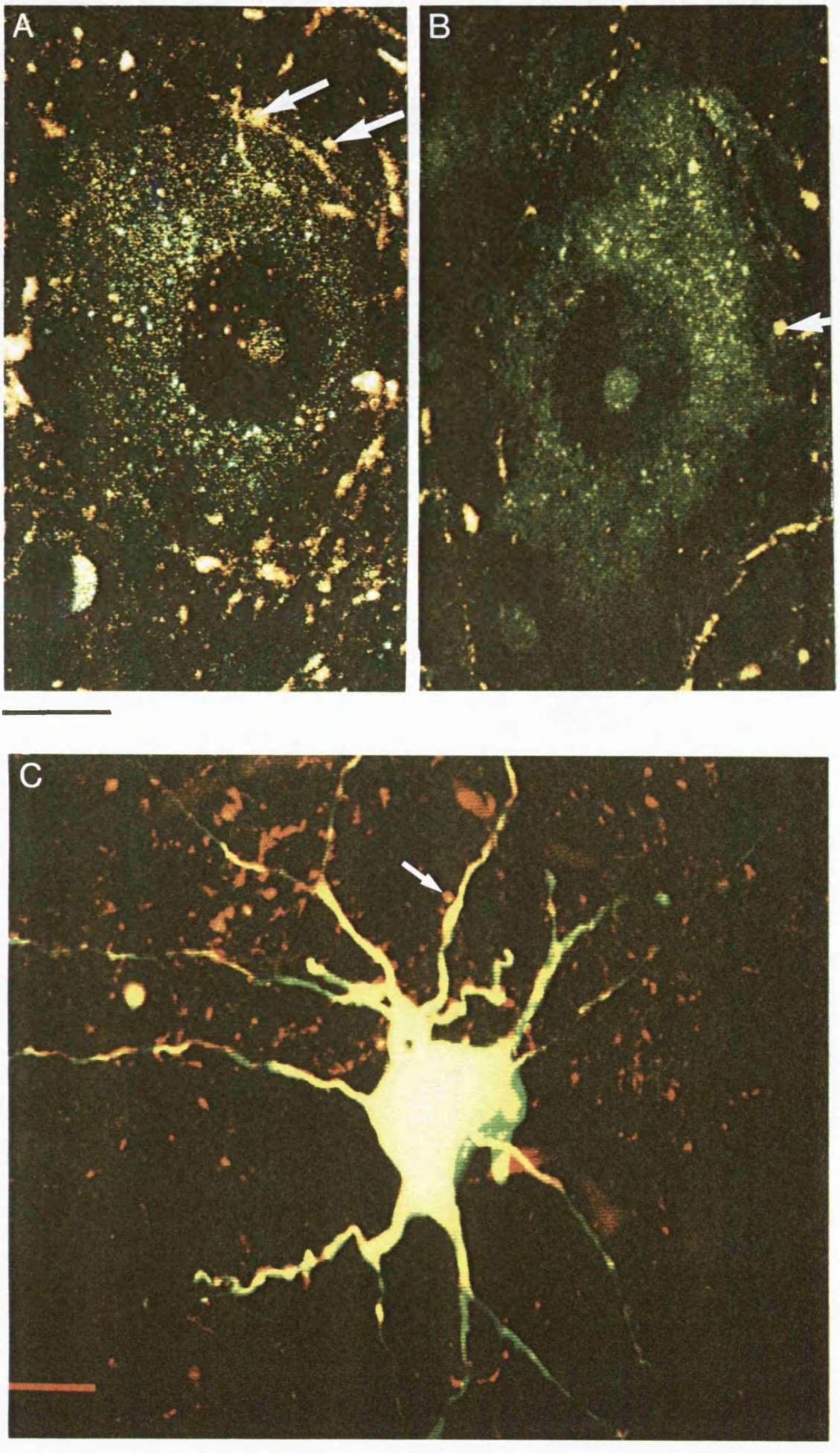
A
B
C

Figure 4.6 Distribution of PV-immunoreactive neurones in the spinal cord at the level of L4. The position of neurones that were PV-immunoreactive was plotted within the spinal cord in four sections at each age. At postnatal day 3 (P3), there were few neurones, all in the ventral horn laminae VII, VIII and IX. At P7, the number of PV-immunoreactive neurones had increased, but they were still located within the same areas. By P14, the number of PV-immunoreactive neurones increased further, and they were also found in laminae VI, V, IV, II, II and I, in the dorsal horn.

Figure 4.7 The ventral horn of a 3 day old spinal cord, from the same section as shown in Figure 4.2a, at higher magnification (x10). This shows the pattern of immuno-staining in 20 μm transverse sections of the spinal cord using the monoclonal antibody to parvalbumin (PV).

(A) shows the pattern of PV-immunoreactivity after common peroneal (CP) nerve crush on postnatal day 2 (P2). **(B)** shows the contralateral control. Even one day after injury there is some difference between the amount of PV-immunoreactivity on the injured compared to the control side. The PV-immunoreactive primary afferent fibres are seen coursing towards the motor columns of the ventral horn. Scale bar = 250 μm.

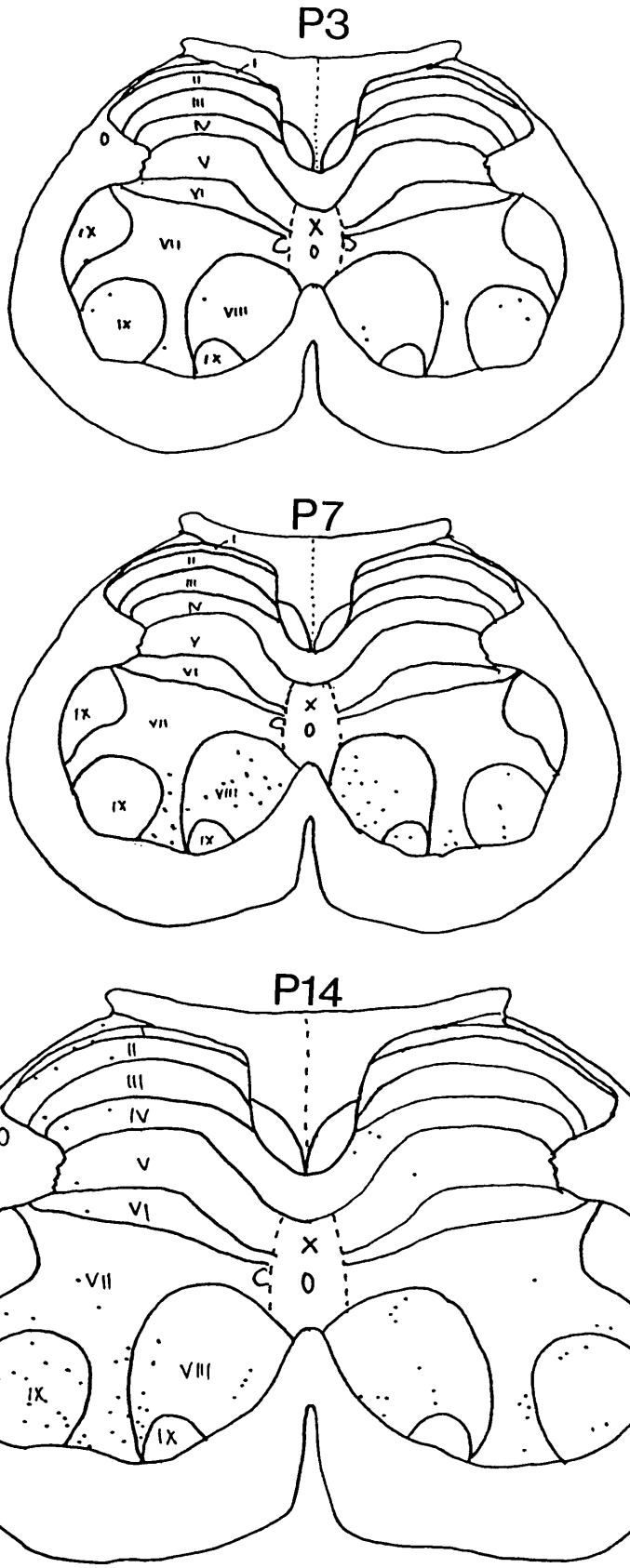
P3
I
II
III
IV
V
VI
VII
VIII
IX
X
O
P7
I
II
III
IV
V
VI
VII
VIII
IX
X
O
P14
II
III
IV
V
VI
VII
VIII
IX
X
O

Figure 4.7 The ventral horn of a 3 day old spinal cord, from the same section as shown in Figure 4.2a, at higher magnification (x10). This shows the pattern of immuno-staining in 20 μm transverse sections of the spinal cord using the monoclonal antibody to parvalbumin (PV).
(A) shows the pattern of PV-immunoreactivity after common peroneal (CP) nerve crush on postnatal day 2 (P2). **(B)** shows the contralateral control. Even one day after injury there is some difference between the amount of PV-immunoreactivity on the injured compared to the control side. The PV-immunoreactive primary afferent fibres are seen coursing towards the motor columns of the ventral horn. Scale bar = 250 μm.

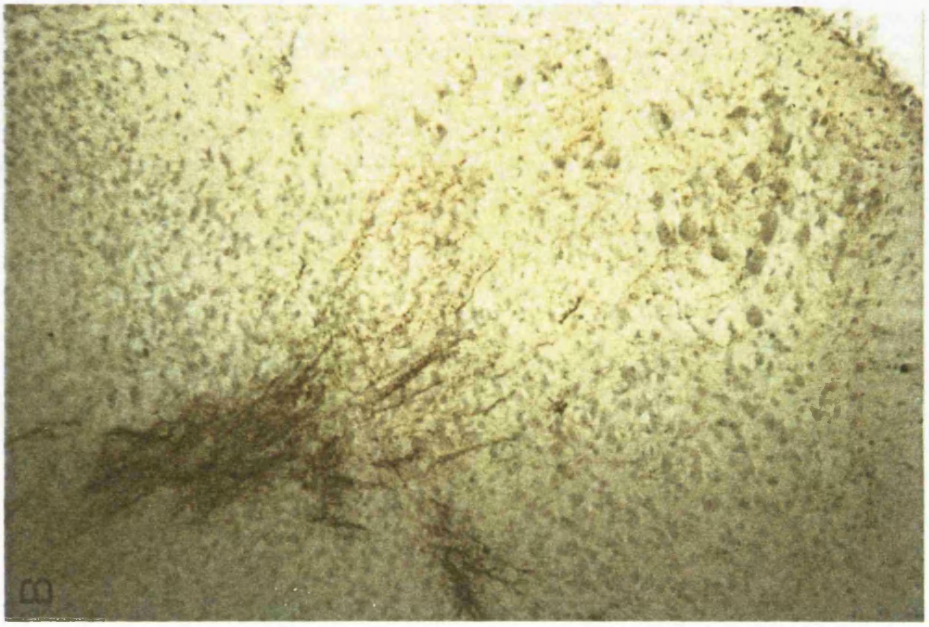
B

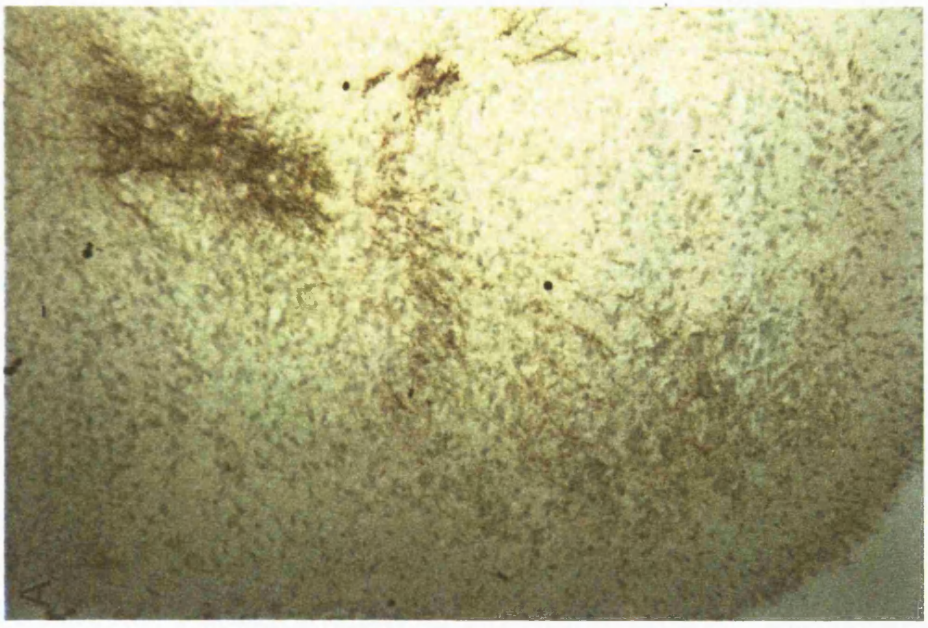
A

Figure 4.8 The ventral horn of a 7 day old spinal cord, from the same section as shown in Figure 4.2b, at higher magnification (x10).
(A) shows is the pattern of PV-immunoreactivity after common peroneal (CP) nerve crush on postnatal day 2 (P2). **(B)** shows the contralateral control. The overall pattern of staining is similar to that at P3. However, the intensity of the PV-immunoreactivity is stronger than at P3. There is less PV-immunoreactivity on the injured compared to the control side of the spinal cord. Scale bar = 250 μm.

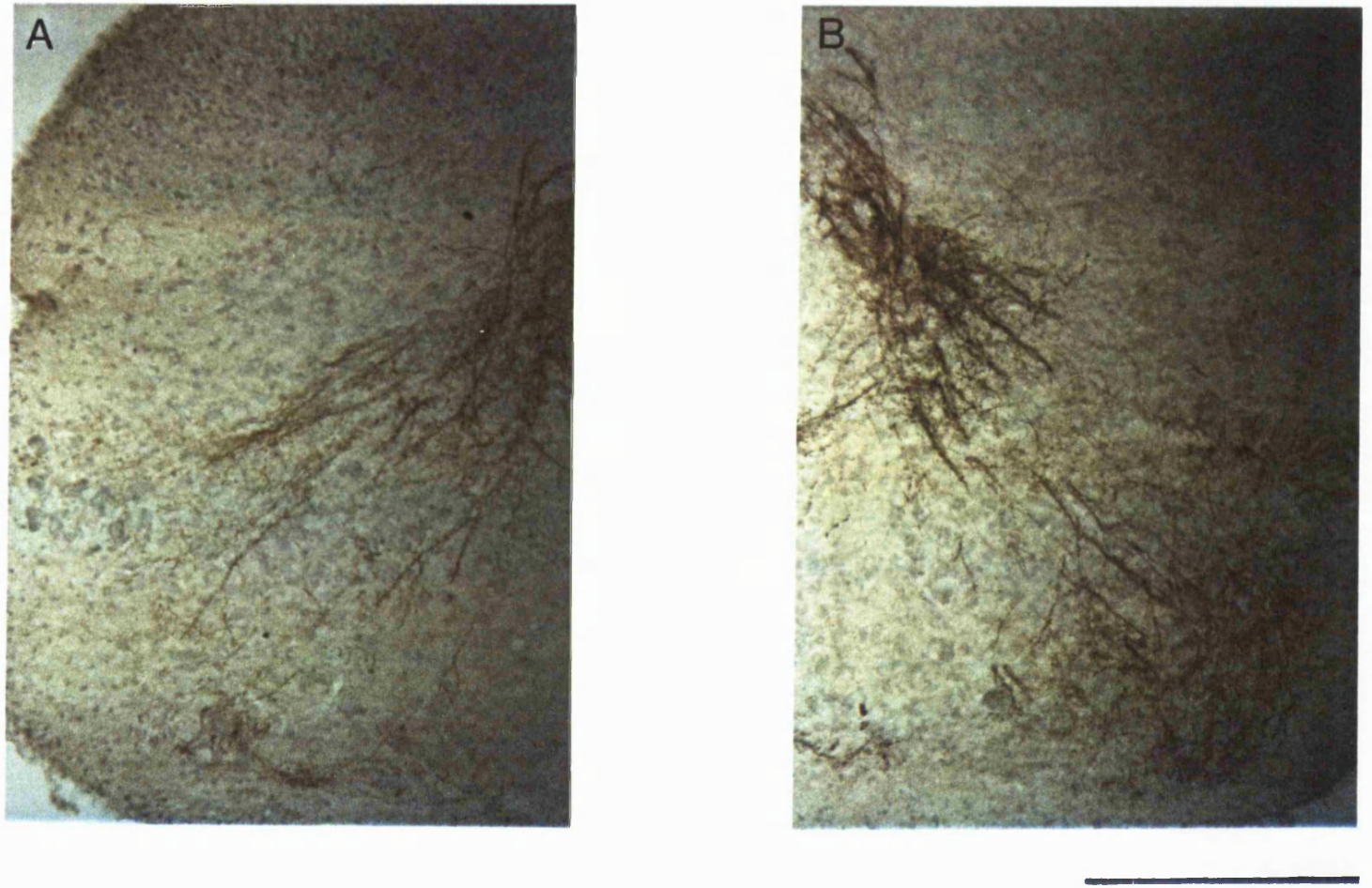
A
B

Figure 4.9 The ventral horn of a 14 day old spinal cord, from the same section as shown in Figure 4.2c, at higher magnification (x10).
(A) shows the pattern of PV-immunoreactivity after common peroneal (CP) nerve crush on postnatal day 2 (P2). **(B)** shows the contralateral control side of the spinal cord. There is an increase in the intensity of staining. There is also greatly reduced staining on the injured side. In addition, many PV-immunoreactive neurones are visible, especially in laminae VII and VIII. These are possibly interneurones. Scale bar = 250 μm.

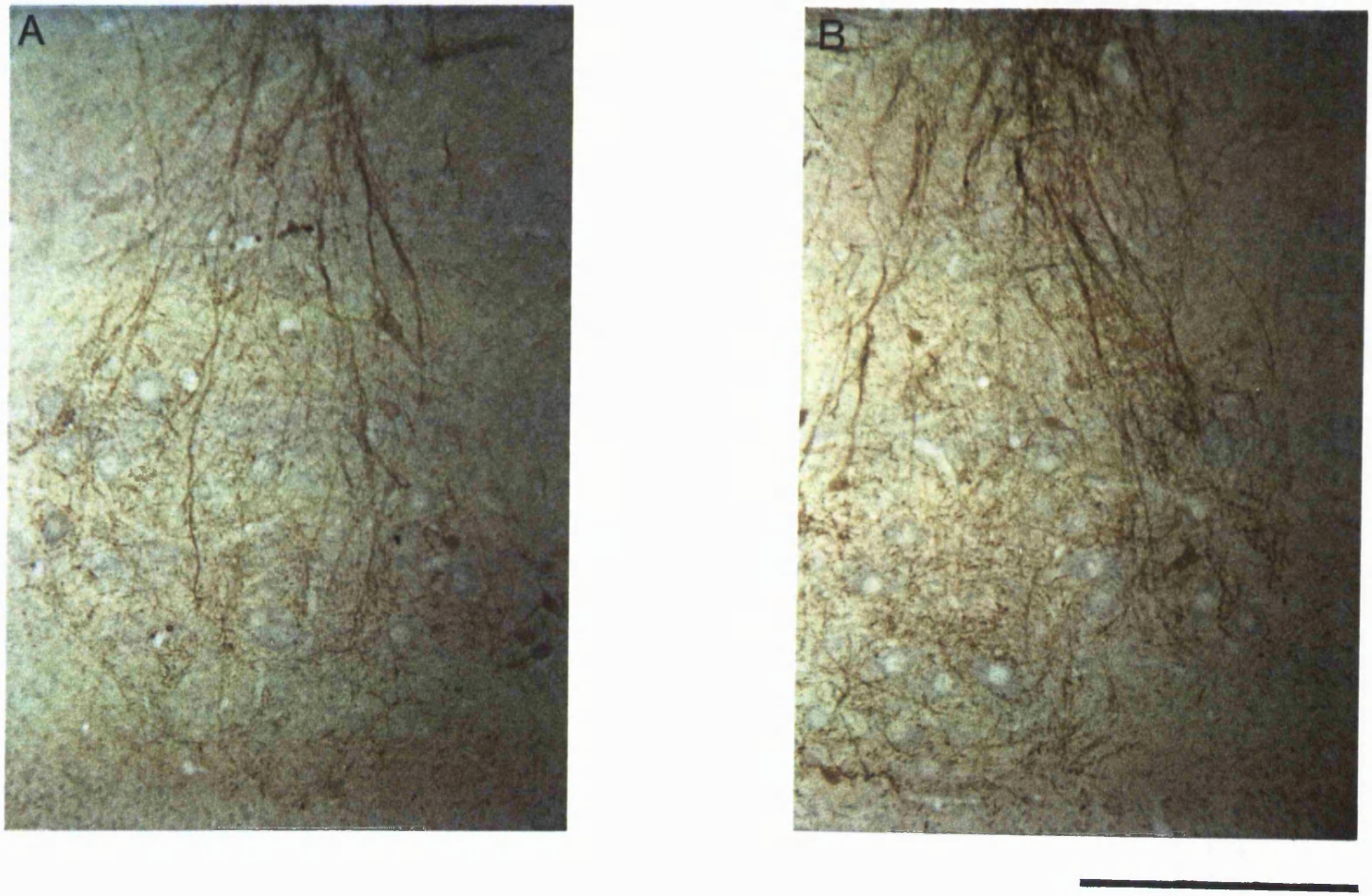
A
B

Figure 4.10 The pattern of serotonin-immunoreactivity on postnatal day 3 (P3), in the ventral horn of the spinal cord in longitudinal sections. Only sections containing tibialis anterior/extensor (TA/EDL) digitorum longus motoneurones prelabelled with Fast Blue and Diamidino Yellow were processed for serotonin immunocytochemistry.

(A) Serotonin-immunoreactive axons around TA/EDL counterstained motoneurones. The serotonin-positive axons appear as beaded axons in the ventral horn. Scale bar = 25 μm.

(C) High power (x100) image of counterstained motoneurones with visible nucleoli, from the same region as in **(A)**. The serotonin-immunoreactive axons are located around the flexor motoneurones. Only those axons that from direct contacts (arrow) were counted. Scale bar = 25 μm.

(B) The region of the ventral horn of an animal in which the common peroneal (CP) nerve was crushed one day before, on postnatal day 2 (P2). The overall pattern of serotonin innervation is similar to that observed on the control side. Scale bar = 25 μm.

(D) High power (x100) image of the same region of the spinal cord as in **(B)**. The density of serotonin-immunoreactivity increases around the flexor motoneurones after CP nerve crush on P2. Scale bar = 25 μm.

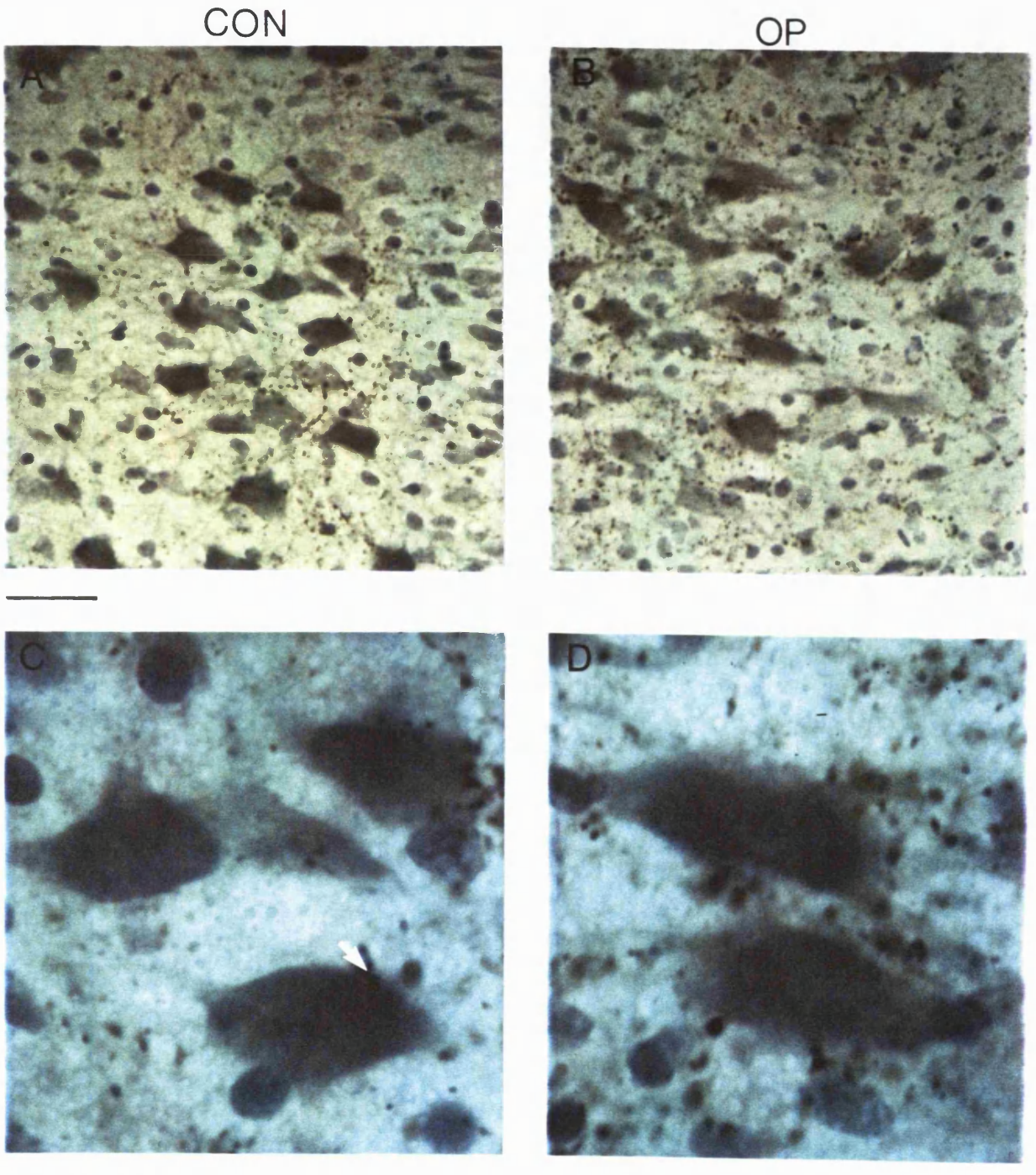
CON
OP
A
B
C
D

Figure 4.11 The pattern of serotonin-immunoreactivity on postnatal day 7 (P7), in the ventral horn of the spinal cord in longitudinal sections.
(A) Serotonin-immunoreactive axons around TA/EDL counterstained motoneurones. The serotonin-positive axons appear as beaded axons in the ventral horn. Scale bar = 25 μm.
(C) High power (x100) image of counterstained motoneurones with visible nucleoli, from the same region as in **(A)**. Scale bar = 25 μm.
(B) The region of the ventral horn of an animal in which the common peroneal (CP) nerve was crushed on postnatal day 2 (P2). The overall pattern of serotonin innervation is similar to that observed on the control side. Scale bar = 25 μm.
(D) High power (x40) image of the same region of the spinal cord as in **(B)**. The density of serotonin-immunoreactivity is higher around the flexor motoneurones six days after CP nerve crush on P2. Scale bar = 25 μm.

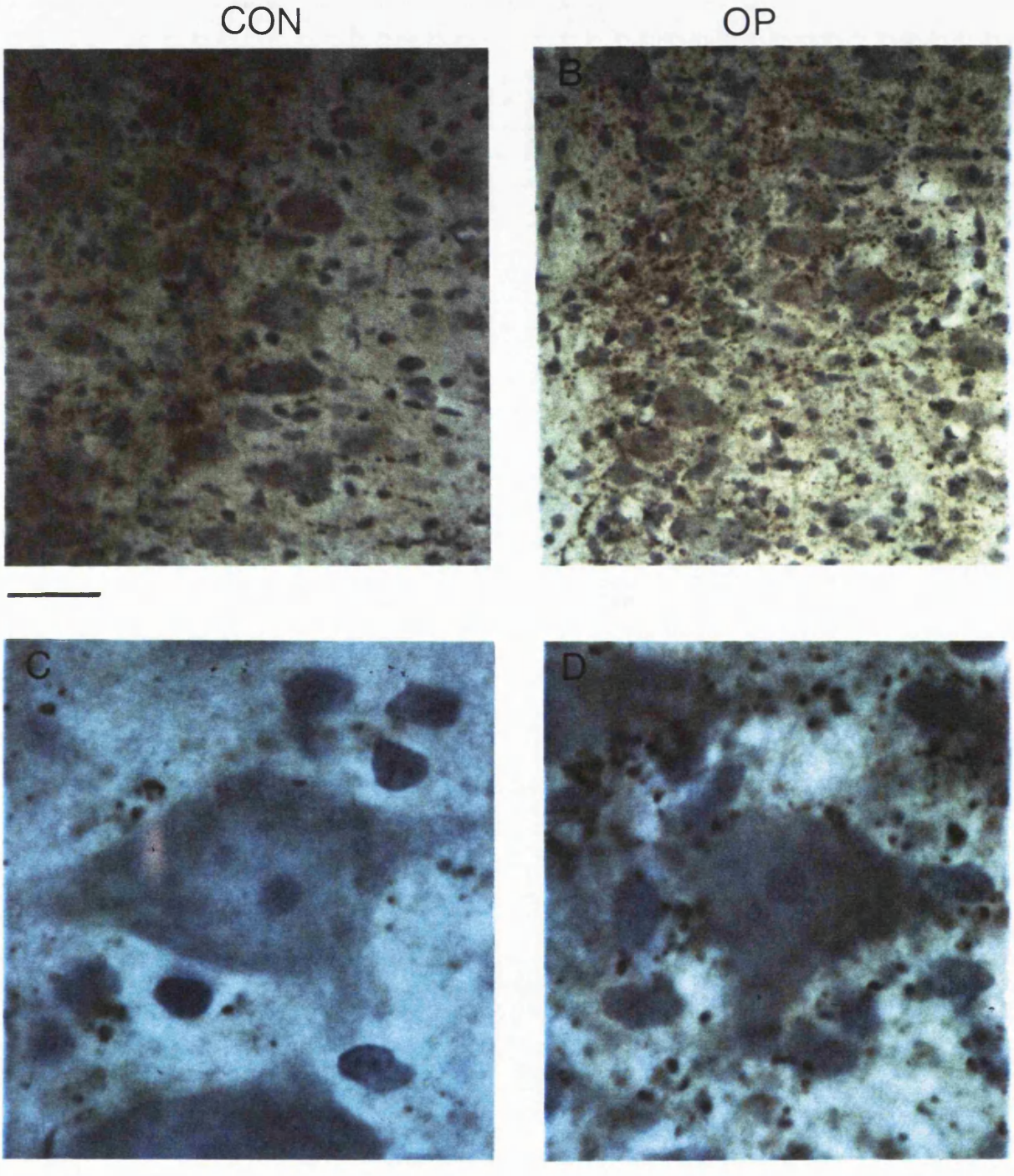
CON
OP
B
C
D

Figure 4.12 Serotonin-immunoreactive afferent axons contacting the dendrite of a Lucifer Yellow (LY) filled motoneurone. LY filled motoneurones were imaged using the BHS filter (seen here as orange/red; small arrows). Serotonin-immunoreactive axons, with texas red as a chromagen, were imaged using the GHS filter (seen here as yellow; large arrows). Images were collected at 1 μm increments (**A** and **B**), and the serotonin-positive appositions within 1 μm of the motoneurones in each image were counted (large arrow). The files were then 'merged' to create a pseudocolour image of the information gathered from both filters. Several images could be projected to create one image of information from several microns along the dendrites (**C**). The interaction of a serotonin-immunoreactive bouton with a LY filled dendrite is shown in (C), which is a projection of four 1μm sections. Scale bar = 5 μm.

A

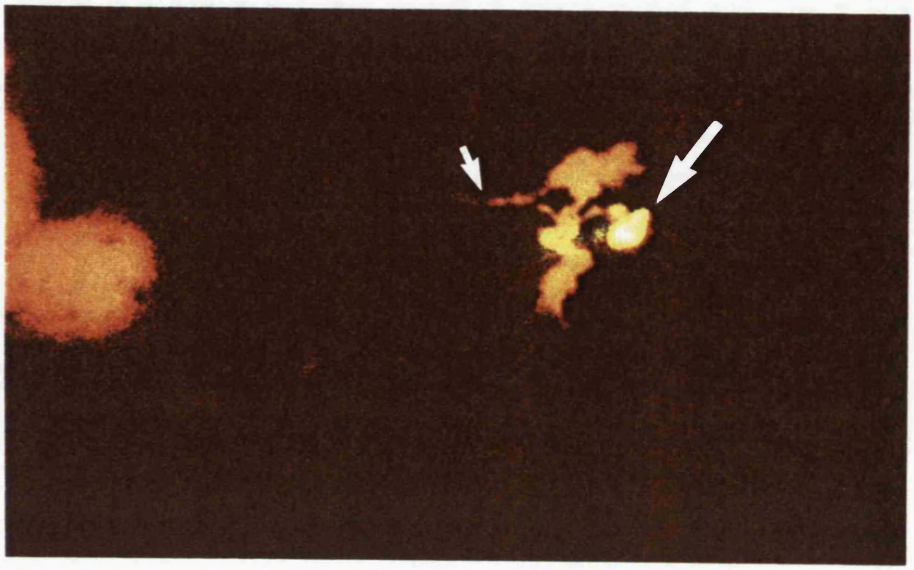

B

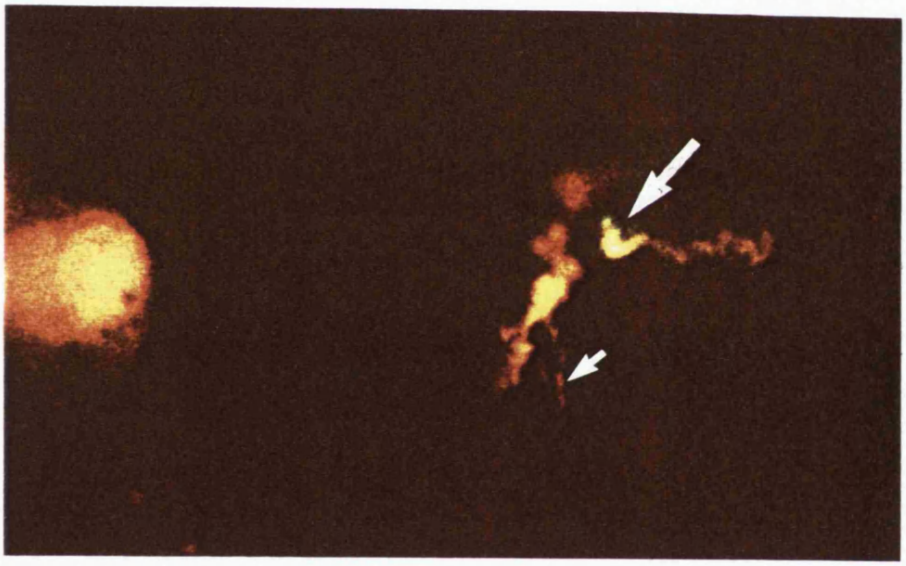

C

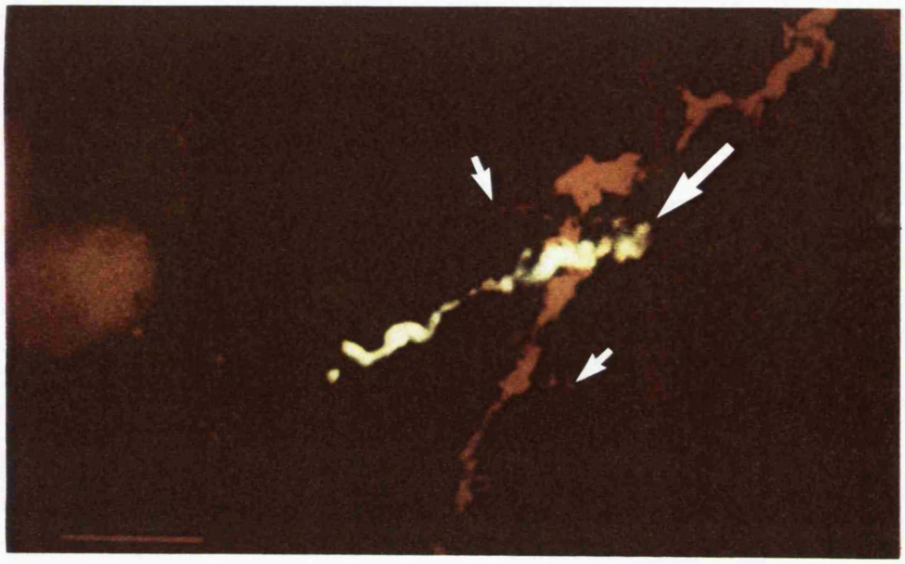

Figure 4.13 Serotonin-immunoreactive afferent axons contacting the soma and dendrites of a tibialis anterior/extensor digitorum longus (TA/EDL) Lucifer Yellow (LY) filled motoneurones. LY filled motoneurones and serotonin-immunoreactive axons were imaged using different filters (see Fig. 4.12). Images were collected at 1 μm increments and the serotonin-positive appositions within 1 μm of the motoneurones in each image were counted. The files were then 'merged' to create a pseudocolour image of the information gathered from both filters.

(A) Soma and proximal dendrites of a normal P7 motoneurone. Serotonin-immunoreactive afferent axons are seen in the area around the flexor motoneurone. Scale bar = 25 μm.

(B) The boxed area in **(A)**. This shows serotonin-immunoreactive afferent axons (orange/red) contacting (arrows) the motoneurone proximal dendrite (green). Scale bar = 5 μm.

(C) Soma of a P7 TA/EDL motoneurone filled with LY, in which the common peroneal nerve was crushed on P2. Serotonin-immunoreactive afferent axons can be seen contacting the soma (arrows). Scale bar = 10 μm.

(D) Distal dendrite of a P7 motoneurone (green) with serotonin-immunoreactive afferent axon (orange/red) contacting it (arrow). Scale bar = 5 μm.

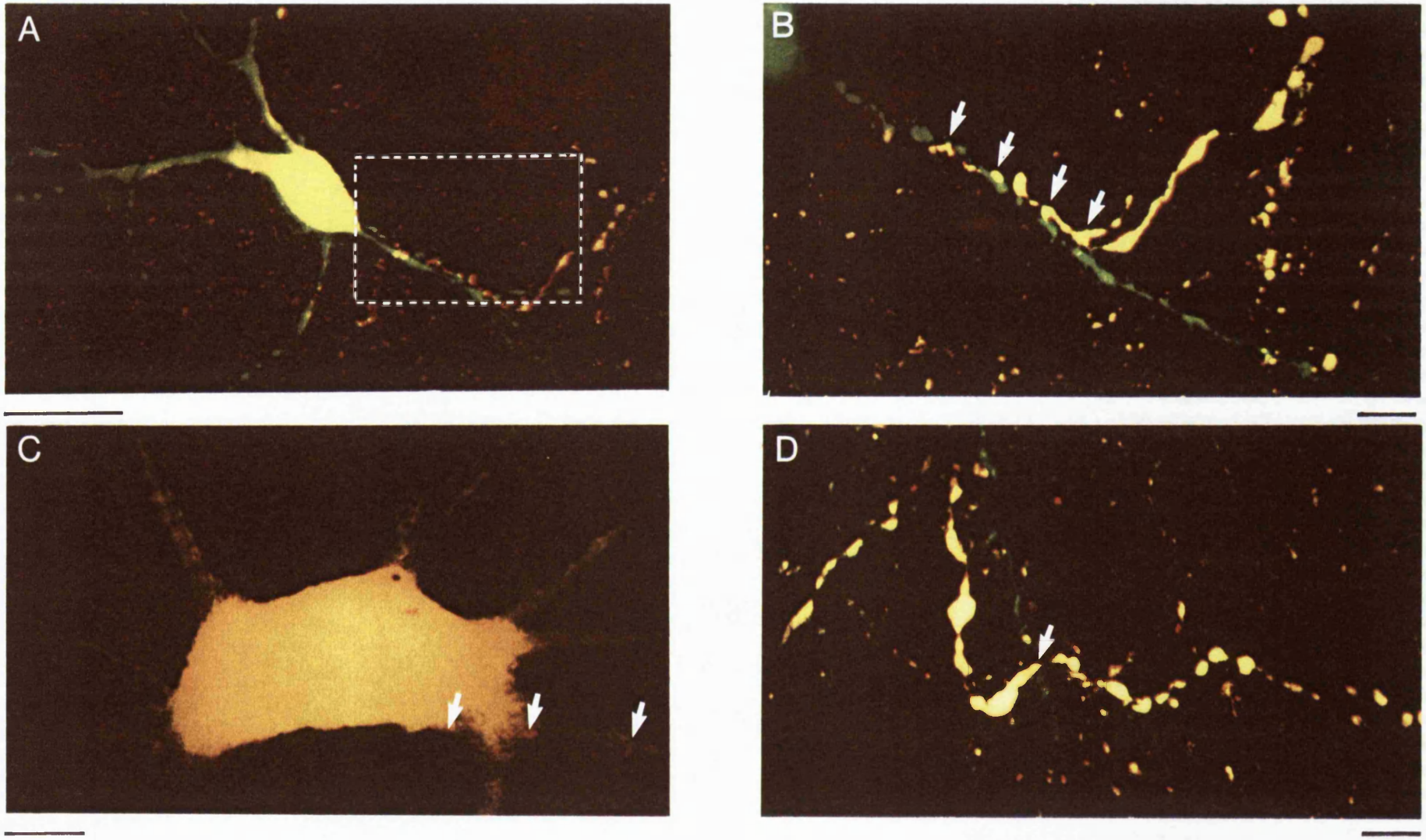
A
B
C
D

Figure 4.14 Camera lucida-like drawings of topographic mapping of serotonin-immunoreactive afferent axons contacting the soma and dendrites of seven day old (P7) tibialis anterior/extensor digitorum longus (TA/EDL) motoneurones. These drawings were obtained from low power (x20) laser scanning confocal images of the motoneurones. The serotonin-immunoreactive boutons were systematically imaged at high power (x60/1.4 oil immersion) on the soma and dendrites of the motoneurone, and their position was plotted on the low power images. This provides information about the distribution of serotonin-positive afferent axons on the somatodendritic surface of the identified motoneurones. Compass points mark the dorsal, ventral, rostral and caudal axes.

(A) A normal P7 motoneurone. Serotonin-immunoreactive afferent axons are absent from the soma, and found mostly on the distal dendrites. Scale bar =100 μm.

(B) A P7 motoneurone in which the common peroneal nerve was crushed on P2. Six out of a total of 58 serotonin-immunoreactive afferent axons were observed contacting the soma of this motoneurone. The majority of the axons still contacted the distal dendrites. Scale bar = 100 μm.

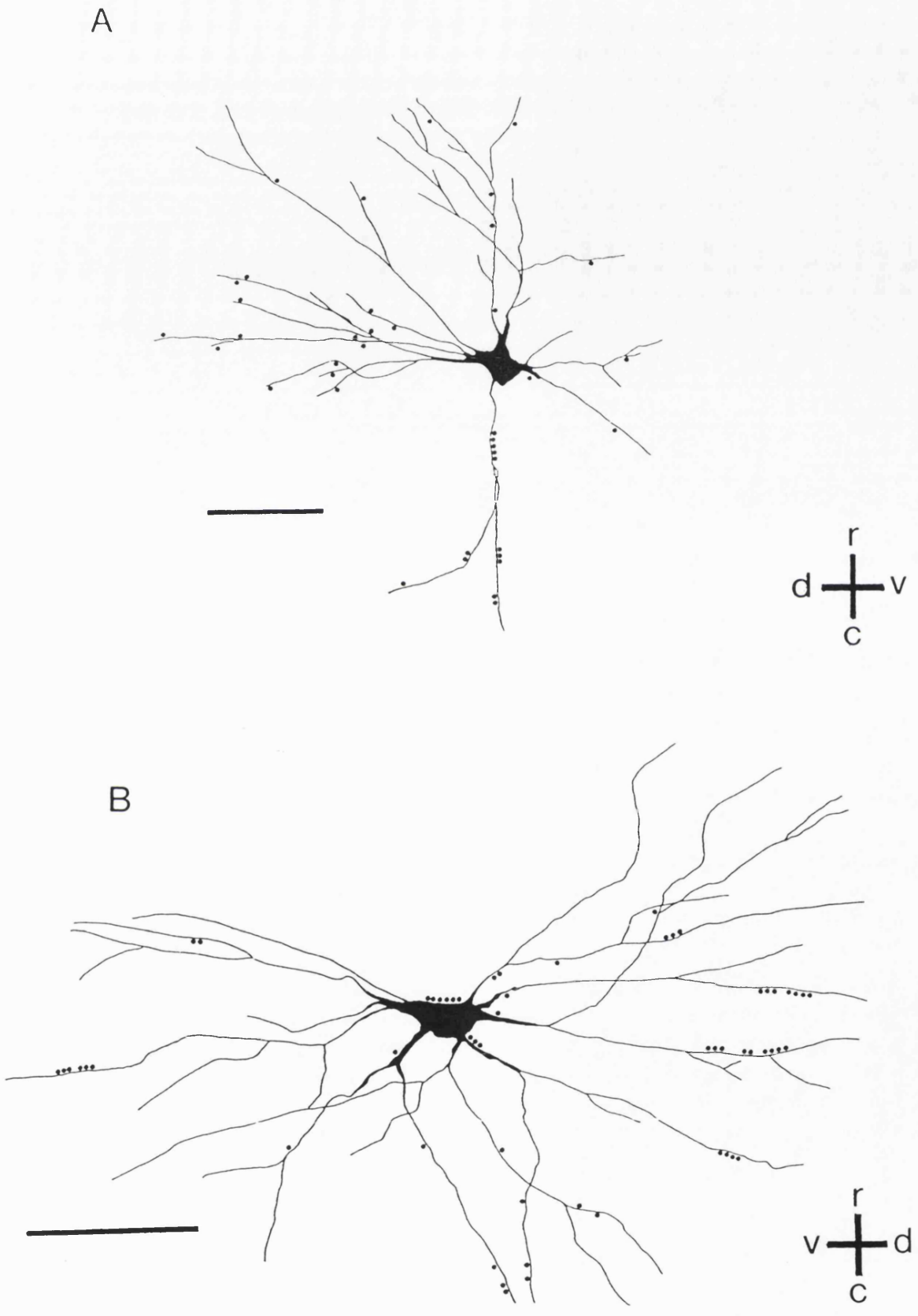
A
r
d
v
c
B
r
v
d
c

Table 4.1

Density of parvalbumin-immunoreactive boutons around the perimeter of identified ankle flexor motoneurones counted using light microscopy[*].

Number in group	Con/op op/con	Age (dpn)	Mean number of appositions	% op/con	Mean distance around perimeter (μm)	% op/con	Mean number of appositions/ 100 μm perimeter	%
n=116	con	3	9.9 ± 4.7	96.0	89.0 ± 11.5 ***ΩΩΩ	98.1	11.1 ± 4.9 ΩΩ	96.4
n=115	op	3	9.5 ± 4.6		87.3 ± 13.4 **ΩΩΩ		10.7 ± 4.6 Ω	
n=99	con	7	11.8 ± 5.7	94.9	111.8 ± 23.5 ≈≈≈	92.5	10.8 ± 4.5 ≈≈	100.9
n=71	op	7	11.2 ± 6.9		103.4 ± 22.7 ≈≈≈		10.9 ± 5.3	
n=60	con	14	11.8 ± 7.4	99.2	127.3 ± 17.2	97.1	9.0 ± 5.3	98.9
n=43	op	14	11.7 ± 7.2		123.6 ± 28.0		8.9 ± 4.7	

[*]Values for each parameter correspond to the mean and standard deviation in each group. The levels of statistical significance are shown by the symbols.

* denotes P3 vs P7; Ω denotes P3 vs P14; ≈ denotes P7 vs P14. The number of symbols represents the levels of significance.

Table 4.2

Density of parvalbumin-immunoreactive boutons around the perimeter of identified ankle flexor motoneurones, quantified using confocal microscopy[apple].

Number in group	Op/con	Age	Mean number of appositions	% op/con	Mean soma area (μm2)	% op/con	Mean number of appositions/ 100μm area	% op/con
n=104	con	3	7.6 ± 5.0***	76.9	462.8 ± 139.0≈≈≈ΩΩΩ	97.2	1.7 ± 1.1**ΩΩΩ	81.1
n=81	op	3	5.6 ± 4.0≈≈≈ΩΩ		449.2 ± 124.0≈≈≈ΩΩΩ		1.3 ± 0.9≈≈≈ΩΩΩ	
n=85	con	7	7.6 ± 4.2***	46.8	601.5 ± 237.5*fff*	98.9	1.3 ± 0.8****fff*	31.6
n=48	op	7	3.2 ± 2.1		590.8 ± 193.7*fff*		0.6 ± 0.4*f*	
n=29	con	14	8.1 ± 4.0***	38.3	937.2 ± 251.1	105	0.9 ± 0.4***	33.3
n=17	op	14	3.1 ± 2.2		983.9 ± 240.6		0.3 ± 0.3	

[apple]Values for each parameter correspond to the mean and standard deviation. The levels of statistical significance are shown by the symbols. * denotes operated vs control; ≈ denotes P3 vs P7; Ω denotes P3 vs P14; *f* denotes P7 vs P14. The number of symbols represents the level of significance.

Table 4.3

Density of serotonin-immunoreactive axons in the ventral horn of sections containing the prelabelled common peroneal motor pool[•].

Animal	Age	Control	Operated	% op/con
GS15	7	125	107	85.60
GS11	7	83	93	112.05
GS24	7	229	196	85.59
GS26	7	602	555	92.19
mean		**259.8 ± 236.3 ***	**237.8 ± 216.4 ***	**93.9 ± 12.5**
GS12	14	128	150	117.19
GS18	14	74	83	112.16
GS25	14	310	267	86.13
GS28	14	495	493	99.60
mean		**251.8 ± 191.0 Ω**	**248.3 ± 180.0 Ω**	**103.8 ± 13.9**
GS16	22	315	266	84.44
GS17	22	406	277	68.23
GS19	22	88	95	107.95
GS27	21	439	479	109.11
mean		**312.0 ± 158.3 ≈**	**279.3 ± 157.1 ≈**	**92.4 ± 19.7**
GS33	adult	788	908	115.23
GS34	adult	853	681	79.84
GS35	adult	777	590	75.93
GS36	adult	1082	1074	99.26
mean		**875.0 ± 142.0**	**813.3 ± 219.3**	**92.6 ± 18.2**

[•]Values for each parameter correspond to mean and standard deviation. The levels of statistical significance are shown by the symbols. * denotes P7 vs adult; Ω denotes P14 vs adult; ≈ denotes P22 vs adult. The number of symbols represents the level of statistical significance.

Table 4.4

Density of serotonin-immunoreactive boutons around the perimeter of identified ankle flexor motoneuornes, quantified using conventional light microscopy[apple].

Number in op/con group	Animal	Age	Mean number of appositions	% op/con	Mean distance around perimeter (μm)	% op/con	Mean number of appostions/ 100 μm perimeter	%
58	con	3	4.8 ± 3.5 **ΩΩΩ	137.5	72.9 ± 13.8 Ω	100.8	6.4 ± 4.3 **ΩΩΩ	142.2
54	op	3	6.6 ± 3.3 ΩΩΩ		73.5 ± 14.5		9.1 ± 4.8 ΩΩΩ	
53	con	7	8.7 ± 5.2 *	128.7	78.2 ± 14.4	94.3	11.0 ± 6.0 **	138.2
55	op	7	11.2 ± 5.5		73.7 ± 13.1		15.2 ± 7.5	

[apple]Values for each parameter correspond to mean and standard deviation. The levels of significance are shown by the symbols. * denotes operated vs control; Ω denotes P3 vs P7. The number of symbols represents the level of significance.

Table 4.5

Topographic location of serotonin-immunoreactive boutons on the soma and dendrites of identified flexor motoneurones intracellularly filled with Lucifer Yellow, for a total of 14 cells, seven of which are normal and seven of which are from animals in which the common peroneal nerve was crushed on postnatal day 2.

Cell	Op/con	Age	Soma area	Surface area	No.appositions	No soma	On dendrites	<75 µm	>75 µm	No./area
1	op	7	727.6	25072.7	30	8	22	2	20	0.0011
2	op	7	361.2	8269.3	35	9	26	4	22	0.0031
3	op	7	544.1	20393.5	58	6	52	10	42	0.0021
4	op	8	729.5	16878.6	84	3	81	16	65	0.0041
5	op	8	349.0	5351.0	156	3	153	84	69	0.0201
6	op	8	407.7	5211.7	111	15	96	71	25	0.0161
7	op	4	356.0	18887.9	173	7	166	57	116	0.0061
mean ± SD		**7.0 ± 1.4**	**496.4 ± 172.1**	**14295 ± 7957**	**92.4 ± 56.8**	**7.3 ± 4.1**	**85.1 ± 57.5**	**34.9 ± 34.7**	**51.3 ± 34.9**	**0.0075 ± 0.0075**
8	con	8	516.0	15396.4	154	8	146	49	97	0.9681
9	con	7	601.5	32563.1	39	0	39	8	31	0.0011
10	con	7	480.9	5082.8	28	0	28	10	18	0.0031
11	con	6	532.1	10046.1	91	0	91	31	60	0.0071
12	con	6	574.0	11154.0	80	2	78	56	22	0.0021
13	con	6	300.7	13868.6	66	0	66	21	45	0.0031
14	con	4	297.5	9374.9	260	8	252	73	179	0.0191
mean ± SD		**6.3 ± 1.3**	**471.8 ± 124.2**	**13927 ± 8862**	**102.6 ± 80.6**	**2.6 ± 3.8**	**100.0 ± 77.3**	**35.4 ± 24.6**	**65.6 ± 57.2**	**0.143 ± 0.36**

Table 4.6

Distribution of serotonin-immunoreactive boutons on identified flexor motoneurones intracellularly filled with Lucifer Yellow, for the same cells as shown in Table 4.5. The position of these boutons on the soma and dendrites is divided into regions corresponding to the dorsal, ventral, rostral and caudal axes.

Cell	Op/con	Age	No. appositions	% dorsal	% ventral	% rostral	% caudal
1	op	7	30	33	33	3	30
2	op	7	35	23	37	14	26
3	op	7	58	55	17	10	17
4	op	8	84	46	21	27	5
5	op	8	156	73	1	6	22
6	op	8	111	27	17	24	32
7	op	4	173	40	18	12	30
mean ± SD		**7.0 ± 1.4**	**92.4 ± 56.8**	**42.4 ±17.4**	**20.6 ± 11.8**	**13.7 ± 8.9**	**23.4 ± 9.6**
8	con	8	154	36	9	31	25
9	con	7	39	41	8	18	33
10	con	7	28	64	21	14	0
11	con	6	91	29	3	37	31
12	con	6	80	29	13	40	19
13	con	6	66	38	14	8	41
14	con	4	260	27	9	15	50
mean ± SD		**6.3 ± 1.3**	**102.6 ± 80.6**	**37.7 ± 12.7**	**11.0 ± 5.7**	**23.3 ± 12.5**	**28.4 ± 16.1**

5. GENERAL DISCUSSION

This study has examined the morphological development of identified rat hindlimb flexor motoneurones and their afferent connections during the early postnatal period. In addition, the response of these neurones following injury to their axons during early development was studied. The tibialis anterior and extensor digitorum longus motor pool were identified using fluorescent retrograde labelling and individual motoneurones were injected intracellularly with Lucifer Yellow to visualise the soma and dendritic tree of the cell. Two types of monosynaptic afferent inputs onto these motoneurones were studied. The terminations of serotonergic descending pathways were visualised, as well as those of the segmental afferent inputs.

5.1. Early postnatal development of rat flexor motoneurones

During early postnatal life, rat motoneurones undergo a change in their phenotype from growing to transmitting cells. During the first and second postnatal weeks there are changes in the morphology and activity patterns of motoneurones. At this stage of development the axons of these cells have more branches than later and occupy a larger peripheral field (Balice-Gordon, Thompson, 1988). This transition occurs at a time when there is a gradual increase in the activity of the motoneurones (Navarrete, Vrbová, 1983) and coordinated locomotor function begins to develop (Westerga, Gramsbergen, 1990).

In this study the normal morphological development of flexor motoneurones was studied in the first nine days of postnatal life. Over this period there was a clear elimination of growth associated processes which were present on the somatodendritic surface of the motoneurones at birth. These processes were long and fine and initially present in all regions of the motoneurone. By P4, however, they had been eliminated from the soma and continued to disappear until

they remained only on distal dendrites. A similar somatofugal loss of processes has been reported in rat thoracic motoneurones (Cummings, Steltzner, 1984).

Changes in dendritic branching structure of motoneurones have been observed during early postnatal development in the kitten (Ulfhake *et al.*1988) and in the rat (Nunez-Abades *et al.*1993). During the limited span covered by this study, no change in the orientation and branching structure of flexor motoneurones was observed. The changes in dendritic branching structure, found in the previously cited studies, occurred predominantly in the distal part of the dendritic tree. However, it is possible that the methods used here did not allow visualisation of these terminal structures. Also, this information may have been lost when imaging fluorescent structures in thick tissue, even using the confocal microscope. Distal dendrites have a very thin diameter (less than 0.6 μm), and the possibility of bleaching occurring during image acquisition must be considered. Thus, whilst it may be possible to say with some confidence that dendritic remodelling does not occur in the proximal dendrites during this period, the branching pattern of very distal dendrites was probably not seen using this technique.

A significant correlation between the soma size and combined diameter of primary dendrites, and the diameter of the stem dendrites and its total dendritic length was observed. Similar correlations have been reported in cat motoneurones (Zwaagstra, Kernell, 1981; Ulfhake, Cullheim, 1988a). The structure and branching pattern of the dendritic tree influence the functional output of the motoneurones (Rall, 1959; Rall *et al.*1967) and is therefore very important. In addition, smaller motoneurones have a higher input resistance and lower excitation threshold and therefore are more active than larger ones (Henneman *et al.*1965). Changes in the size and branching structure of slow and fast motoneurones have been described during postnatal development (Westerga, Gramsbergen, 1992). These developmental changes in the morphology of the

motoneurones may be responsible for functional changes that are observed during early postnatal life.

It is clear that there are changes occurring in the motoneurone during early postnatal development, and that this eventually results in the adult morphology and patterns of activity. Some of these events may be preprogrammed, and occur as a result of the switching on and off of various combinations of genes during development. Even if this is the case, the environment that a motoneurone finds itself in will influence its phenotype.

One factor that might influence the phenotype of the motoneurone is the position of afferent synapses onto the surface of the cell. This study showed that there was a postnatal decrease in the density of parvalbumin-positive innervation onto the motoneurones (see (Zhang *et al.*1990)) at a time when there is an increase in the density of serotinergic innervation (see (Rajaofetra *et al.*1989b; Rajaofetra *et al.*1989a)). The position and density of synaptic contacts onto the growth cones of developing motoneurones has been suggested as a possible mechanism for control of dendritic branching (Vaughn *et al.*1974; Vaughn, 1989). If this is the case the changes in afferent inputs observed during this study would affect the patterns of dendritic branching.

5.1.1. Role of afferents in dendritic remodelling

There is some evidence for plasticity of synaptic connections between motoneurones and their afferents during the early postnatal period (Fitzgerald, Vrbová, 1985; Fitzgerald, 1985b; Himes, Tessler, 1989). A role for afferent contacts in influencing the branching patterns of the dendritic trees of the postsynaptic motoneurones has been proposed (Vaughn, 1989). The growth of dendrites of frog motoneurones into preformed synaptic fields (Jackson, Frank, 1987) would seem to confirm this. According to this hypothesis, dendritic density should be directly related to the quantity of synaptic sites present. For instance, there is reduced branching of cerebellar Purkinje cells following irradia-

tion resulting in reductions in afferent fibres (Berry, Bradley, 1976b). However, the orientation of the initial outgrowth of the dendrites of rat spinal accessory motoneurones (studied using DiI) occurs before the afferent axons have entered the ventral horn (Snider *et al.*1992b). This does not preclude afferents from influencing the shape of dendritic trees at a later time. It is clear that there are other factors which effect the direction of growth and branching pattern of mammalian motoneurones. The timing of the interaction from different afferent systems during development, the most significant probably being from interneurones, may effect the resulting dendritic growth.

In this study, there was no observable change in the dendritic branching structure of the motoneurones during normal early postnatal development. There was, however, an increase in the number of serotonergic appositions and a small decrease in the number of parvalbumin-positive contacts onto the motoneurones during this period. In addition, there was a decrease in the number of PV-positive boutons and an increase in the number of serotonin-positive contacts onto motoneurones following neonatal injury. So, despite the changes in these specific types of afferent inputs no changes in the branching structure of the motoneurones was observed. This is in contrast to other studies in adult have shown changes in dendritic branching after injury in rats (Sumner, Watson, 1971; Standler, Bernstein, 1982), and in cats (Brannstrom *et al.*1992a; Brannstrom *et al.*1992b). There is also evidence of changes in dendritic structure 14 days after neonatal injury in the rat (O'Hanlon, Lowrie, 1993a). It is probable that changes in the dendritic branching pattern have not happened by P9, and that they occur thereafter.

The retrograde influence of the target muscle could also affect the development of motoneurones. The peripheral nerve was damaged in the neonate to investigate any changes in the morphology of flexor motoneurones as a result of disconnection from the target.

5.1.2. Response to neonatal nerve injury of rat flexor motoneurones

In the rat, disruption of the interaction of the motoneurone with its target muscle during the first few days after birth results in massive cell death (see (Lowrie, Vrbová, 1992)), indicating that motoneurones at this stage of their development are somehow dependent on the contact with their target.

The results of this study show that following injury to the CP nerve two days after birth, over 50% of flexor motoneurones to die. The morphology of these cells during the first seven days after injury was examined, in the same way as for normal development. It appeared that the normal maturation of the surface of the motoneurones was arrested. The reduction in surface growth associated processes was halted, so that on P4 the soma and proximal dendrites were still densely covered with long filopodial processes. There was an apparent increase in the incidence of these growth associated processes following injury to the axon of the cell. There was also evidence of some aberrant growth of dendrites. Injury causes changes in the metabolism of the cell (LaVelle, LaVelle, 1958) and possibly prolongs the period that the motoneurones are in a growth state. It is not clear when, or if, motoneurones continue to develop normally, or why some should die whilst others survive.

Using cholera toxin-HRP, the total visible length of the dendritic tree of surviving flexor motoneurones has been seen to be larger than normal at P14 (O'Hanlon, Lowrie, 1993a). However, this increase in the size of the dendritic tree was only transient, and the subsequent growth was slower than normal. When adult, these injured motoneurones have abnormal dendritic morphologies (O'Hanlon, Lowrie, 1992; O'Hanlon, Lowrie, 1993c). The total visible dendritic length is 30% smaller than normal, the predominant reduction being in the medial sectors resulting from a reduction in the branching of dendrites. This may result from the reduction in afferent connections, especially interneurones, in that sector. The soma area was also shown to be smaller than normal. This was

This study suggested that there was no growth of the dendritic tree of normal motoneurones in the early postnatal period. Other studies, using different techniques, have shown significant growth during this period (see Bellinger and Anderson, 1987), so it is possible that the method used here may not show growth that may be occurring. One of the reasons for this may be the use of fluorescent material, where there is bleaching of the finer distal processes during the acquisition of the images. This is the region of the motoneurones in which growth is most probably occurring and so if it was not being imaged no growth would be observed. It is also possible that information was lost in the projection of the images from three dimensions into two dimensions for Sholl analysis. The distal processes deeper within the tissue may be obscured by overlying processes. A alternative method of analysis is suggested by Berry (Berry *et al.*, 1976). This involves topographical analysis of the branching patterns and branch lenghts of the individual dendrites of the motoneurones and may provide a more accurate method of analysing the growth of the cells. In light of this, it is more accurate to conclude that this study did not illustrate growth of postnatal motoneurones, or any change in dendritic branching of motoneurones following injury in the early postnatal period, but that this may be a limitation of the methods used.

also seen in the present study which showed that motoneurones that survived to three months had a smaller soma area than contralateral controls.

The size of flexor motoneurones and branching structure of their dendrites, was studied up to one week after crush injury in this study. Changes in the somato-dendritic surface of the motoneurones were observed, but there was no observable change in the orientation or branching structure of the small number of motoneurones subjected to Sholl analyses. It is possible that some of the long processes, observed in a few of the injured motoneurones, may continue to grow and form dendrites. Thus, by P14 see (O'Hanlon, Lowrie, 1993a), there would be an observable change in the branching structure of the dendritic tree. This period of exuberant growth may only occur transiently after injury. The dendritic tree may then lose the growth associated processes, as is observed during normal development in flexor (this study) and in thoracic motoneurones (Cummings, Steltzner, 1984). However, the retarded rate of growth observed after neonatal injury, and the presence of abnormally projecting dendrites, may contribute to the abnormal morphologies seen in adult motoneurones that survive injury at birth (O'Hanlon, Lowrie, 1993c; O'Hanlon, Lowrie, 1993b). In this study dendritic morphologies of injured motoneurones were followed only until P7. It would be interesting to study the period after the end of this study (P7), and before P14, when abnormal dendritic morphologies have been observed (O'Hanlon, Lowrie, 1993a). It may be possible to determine if there is a process of transformation of the growth associated processes into dendrites. ✳

Temporary disconnection of the neonatal motoneurone from its peripheral target appears to result in the cell failing to undergo some critical developmental changes and renders them vulnerable to the effects of factors that result in their death. The mechanisms for the retrograde trophic influence of the muscle on the motoneurones are not clearly understood. The muscle may lend trophic support in the form of chemical trophic factors such as CNTF and BDNF (Sendtner *et al.*1990; Sendtner *et al.*1992b; Sendtner *et al.*1992a). When the

connection is severed, this support, (or some other retrograde influence), is no longer available to the young motoneurones and they can no longer survive in their environment. It is also possible that this death results from excessive synaptic activation via glutamate, the main excitatory neurotransmitter to motoneurones, resulting in excitotoxic cell death (see (Choi, 1992b)). Since neonatal motoneurones appear to have a higher density of NMDA receptors than adults (Kalb *et al.*1992), they may be especially susceptible to excessive application of glutamate. After injury during this critical neonatal period, surviving motoneurones become hyperactive and display inappropriate reflexes (Navarrete, Vrbová, 1984; Navarrete *et al.*1990), suggesting that injury affects the maturation of the motoneurones and possibly of their synaptic connectivity.

Therefore, these changes may not just be due to disconnection from the target. Crushing the peripheral nerve also causes injury to the peripheral projection of the dorsal root ganglion cells and results in cell death (Bondok, Sansone, 1984; Arvidsson *et al.*1986b; Himes, Tessler, 1989; Yip *et al.*1984) and other afferent systems have been demonstrated to change. This study showed that after common peroneal nerve crush on P2, there was an increase in the number of serotonin-immunoreactive contacts onto flexor motoneurones. There was also a decrease in the number of PV-immunoreactive contacts. Previous studies have shown an increase in serotonergic innervation to motoneurones following death of DRG's (Polistina *et al.*1990; Wang *et al.*1991b). Topographic mapping of the serotonin-positive appositions contacting the soma and dendrites of motoneurones intracellularly filled with Lucifer Yellow showed what appeared to be a redistribution of serotonin-positive afferents after injury, with a greater percentage being found on the soma. The increase in the incidence of growth associated processes on the somatodendritic surface of the motoneurones following neonatal injury may provide a potential new site for the formation of synapses and may also be an indication of changes in the afferent synaptology onto motoneurones. Whether this increase in serotonin-immunoreactive inner-

vation remains beyond the first postnatal week after injury needs to be investigated. In addition, DRGs from adjacent uninjured roots may sprout and form contacts with injured motoneurones after P7.

These changes in the sites of afferent inputs onto the motoneurones after injury may contribute to the changes in activity observed in the same motoneurones (Navarrete, Vrbová, 1984; Navarrete *et al.*1990), and cell death may result from inappropriate synaptic activation of vulnerable motoneurones which have lost the trophic support of their targets. Changes in the phenotype of the motoneurones have been observed in response to injury. There is a delay in the up-regulation of the enzyme ChAT after neonatal injury in the rat (Greensmith, Vrbová, 1990). There are also changes in the production of other proteins after injury, such as GAP 43 (Schreyer, Skene, 1991). If there are morphological changes in the motoneurones following injury, it might be expected that there would be changes in the amounts of both the mRNA and the protein products of cytoskeletal proteins such as actin, tubulin, MAPs and neurofilament. The expression of genes specifically associated with injury, such as c-fos and c-jun could also be examined. This could be investigated both during normal development and in neonatally injured motoneurones, using *in situ* hybridisation and immunocytochemistry. This information would indicate which regions of the motoneurones change in response to neonatal injury, and which areas of the cell grow during this developmental period.

6. APPENDIX 1

6.1. Modified Hanker-Yates method for the Visualization of Horseradish Peroxidase.

1. The spinal cord was cut above L3 and below L6. The right dorsal horn was pierced with a fine micropin to allow identification of each side of the spinal cord.
2. The block of tissue was frozen and cut into sections 50 µm thick on a freezing microtome (Pelcool). Sections were collected into containing Millonig's phosphate buffer.
3. The sections were briefly washed in distilled water.
4. The sections were incubated in cobalt/nickel solution for 15 minutes.
5. The sections were rinsed in distilled water and then washed twice, for 10 minutes each time, in Millonig's phosphate buffer.
6. The sections were reacted in Hanker-Yates solution for 10-25 minutes, until the HRP-filled cells were clearly visible.
7. The sections were washed in 2 changes of Millonig's phosphate buffer for 5 minutes each.
8. The sections were mounted onto gelatinised glass slides (0.5%) and dried overnight.
9. The sections were counterstained with gallocyanin, after a brief was in distilled water, for 10-25 minutes.
10. The sections were dried, then dehydrated through graded alcohols and cleared in xylene and coverslipped.

6.1.1. Solutions for Hanker-Yates Method

1. Millonig's phosphate buffer.

$NaH_2PO_4.2H_2O$	19.08 g
1M NAOH	96.3 ml

Make up to 1 litre with distilled water.

Adjust to pH 7.3; store at 4°C.

2. Cobalt/nickel solution.

1% cobalt chloride	300 ml
1% ammonium nickel sulphate	200 ml

Mix prior to use.

3. Cacodylate buffer.

0.1 M sodium cacodylate	500 ml
(21.4 g/500 ml distilled water)	
0.2 M HCL	
(17.22 ml conc. HCL/litre distilled water)	

Adjust to pH 5.1-5.2. Make up to 2 litres in distilled water. Store at 4 °C.

4. Hanker-Yates solution.

Hanker-Yates combined reagent (sigma VI)	150 mg
Cacodylate buffer (pH 5.1-5.2)	100 ml
30% H_2O_2	1 drop

Make up prior to use. Use within 1 hour.

6.1.2. Counterstining with Gallocyanin

Preparation of gallocyanin.

Gallocyanin	0.3 g
Chromalum	10 g

Make to 100 ml in distilled water.

Dissolve chromalum in heated water. Add gallocyanin. Boil and simmer for 20-30 minutes. Cool; make to 100 ml. Filter and store at room temperature.

7. APPENDIX 2

7.1. Parvalbumin Immunocytochemistry

1. Transverse sections of the spinal cord were cut on a cryostat (Bright) at either 20 μm (on gelatinised slides), or 50 μm (free-floating).
2. Sections were washed in PBS + 0.1% Bovine serum albumin (BSA) + 0.3% Triton-X-100, 3 times for 5 minutes.
3. Sections were incubated in Normal Horse Serum (NHS; Vector) 1:30 in PBS + 0.3% Triton at room temperature for 1 hour.
4. Sections were washed in PBS + 0.3% Triton 3 times for 5 minutes.
5. Sections were incubated in the primary antibody, monoclonal Mouse Anti-Parvalbumin (Sigma) 1:1000 in PBS + 0.3% Triton for 48 hours at $4^{o}C$. Sections for controls were incubated in NHS.
6. Sections were washed in PBS 2 times for 10 minutes.
7. Sections were incubated in the secondary biotinilated anti-mouse antibody raised in rat (Vector) 1:200 in PBS.
8. Sections were washed 2 times in PBS.
9. Sections for visualisation with Texas Red Avidin D as the chromagen were washed in bicarbonate buffered saline.
10. Sections for visualisation with HRP as the chromagen were reacted using the Elite ABC vectorstain kit (Vector). This was made up 1/2 an hour before use. The sections were incubated for 1 hour, washed in PBS 2 times and reacted with 20 mg/1 ml Diaminodenzidine (DAB; Sigma) in PBS for 10 minutes at room temperature.
11. Sections were then dried, dehydrated through graded alcohols, cleared in xylene and coverslipped.
12. Sections for visualisation with fluorescence were incubated for 2 hours in 1:100 Texas Red Avidin D in $NaHCO_3$ buffered saline. They were the washed twice in the buffered saline for 10 minutes each, dried, dehydrated through

graded alcohols, cleared in methyl salicylate (Sigma), mounted in Entellan (Sigma) and coverslipped.

Bicarbonate Buffered Saline (0.05 M).

NaCl	0.9 g
Na HCO_3	4.2 g

Make up to 1 litre in distilled water.

8. APPENDIX 3

8.1. Serotonin Immunohistochemistry

1. Transverse sections of the spinal cord were cut on a cryostat (Bright) at either 20 μm (on gelatinised slides), 100 μm using the hemicords containing intracellularly filled cells (free-floating).
2. Sections were washed in PBS + 0.1% Bovine serum albumin (BSA) + 0.3% Triton-X-100, 3 times for 5 minutes.
3. Sections were incubated in Normal Goat Serum (NGS; Vector) 1:30 in PBS + 0.3% Triton at room temperature for 1 hour.
4. Sections were washed in PBS + 0.3% Triton 3 times for 5 minutes.
5. Sections were incubated in the primary antibody, polyclonal Rabbit Anti-Serotonin (Affinity) 1:1000 in PBS + 0.3% Triton for 48 hours at $4^{o}C$. Sections for controls were incubated in NGS.
6. Sections were washed in PBS 2 times for 10 minutes.
7. Sections were incubated in the secondary biotinilated anti-rabbit antibody raised in goat (Vector)1:200 in PBS.
8. Sections were washed 2 times in PBS.
9. Sections for visualisation with Texas Red Avidin D as the chromagen were then washed in bicarbonate buffered saline.
10. Sections for visualisation with HRP as the chromagen were reacted using the Elite ABC vectorstain kit (Vector). This was made up 1/2 an hour before use. The sections were incubated for 1 hour, washed in PBS 2 times and reacted with 20 mg/1 ml Diaminodenzidine (DAB; Sigma) in PBS for 10 minutes at room temperature.
11. Sections were then dried, dehydrated through graded alcohols, cleared in xylene and coverslipped.
12. Sections for visualisation with fluorescence were incubated for 2 hours in 1:100 Texas Red Avidin D in $NaHCO_3$ buffered saline. They were the washed

twice in the buffered saline for 10 minutes each, dried, dehydrated through graded alcohols, cleared in methyl salicylate (Sigma), mounted in Entellan (Sigma) and coverslipped.

BIBLIOGRAPHY

Abercrombie M (1961) The bases of the locomotory behaviour of fibroblasts. Exp Cell Res 8:188-198.

Abercrombie M (1982) Cell Behaviour. Cambridge: C.U.P..

Aguayo A, Bray GM, Perkins CS, Duncan ID (1979) Axon-sheath cell interactions in peripheral and central nervous system transplants. Soc Neurosci Symp 4:361-383.

Aguayo A, David S, Richardson P, Bray D (1982) Axonal elongation in peripheral and central nervous system transplants. Adv Cell Neuobiol 3:215-234.

Aldskoguis H, Risling M (1981) Effect of sciatic neurectomy on neuronal number and size distribution in the L7 ganglion of kittens. Exp Neurol 74:597-604.

Aldskoguis H, Arvidsson J, Grant G (1985) The reaction of primary sensory neuorns to peripheral nerve injury with particular emphasis on transganglionic changes. Brian Research Reveiws 10:27-46.

Altman J, Sundarshan K (1975) Postnatal development of locomoion in the laboratory rat. Animal Behaviour 23:896-920.

Altman J (1982) The cerebellum - New vistas. Berlin: Springer.

Altman J, Bayer SA (1984) Development of the Rat Spinal Cord. Advances in Anatomy and Embryology 85:

Anderson EG (1972) Bulbospinal serotonin-projecting neurones and motor control. Proc Fed Am Soc Exp Biol 31:107-112.

Anglister L, Farber IC, Shahar A, Grinvald A (1982) Localization of voltage sensitive Ca++ channels along developing neurites: their possible role in regulating neurite growth. Developmental Biology 94:351-356.

Appel SH (1993) Excitotoxic neuronal cell death in amyotrophic lateral sclerosis. Trends Neurosci 16:3-5.

Arakawa YM, Sendtner M, Thoenen H (1990) Survival effect of ciliary neurotophic factor (CNTF) on chick embryonic motoneurones in culture: comparison with other neurotrophic factors and cytokines. Journal of Neuroscience 10:3507-3515.

Arvidsson J, Ygge J, Grant G (1986a) Cell loss in lumbar dorsal root ganglia and transganglionic degeneration after sciatic nerve resection in the rat. Brian Research 373:15-21.

Arvidsson J, Ygge J, Grant G (1986b) Cell loss in lumbar dorsal root ganglia and transganglionic degeneration after sciatic nerve resection in the rat. Brian Research 373:15-21.

Arvidsson J, Risling M, Cullheim S, Dagerlind H, Shupliakov O, Ulfhake B, Hokfelt T (1992) On the distribution of GAP-43 and its relation to serotonin in

adult monkey and cat spinal cord and lower brain stem. European Journal of Neuroscience 4:777-784.

Ashwell K (1991) The distribution of microglia and cell death in the fetal rat forebrain. Developmental Brain Research 58:1-12.

Azvidsson U, Schalling M, Cullheim S, Ulfhake B, Terenius L, Verhfsad A, Hokfelt T (1990) Evidence for coexistence between calcitonin gene-related peptide and serotonin in the bulbospinal pathway in the monkey. Brian Research 532:47-57.

Baimbridge KG, Celio MR, Rogers JH (1992) Calcium-binding proteins in the nervous system. Trends Neurosci 15(8):303-309.

Balice-Gordon RJ, Thompson WJ (1988) Synaptic rearrangements and alterations in motor unit properties in neonatal rat extensor digitorum longus muscle. Journal of Physiology 398:191-210.

Barde Y-A (1989) Trophic factors and neuronal survival. Neuron 2:1525-1534.

Barr ML, Hamilton JD (1948) A quantitative study of certain morphological changes in spinal motor neurones during the axon reaction. J Comp Neurol 89:93-122.

Barron KD, Tuncbay TO (1964) . Journal of Neuropathology and Experimental Neurology 23:368.

Barron KD, Oldershaw JB, Bernsohn J (1966) . Journal of Neuropathology and Experimental Neurology 25:443.

Barron KD, Chiang TY, Daniels AC, Doolin PF (1971) Progress in Neuropathology. New York: Grune and Stratton.

Basbaum AL, Clanton CH, Fields HL (1978) Three bulbospinal pathways from the rostral medulla of the cat. An autoradiographic study of pain modulatory systems. J Comp Neurol 178:209-224.

Beal FM, Hyman BT, Koroshetz W (1993) Do defects in mitochondrial energy metabolism underlie the pathology of neurodegenerative diseases? Trends Neurosci 16:125-131.

Becker DL, Cook JE (1990) Changes in goldfish retinal ganglion cells during axonal regeneration. Proceedings of the Royal Society of London B 241:73-77.

Becker DL, Navarrete R (1990) Dye-coupling between lumbar motoneurones in the embyronic and neonatal rat spinal cord: an *in vitro* study. Journal of Physiology 423:98P.

Becker DL, Dekkers J, Navarrete R, Green C, Cook JE (1991) Enhancing the laser scanning confocal microscopic visualisation of lucifer yellow filled cells in whole-mounted tissue. Scanning Microscopy 5(3):619-624.

Bekoff A (1976) Ontogeny of leg motor output in the chick embryo: A neuronal analysis. Brian Research 106:271-291.

Bellinger DL, Anderson WJ (1987a) Postnatal development of cell columns and

their associated dendritic bundles an the lumbosaccral spinal cord of the rat. I. The ventrolateral cell column. Experimental Brain Research 35:55-67.

Bellinger DL, Anderson WJ (1987b) Postnatal development of cell columns and their associated dendritic bundles in the lumbosaccral spinal cord of the rat. II. The ventromedial cell column. Developmental Brain Research 35:69-82.

Bennett MR, Pettigrew AG (1974) The formation of synapses in striated muscle during development. Journal of Physiology 241:515.

Berger AJ, Takahashi T (1990) Serotonin enhances a low-voltage-activated calcium current in rat spinal motoneurones. Journal of Neuroscience 10(6):1922-1928.

Bernstein JJ, Guth L (1961) Nonselectivity in establishment of neuromuscular connections following nerve regeneration in the rat. Exp Neurol 2624:262-275.

Bernstein JJ, Standler NA (1983) Dendritic alteration of rat spinal motoneuornes after dorsal horn mince: Computer reconstruction of dendritic fields. Exp Neurol 82:532-540.

Berry M, Bradley P (1976a) The application of network analysis to the study of branching patterns of large dendritic fields. Brian Research 109:111-132.

Berry M, Bradley P (1976b) The growth of the dendritic trees of Purkinje cells in irradiated agranular cerebellar cortex. Brian Research 116:361-387.

Berry M (1980) Dendritic growth and the control of neuronal form. Current Topics in Developmental biology 15:67-102.

Berry M, McConnel P, Sievers J (1980) Dendritic growth and the control of neuronal form. Current Topics in

Betz H, Bourgeois J-P, Changeux J (1980) Evolution of cholinergic proteins in developing slow and fast skeletal muscles in chick embryo. Journal of Physiology 302:265-279.

Black JA, Foster RE, Waxman SG (1982) Rat optic nerve: freeze-fracture studies during development of myelinated axons. Brian Research 250:1-20.

Bondok AA, Sansone FM (1984) Retrograde and transganglionic degeneration of sensory neurones after a peripheral lesion at birth. Exp Neurol 86:522-530.

Borke RC (1983) Intrasomatic changes in the maturing hypoglossal nucleus after axon injury. Journal of Neurocytology 12:873-883.

Bowe CM, Yu MC, Waxman SG (1988) Morphological changes in spinal motor neurones giving rise to long-term regenerated sciatic nerve axons. Brian Research 463:69-77.

Bowe CM, Hildebrand C, Kocsis JD, Waxmann SG (1989) Morphological and physiological properties of neurones after long-term axonal regeneration: observtions on chronic and delayed sequelae of peripheral nerve injury. Journal of Neurological Sciences 91:259-292.

Bowe CM, Evans NH, Vlacha V (1992) Progressive morphological abnormalities

observed in rat spinal motor neuorns at extended intervals after axonal regeneration. J Comp Neurol 321:576-590.

Bowker RM, Steinbruch HWM, Coulter JD (1981) Serotonergic and peptidergic projection to the spinal cord demonstrated by a combinedretrograde HRP hisochemical and immunocytochemical staining method. Brian Research 21:412-417.

Bowker RM, Westlund KN, Sullivan MC, Wilbur JF, Coulter JD (1983) Descending serotonergic peptidergic and cholinergic pathways from the raphe nuclei: a multple transmitter complex. Brian Research 288:33-48.

Bowker RM (1986) Serotonergic and peptidergic inputs to the primate ventral spinal cord as visualized with multiple chromagens on the same tissue section. Brian Research 375:345-350.

Bowker RM, Abbott LC (1990) Quantitative re-evaluation of descending serotinergic and non-serotinergic projections from the medulla of the rodent: evidence for co-existence of serotonin and peptides in the same spinally projecting neurones, but not from the nucleus raphe magnus. Brian Research 512:15-25.

Boyde A (1992) Three- dimensional inages of Ramon y Cajal's origional preparations, as viewed by confocal microscopy. Trends Neurosci 15(7):246-248.

Brannstrom T, Havton L, Kellerth JO (1992a) Changes in size and dendritic arborization patterns of adult cat a-motoneurones following permanent axotomy. J Comp Neurol 318:439-451.

Brannstrom T, Havton L, Kellerth JO (1992b) Restorative effects of reinnervation on the size and dendritic arborization patterns of axotomized cat spinal a-motoneurones. J Comp Neurol 318:452-461.

Braun K, Schachner M, Scheich H, Heizmann CW (1986) Cellular localization of the Ca++-binding protein parvalbumin in the developmental avian cerebellum. Cell and Tissue Research 243:69-78.

Bray D (1970) Surface movements during growth of single explanted neurones. Proc Natl Acad Sci USA 65:905-910.

Bray D (1973a) Model for membrane movements in the neuronal growth cone. Nature 244:93-96.

Bray D (1973b) Branching patterns of individual sympathetic neurones in culture. Journal of Cell Biology 56:702-712.

Bray D, Bunge MB (1973) Ciba Foundaton Symposium: The growth cone in neurite extension. Amsterdam: Ciba Foundation.

Bray D, Thomas C, Shaw G (1978) Growth cone formation in cultures of sensory neurones . Proc Natl Acad Sci USA 81:5626-5629.

Bray D (1982) Cell Behaviour. Cambridge: C.U.P..

Bregman BS, Goldberger ME (1982) Anatomical plasticity and sparing of function after spinal cord damage in newborn and adult cats. Science 217:553-555.

Bregman BS (1987) Development of serotonin immunoreactivity in the rat spinal cord and its plasticity after spinal cord lesions. Developmental Brain Research 34:245-263.

Brenneman DE, Neale EA, Habig WH, Bowers LM, Nelson PG (1983) Developmental and neurochemical specificity of neuronal deficits produced by electrical impulse blockade in dissociated spinal cord cultures. Developmental Brain Research 9:13-27.

Brenneman DE, Forsythe ID, Nicol T, Nelson PG (1990) N-methyl-D-aspartate receptors influence neuronal survival in developing spinal cord cultures. Developmental Brain Research 51:63-68.

Brown AG, Fyffe RE (1981) Direct observations on the contact made between Ia afferent fibres and a-motoneurones in the cat's lumbosaccral spinal cord. Journal of Physiology 313:121-140.

Brown MC, Butler RG (1976) Regeneration of afferent and efferent fibres to muscle spindles after nerve injury in adult cats. Journal of Physiology 260:253-266.

Brown MC, Jansen JKS, Van Essen D (1976) Polyneuronal innervation of skeletal muscle in new-born rats and its elimination during maturation. Journal of Physiology 261:387-422.

Buhl EH, Lubke J (1988) Intracellular lucifer yellow injection in fixed brain slices combined with retrograde tracing, light and electron microscopy. Neuroscience 28:3-16.

Bunge MB (1977) Initial endocytosis of peroxidase or ferritin by growth cones of cultured nerve cells. Journal of Neurocytology 6:407-439.

Burke RE (1967) Composite nature of the monosynaptic excitatory postsynaptic potential. J Physiol 30:1114-1137.

Burke RE, Walmsley B, Hodgson JA (1979) HRP anatomy of group Ia afferent contacts on alpha motoneurones. Brian Research 160:347-352.

Burke RE (1981) Motor units: anatomy, physiology and functional organisation. In: (Brookes VB ed), pp 345-422. Bethesda: Amer. Physiol. Soc..

Burke RE, Dum RP, Fleshman JW, Glenn LL, Lev-Tov A, O'Donovan MJ, Pinter MJ (1982) An HRP study of the relation between cell size and motor unit type in cat ankle extensor motoneurons. J Comp Neurol 209:17-28.

Burls A, Krishnan S, Lowrie MB, Vrbová G (1991) Absence of nerve-muscle interaction influences the survival of developing motoeurones. European Journal of Neuroscience 3:216-221.

Callaway JH, Soha JM, Van Essen D (1987) Competition favouring inactive over active motor neurons during synapse elimination. Nature 328:422-426.

Cameron WE, Averill DB, Berger AJ (1983) Morphology of cat phrenic motoneurones as revealed by intracellular injection of HRP. J Comp Neurol 219:70-80.

Cameron WE, Averill DB, Berger AJ (1988) Quantitative analysis of the dendritic tree of cat phrenic motoneurones stained intracellularly with horseradish peroxidase. J Comp Neurol 230:91-101.

Cameron WE, Fang H (1989) Morphology of developing motoneurones innervating the medial gastrocnemius of the cat. Developmental Brain Research 49:253-263.

Cameron WE, Fang H, Brozanski BS, Guthrie RD (1989) The postnatal growth of motoneurones at three levels of the cat neuraxis. Neuroscience Letters 104:274-280.

Cameron WE, Brozanski BS, Guthrie RD (1990) Postnatal development of phrenic motoneurones in the cat. Developmental Brain Research 51:142-145.

Cameron WE, Kalipatnapu P, Jodkowski JS, Guthrie RD (1991) Morphometric analysis of phrenic motoneurones in the cat during postnatal development. J Comp Neurol 314:763-776.

Carlson J, Lias AC, Dyck PJ (1979) Axonal atrophy from permanent peripheral axotomy in adult cat. Journal of Neuropathology and Experimental Neurology 38:579-585.

Cavanaugh MW (1951) Quantitative effects of the peripheral innervation area on nerves and spinal ganglion cells. J Comp Neurol 94:181.

Celio MR (1990) Calbindin D-28k and parvalbumin in the rat nervous system. Neuroscience 35(2):375-475.

Cerf JA, Chako LW (1958) Retrograde reaction in motoeurone dendrites following ventral root section in the frog. J Comp Neurol 109:205-220.

Chang TPO, Reese TS (1986) Polarised compartmentalization of organelles in growth cones from developing optic tectum. Journal of Cell Biology 85:1473-1480.

Chen EW, Chui AY (1992) Early stages in the development of spinal motor neuornes. J Comp Neurol 320:291-303.

Chen S, Hillman DE (1982) Marked reorganization of Purkinje cell dendrites and spines in adult rat following vacating of synapses due to deafferentation. Brian Research 245:131-135.

Chevalier A (1978) Etude de la migration des celles somatiques dans le mesoderm somatopleural de l'ebauche del'aile. Roux's Archive of Developmental Biology 184:57-73.

Chimykhova NM, Karamin OA, Kozhanov VM (1991) Sensorimotor connections in the lumbar spinal cord of the young rat: a morphological study. Neuroscience 43:569-576.

Cho EYP, So K-F (1992) Characterization of the sprouting response of axon-like processes from retinal ganglion cells after axotomy in adult hamsters: a model using intravitreal implantation of a peripheral nerve. Journal of Neurocytology 21:589-603.

Choi DW (1985) Glutamate neurotoxicity in cortical cell culture is calcium dependant. Neuroscience Letters 58:293-297.

Choi DW (1987) Ionic dependance of glutamate neurotoxicity in cortical cell culture. Journal of Neuroscience 7:369-379.

Choi DW (1988) Glutamate neurotoxicity and diseases of the nervous system. Neuron 1:623-634.

Choi DW (1992a) Bench to bedside: The glutamate connection. Science 258:241-243.

Choi DW (1992b) Excitotoxic cell death. Journal of Neurobiology 23:1261-1276.

Christie G (1964) Developmental stages in somite and post-somite rat embryos, based on external appearence, and including some features of the macroscopic developmental oral cavity. J Morphol 114:263-280.

Chu-Wang IW, Oppenheim RW (1978) Cell death of motoneurones in the chick embryo spinal cord. I. Light and electron microscopic study of naturally occuring and induced cell loss duing development. J Comp Neurol 177:33-58.

Chung K, Coggeshall RE (1984) The postnatal development of the tract of Lissauer in the rat. J Comp Neurol 229:471-475.

Chymkhova NM, Karamin OA, Kozhanov VM (1991) Sensorimotor conections in the lumbar spinal cord of the young rat: a morphological study. Neuroscience 43:569-576.

Clowry GJ, Dekkers J, Navarrete R (1991) Effect of neonatal motoneurone axotomy on serotonergic innervation in the rat lumbar spinal cord. Abstracts of the 14th Annoal Meeting of the European Neuroscience Association 3143.

Connold AL, Evers JO, Vrbová G (1986) Effect of low calcium and protease inhibitors on synapse elimination during postnatal development in the rat soleus muscle. Developmental Brain Research 28:99-107.

Connold AL, Fisher TJ, Maudarbocus S, Vrbová G (1992) Response of developing rat fast muscles to partial denervation. Neuroscience 46:981-988.

Conradi S, Skolglund S (1969) Observations on the ultrastructure of the initial motor axon segment and dorsal root boutons on the motoneurons in the lumbosacral spinal cord of the cat during postnatal development. Acta Physiologica Scandinavia 333:53-79.

Conradi S, Ronnevi L-O (1975) Spontaneous elimination of synapses on cat spinal motoneuornes after birth: do half of the synapses on the cell bodies disappear? Brian Research 92:505-510.

Conradi S, Ronnevi L-O (1977) Ultrastructure and synaptology of the initial axon segment of cat spinal motoneurones during early postnatal development. Journal of Neurocytology 6:195-210.

Conradi S, Cullheim S, Gollvik L, Kellerth JO (1983) Electron microscopic ob-

servations on the synaptic contacts of group 1a muscle spindle afferents in the cat lumbosacral spinal cord. Brian Research 265:31-39.

Cragg BG, Thomas PK (1961) Changes in conduction velocity and fibre size proximal to peripheral nerve lesions. Journal of Physiology 157:315-327.

Crews L, Wigston DJ (1990) The dependance of motoneurones on their muscle during postnatal development of the mouse. Journal of Neuroscience 10(5):1643-1653.

Croall DE, Demartino GN (1991) Calcium-activated neutral protease (calpain) system: structure, function nad regulation . Physiological Review 71:813-847.

Cullheim S, Kellerth JO, Conradi S (1977) Evidence for direct synaptic interconnections between cat spinal a-motoneurones via the recurrent axon collateral: a morphological study using intracellular injection of horseradish peroxidase. Brian Research 132:1-10.

Cullheim S (1978) Relations between cell body size, axon diameter and axon conduction velocity of cat sciatic a-motoneurones stained with horseradish peroxidase. Neuroscience Letters 8:17-20.

Cullheim S, Ulfhake B (1979a) Relations between cell body size, axon diameter and axon conduction velocity of triceps surae alpha motoneurones during postnatal development. J Comp Neurol 188:679-686.

Cullheim S, Ulfhake B (1979b) Observations on the morphology of intracellularly stained gamma-motoneurones in relation to their axon conduction velocity. Neuroscience Letters 13:47-50.

Cullheim S, Lipsenthal L, Burke RE (1984) Direct monosynaptic contacts between type-identified alpha-motoneurones in the cat. Brian Research 308:196-199.

Cullheim S, Ulfhake B (1985) Postnatal changes in the termination pattern of recurrent axon collaterals of triceps surae a-motoneurones in the cat. Developmental Brain Research 17:63-73.

Cullheim S, Fleshman JW, Glenn LL, Burke P (1987a) Membrane area and dendritic structure in type-identified triceps surae a-motoneurones. J Comp Neurol 255:68-81.

Cullheim S, Fleshman JW, Glenn LL, Burke RE (1987b) Three-dimensional architecture of dendritic trees in type-identified alpha-motoneurones. J Comp Neurol 255:82-96.

Cummings JP, Steltzner DJ (1984) Prenatal and postnatal development of lamina IX neurones in the rat thoracic spinal cord. Exp Neurol 83:155-166.

Dahlstrom A, Fuxe K (1964) Evidence for the existence of monoamine-containing neurones in the central nervous system-I. Demonstration of monoamines in the cell bodies of brain stem neurones. Acta Physiologica Scandinavia 62:1-55.

Dekkers J, Becker DL, Navarrete R, Cook JE (1990) A morphological study of developing rat hindlimb flexor motoneuones. Proceedings of the Physiological Society 430:115P.

Dekkers J, Becker DL, Cook JE, Navarrete R (1994) Early postnatal changes in the somatodendritic morphology of ankle flexor motoneurones in the rat. European Journal of Neuroscience 6:87-97.

Delgado-Garcia JM, Del Pozo F, Spencer RF, Baker R (1988) Behaviour of neurons in the abducens nucleus of the alert cat - III. Axotomised neurones. Neuroscience 24(1):143-160.

Dennis MJ, Ziskind-Conhaim L, Harris AJ (1981) Development of neuromuscular junctions in rat embryos. Developmental Biology 81:266-279.

Detwiler SR (1936) Neuroembryology: An experimental study. New York: Macmillan.

Diamond J, Miledi R (1962) A study of foetal and newborn rat muscle fibres. Journal of Physiology 162:393-408.

Dryden WF, Erulker SD, de la Haba G (1974) Properties of the cell membrane of developing skeletal muscle fibres in culture and its sensitivity to acetlycholine. Clinical and Experimental Pharmacology 1:369-387.

Dunn GA (1982) Cell Behaviour. Cambridge: C.U.P..

Duxon MJ (1982) The effect of postsynaptic block on development of the neuromusccular junction in postnatal rats. Journal of Neurocytology 11:395-408.

Duxon MJ, Vrbová G (1985a) Inhibition of acetylcholinesterase accelerates axon terminal withdrawal. Neuroscience Letters 14:337-363.

Duxon MJ, Vrbová G (1985b) Inhibition of acetylcholinesterase accelerates axon terminal withdrawal. Journal of Neurocytology 14:337-363.

Duxon MJ, Ross JJ, Harris AJ (1986) Transfer of differentiated synaptic terminals from primary myotubes to new-formed muscle cells during embryonic development in rats . Neuroscience Letters 71:147-152.

Eccles JC, Eccles RM, Lundberg A (1957) The convergence of monosynaptic axcitatory afferents onto many different species of alpha-motoneurone. Journal of Physiology 137:22-50.

Eccles JC, Libet B, Young RR (1958) The behaviour of chromatolyzed motoneurones studied by intracellular recording. Journal of Physiology 143:11-40.

Eccles JC, Llinas R, Sasaki K (1966) The excitatory synaptic action of climbing fibres on the Purkinje cells of the cerebellum. Journal of Physiology 182:268-296.

Eide PK, Mjellem N, Hole K (1990) The role of spinal cord 5-HT1a and 5-HT 1b receptors in the modulation of a spinal nociceptive reflex. Brian Research 536:195-200.

Engel AK, Kreutzberg GW (1986) Changes of acetylcholinesterase molecular forms in regenerating motor neurones. Neuroscience 18:467-473.

Engel AK, Kreutzberg GW (1988) Neuronal surface changes in the dorsal vagal

nucleus of the guinea pig in response to axotomy. J Comp Neurol 275:181-200.

Engel AK, Tetzlaff W, Kreutzberg GW (1988) Axonal transport of 16S acetylcholinesterase is increased in regenerating peripheral nerve in guinea pig, but not in rat. Neuroscience 24:729-738.

Ezerman EB, Ishikawa H (1967) Differentiation of the sarcoplasmic reticulum and T-system in developing chick skeletal muscle in vitro. Journal of Cell Biology 35:405-420.

Faber DS, Zottoli SJ (1981) Axotomy-induced changes in cell structure and membrane excitabilty are sustained in a vertebrate central neurone. Brian Research 223:436-443.

Fambrough D, Rash JE (1971) Development of acetylcholine sensitivity during myogenesis. Developmental Biology 26:55-68.

Feasby TE, Bostock H, Sears TA (1981) Conduction in regenerating dorsal fibres. Journal of Neurological Sciences 49:439-454.

Feldman JL, Loewy AD, Speck DF (1985) Projections from the ventral respiratory group to phrenic and intercostal motoneurones in cat: An autoradiographic study. Journal of Neuroscience 5:1993-2000.

Fellous A, Lennon AM, Francon J, Nunez R (1979) Thyroid hormones and neurotube assembly *in vitro* during brain development. European Journal of Biochemistry 101:365-376.

Filogamo G, Gabella G (1967) The development of neuromuscular correlations in vertebrates. Arch Biol 78:9-60.

Fitzgerald M (1985a) The post-natal development of cutaneous afferent fibre input and receptive field organisation in the rat dorsal horn. Journal of Physiology 364:1-18.

Fitzgerald M (1985b) The sprouting of saphenous nerve terminals in the spinal cord following early postnatal nerve section in the rat. J Comp Neurol 240:407-413.

Fitzgerald M, Vrbová G (1985) Plasticity of acid phosphatase (FRAP) afferent terminal fields and of dorsal horn cell growth in the neonatal rat. J Comp Neurol 240:414-422.

Fitzgerald M, Shortland P (1988) The effect of neonatal peripheral nerve section on the somadendritic growth of sensory projection cells in the rat spinal cord. Developmental Brain Research 42:129-136.

Fitzgerald M, Woolf CJ, Shortland P (1990) Collateral srpouting of the central terminals of cutaneous primary afferent neurones in the rat spinal cord: pattern, morphology, and influence of targets. J Comp Neurol 300:370-385.

Fleshman JW, Munson JB, Sypert GW (1981) Homonymous projection of individual group 1a-fibres to physiologically characterized medial gastrocnemious motoneurones in the cat. Journal of Neurophysiology 46:1339-1348.

Foehring RC, Sypert GW, Munson JB (1986) Properties of self-reinnervated mo-

tor units of medial gastrcnemius of cat. II Axotomised motoneurones and the time course of recovery. Journal of Neurophysiology 55(5):947-965.

Francon J, Lennon AM, Fellous A, Pierre M, Nunez R (1982) Heterogeneity of microtubule-associated proteins and brain development. European Journal of Biochemistry 129:465-472.

Frank E, Fischbach GD (1979) Early events in neruomuscular junction formation *in vitro*: induction of ACh receptor clusters in the postsynaptic membrane and morphology of newly formed synapses. Journal of Cell Biology 83:143-158.

Frank E, Westerfield M (1982) Synaptic organization of sensory and motor neurones innervating triceps brachii muscles in the bullfrog. Journal of Physiology 324:479-494.

Frank E, Westerfield M (1983) Development of sensory-motor synapses in the spinal cord of the frog. Journal of Physiology 343:593-610.

Fujita S (1963) The matrix cell cytogenesis in the developing central nervous system. J Comp Neurol 120:37-42.

Fujita S (1966) Application of light and electron microscope autoradiaography to the study of cytogenesis in the fore-brain. In: Evolution of the Forebrain (Harsler R, Stephen H eds), pp 18-196. New York: Plenum Press.

Fulton BP, Walton KD (1986) Electrophysiological properties of neonatal rat motoneurones syudied *in vitro*. Journal of Physiology 370:651-678.

Gharagozloo A, Holohean AM, Hackman JC, Davidoff RA (1990) Serotonin and GABA-induced depolarizations of frog primary afferent fibres. Brian Research 532:19-24.

Gilbert M, Steltzner DJ (1979) The development of descending and dorsal root connections in the lumbosacral cord of the postnatal rat. J Comp Neurol 184:821-838.

Giulian D, Baker TJ (1986) Characterization of amoeboid microglia isolated from developing mammalisn brain. Journal of Neuroscience 6:2163-2178.

Giulian D, Robertson C (1990) Inhibition of mononuclear phagocytes reduces ischemic injury in the spinal cord. Ann Neurol 27:33-42.

Giulian D, Vaca K, Corpuz M (1993) Brain glia release factors with opposing actions upon neuronal survival. Journal of Neuroscience 13:29-37.

Goldberg JI, Mills LR, Kater SB (1991) Novel effects of serotonin on neurite outgrowth in neurons cultured from embryos of *Helisoma triviolis*. Journal of Neurobiology 22(2):182-194.

Goldberger ME, Murray M (1982) Lack of sprouting and its prescence after lesions of the cat spinal cord. Brian Research 241:227-239.

Gordon T, Perry R, Tuffeny AR, Vrbová G (1974) Possible mechanisms determining synapse formation in developing skeletal muscles of the chick. Cell and Tissue Research 155:13-25.

Gordon T, Hoffer JA, Jhamandas J, Stein RB (1980) Long-term effects of axotomy on neural activity during cat locomotion. Journal of Physiology 303:243-263.

Gordon T (1988) To what extent can the normal organization of the motor unit properties be reestablished after muscle reinnervation? In: The current status of peripheral nerve regeneration. New York: Alan R. Liss.

Grafstein B, McQuarrie IG (1979) Neuronal Plasticity. New York: Raven.

Gramsbergen A, IJkema-Paasen J (1984) Early Brain Damage. New York: Academic Press.

Grant G (1965) Degenerative changes in dendrites following axonal transection. Experimentia 21:722-733.

Grant G (1968) Silver impregnation of degenerating dendrites, cells and axons central to axonal transection. II. A Nauta study on spinal motor neurones in kittens. Experimental Brain Research 6:284-293.

Grant G, Westman J (1968) Degenerative changes in dendrites central to axonal transection. Eletron microscopical observations. Experimentia 24:169-170.

Grant G (1975) Retrograde dendritic degeneration. Advances in Neurobiology 12:

Grant G, Ygge J (1981) Somatotopic organization of the thoracic spinal nerve in the dorsal horn demonstrated with transganglionic degeneration. J Comp Neurol 202:357-364.

Greensmith L, Vrbová G (1989) Effect of muscle paralysis on motoneurone survival in neonatal rats. Proceedings of the Physiological Society 148P.

Greensmith L, Vrbová G (1990) Regulation of choline acetlytransferase in developing rat motoneurones. Journal of Physiology 426:59P.

Greensmith L, Hasan HI, Vrbová G (1991) Nerve injury in anaesthetized rats increases the subsequent susceptibility of motoneurones to NMDA-induced neurotoxicity. Journal of Physiology 434:20P.

Greensmith L, Navarrete R (1991) Developmental expression of MHC antigens in the rat spinal cord following neonatal nerve injury. European Journal of Neuroscience Suppl 4:4165.

Greensmith L, Vrbová G (1991) Neuromuscular contacts in the developing rat soleus depend on muscle activity. Developmental Brain Research 62:121-129.

Greensmith L, Dekkers J, Navarrete R (1992) Early changes of parvalbumin-immunoreactive primary afferent fibres in the rat spinal cord following noenatal nerve injury. Society for Neuroscience abstracts IN PRESS:

Gundarsen K (1990) Spontaneous activity at long-term silenced synapses in rat muscle. Journal of Physiology 430:339-418.

Gundersen RW, Barrett JN (1979) Neuronal chemotaxis: Chick dorsal-root ax-

ons turn toward high concentrations of nerve growth factor. Science 206:1079-1080.

Gundersen RW, Barrett JN (1980) Characteristics of the turning reponse of dorsal root neurites towards nerve growth factor. Journal of Cell Biology 87:546-554.

Gustafsson B (1979) Changes in motoneurones passive electrical properties following axotomy. Journal of Physiology 293:197-215.

Gustafsson B, Pinter MJ (1984) Effects of axotomy on the distribution of passive electrical properties of cat motoneurones. Journal of Physiology 356:433-442.

Gutmann E, Young JZ (1944) Reinnervation of muscle after various periods of atrophy. Journal of Anatomy 78:15-43.

Hall GF, Cohen MJ (1988) The pattern of dendritic sprouting and retraction induced by axotomy of lamprey central neurons. Journal of Neuroscience 8:3584-3597.

Hall GF, Poulos A, Cohen MJ (1989) Sprouts emerging from the dendrites of axotomized lampry central neurons have axonlike ultrastructure. Journal of Neuroscience 9:588-599.

Halpain S, Greengard P (1990) activation of NMDA receptors induces rapid dephosphorylation of the cytoskeletal protein MAP2. Neuron 5:237-246.

Hamburger V (1934) The effects of wing bud extirpilation on the development of the central nervous system in chick embryos. J Exp Zool 68:449-494.

Hamburger V (1948) The mitotic patterns in the spinal cord of the chick embryo and their relation to histogenic processes. J Comp Neurol 88:221-284.

Hamburger V, Levi-Montalcini R (1949) Proliferation, differentiation and degeneration in the spinal ganglia of the chick embryo under normal and experimetal conditions. J Exp Zool 111:457-501.

Hamburger V, Balaban M (1963) Observations and experiments on spontaneous rhythmical behaviour in the chick embryo. Developmental Biology 7:533-545.

Hamburger V, Balaban M, Oppenheim RW, Wenger E (1965) Periodic motility of normal and spinal chick embryos between 8 and 17 days of incubation. J Exp Zool 159:1-13.

Hamburger V, Wenger E, Oppenheim RW (1966) Motility in the chick embryo in the absence of sensory input. J Exp Zool 133:160.

Hamburger V (1975) Cell death in the development of the lateral motor columns of the chick embryo. J Comp Neurol 160:535-546.

Hamburger V, Brunso-Bechtold JK, Yip JW (1981) Neuronal death in the spinal ganglia of the chick embryo and its reduction by nerve growth factor. Journal of Neuroscience 1:60-71.

Hamburger V (1992) History of the Discovery of Neuronal death in Embryos.

Journal of Neurobiology 23:1116-1123.

Harris AJ (1981) Embryonic growth and innervation od rat skeletal muscles. I. Neural regulation of muscle fibre numbers. II. Neural regulation of muscle cholinesterase. III. Neural regulation of junctional and extra-junctional acetylcholine receptor clusters. Philos Trans R Soc Lond [Biol] 293:257-314.

Harrison RG (1910) The outgrowth of the nerve fibre as a mode of protoplasmic movement. J Exp Zool 9:787-846.

Havton L, Kellerth JO (1984) Retrograde effects of axotomy on the intramedullary axon collateral systems and recurrent inhibitory reflexes of cat spinal motoneurones. Neuroscience Letters 52:13-17.

Havton L, Kellerth JO (1987) Regeneration by supernumery axons with synaptic terminals in spinal motoneurones of cats. Nature 325:711-714.

Havton L, Kellerth JO (1989) A physiological study of the monosynaptic reflex responses of cat a-motoneurones following peripheral nerve injury. Experimental Brain Research 488:149-162.

Havton L, Kellerth JO (1990a) Plasticity of recurrent inhibitory reflexes in cat spinal motoneurones following peripheral nerve injury. Experimental Brain Research 79:75-82.

Havton L, Kellerth JO (1990b) Elimination of intramedullary axon collaterals of cat spinal a-motoneurones following peripheral nerve injury. Experimental Brain Research 79:65-74.

Haydon PG, McCobb DP, Kater SB (1987) The regulation of neurite outgrowth growth cone motility and electrical synaptogenisis by serotonin. Journal of Neurobiology 18:197-215.

Heizmann CW, Röhrenbeck J, Kamphuis W (1990) Parvalbumin, molecular and functional aspects. Adv Exp Med Biol 269:57-66.

Heizmann CW, Braun K (1992) Changes in Ca2+-binding proteins in human neurodegenerative disorders. Trends Neurosci 15(7):259-264.

Henkel CK, Brunso-Bechtold JK (1991) Dendritic morphology and development in the ferret lateral superior olivary nucleus. J Comp Neurol 313:259-272.

Henneman E (1957) Relation between size of neurones and their susceptibility to discharge. Science 126:1345-1346.

Henneman E, Somjen G, Carpenter DO (1965) Functional significance of cell size in spinal motoneurones. Journal of Neurophysiology 28:560-580.

Henneman E (1979) Functional organization of motoneurone pools: the size-principal. In: Integration in the Nervous System (Asanuma H, Wilson VJ eds), Tokyo: Igaku-Shoin.

Henrikson CK, Vaughn JE (1974) Fine structural relationship between neurites and radial glial processes in developing mouse spinal cord. Journal of Neurocytology 3:659-675.

Hevner RF, Wong-Riley MTT (1990) Regulation of cytochrome oxidase protein levels by functional activity in the macaque monkey visual system. Journal of Neuroscience 10:1331-1340.

Hicks SP, D'Amato CJ (1975) Motor-sensory cortex-corticospinal system and developing locomotion and placing in rats. Am J Anat 143:1:1-42.

Himes BT, Tessler A (1989) Death of some dorsal root ganglion neuones and plasticity of others following sciatic nerve section in adult and neonatal rats. J Comp Neurol 284:215-230.

Hinds JW, Hinds PL (1972) Reconstruction of dendritic growth cones in neonatal mouse olfactory bulb. Journal of Neurocytology 1:169-187.

Hoffman PN, Lasek RJ (1975) The slow component of axonal transport. Identification of major structural polypeptides of the axon and their generality among mammalian neurones. Journal of Cell Biology 66:351-366.

Hoffman PN, Cleveland JW, Griffin PW, Cowan NJ, Price DL (1987) Neurofilament gene expression: a major determinant of axonal caliber. Proc Anat Soc 84:3471-3476.

Hohlfield R, Sterz RA, Peper K (1981) Prejunctional effects of anticholinesterase drugs at the endplate. Mediated by presynaptic acetlycholine receptors or by postsynaptic potassium efflux? Pflugers Arch 391:213-218.

Holland PC, MacLennan DH (1976) Assembly of the sarcoplasmic reticulum. Biosynthesis of adenosine triphosphate in rat skeletal muscle cell culture. Journal of Biochemistry 251:2030-2036.

Hollyday M, Hamburger V (1976) Reduction of the naturally occuring motor neuron loss by enlargement of the periphery. J Comp Neurol 170:311-320.

Hollyday M, Hamburger V (1977) An autoradiographic study of the formation of the lateral motor column in the chick embryo. Brian Research 132:197-208.

Hollyday M, Hamburger V, Farris JMG (1977) Localization of motor neuron pools supplying identified muscles in normal and supernumerary legs of chick embryo. Proc Natl Acad Sci USA 74:3582-3586.

Holstege JC, Kuypers HJM (1987a) Brainstem projections to lumbar motoneurones in rat-I. An ultrastructural study using autoradiography and the combination of autoradiography and horseradish peroxidase histochemistry. Neuroscience 21:345-367.

Holstege JC, Kuypers HJM (1987b) Brainstem projections to spinal motoneurones: an update. Neuroscience 23:809-821.

Holstege JC, Kuypers HJM (1987c) The anatomy of brain stem pathways to the spinal cord in cat. A labelled amino acid tracing study. In: Descending Pathways th the Spinal Cord. Progress in Brain Researh (Kuypers HGJM, Martin GF eds), pp 145-175. Amsterdam: Elsevier.

Holtzner H, Marshal J, Fick H (1957) An analysis of myogenesis by the use of fluorescent antimyosin. Journal of Biophysics,Biochemistry and Cytology 3:705-724.

Holtzner H (1959) Some further uses of antibobies for analysing the structure and development of muscle. Experimental Cell Research 7:234-243.

Holtzner H, Sanger JW (1972) Research in muscle development and the muscle spindle. Excerpta Medica, International congress series.

Homma S, Sako H, Kohno K, Okado N (1988) The pattern of distribution of serotonergic fibres in the anterior horn of the chick embryo spinal cord. Anatomy and Embryology 179:25-31.

Honig MG, Hume RI (1989) DiI and DiO: versatile fluorescent dyes for neuronal labelling and pathway tracing. Trends Neurosci 9:333-335.

Hubel DH, Weisel TN (1962) Receptive fields, binocular interaction and functional architecture of the cat's striate cortex. Journal of Physiology 160:106-154.

Hubel DH, Weisel TN (1963) Receptive fields of cells in striate cortex of very young, visually inexperienced kittens. Journal of Neurophysiology 26:994-1002.

Hubel DH, Weisel TN, LeVay S (1977) Plasticity of ocular dominance columns in the monkey striate cortex. Philos Trans R Soc Lond [Biol] 275:377-409.

Hudson G, Lazarow A, Hartman JF (1961) A quantitative electron microscopic study of mitochondria in motor neurones following axonal section. Experimental Cell Research 24:440-456.

Hulsebosch CE, Coggeshall RE, Chung K (1986) Numbers of rat dorsal root axons and ganglion cells during postnatal development. Developmental Brain Research 26:105-113.

Hume RI, Role LW, Fischbach GD (1983) Acetylcholine release from growth cones detected with patches of acetylcholine receptor-rich membranes. Nature 305:632-634.

Hylden JLK, Hayashi H, Ruda MA, Dubner R (1986) Serotonin innervation of physiologically identified lamina 1 projection neurones. Brian Research 370:401-404.

Iansek R, Redman SJ (1973) The amplitude, time course and charge of unitary post-synaptic potentials evoked in spinal motoneurone dendrities. J Physiol 234:665-688.

Innoceti GM, Clarke s, Koppel H (1983) Transitory macrophages in the white matter of the developing visual cortex. II. development and relations with axonal pathways. Developmental Brain Research 11:55-66.

Ishida I, Deguchi T (1983) Effect of depolarizing agents on choline acetly transferase and acetlycholinesterase activities in primary cell cultures of spinal cord. Journal of Neuroscience 3:1818-1823.

Ishizka N, Mannen H, Hongo T, Sasaki S (1979) Trajectory of group Ia afferent fibres stained with horseradish peroxidase in the lumbosacral spinal cord of the cat: Three dimensional reconstructions from serial sections. J Comp Neurol 186:189-212.

Iwahara T, van Hartesveldt C, Garcia-Rill E, Skinner RD (1991) L-DOPA-induced air-stepping in decerebrate developing rats. Developmental Brain Research 58:257-264.

Izzard CS, Lochner LR (1976) Cell-to-substrate contacts in living fibroblasts: An interference reflection study with an evaluation of the technique. J Cell Sci 21:129-159.

Jackson C, Frank E (1987) Development of synaptic connections between muscle sensory and motor neurones: Anatomical evidence that postsynaptic dendrites grow into a preformed sensory neuropil. J Comp Neurol 255:538-547.

Jackson PC, Diamond J (1981) Regenerating axons reclaim sensory targets from collateral nerve sprouts. Science 214:926-928.

Jacobson M (1970) Histogenesis and morphogenesis of the nervous system. In: Developmental Neurobiology (pp 1-64. New York: Holt, Rinehart, Winston.

Jacobson M (1982) Neuronal Development. New York: Plenum Press.

Jaffe LF (1979) Membrane Transduction Mechanisms. New York: Raven Press.

Jaffe LF (1981) The role of ionic currents in establishing developmental pattern. Philos Trans R Soc Lond [Biol] 295:553-566.

Jankowska E, Lindstrom A (1972) Morphology of interneurones mediating 1a reciprocal inhibition of motoneurones in the spinal cord of the cat. J Biochem Tokyo 226:805-823.

Jaramillo F, Vicini S, Schuetze SM (1988) Embryonic acetylcholine receptors guarantee spontaneous contractions in rat developing muscle. Nature 335:66-68.

Johnson IP, Sears TA (1989a) Ultrastructure of axotomized alpha and gamma motoneurones in the cat thoracic spinal cord. Neuropathol Appl Neurobiol 15:149-163.

Johnson IP, Sears TA (1989b) Organelle changes in cat thoracic a- and g-motoneurones following axotomy. Brian Research 489:400-405.

Johnson KE (1969) Altered contact behaviour of presumptive mesodermal cells from hybrid amphibian embryos arrested in development. J Exp Zool 170:325-332.

Johnson KE (1970) The role of changes in cell contact behaviour in amphibian gastrulation. J Exp Zool 175:391-428.

Jones S,L., Light AR (1990) Termination patterns of serotinergic medullary raphespinal fibres in the rat lumbar spinal cord: an anterograde immunohistochemical study. J Comp Neurol 297:267-282.

Jones SI, Light AR (1992) Serotonergic medullary raphespinal projection to the lumbar spinal cord in the rat: a retrograde immunohistochemical study. J Comp Neurol 322:599-610.

Kalb RG, Lidow M, Halsted MJ, Hochfield S (1992) N-methyl-D-aspartate receptors are transiently expressed in the developing spinal cord ventral horn. Proc Natl Acad Sci USA 89:8502-8506.

Kashihara Y, Kuno M, Miyata Y (1987) Cell death of axotomized motoneurones in neonatal rats, and its prevention by peripheral reinnervaion. Journal of Physiology 386:135-148.

Kater SB, Mattson MP, Cohan C, Connor J (1988) Calcium regulation of the neuronal growth cone. Trends Neurosci 11(7):315-321.

Kerai B, Greensmith L, Vrbová G, Navarrete R (1993) Effect of transient neonatal paralysis on soleus motoneurone growth in the rat. Journal of Physiology 467:111P.

Kernell D, Zwaagstra B (1981) Input conductance, axonal conduction velocity and cell size among hindlimb motoneurones of the cat. Brian Research 204:311-326.

Kerns JM, Peters A (1974) Ultrastructure of a large ventro-lateral dendritic bundle in the rat ventral horn. Journal of Neurocytology 3:533-555.

Krishnan S, Lowrie MB, Vrbová G (1985) The effect of reducing the peripheral field on motoneurone development in the rat. Developmental Brain Research 19:11-20.

Kudo N, Yamada T (1987) Morphological and physiological studies of development of the monosynaptic reflex pathway in the rat lumbar spinal cord. Journal of Physiology 389:441-459.

Kudo N, Furukawa F, Okado N (1993) Development of descending fibres to the rat embryonic spinal cord. Neuroscience Research 16:131-141.

Kuno M, Llinas R (1970a) Alterations of synaptic action on chromatolysed motoneruones in the cat. Journal of Physiology 210:823-838.

Kuno M, Llinas R (1970b) Enhancement of synaptic transmission by dendritic potentials in chromatolyzed motoneurones of the cat. Journal of Physiology 210:725-739.

Kuno M, Miyata Y, Munoz-Martinez EJ (1974) Differential reactions of fast and slow alpha motoneurones to axotomy. Journal of Physiology 240:725-739.

Kuno M (1990) Target dependence of motoneuronal survival: the current status. Neuroscience Research 9:155-172.

Lagerback PA, Ulfhake B (1987) Ultrastructural observations on beaded a-motoneurone dendrites. Acta Physiol Scand 129:61-66.

Lance-Jones C, Landmesser LT (1980a) Motoneurones projection patterns in chick hind limb following partial reversals of the spinal cord. Journal of Physiology 302:581-602.

Lance-Jones C, Landmesser LT (1980b) Motoneurone projection patterns in embryonic chick limbs following partal deletions in the spinal cord. Journal of Physiology 302:559-580.

Lance-Jones C, Landmesser LT (1981a) Pathway selection by chick lumbrosacral motoneurones during normal development. Proceedings of the Royal Society of London B 214:1-18.

Lance-Jones C, Landmesser LT (1981b) Pathway selection by embryonic chick motoneuornes in an experimentally altered environment. Proceedings of the Royal Society of London B 214:19-52.

Landis SC (1983) Neuronal growth cones. Annu Rev Physiol 45:567-580.

Landmesser LT, Pilar G (1974) Synaptic transmission and cell death during normal ganglionic development. Journal of Physiology 241:737-749.

Landmesser LT (1978) The development of motor projection patterns in the chick hind limb. Journal of Physiology 284:391-414.

Landmesser LT, O'Donovan MJ (1984) activation patters of embryonic chick hind limb muscles recorded in ovo and in an isolated spinal cord preparation. Journal of Physiology 347:189-204.

Lau KC, So K-F, Tay D, Jen LS (1991) Elimination of transient dendritic spines in ipsilaterally projecting retinal ganglion cells in rats with neonatal unilateral thalamotomy. Neuroscience Letters 121:255-258.

LaVelle A, LaVelle FW (1958) Neuronal swelling and chromatolysis as influenced by the state of cell development. Am J Anat 102:219-241.

LaVelle A, Sechrist JW (1970) Immature and mature reaction patterns in neurons after axon section. Anatomical Record 166:335.

LaVelle A (1973) Levels of maturation and reactions to injury during neuronal development. Progress in Brain Research 40:162-166.

Lee MT, O'Donovan MJ (1991) Organization of hindlimb muscle afferent projections to lumbosacral motoneuones in the chick embryo. Journal of Neuroscience 11:2564-2573.

Letourneau PC (1981) Immunocytochemical evidence for colocalization in neruite growth cones of actin and myosin and their relationship to cell-substratum adhesion. Developmental Biology 85:113-122.

Letourneau PC (1982) Neuronal Development. New York: Plenum Press.

Letourneau PC, Ray PN, Bernfield MR (1982) Biological regulation and development. New York: Plenum Press.

Letterier JF, Shelanski M (1982) Interactions between neurofilaments and microtubule-associated proteins: A possible mechanism for intra-organelle bridging. Journal of Cell Biology 95:982-986.

Leuba G, Garey LJ (1984) Development of dendritic patterns in the geniculate nucleus of the monkey: a quantitive Golgi study. Developmental Brain Research 16:285-299.

Levi-Montalcini R (1972) Immunosympathectomy. Amsterdam: Elsevier.

Levitt P, Rakic P (1980) Immunoperoxidase localization of glial fibrially acidic protein in radial glial-cells and astrocytes of the developing rhesus-monkey brain. J Comp Neurol 193:815-840.

Lewin GR, Winter J, McMahon SB (1992) Regulation of afferent connectivity in the adult spinal cord by nerve growth factor. European Journal of Neuroscience 4:700-707.

Lewis SA, Lee M, Cowan NJ (1985) Five mouse tubulin isotypes and their regulated expression during development. Journal of Cell Biology 101:852-861.

Lichtman JW, Purves D (1980) The elimination of redundant perganglionic innervation to hamster sympathetic ganglion cells in early post-natal life. Journal of Physiology 301:213-228.

Lieberman AR (1971) The axon reaction: A review of the principal features of perikaryal responses to injury. Int Rev Neurobiol 14:49-124.

Lieberman AR (1974a) Essays on the Nervous Sysytem. Clarendon Press.

Lieberman AR (1974b) Some factors affecting neuronal responses to axonal lesions. In: Essays on the Nervous System (Bellairs R, Gray E,G. eds), pp 71-105. Oxford: Clarendon Press.

Linda H, Risling M, Cullheim S (1985) 'Dendraxons' in regenerating motoneurones in the cat: do dendrites generate new axons after central axotomy? Brian Research 358:329-333.

Linda H, Bergstrand A, Cullheim S, Risling M (1990a) Changes in synaptic input on cat spinal motoneurones following an intramedullar axotomy. Abstracts of the 13th Annual Meeting of the European Neuroscience Association 3:3221.

Linda H, Cullheim S, Risling M (1990b) Changes in synaptic input on cat spinal motoneurones following an intracellular axotomy. European Neuroscience Association Abstracts 3:3221.

Lindsay HA, Barr ML (1955) Further observations on the behaviour of nuclear structures during depletion and restoration of nissl material. Journal of Anatomy 89:47-62.

Ling EA, TAn CK (1974) Amoeboid microglial cells in the corpus callosum of neonatal rats. Arch Histol Japn 36:265-280.

Lipton SA, Kater SB (1989) Neurotransmitter regulation of neuronal outgrowth, plasticity and survival. Trends Neurosci 12(7):265-270.

Llinas R, Sugimori M (1979) Calcium conductances in Purkinje cell dendrites: their role in development and integration. Progress in Brain Research 51:323-334.

Llinas R (1988) The intrinsic electrophysiological properties of mammalian neurones: insights into central nervous system function. Science 242:1654-1664.

Lowrie MB, Krishnan S, Vrbová G (1982) Recovery of slow and fast muscles following nerve injury during early postnatal development in the rat. Journal of

Physiology 331:51-66.

Lowrie MB, Krishnan S, Vrbová G (1987) Permanent changes in muscle and motoneurones induced by nerve injury during a critical period of development of the rat. Developmental Brain Research 31:91-101.

Lowrie MB, Vrbová G (1992) Dependence of postnatal motoneurones on their targets: reveiw and hypothesis. Trends Neurosci 3:80-84.

Lund RD (1978) Development and plasticity of the brain. New York: Oxford University Press.

Luscher H-R, Ruenzel P, Henneman E (1980) Topographic distribution of terminals of 1A and group II fibres in spinal cord, as revealed by postsynaptic population potentials. Journal of Neurophysiology 43(4):965-985.

Luscher H-R, Clamann HP (1992) Relation between structure and function in information transfer in spinal monosynaptic reflex. Physiological Review 72:71-95.

Lux HD, Schubert P (1975) some aspects of the electroanatomy of dendrites. Advances in Neurology 12:29-44.

Maehlen J, Nennesmo I, Olsson T, Schroder HD, Kristensson K (1989) Peripheral nerve injurt causes transient expression of MHC class I antigens in rat neurones and skeletal muscles. Brian Research 481:368-372.

Manabe T, Araki I, Takahashi T, Kuno M (1991) Membrane currents recorded from sexually dimorphic motoneurones ofthe bulbocavenosus muscle in neonatal rats. Journal of Physiology 440:419-435.

Manthorpe M, Skaper SD, Williams LR, Varon S (1986) Purification of adult rat sciatic nerve ciliary neurotrophic factor. Brian Research 367:282-286.

Mariani J, Changeux J (1981) Ontogenesis of olivocerebellar relationships. I. Studies by intracellular recordings of the multiple innervation of Purkinje cells by climbing fibres in the developing rat cerebellum. Journal of Neuroscience 1:696-702.

Martin GF, Ghooray G, Ho RH, Pindzola RR, Xu XM (1991) The origin of serotoninergic projections in the lumbosacral spinal cord at different stages of development in the North American opossum. Developmental Brain Research 58:203-213.

Mates SL, Lund JS (1982) Spine formation and maturation of type 1 synapses on spiny stellate neurones in primate visual cortex. J Comp Neurol 221:91-97.

Matsumoto A, Arnold AP, Micevych PE (1989) Gap junctions between lateral spinal motoneurones in the rat. Brian Research 495:362-366.

Mattson MP, Kater SB (1987) Calcium regulation of neurite elongation and growth cone motility. Journal of Neuroscience 7(12):4034-4043.

Matus A, Bernhardt R, Bodmer R (1986) Microtubule-associated protein 2 and tubulin are differnetly distributed in dendrites of developing neurones. Neuroscience 17:371-389.

Matus A (1987) The Making of the Nervous System. Oxford: O.U.P..

Matus A (1988) Microtubule associated proteins: Their potential role in determining neuronal morphology. Annual Review of Neuroscience 11:29-44.

Matus A (1990) Microtubule-associated proteins. Current Opinion in Cell Biology 2:13-14.

Mazza E, Nunez-Abades PA, Spielmann JM, Cameron WE (1992) Anatomical and electrotonic coupling in developing genioglossal motoneurones of the rat. Brian Research 598:127-137.

McCobb DP, Best PM, Beam KG (1989) Development alters the expression of calcium currents in chick limb motoneurones. Neuron 2:1633-1643.

McCobb DP, Best PM, Beam KG (1990) The differentiation of excitability in embryonic chick limb motoneurones. Journal of Neuroscience 10:2974-2984.

McGreer PL, Itagaki S, Tago H, McGreer EG (1987) Reactive microglia in patients with senile dementia of the Alzheimer type are postitive for the histocompatibility glycoprotein HLA-DR. Neuroscience Letters 79:195-200.

Mendell LM, Henneman E (1971) Terminals of single 1a fibres: Location, density and distribution within a pool of 300 homonymous motoneurones. Journal of Neurophysiology 34:171-187.

Mendell LM, Munson JB, Scott JG (1974) Connectivity changes of Ia afferents on axotomized motonerones. Developmental Brain Research 73:338-342.

Mendell LM, Munson JB, Scott JG (1976) Alterations of synapses on axotomized motoneurones. Journal of Physiology 255:67-79.

Mentis GZ, Greensmith L, Vrbová G (1993) Motoneurones destined to die are rescued by blocking *N*-methyl-D-aspartate receptors by MK-801. Neuroscience 54:283-285.

Miletic V, Hoffert MJ, Ruda MA, Dubner R (1984) Serotonergic axonal contacts on identified cat spinal dorsal horn neurones and their correlation with nucleus raphe magnus stimulation. J Comp Neurol 228:129-141.

Miller HW, Tetzlaff W, Naus CCG, Bisby MA, Bloom FE, Milner RJ (1987) The differential expression of a-tubulin genes during neuronal development is reiterated during neuronal regeneration. Abstr Soc Neurosci 13:1706.

Molander C, Kinnman E, Aldskoguis H (1988) Expansion of spinal cord sensory afferent projection following combined sciatic nerve crush. J Comp Neurol 276:436-441.

Morest DK (1968) Growth of cerebral dendrites and synapses. Anatomical Record 160:516.

Murabe Y, Samo Y (1982) Morphological studies on neuroglia. VI. Distribution of 'brain macrophages' in brains of neonatal and adult rats, as determined by means of immunohistchemistry. Cell and Tissue Research 225:469-485.

Murphy EH, Brown J, Iannuzzelli PG, Baker R (1990) Regeneration and soma size changes following axotomy of the trochlear nerve. J Comp Neurol 295:685-697.

Murphy AS, Flavin M (1983) Microtubule assembly using microtubule-associated protein MAP2 prepared in defined states of phosphorylation with protein kinase and phosphatase. European Journal of Biochemistry 137:37-46.

Murray M, Grafstein B (1969) Changes in the morphology and amino acid incorporation of regenerating goldfish optic neurones. Exp Neurol 23:544-560.

Nardi JB (1983) Neuronal pathfinding in developing wings of the moth. Developmental Biology 95:163-174.

Navarrete R, Vrbová G (1983) Changes of activity patterns in slow and fast muscle during postnatal development. Developmental Brain Research 8:11-19.

Navarrete R, Vrbová G (1984) Differential effect of nerve injury at birth on the activity pattern of reinnervated slow and fast muscles of the rat. Journal of Physiology 351:675-685.

Navarrete R, Vrbová G (1985) Precocious activation of locomotor activity by L-DOPA in the neonatal rat. Neuroscience Letters 22:S556.

Navarrete R, Shahani U, Vrbová G (1986) Permanent changes of motor reflexes induced by postnatal nerve injury in the rat. Proc Phys Soc 40P.

Navarrete R, Walton KD, Llinas R (1987) Spinal network development and its relation to hind-limb movement: an in vitro electrophysiological study in the neonatal rat. Society for Neuroscience abstracts 13:824.

Navarrete R, Walton KD, Llinas R (1988a) Postnatal changes in the electrical properties of muscle identified rat motoneurones: an *in vitro* study. Society for Neuroscience abstracts 14:1060.

Navarrete R, Walton KD, Llinas R (1988b) Postnatal changes in the electrical properties of muscle- identified rat motoneurones. Society for Neuroscience abstracts 14:1060.

Navarrete R, Walton KD (1989a) Postnatal changes in electrotonic coupling between rat lumbar motoneurones studied in an *in vitro* spinal cord-hindlimb preparation. Proc Phys Soc 24p.

Navarrete R, Walton KD (1989b) Calcium conductances trigger doublet firing in neonatal rat motoneurones *in vitro*. Proc Phys Soc 415:70p.

Navarrete R, Shahani U, Vrbová G (1990) Long-lasting modification of reflexes after neonatal nerve injury in the rat. Journal of the Neurological Sciences 96:257-267.

Navarrete R, Vrbová G (1993) Activity-dependent interactions betweem motoneurones and muscles: their role in the development of the motor unit. Progress in Neurobiology 41:93-124.

Nicholas AP, Pieribone VA, Arvidsson U, Hokfelt T (1992) Serotonin-, substance P- and glutamate/aspartate-like immunoreactivities in medullo-spinal pathways

of rat and primate. Neuroscience 48:545-559.

Nicolopoulos-Stournaras S, Iles JF (1983) Motor neuron columns in the lumbar spinal cord of the rat. J Comp Neurol 217:75-85.

Nishida E, Kuwaki T, Sakai H (1981) Phosphorylation of microtubule-associated proteins (MAPs) and pH of the medium control the interaction between MAPs and actin filaments. J Biochem Tokyo 90:575-578.

Nissl F (1892) Uber die Veranderungen der Ganglienzellen am Facialiskern des Kaninchens nach Ausreissung der Nerven. Allgem Z f Psychiat 48:197-198.

Nunez-Abades PA, He F, Barrionuevo G, Cameron WE (1993) Morphology of developing rat genioglossal motoneurones studied *in vitro*: changes in length, branching pattern, and spatial distribution of dendrites. J Comp Neurol

O'Brien RAD, Ostberg AJC, Vrbová G (1978) Observations on the elimination of polyneuronal innervation in developing mammalian skeletal muscle. Journal of Physiology 282:571-582.

O'Brien RAD, Vrbová G (1978) Acetlycholine synthesis in nerve endings to slow and fast muscles in developing chicks: effect of muscle activity. Neuroscience 3:1227-1230.

O'Brien RAD, Ostberg A, Vrbová G (1982) The reorganization of neuromuscular junctions during development in the rat: Membranes in Growth and Development. New York: Alan R.Liss.

O'Brien RAD, Ostberg A, Vrbová G (1984) Protease inhibitors reduce the loss of nerve terminals induced by activity and calcium in developing rat soleus muscles *in vitro* . Neuroscience 12:637-646.

O'Brien RJ, Fischbach GD (1986a) Isolation of embryonic chick motoneurones and their survival *in vitro*. Journal of Neuroscience 6:3265-3274.

O'Brien RJ, Fischbach GD (1986b) Characterization of excitatory amino acid receptors expressed by embryonic chick motoneurones *in vitro*. Journal of Neuroscience 6:3275-3283.

O'Donovan MJ, Landmesser LT (1987) The development of hindlimb motor activity studied in the isolated spinal cord of the chick embryo. Journal of Neuroscience 7(10):3256-3264.

O'Hanlon GM, Lowrie MB (1992) Localised morphological changes in sciatic pool motoneurones following nerve crush in rats. Journal of Anatomy 180:360P.

O'Hanlon GM, Lowrie MB (1993a) Postnatlal dendritic development of sciatic motoneuornes under normal conditions and following neonatal nerve injury in the rat. Journal of Anatomy 183:189-D1.

O'Hanlon GM, Lowrie MB (1993b) Evidence for age-dependent changes in motoneurone dendritic morphology following nerve-crush in the rat. Neuroscience 57:995-1005.

O'Hanlon GM, Lowrie MB (1993c) Neonatal nerve injury causes long-term

changes and distribution of motoneuron dendrites in the rat. Neuroscience 56(2):453-464.

O'Leary DDM, Cohen WM (1984) Survival of isthmo-optic neurons after early removal of one eye. Developmental Brain Research 12:293-310.

Okado N, Sako H, Homma S, Ishikawa K (1991) Development of serotonergic system in the brain and spinal cord of the chick. Progress in Neurobiology 38:93-123.

Oppenheim RW (1975) The role of supraspinal input in embryonic motility: a re-examination in the chick. J Comp Neurol 160:37-50.

Oppenheim RW, Maderdrut JL, Wells DJ (1982) Cell death of motoneurones in the chick embryo spinal cord. IV. Reduction of naturally occuring cell death in the thoracolumbar cloumn of Terni by nerve growth factor. J Comp Neurol 210:174-189.

Oppenheim RW (1991) Cell death during development of the nervous system. Annual Review of Neuroscience 14:453-501.

Oppenheim RW (1992) High hopes of a trophic factor. Nature 358:451-452.

Oppenheim RW, Qui-Wei Y, Prevette D, Yan Q (1992) Brain-derived neurotrophoc factor rescues developing avian motoneuornes from cell death. Nature 360:755-757.

Otsuka M, Konishi S (1975) Electrophysiology of mammalian spinal cord *in vitro*. Nature 252:733-734.

Ozaki S, Kudo N, Okado N (1991) Serotonin-positive fibres within the spinal motor nucleus of the newborn rat, with special reference to co-localization of substance P. Neuroscience Letters 130:145-148.

Patel SN, Poo MM (1982) Orientation of neurite outgrowth by extracellular electric fields. Journal of Neuroscience 2(4):483-496.

Perry VH, Linden R (1982) Evidence for dendritic competition in the developing retina. Nature 297:683-685.

Perry VH, Hume DA, Gordon S (1985) Immunohistochemical localization of macrophages and microglia in the adult and developing mouse brain. Cell and Tissue Research 15:313-326.

Perry VH, Gordon S (1988) Macrophages and microglia in the nervous system. Tends Neurosci 11:273-277.

Petit TL, LeBoutillier JC, Gregorio A, Libstug H (1988) The pattern of dendritic development in the cerebral cortex of the rat. Developmental Brain Research 41:209-219.

Peyronnard JM, Charron JP, Lavoie J, Messier JP (1988) Motor, sympathetic and sensory innervation of rat skeletal muscle. Brian Research 373:288-302.

Phelps PE, Barber RP, Houser CR, Crawford GD, Salvaterra PM, Vaughn JE (1984) Postnatal development of neurones containing choline acetyltransferase

in rat spinal cord: an immunocytochemical study. J Comp Neurol 229:347-361.

Phelps PE, Barber RP, Brennan LA, Maines VM, Salvaterra PM, Vaughn JE (1990) Embryonic development of four different substes of cholinergic neurones in rat cervical spinal cord. J Comp Neurol 261:9-26.

Piehl f, Arvidsson U, Johnson H, Cullheim S, Villar M, Dagerlind A, Terenius L, Hokfelt T, Ulfhake B (1991) Calcitonin gene-related peptide (CGRP)-like immunorectivity and CGRP mRNA in thr rat spinal cord motoneurones after different types of lesions. European Journal of Neuroscience 3:737-757.

Pilar G, Tuttle J, Vaca K (1981) Functional maturation of motor nerve terminals in the avian iris: ultrastructure, transmitter metabolism and synaptic reliability. Journal of Physiology 106:457-468.

Pilowsky PM, de Castro D, Llewellyn-Smitth I, Lipski J, Voss MD (1990) Serotonin immunoreactivity boutons make synapses with feline phrenic motoneurones. Journal of Neuroscience 10(4):1091-1098.

Polistina DC, Murray M, Goldberger ME (1990) Plasticity of dorsal root and descending projections after partial deafferentation of the adult rat spinal cord. J Comp Neurol 299:349-363.

Pollin MM, McHanwell S, Slater CR (1991) The effect of age on motor neurone death following axotomy in the mouse. Development 112:83-89.

Price DL, Porter KR (1972) The response of ventral horn neurones to axonal transection. Journal of Cell Biology 53:24-37.

Provine RR (1971) Embryonic spinal cord: synchrony and spatial distribution of polyneuronal burst discharges. Brian Research 29:155-158.

Purves D, Vrbová G (1974) Some characteristics of myotubes cultured from slow and fast chick muscles. Journal of Cell Physiology 84:97-100.

Purves D (1980) Neuronal competition. Nature 287:585-587.

Purves D, Lichtman JW (1980) Elimination of synapses in the developing nervous system. Science 210:153-157.

Purves D, Lichtman JW (1985) Principles of Neural Development. Sunderland: Sinauer.

Rajaofetra N, Sandillon F, Geffard M, Privat A (1989a) Pre- and post-natal ontogeny of serotonergic projections to the rat spinal cord. Journal of Neuroscience Research 22:305-321.

Rajaofetra N, Sandillon F, Geffard M, Privat A (1989b) Pre- and post-natal ontogeny of serotonergic projections in the rat spinal cord. Journal of Neuroscience Research 22:305-321.

Rakic P (1971) Guidance of neurones migrating to the fetal monkey cortex. Brian Research 33:471-476.

Rakic P (1972) Mode of cell migration to the superficial layers of fetal monkey neocortex. J Comp Neurol 145:61-84.

Rakic P (1974) Neurons in rhesus monkey visual cortex: Systematic relation between time of origin and eventual disposition. Science 183:425-427.

Rakic P (1975) Role of cell interaction in development of dendritic patterns. Advances in Neurology 12:117-134.

Rall W (1959) Branching dendritic tree and motoneurone membrane resistance. Exp Neurol 1:491-527.

Rall W (1964) Neural Theory and Modelling. Stanford: Stanford University Press.

Rall W, Burke RE, Smith TG, Nelson PG, Frank K (1967) Dendritic location of synapses and possible mechanisms for the monosynaptic EPSP in motoneurones. Journal of Neurophysiology 30:1169-1193.

Rall W, Rinzel J (1973) Branch input resistance and steady attenuation for input to one branch of a dendritic neuron model. Biophys J 13:648-688.

Ramirez V, Ulfhake B (1991) Postnatal development of cat hindlimb motoneurones supplying the intrinsic muscles of the foot sole. Developmental Brain Research 62:189-202.

Ramirez V, Ulfhake B (1992) Anatomy of dendrites in motoneurones supplying the intrinsic muscles of the foot sole in the aged cat: evidence for dendritic growth and neo-synaptoganisis. J Comp Neurol 316:1-16.

Ramoa AS, campbell G, Shatz CJ (1988) Dendritic growth and remodeling of cat retinal ganglion cells during fetal and postnatal development. Journal of Neuroscience 8(1):4329-4261.

Ramon y Cajal S (1890) Sur l'origine et les ramifications des fibres nerveuses de la moelle embryonnaire. Anat Anz 5:85-95.

Ramon y Cajal S (1929) Degeneration and Regeneration of the Nervous System. New York: Hafner.

Rao K, Lund RD (1989) Degeneration of optic axons induces expression of major histocompatibility antigens. Brian Research 488:332-335.

Rasmussen CD, Means AR (1989) The presence of parvalbumin in a non-muscle cell line attenuates progression through mitosis. Mol Endocrinol 3:588-596.

Redfern PA (1970) Neuromuscular transmission in newborn rats. Journal of Physiology 209:701-709.

Reh T, Constantine-Paton M (1985) Eye-specific segregation requires neural activity in three-eyed *Rana pipiens*. Journal of Neuroscience 5:1132-1143.

Renshaw B (1946) Central effects of centripetal impulses in axons of spinal ventral roots. Journal of Neurophysiology 9:191-204.

Rich KM, Luszczynski JR, Osbourn PA, Johnson EM (1987) Nerve growth factor protects adult sensory neurons from cell death and atrophy caused by nerve injury. Journal of Neurocytology 16:261-268.

Riederer B, Matus A (1985) Differential expression of distinct microtubule-associated proteins during brain development . Proc Natl Acad Sci USA 82:6006-6009.

Riederer B, Cohen R, Matus A (1986) Map5: a novel microtubule-associated protein under strong developmental regulation. Journal of Neurocytology 15:763-775.

Rio-Hortega P (1939) Cytology and cellular pathology of the nervous system. New York: Hocker.

Risling M, Aldskoguis H, Hildebrand C, Remahl S (1983a) Effects of sciatic nerve resection on L7 spinal roots and dorsal root ganglia in adult cats. Exp Neurol 82:568-580.

Risling M, Aldskoguis H, Hildebrand C, Remahl S (1983b) Effects of trigeminal nerve resection on L7 DRG and spinal roots in adult cats. Exp Neurol 82:568-580.

Risling M, Hildebrand C, Cullheim S (1984) Invasion of the L7 ventral root and pia mater by new axons after sciatic nerve crush in kittens. Exp Neurol 83:84-97.

Rivero-Melian C, Grant G (1987) The distribution of lumbar dorsal root fibres to spinocerebellar cell groups in the lumbar region in the rat: A double labelling study with choleragenoid-horseradishperoxidase conjugate and fluoro-gold. Neuroscience Suppl 22:2300.

Rivero-Melian C, Grant G (1990) Distribution of lumbar dorsal root fibres in the lower thoracic and lumbosacral spinal cord of the rat studied with choleragenoid horse radish peroxidase. J Comp Neurol 299:470-481.

Romanes GJ (1946a) Motor localization and the effects of nerve injury on the ventral horn cells of the spinal cord. Anatomy 80:117-131.

Romanes GJ (1946b) The motor pools of the spinal cord. Journal of Anatomy 98:171-131.

Rose PK (1982) Branching structure of motoneurone stem dendrites: Study of neck muscle motoneurones intracellularly stained with horseradish peroxidase in the cat. Journal of Neuroscience 2(11):1596-1607.

Rose SPR (1991) How chicks make memories: the cellular cascade from c-fos to dendritic remodelling. Trends Neurosci 14:390-397.

Rothman SM, Olney JW (1987) Excitotoxicity and the NMDA receptor. Trends Neurosci 10(7):299-302.

Rubin E, Purves D (1980) Segmental organization of sympathetic preganglionic neurones in the mammalian spinal cord. J Comp Neurol 192:163-174.

Ryall RW, Piercy MF (1971) Excitation and inhibition of Renshaw cells by impulses in peripheral afferent nerve fibres. Journal of Neurophysiology 34:242-251.

Saito K (1979) Development of spinal reflexes in the rat fetus studied *in vitro*. Journal of Physiology 294:581-594.

Sako H, Kojima T, Okado N (1986) Immunohistochemical study on the development of serotoninergic neurones in the chick: II. Distribution of cell bodies and fibres in the spinal cord. J Comp Neurol 253:79-91.

Sanders FK, Whitteridge D (1946) Conduction velocity and myelin thickness in regenerating nerve fibres. Journal of Physiology 105:152-174.

Sato M, Mizuno N, Konishi A (1977) Postnatal differentiation of cell body volumes of spinal motoneurones innervating slow-twitch and fast-twitch muscles. J Comp Neurol 175:27-36.

Sauer FC (1935) Mitosis in the neuroal tube. J Comp Neurol 62:377-405.

Scheibel AB (1991) Development of axonal and dendritic neuropil as a function of evolvoing behaviour. A Book 381-398.

Scheibel ME, Scheibel AB (1970) Organisation of spinal motoneuone dendrites in bundles. Exp Neurol 28:106-112.

Scheibel ME, Scheibel AB (1971) Developmental relationship between spinal motoneuorne dendritic bundles and patterned activity in the forelimb of cats. Exp Neurol 30:367-373.

Scheibel ME, Davies TL, Scheibel AB (1973) Maturation of reticular dendrites: Loss of spines and development of bundles. Exp Neurol 38:301-310.

Scheibel ME, Scheibel AB (1973) Dendritic bundles in the ventral commisure of the cat spinal cord. Exp Neurol 39:482-488.

Schinstine M, Cornbrookes CJ (1990) Axotomy enhances the outgrowth of neurites from embryonic rat septal-basal neurones on a laminin substratum. Exp Neurol 108:10-22.

Schmalbruch H (1984) Motoneurone death after sciatic nerve section in newborn rats. J Comp Neurol 224:252-258.

Schreyer DJ, Jones EHG (1988a) Topographic sequence of outgrowth of corticospinal axons in the rat: a study using retrograde axonal labelling with Fast Blue. Developmental Brain Research 38:89-101.

Schreyer DJ, Jones EHG (1988b) Topographic sequence of outgrowth of corticospinal axons in the rat: a study using retrograde axonal labelling with Fast Blue. Developmental Brain Research 38:89-101.

Schreyer DJ, Skene JHP (1991) Fate of GAP-43 in ascening spinal axons of DRG neurons after peripheral nerve injury: delayed accumulation and correlation with regenerative potential. Journal of Neuroscience 11:3738-3751.

Schudt C, Gaertner U, Dolken G, Pette D (1976) Calcium-related changes of enzyme activities in energy metabolism of cultured embryonic chick myoblasts and myotubes. European Journal of Biochemistry 60:579-586.

Seil FJ (1988) Axonal sprouting in response to injury. Neural Regeneration and

Sendtner M, Kreutzberg GW, Thoenen H (1990) Ciliary neurotrophic factor prevents the degeneration of motor neurons after axotomy. Nature 345:440-441.

Sendtner M, Holtmann B, Kolbeck R, Thoenen H, Barde Y-A (1992a) Brain-derived neurotrophic factor prevents death of motoneurones in newborn rats after nerve section. Nature 360:757-759.

Sendtner M, Schmalbruch H, Stockil KA, Carroll P, Kreutzberg GW, Thoenen H (1992b) Ciliary neurotropic factor prevents degeneration of motor neurons in mouse mutant progressive motor neuropathy. Nature 358:502-504.

Sendtner M, Stockil KA, Thoenen H (1992c) Synthesis and localization of ciliary neurotropic factor in the sciatic nerve of the adult rat after lesion znd during regeneration. Journal of Cell Biology 118:139-148.

Shatz CJ, Kirkwood PA (1984) Prenatal development of functional connections in the cat's retinogeniculate pathway. Journal of Neuroscience 4(5):1378-1397.

Sheard PW, Duxon MJ, Harris AJ (1991) Neuromuscular transmission to identified promary and secondary myotubes: a re-evaluation of polyneuronal innervation patterns in rat embryos. Developmental Biology 148:459-472.

Shieh JY, Leong SK, Wong WC (1983) Origin of the rubrospinal tract in neonatal, developing and mature rats. J Comp Neurol 214:79-86.

Sholl DA (1953) Dendrtic organisation in the neurones of the visual and motor cortices of the cat. Journal of Anatomy 87:387-401.

Shortland P, Woolf CJ (1993) Chronic peripheral nerve section results in a rearrangement of the central axonal arborizations of axotomized A beta primary afferent neurons in the rat spinal cord. J Comp Neurol 330:65-82.

Silos-Santiago I, Snider WD (1992) Development of commisural neurones in the embryonic rat spinal cord. J Comp Neurol 325:514-526.

Singer P, Mehler S (1980) 2-deoxy-[14C]glucose uptake in rat hypoglossal nucleus after nerve transection. Exp Neurol 69:617-626.

Singer P, Mehler S (1983) Role of electrical activity in axotomy-induced glucose use. Exp Neurol 80:601-612.

Skagerberg G, Bjorkland A (1985) Topographic principles in the spinal projections of serotonergic and non-serotonergic brainstem neurons in the rat. Neuroscience 15:445-480.

Skene JHP, Willard AL (1981) Shanges in axonally transported proteins during axon regeneration in toad retinal ganglion cells. Journal of Cell Biology 89:86-95.

Skene JHP, Jacobson RD, Snipes GJ, McGuire CB, Norden JJ, Freeman JA (1986) A protein induced during nerve growth (GAP-43) is a major component of growth cone membranes. Science 233:783-786.

Skene JHP (1989) Axonal growth-associated proteins. Annual Review of Neuroscience 12:127-156.

Skoff RP, Hamburger V (1974) Fine structure of dendritic and axonal growth cones in embryonic chick spinal cord. J Comp Neurol 153:107-148.

Smith CJ (1983) The development and postnatal organisation of primary afferent projections to the rat thoracic spinal cord. J Comp Neurol 220:29-43.

Smith CJ, Hollyday M (1983) The development and postnatal organization of motor nuclei in the rat thoracic spinal cord. J Comp Neurol 220:16-28.

Snider WD, Thanedar S (1989) Target dependence of hypoglossal neurons during development and in maturity. J Comp Neurol 279:489-498.

Snider WD, Palavali V (1990) Early axon and dendritic outgrowth of spinal accessory motor neurones studied with DiI in fixed tissues. J Comp Neurol 297:227-238.

Snider WD, Tsering C (1990) Interactions between motor neuron dendrites and dorsal root afferent axons in developing mammalian spinal cord. Society for Neuroscience abstracts 16:463.6.

Snider WD, Elliott JL, Yan Q (1992a) Axotomy-induced neuronal death during development. Journal of Neurobiology 23:1231-1246.

Snider WD, Zhang L, Yusoof S, Gorukanti N, Tsering C (1992b) Interactions between dorsal root axons and their target motor neurons in developing mammalian spinal cord. Journal of Neuroscience 12(9):3494-3508.

Solbach S, Celio MR (1991) Ontogeny of the calcium binding protein parvalbumin in the rat nervous system. Anatomy and Embryology 184:103-124.

Sotelo C, Taxi J (1970) Ultrastructural aspects of electrotonic junctions in the spinal cord of the frog. Brian Research 17:137-141.

Spitzer NC (1981) Development of membrane properties in vertebrates. Trends Neurosci July:169-172.

Srihari T, Vrbová G (1978) The role of muscle activity in the differentation of neuromuscular junctions in slow and fast chick muscles. Journal of Neurocytology 7:529-540.

Standler NA, Bernstein JJ (1982) Degeneration and regeneration of motoneurone dendrites after ventral root crush: computer reconstruction of dendritic fields. Exp Neurol 75:600-615.

Steltzner DJ (1971) The normal postnatal development of synaptic end-feet in the lumbar spinal cord and of responses in the hind limbs of the albino rat. Exp Neurol 31:337-357.

Steltzner DJ (1982) The role of descending systems in maintaining intrinsic spinal function: A devlopmental approach. Brain Stem Control of Spinal Mechanisms 297-321.

Stevens RT, Apkarian AV, Hodge CJ (1985) Funicular cause of catecholamine

fibres innervating the lumbar spinal cord of the rat. Brian Research 336:243-251.

Stockil KA, Lottspeich F, Sendtner M, Mariakowski P, Carrol P, Gotz R, Lindholm D, Thoenen H (1991) Molecular cloning, expression an dregional distribution of rat ciliary neurotrophic factor. Nature 342:920-923.

Stockli KA, Lillien LE, Naher NM, Breitfeld G, Hughes RA, Raff MC, Thoenen H, Sendtner M (1991) Regional distribution, developmental changes, and cellular localization of CNTF-mRNA abd protein in the rat brain. Journal of Cell Biology 115:447-459.

Sumner BEH, Watson WE (1971) Retraction and expansion of the dendritic tree of motor neurones of adult rats induced *in vivo*. Nature 233:273-275.

Sumner BEH, Sunderland FI (1973) Quantitative electron microscopy on the injured hypoglossal nucleus in the rat. Journal of Neurocytology 2:315-328.

Sumner BEH (1975) A quantitative analysis of the response of presynaptic boutons to postsynaptic motor neuron axotomy. Exp Neurol 46:605-615.

Sumner BEH (1976) Quantiative ultrastructural observations on the inhibited recovery of the hypgossal nucleus from the axotomy response when regeneration of the hypoglossal nerve is prevented. Experimental Brain Research 26:141-150.

Swett JE, Hong C, Miller PG (1991) All peroneal motoneurones of the rat survive crush injury but some fail to reinnervate their origional targes. J Comp Neurol 304:234-252.

Tan H, Miletic V (1990) Bulbospinal serotinergic pathways in the frog *Rana pipiens*. J Comp Neurol 292:291-302.

Tanaka H, Landmesser LT (1986) Cell death of lumbosacral motoneurones in chick, quail and chick-quail chimera embryos. A test of the quantitative matching hypothesis of neuronal cell death. Journal of Neuroscience 6:2889-2899.

Tanaka H, Mori S, Kimura H (1992) Developmental changes in the serotonergic innervation of hindlimb extensor motoneurones in the rat. Developmental Brain Research 65:1-12.

Tashiro T, Sadota T, Takahashi O, Matsushima r, Mizuno N (1988) Distribution of axons exhibiting both enkephalin- and serotinergic-like immunoreactivities in the lumbar cord segments: an immunohistochemical study in the cat. Brian Research 440:357-362.

Tello JF (1917) Genesis de las terminaciones nerviosas mortices y sensitivas. I. En el sistemo locomotor de los vertebratos superioves histogenesis muscular. Trabos Lab Invest Biol Madrid 15:101-199.

Tessler A, Himes BT, Krieger NR, Murray M, Goldberger ME (1985) Sciatic nerve transection produces death of dorsal root ganglion cells and reversible loss of Substance P in spinal cord. Brian Research 332:209-218.

Tetzlaff W, Graeber MB, Bisby MA, Kreutzberg GW (1988) Increased glial fibrillary acidic protein synthesis in astrocytes during retrograde reaction of the rat

facial nucleus. Glia 1:90-95.

Titmus MJ, Faber DS, Zottoli SJ (1986) Altered excitability of goldfish mauthner cell following axotomy: I. Characterisation and correlations with somatic and axonal morphological reactions. Journal of Neuroscience 55(6):1424-1439.

Titmus MJ, Faber DS (1990) Axotomy-induced alterations in the electrophysiological characteristics of neurons. Progress in Neurobiology 35:1-51.

Tork I (1985) Raphe nuclei and serotonin containing systems. The Rat Nervous System

Tracey DJ (1985) Ascending and descending pathways in the spinal cord. In: The Rat Nervous System (pp 311-324. Achademic Press Australia.

Tremblay LE, Maheux R, Bedard P (1986) Substance P in the lumbar spinal cord of the rat affects the motor response to 5HT and TRH. Neuropharmacology 25:419-424.

Tucker RP (1990) The roles of microtuble-associated proteins in brain morphogenesis: A review. Brian Research Reveiws 15:101-120.

Ulfhake B, Arvidsson U, Cullheim S, Hokfelt T, Brodin E, Verhofstad A, Visser T (1978) An ultrastructural study of 5-HT-, thyrotropin-releasing hormone-, and substance P-immunoreactive axonal boutons in the motor nucleus of spinal cord segment L7-S1 in the adult cat. Neuroscience 23:917-929.

Ulfhake B, Cullheim S (1981) A quantitative light microscopic study of the dendrites of cat spinal g-motoneurones after intracellular staining with horseradish peroxidase. J Comp Neurol 202:585-596.

Ulfhake B, Kellerth JO (1981) A quantitative light microscopic study of the dendrites of cat spinal a-motoneurones after intracellular staining with horseradish peroxidase. J Comp Neurol 202:571-583.

Ulfhake B, Kellerth JO (1983) A quantitative morphological study of HRP-labelled cat a-motoneurones supplying different hindlimb muscles. Brian Research 264:1-19.

Ulfhake B, Kellerth JO (1984) Electrophysiological and morphological measurments in cat gastrocnemius and soleus a-motoneurones. Brian Research 307:167-179.

Ulfhake B, Cullheim S, Hokfelt T, Visser TJ (1987) The combined use of immunohistochemistry and intracellular staining with horseradish peroxidase for light and electron microscopic studies of transmitter identified inputs to functionally characterised neurones. Brian Research 419:387-391.

Ulfhake B, Cullheim S (1988a) Postnatal development of cat hind limb motoneurones. III: Changes in size of motoneurones supplying the triceps surae muscle. J Comp Neurol 278:103-102.

Ulfhake B, Cullheim S (1988b) Postnatal development of cat hind limb motoneurones. II: in vivo morphology of dendritic growth cones and the maturation of dendritic morphology. J Comp Neurol 278:88-102.

Ulfhake B, Cullheim S, Franson P (1988) Postnatal development of cat hind limb motonerones. I: changes in length, branching structure, and spatial distribution of cat triceps surae motoneurones. J Comp Neurol 278:69-87.

Uylings HBM, van Eden CG, Hofman MA (1986) Morphology of size/volume variables and comparison of their bivariate relations in the nervous system under different conditions. Journal of Neuroscience Methods 18:19-37.

Valentino KL, Jones EG (1982) The early formation of the corpus callosum: a light and electron microscopic study in foetal and neonatal rats. Journal of Neurocytology 11:583-609.

van Donger PAM, Grillner S, Hokfelt T (1986) 5-hydroxytryptamine (serotonin) causes a reduction in the afterhyperpolarization following the action potential in lamprey motoneurones and premotor intersor. Brian Research 536:320-325.

Vaughn JE, Henrikson CK, Grieshaber JA (1974) A quantitative study of synapses on motor neuron dendritic growth cones in developing mouse spinal cord. Journal of Cell Biology 60:664-672.

Vaughn JE, Simms TJ (1978) Axonal growth cones and developing axonal collaterals form synaptic junctions in embryonic mouse spinal cord. Journal of Neurocytology 7:337-363.

Vaughn JE, Barber RP, Sims T (1988) Dendritic development and preferential growth into synaptogenic fields. Synapse 2:69-78.

Vaughn JE (1989) Fine structure of synaptogenesis in the vertebrate central nervous system. Synapse 3:255-285.

Vejsada R, Hnìk P, Navarrete R, Palecek J, Soukup T, Borecka U, Payne R (1991) Motor functions in rat hindlimb muscles following neonatal sciatic nerve crush. Neuroscience 40:267-275.

Viereck C, Tucker RP, Binder LI, Matus A (1988) Phylogenetic conservation of brain microtubule-associated proteins MAP2 and tau. Neuroscience 26:893-904.

von Bussmann KA, Garey LJ, Jen LS (1993) Injury-resistant retinal ganglion cells that are rich in cytochrome oxidase. NeuroReport 4:247-250.

Vrbová G, Navarrete R, Lowrie MB (1985) Matching of muscle proprerties and motoneurones firing patterns during early stages of development. Journal of Experimental Biology 115:113-123.

Walton KD, Fulton BP (1983) Hydrogen peroxide as a source of molecular oxygen for in vitro mammalian CNS preparations. Brian Research 278:387-393.

Walton KD, Fulton BP (1986) Ionic mechanisms underlying the firing properties of rat neonatal motoneurones studied *in vitro*. Neuroscience 19(3):669-683.

Walton KD, Navarrete R (1991) Postnatal changes in motoneurones electrotonic coupling studied in the *in vitro* rat lumbar spinal cord. Journal of Physiology 433:283-305.

Wang S-D, Goldberger ME, Murray M (1991a) Normal development and the ef-

fects of early rhizotomy on spinal systems in the rat . Developmental Brain Research 64:57-69.

Wang S, Goldberger ME, Murray M (1991b) Plasticity of spinal systems after unilateral lumbosacral dorsal rhizotomy in the adult rat. J Comp Neurol 304:555-568.

Wassle H (1988) Dendritic maturation of retinal ganglion cells. Trends Neurosci 11(3):87-89.

Watson WE (1965) An autoradiographic study of the incorporation of nucleic-acid precursors by neurones and glia during nerve regeneration. Journal of Physiology 180:741-753.

Watson WE (1968a) The change in dry mass of hypoglossal neurones by puromycin, and the effects of nerve injury. Journal of Physiology 201:80P.

Watson WE (1968b) Observations on the nucleolar and total cell body nucleic acid of injured nerve cells. Journal of Physiology 196:655-676.

Watson WE (1970) Some metabolic responses of axotomised neurones to contact between their axons and denervated muscle. Journal of Physiology 210:321-343.

Watson WE (1972) Some quantitative observations upon the responses of neuroglial cells which follow axotomy of adjacent neurones. Journal of Physiology 225:415-435.

Watson WE (1974) Cellular responses to axotomy and to related procedures. Br Med Bull 30:112-115.

Waxman SG, Foster RE (1980) Ionic channel distribution and heterogeneity of the axon membrane in myelinated fibres. Brian Research Reveiws 2:205-234.

Weber ED, Steltzner DJ (1980) Synaptogenesis in the intermediate gray region of the lumbar spinal cord in the postnatal rat. Brian Research 185:17-37.

Weisel TN, Hubel DH (1965) Comparison of the effects of unilateral and bilateral eye closure on cortical unit responses in kittens. Journal of Neurophysiology 28:1029-1040.

Weiss P (1939) Principles of development. New York: Henry Holt and Company.

Weiss P (1941) Nerve patterns: Mechanics of nerve growth. Growth 5:163-203.

Weiss P (1961) Guiding priciples in cell locomotion and cell aggregation. Exp Cell Res 8:346-401.

West NR, Collins GH (1991) Relationship of wallerian degeneration to regrowing axons. Journal of Neuropathology and Experimental Neurology 50:693-703.

Westerga J, Gramsbergen A (1990) The development of locomotion in the rat. Developmental Brain Research 57:163-174.

Westerga J, Gramsbergen A (1992) Structural changes of the soleus and the tibialis anterior motoneurone pool during development in the rat. J Comp Neurol 319:406-416.

Whitelaw V, Hollyday M (1983a) Position-dependant motor innervation of the chick hindlimb following serial and parallel duplications of limb segments. Journal of Neuroscience 3:1216-1225.

Whitelaw V, Hollyday M (1983b) Neural pathway constraints in the motor innervation of the chick hindlimb following dorsoventral rotations of distal limb segments. Journal of Neuroscience 3:1226-1233.

Wilke V (1984) Optical scanning microscory - The laser scan microscope. Scanning 7:88-96.

Wong ROL, Yamawaki RM, Shatz CJ (1992) Synaptic contacts and the transient dendritic spines of developing retinal ganglion cells. European Journal of Neuroscience 4:1387-1397.

Wong-Riley MTT, Merzenich MM, Leake PA (1978) Changes in endogenous enzymatic activity to DAB induced by neuronal activity. Brian Research 141:185-192.

Wong-Riley MTT (1979) Changes in the visual system of monocularly sutured or enucleated cats demonstrable with cytochrome oxidase histochemistry. Brian Research 171:11-28.

Wong-Riley MTT (1989) Cytochrome oxidase: an endogenous metabolic marker for neuronal activity. Trends Neurosci 12:94-101.

Xie ZP, Poo MM (1986) Initial events in the fromation of neruomuscular synapse: Rapid induction of acetylcholine release from embryonic neuron. Proc Natl Acad Sci USA 83:7069-7073.

Yaffe D (1969) Cellular aspects of muscle differentiation in vitro. Current Topics in Developmental biology 4:37-75.

Yan Q, Elliott J, Snider WD (1992) Brain-derived neurotrophic factor rescues spinal motor neurones from axotomy-induced cell death. Nature 360:753-755.

Yawo H (1987) Changes in the dendritic geometry of mouse superior cervical ganglion cells following postganglionic axotomy. Journal of Neuroscience 7(11):3703-3711.

Yelnik J, Percheron G, Francois C (1984) A Golgi analysis of the primate globus palidus. II. Quantitative morphology and spatial orientation of dendritic arbourisations. J Comp Neurol 227:200-213.

Ygge J, Aldskoguis H (1984a) Intercostal nerve transection and its effect on the dorsal root ganglion. A quantitative study on thoracic ganglion numbers and sizes in the rat. Experimental Brain Research 55:402-408.

Ygge J, Aldskoguis H (1984b) Intercostal nerve transection and its effect on the dorsal root ganglion. A quantitative study on ganglion cell numbers and sizes. Experimental Brain Research 55:402-408.

Ygge J (1989) Neuronal loss in lumbar dorsal root ganglia after proximal compared to distal sciatic nerve resection: a quantitative study in the rat. Brian Research 479:193-195.

Yip HK, Rich KM, Lampe PA, Johnson EM (1984) The effects of nerve growth factor and its antiserum on the postnatal development and survival after injury of sensory neurones in rat dorsal root ganglia. Journal of Neuroscience 4(12):2986-2992.

Young SH, Poo MM (1983) Spontaneous release of transmitter from growth cones of embryonic neurones. Nature 305:634.

Yu WHA (1988) Sex difference in neuronal loss induced by axotomy in the rat brain stem motor nuclei. Exp Neurol 102:230-235.

Zelena J, Hnìk P (1960) Abscence of spindles in muscles of rats reinnervated during development. Physiol Bohemoslov 9:373-381.

Zhang B, Goldberger ME, Murray M (1993) Proliferation of SP- and 5HT-containing terminals in lamina II of rat spinal cord following dorsal rhizotomy: quantitative EM-immunocytochemical studies. Exp Neurol 123:51-63.

Zhang J-H, Morita Y, Hironaka T, Emson PC, Tohyama M (1990) Ontological study of calbindin-D-like and parvalbumin-like reactivities in rat spinal cord and dorsal root ganglia. J Comp Neurol 302:715-728.

Zhu P-H, Vrbová G (1992) The role of Ca++ in the elimination of polynauronal innervation of rat soleus muscle fibres. European Journal of Neuroscience 4:433-437.

Ziskind-Conhaim L (1988) Physiological and morphological changes in developing peripheral nerves of rat embryos. Developmental Brain Research 42:15-28.

Zwaagstra B, Kernell D (1981) Sizes of soma and stem dendrites in intracellularly labelled a-motoneurones of the cat. Brian Research 204:295-309.